Morphology, Systematics & Palaeoecology of Pachycormid Fishes

Claire E. Dobson

Thesis submitted for the Degree of Doctor of Philosophy

Department of Earth Sciences

St Hugh's College, University of Oxford

Supervised by:

Prof. Matt Friedman, Dr Sam Giles & Prof. Roger Benson

Trinity Term 2019

Declaration

The contents of this thesis are all my own work, except where otherwise stated. Work done in collaboration with others is outlined at the start of each chapter.

Claire Dobson, Oxford

Abstract

Pachycormiformes are one of the earliest diverging groups of stem teleosts, and are distinguished by substantial ecomorphological disparity: from mid-sized predators, to giant suspension-feeders. Despite this, and their relatively abundant fossil record, they lack detailed study. Here, I use computed tomography scanning to re-examine and redescribe well-preserved suspension-feeding (*Martillichthys*) and predatory (*Pachycormus*) pachycormiforms. I report previously unobserved aspects of the gill skeleton (*Martillichthys*), neurocranium (both) and pectoral girdle (*Pachycormus*). I also identify features previously unreported in pachycormiforms, including a median vomer (*Martillichthys*: considered a teleost character but likely convergent), a urohyal (*Pachycormus*: considered a teleost character), and a metapterygium-like radial (*Pachycormus*: considered a primitive actinopterygian character). These morphological observations, along with molecular and stratigraphic data, inform phylogenetic analyses using maximum parsimony and Bayesian methods in order to resolve pachycormiform interrelationships, estimate divergence times, and test a hypothesized second origin of suspension-feeders within the group. Results corroborate previous hypotheses of pachycormiform relationships, but the inclusion of stratigraphic data results in an alternative pattern of relationships. Finally, I use quantitative biostratigraphic models, incorporating fossil record heterogeneity, to estimate credible intervals of suspension-feeding pachycormiform extinction and suspension-feeding chondrichthyan emergence. I find some chondrichthyan lineages may have appeared as early as the Early Cretaceous, and cannot reject that pachycormiforms may have persisted into the Eocene. However, the presence of other putative suspension-feeding chondrichthyans in

the Cretaceous that are absent in the Cenozoic suggests modern lineages may (as hypothesized here and elsewhere) have emerged following the faunal turnover of the end Cretaceous. This thesis builds a clearer picture of pachycormiform morphology and interrelationships, which can be used as a model to interpret the ecology and evolution of other fossils of pachycormiforms and stem teleosts. It also provides further context for the evolution of modern teleosts and how the extinction of pachycormiforms impacted modern marine diversity.

Extended Abstract

Teleosts are the largest group of bony vertebrates, representing over half of modern vertebrate diversity. However, while the sister group of the teleost total-group has recently been well established as holosteans, uncertainty still surrounds the composition and relationships of the teleost stem. Many have argued that this is due to a lack of detailed analysis and recognition of key synapomorphies in these early groups. Pachycormiformes, the group currently accepted as one of the earliest diverging stem teleosts, are often distinguished by substantial ecomorphological disparity: from mid-sized pelagic predators such as *Pachycormus* and *Hypsocormus*, to giant bodied suspension-feeders such as *Martillichthys* and *Leedsichthys* that represent the first and only currently recognized example of suspension-feeding in large bodied teleosts. Often branded as enigmatic, the Pachycormiformes have not been studied in close detail, despite being represented by numerous well-preserved specimens from Jurassic and Cretaceous deposits around the world. In particular, three-dimensional pachycormiform fossils from localities including the Strawberry Bank deposit of Ilminster and Dogsthorpe Pit of Peterborough provide an opportunity to observe internal and external structures in their full anatomical context rather than as isolated structures.

In this thesis, I use micro-computed tomography (μCT) scanning to re-examine and redescribe well preserved, three-dimensional specimens of suspension-feeding (*Martillichthys*) and predatory (*Pachycormus*) examples of pachycormiform taxa. In chapters 2 and 3, I describe new aspects of the gill skeleton, neurocranium and hyoid arch of *Martillichthys*,

including: gill rakers (previously considered absent); a spatulate anterior corpus of the parasphenoid; and a possible median vomer (a character generally considered to unite crownward teleosts, but which may be more widely distributed among teleost and non-teleost taxa). I also consider the merits of a hypothesis proposing a second origin of suspension-feeding within pachycormiforms, based on variation in skull geometries between the suspension-feeding pachycormiforms, and the presence of derived features shared by *Bonnerichthys* and the billfish-like predator *Protosphyraena*. For *Pachycormus*, I provide revised descriptions of the mandible, gill basket, neurocranium and pectoral girdle, newly identifying six pectoral radials, the last of which is forked distally and resembles the metapterygium seen in non-teleost actinopterygians. I also reinterpret a structure previously described as a ventral toothplate as a urohyal resembling the teleostean urohyal, previously only described in 'pholidophorids' and more crownward teleosts.

My third chapter also includes a phylogenetic analysis of crown neopterygians, using a pre-existing morphological character matrix that I adapt based on the descriptions given in this thesis and a thorough literature review. To this, I also add new and updated characters, and new taxa including the currently hypothesized sister group to pachycormiforms: aspidorhynchids. I then use this character-by-taxon matrix to investigate pachycormiform interrelationships, using both maximum parsimony and Bayesian methods. In addition, I perform a Fossilized Birth-Death analysis, incorporating sequence data from 12 nuclear genes and stratigraphic data in order to estimate divergence times among pachycormiforms. Finally, I perform a stepping stone analysis to explore the alternative hypothesis of relationships suggested in my second chapter. Both my maximum parsimony and Bayesian

analyses corroborate the patterns of relationships recovered in previous studies: *Euthynotus* is resolved as the sister taxon to all other pachycormiforms, with remaining pachycormiforms divided between two clades. These two clades are characterized by divergent ecologies among their most nested members: the billfish-like macropredators (*Protosphyraena* and *Australopachycormus*), and the giant suspension-feeders (*Bonnerichthys*, *Rhinconichthys*, *Asthenocormus*, *Leedsichthys* and *Martillichthys*). The more generalist predators *Hypsocormus* and *Orthocormus*, and *Pachycormus*, *Saurostomus* and *Ohmdenia*, respectively, fall as early diverging members of these lineages. As with previous studies, I also resolve *Ohmdenia* as the sister to all suspension-feeding pachycormiforms, potentially representing an intermediary taxon between the mid-sized predators and the giant suspension-feeders. However, the inclusion of stratigraphic data when estimating divergence times results in a loss of resolution and an alternative pattern of relationships. In this, the suspension-feeding pachycormiforms are resolved as sister group to all other pachycormiforms, rather than being nested within the clade containing *Pachycormus*, *Saurostomus* and *Ohmdenia*, which now form a separate group that is sister to a clade containing *Euthynotus*, *Hypsocormus*, *Ohmdenia*, *Australopachycormus* and *Protosphyraena*.

My final chapter provides constraints on the timing of the extinction of giant suspension-feeding pachycormiforms, as well as the origin of modern giant suspension-feeding chondrichthyans, such as whale sharks, basking sharks and mobulid rays. This has an important bearing on hypotheses that link the presumed extinction of pachycormiforms at the Cretaceous-Paleogene boundary to the appearance of suspension-feeding chondrichthyans in the Paleogene. Based on the fossil records of these taxa, I hypothesize that the extinction

of suspension-feeding pachycormiforms at the Cretaceous-Paleogene boundary provided ecological opportunity for modern suspension-feeders to emerge in the Cenozoic. To test this, I use occurrence data from the fossil record of suspension-feeding chondrichthyan groups and suspension-feeding pachycormiforms to estimate Bayesian credible intervals for emergence (chondrichthyans) and extinction (pachycormiform) times beyond their observed ranges. I also apply a recovery function to account for preservation heterogeneity among fossil horizons. My results cannot reject the emergence of chondrichthyan groups in the Mesozoic except cetorhinids, which emerge in the Eocene. At the same time, I cannot reject the possibility of pachycormiform extinction occurring as late as the mid Eocene (Lutetian) for the extinction of pachycormiforms. Although this neither corroborates nor rejects my hypothesis, there are a number of Cretaceous suspension-feeding chondrichthyans that appear unrelated to modern lineages. This suggests that there was a Cretaceous radiation of giant suspension-feeders that disappeared as part of the faunal turnover of taxa at the Cretaceous-Paleogene boundary, which would corroborate previous hypotheses of an extinction and replacement pattern of giant bodied suspension-feeders at the end Cretaceous mass extinction. I suggest that the loss of pelagic foraminifera and decline of primary productivity in pelagic environments may be associated with the extinction of giant suspension-feeding taxa in the Cretaceous. Therefore, I identify some putative suspension-feeding chondrichthyans, such as *Archeomanta*, *Cretomanta* and *Pseudomegachasma*, that may form part of the faunal turnover of the Cretaceous along with pachycormiforms. These putative suspension-feeders could be studied using the methods applied in this thesis to build a clear picture of extinction patterns in Cretaceous taxa, and how this relates to the emergence estimates for modern giant chondrichthyan suspension-feeders. However, these

taxa are very poorly known in the fossil record, so any study into patterns of their extinction could only happen following the identification of more material attributable to them.

By re-describing valuable, but understudied, articulated pachycormiform fossils from both the predatory and suspension-feeding groups, I hope to provide an anatomical model with which to interpret other, more poorly preserved fossils. The identification of teleostean characters, such as a urohyal, may also help improve our understanding of when key teleost characters arose, and how other early taxa fit are placed on the teleost stem. Finally, my work on estimating the emergence of chondrichthyans in the light of pachycormiform extinction helps to place Mesozoic taxa (and their extinction) into the context of modern diversity, and provide clues as to how previous diversity and mass extinction events have influenced the composition of modern marine ecosystems.

Acknowledgements

Completing my PhD is one of the hardest things I will ever do, not least when I have jumped from a molecular-focussed background to a palaeontology-focussed PhD, and I couldn't have done it without the help and support of my supervisors, friends and family. I would first like to thank my supervisor, Matt Friedman. Despite being on the other side of the Atlantic, Matt has always managed to help guide me through the harder parts of my PhD and give me the time I needed when I asked for his support. He has helped me think about the questions of my PhD in new ways, and taught me what it takes to be an independent researcher. I am extremely grateful for the opportunity to be his student, and to learn so much from him.

I would also like to thank my other supervisor, Sam Giles, who was my UK-based supervisor once Matt moved to the States, and continued to support and supervise me from Birmingham throughout my final year. She helped to teach me so much about how to conduct my research, from the secrets to making Mimics and Blender work to how to communicate my work at conferences, and how to write well. It has been a privilege to work with both Matt and Sam over the last three years. Finally, I'd like to thank my third supervisor, Roger Benson, who stepped in at the start of my third year once Sam moved to Birmingham. His office was always open for a chat, and his searching questions always got me thinking about how to improve and direct my research. It goes without saying that without my supervisors, my PhD wouldn't be what it is today, but I cannot thank them enough for their patience, support and guidance that helped me get to this stage and accomplish so much.

I'd like to give a huge thank you to Zerina Johanson, who supervised me during my master's degree at the Natural History Museum. She has been a constant source of support and guidance, and somehow managed to read my work at the speed of light whenever I asked for her help. She has done more for my PhD than I can list, from finding fossils in the collections, to finding me books and papers in the endless maze of NHM libraries, to reading various forms of my thesis and providing constructive feedback. I cannot thank her enough for her endless support throughout my master's and PhD, and I hope she knows how much I appreciate everything she did for me.

On a similar note, my next thanks go to Jeff Liston, who has been ready to help whenever I get in touch. He's been great company at conferences to chat about my work, and he has been there to support me during the various milestones of my PhD, including presenting my first posters and talks at conferences, and getting my first paper published. His knowledge of pachycormiforms, and his publications on them, have been integral to my PhD and I have hugely appreciated the time he's given to mentoring me throughout it.

Additionally, my PhD would not have been possible without access to museums, collections and facilities such as μCT scanners. Emma Bernard gave me access to the Natural History Museum fish collections; Farah Ahmed and Amin Garbout gave me access to the μCT scanner in the NHM Image and Analysis Centre; Henry Taylor took incredibly detailed photos of *Martillichthys* in the NHM Photography Studio and Picture Library; and Ben Moon μCT scanned various *Pachycormus* specimens at Bristol University (as well as providing endlessly helpful answers to any and all questions I had). I'd also like to thank

Alessio Capobianco for his help and guidance when interpreting his R script for my final project.

During the day to day of my PhD, my friends at the Earth Sciences department (and beyond) have kept me going when things got tough. My office mates: Sophie Gill, Dan Spencer, Sascha Holland, Lucy Kissick and Sam Eggins were always ready for a tea break (or perhaps the occasional cheese board) whenever I needed it, and respected my need to sometimes have lunch "al desko". Outside my office, Ellen Cliff, Ricky Sengupta, Clancy Zhi Jian and Gwen Antell were always ready with yet more tea and a sympathetic ear when I needed their time. The palaeo cohort from previous years: Mimi Harrison, Gemma Benevento, Harrie Drage, Serjoscha Evers and Dave Ford provided endless practical advice and resources to keep my PhD moving when it felt like I was going to run out of steam. In particular, Neil Brocklehurst managed to debug my code when I faced error messages that I just couldn't fix, and gave time to talk to me about my work when I reached a dead end.

Outside of my PhD, I want to thank my wonderful boyfriend Josh, who has been eternally patient, understanding and supportive, even when I was stressed or working ridiculous hours to get my work done. His support, and the support of his wonderful family, has been invaluable and I can't thank any of them enough for their kindness, generosity and encouragement throughout my PhD. Josh has been there throughout the best and worst times of my PhD, and I appreciate it immensely. Thank you.

Finally, but most importantly, I'd like to thank my fantastic and hugely supportive parents, my brother James, and my grandparents. They have supported my ambitions no matter what, and have been in my corner throughout everything that's happened during my education and career so far. They have given me everything they could, and more, to make sure I could keep pursuing my ambitions, and have been ready to help me however or whenever they could. I wouldn't be here without them, and I wouldn't be the person I am now if it wasn't for their love, guidance and support. I can't put into words how much I appreciate everything they do.

Anatomical conventions

When referring to skull roofing bones throughout this thesis, I use conventional actinopterygian terminology to facilitate comparison with other descriptions (see Gardiner & Schaeffer 1989 and Gardiner *et al.* 2005 for discussion of homology between actinopterygian and sarcopterygian skull bones).

List of Abbreviations

Anatomy

A.C.Pr Anterior coracoid process

A.Chy Anterior ceratohyal

a.gr Aortic groove

A.Pr Anterior process

Ad.F Adductor fossa

AH.A.F Afferent hyoid artery foramen

AH.A.G Afferent hyoid artery groove

ainp I Articulation site for pharyngobranchial I

Ang Angular

Ant Antorbital

Art Articular

asp Ascending processes

asr Articulation site for radials

b.fs Basal fissure

Bb Basibranchial

Bb.P Basibranchial toothplate

Bc Braincase

Bf Bifurcation

Boc Basioccipital

Bs Base

Bsr Branchiostegal rays

C.T.P Coronoid toothplate

Cb Ceratobranchial

Cl Cleithrum

Clv Clavicle

Cor Coronoid

Cor.F	Coronoid fang
Cor.Pr	Coronoid process
Cor.T	Coronoid teeth
Crr	Coracoid
D.Sco	Dorsal sclerotic ossicle
Dent	Dentary
dmc	Dorsal muscle canal
Dmp	Dermopalatine
Dmp.T	Dermopalatine teeth
dmr	Dorsal median ridge
Dpt	Dermopterotic
Dsp	Dermosphenotic
Eb	Epibranchial
Ectp	Ectopterygoid
Entp	Entopterygoid
Eoc	Exoccipital
epl	Ethmopalatine ligament attachment site
fdn	Foramen for diagonal nerve
fica	Carotid artery foramen
Fim	Fimbriations
Fm	Foramen magnum
FN.F	Hyomandibular branch of the facial nerve foramen
FN.Gr	Facial nerve groove
foca	Foramen for occipital artery
focn	Foramen for occipital nerve
fpal	Foramen for the palatine nerves
fpsa	Facet for pseudobranchial arteries
Fr	Frontal
Fr.Gp	Frontal gap
FRs	Fin rays

fs.X	Foramen for subsidiary branch of vagus nerve
Gl.F	Glenoid fossa
gpal	Grooves for the palatine nerves
grao	Groove for the dorsal aorta
Gul	Gular
H.Fa	Hyoid facet
Hb	Hypobranchial
Hhy	Hypohyal
Hhy.R	Hypohyal ridge
Hyo	Hyomandibula
Hyo.O.P	Hyomandibular opercular process
Ic	Intercalar
Ihy	Interhyal
II–V	Radials II–V
Iop	Interoperculum
Ior	Infraorbital
jc	jugular canal
L.Eth	Lateral ethmoid
Mand	Mandible
MCor	Mesocoracoid arch
Mpt	Metapterygoid
MQ.J	Mandibular-quadrate joint
MSC	Mandibular sensory canal
Mtg	Metapterygium
Mtgo	Metapterygium ossification
Mx	Maxilla
mx.n	Maxillary nerve foramen
Mx.T	Maxillary teeth
myo	Myodome
N	Nasal

Nar	Naris
ncg	Notochordal groove
ncp	Notochordal pit
Obsp	Orbitosphenoid
oc.f	Otoccipital fissure
Op	Operculum
Opso	Opisthotic
Ospt	Orbital septum
Ot.R	Otic region
P.C.Pr	Posterior coracoid process
P.Chy	Posterior ceratohyal
P.Cl	Postcleithrum
P.F	Pectoral fin
P.Op.Pr	Postorbital process
P.Pr	Posterior process
P.Tmp	Post-temporal
Par	Parietal
Part	Prearticular
Pb	Pharyngobranchials
Pmx	Premaxilla
Pmx.T	Premaxillary teeth
Pop	Preoperculum
Pr	Projections
Pro	Prootic
Psp	Parasphenoid
Ptg	Propterygium
Pto	Pterotic
Quad	Quadrate
R	Ridge
R.Fa	Radial facet

Rad	Radials
Rde	Rostrodermethmoid
Rde.T	Rostrodermethmoid teeth
Rks	Rakers
rscm	Attachment site for subcelaphic muscles
S.C	Sensory canal
S.Cl	Supracleithrum
S.O	Serrated appendage
S.R	Skull roofing bones
Sang	Surangular
Scc	Scapulocoracoid
Sco	Sclerotic ossicle
Scp	Scapula
Slk	Stalk
smc	Median crest
Smx	Supramaxilla
Sop	Suboperculum
Sop.Pr	Subopercular process
Sor	Suborbital
Sph	Sphenotic
Sq	Squamation
Su.C	Supraorbital canal
Sym	Symplectic
T.P	Thickened portion
T.R	Thickened ridge
Uro	Urohyal
v.fn	Vestibular fontanelle
V.Sco	Ventral sclerotic ossicle
VII.hym	Hyomandibular branch of the palatine nerve
VII.pal	Facial branch of the palatine nerve

vmc	Ventral muscle canal
Vmr	Vomer
X	Vagus nerve foramen

Institutions

AMHN	American Museum of Natural History, New York, USA
AUMP	Auburn University Museum of Paleontology, Alabama, USA
BRLSI	Bath Royal Literary and Scientific Institution, Bath, UK
BSPG	Bayerische Staatssammlung für Geologie und Paläontologie, München
CAMSM	Sedgwick Museum of Geology, University of Cambridge, UK
CM	Carnegie Museum, Pittsburg
DMNH	Delaware Museum of Natural History, Delaware, USA
FMNH	Field Museum of Natural History, Chicago, USA
FHSM	Sternberg Museum of Natural History, Fort Hays State University, Kansas, USA
GLAHM	Hunterian Museum, University of Glasgow, Scotland, UK
GPIT	Institut für Geowissenschaften, Eberhard Karls Universität Tübingen, Tübingen, Germany
KUVP	University of Kansas Museum of Natural History, Lawrence, Kansas, USA
I	Museo de Arqueologia, Antofagasta, Chile
IRSNB	Institut royal des Sciences naturelles de Belgique, Brussels, Belgium
IAA	Instituto Antártico Argentino, Argentina
JM.SOS	Jura Museum, Eichhstätt, Germany
LACM	Los Angeles County Museum of Natural History, Los Angeles, California, USA
LEICT	Museum and Art Gallery, Leicester, UK
LEIUG	University of Leicester Department of Geology, UK
MB	Institut und Museum für Geologie und Paläontologie, Museum für Naturkunde, Berlin
MCZ	Museum of Comparative Zoology, Harvard University, Massachusetts, USA

MLP	Museo de La Plata, División Paleontología Vertebrados, La Plata, Buenos Aires, Argentina
MOZ	Museo Provincial Dr. Prof. Juan Augusto Olsacher, Argentina
MMNS	Mississippi Museum of Natural Science, Jackson, Mississippi, USA
MNHN	Muséum National d'Histoire Naturelle, Paris, France
NHMUK	Natural History Museum, London (formerly BMNH)
NSM	National Museum of Science and Nature, Tsukuba, Ibaraki, Tokyo, Japan
NJSM	New Jersey State Museum, Trenton, New Jersey, USA
OUMNH	Oxford University Museum of Natural History, UK
PETMG	Peterborough Museum and Art Gallery, Peterborough, UK
PHBW	Privatsammlung Harry Breitkreutz, Enger, Germany
PMM	Privatsammlung Matthias Metz, Bünde, Germany
QM	Queensland Museum, Brisbane, Australia
RMM	Red Mountain Museum, McWane Science Centre, Alabama, USA
ROM	Royal Ontario Museum, Toronto, Canada
SAM	South Australian Museum, Adelaide, Australia
SM	Senckenberg Museum, Frankfurt, Germany
SMU	Schuler Museum of Paleontology, Southern Methodist University, Texas, USA
SDSM	Museum of Geology, South Dakota School of Mines & Technology, South Dakota, USA
SMNK	Staatliche Museum für Naturkunde Karlsruhe, Germany
SMNH	Swedish Museum Natural History, Stockholm, Sweden
T	Teylers Museum, Haarlem, Netherlands
UAM	Vertebrate Paleontology Collection, Alabama Museum of Natural History, Alabama, USA
UCM	University of Colorado Museum, Colorado, USA
UCMP	University of California Museum of Paleontology, Berkeley, California, USA
UNSM	University of Nebraska State Museum, Nebraska, USA
WMfN	Westphalisches Museum für Naturkunde, Münster, Germany

Contents

Declaration i

Abstract iii

Extended Abstract v

Acknowledgements xi

Anatomical conventions xv

List of Abbreviations xvii

1. Introduction **1**

1.1. Actinopterygii and Teleostei 1

1.2. Teleost monophyly 6

1.3. Patterson's work on the teleost stem 11

1.4. The sister group to teleosts 12

1.5. Pachycormiformes 15

1.6. Pachycormiform interrelationships 22

1.6.1. The history of Pachycormiformes 22

1.6.2. Current understanding of pachycormiform interrelationships 31

1.6.3. Evolutionary trends of the 'protosphyraenid' clade 33

1.6.4. Evolutionary trends of the 'suspension-feeding' clade 35

1.6.5. Uncertainties surrounding pachycormiform relationships 36

1.7. Pachycormiform ecology 42

1.7.1. Predatory pachycormiforms 43

1.7.2. Ohmdenia 44

1.7.3. Edentulous pachycormiforms *44*

1.8. Mesozoic marine ecosystems 47

1.9. Outstanding questions 51

2. Cranial osteology of *Martillichthys renwickae* with comments on the evolution and ecology of edentulous pachycormiforms 59

2.1. Abstract 59

2.2. Introduction 60

2.3. Materials and methods 63

2.3.1. Materials *63*

2.3.2. Methods *66*

2.4. Systematic palaeontology 66

2.5. Morphological description 68

2.5.1. Skull roof *70*

2.5.2. Braincase, parasphenoid, and associated bones *73*

2.5.3. Upper jaw *76*

2.5.4. Mandible *78*

2.5.5. Gill skeleton *81*

2.5.6. Hyoid arch and palate *85*

2.5.7. Cheek, circumorbital bones and sclerotic ossicles *88*

2.5.8. Operculogular series *89*

2.6. Discussion 91

2.6.1. Revisions and additions to previous descriptions *91*

2.6.2. Phylogenetic placement of Martillichthys *98*

2.6.3. Implications for edentulous pachycormiform evolution and ecology 106

2.7. Conclusions 110

3. Cranial osteology of *Pachycormus*, relationships and divergence times among pachycormiforms 113

3.1. Abstract 113

3.2. Introduction 114

3.3. Methods 120

3.3.1. Materials 120

3.3.2. X-ray computed tomography scanning 122

3.4. Systematic palaeontology 123

3.5. Morphological description 125

3.5.1. General observations 125

3.5.2. External dermal skeleton 126

3.5.3. Braincase and parasphenoid 126

3.5.4. Upper jaw 133

3.5.5. Mandible 135

3.5.6. Palate 138

3.5.7. Sclerotic ossicle, circumorbital bones and cheek 141

3.5.8. Dorsal gill skeleton 143

3.5.9. Ventral gill skeleton 144

3.5.10. Hyoid arch 148

3.5.11. Operculogular series 150

3.5.12. Pectoral girdle 152

3.5.13. Previously unknown structure *158*

3.6. Phylogenetic analyses 159

3.6.1. Matrix construction and coding *159*

3.6.2. Pachycormiform-only matrix *162*

3.6.3. Phylogenetic analyses *163*

Maximum parsimony. 163

Bayesian analyses. 163

Stepping stone analysis. 165

3.7. Results 167

3.7.1. Phylogenetic analyses *167*

Maximum parsimony analysis. 167

Bayesian analysis. 172

Fossilized Birth-Death model analysis. 175

Stepping stone analysis. 177

3.8. Discussion 177

3.8.1. Revisions to past descriptions and comparisons to other taxa *177*

3.8.2. Characters diagnosing Pachycormus *as a pachycormiform* *192*

3.8.3. The monophyly of Orthocormus *and* Hypsocormus *192*

3.8.4. 'Protosphyraenid' vs. 'suspension-feeding' pachycormiforms *196*

3.8.5. Pachycormiform monophyly and the teleost stem *197*

3.8.6. The age of pachycormiforms *199*

3.8.7. Notes on pachycormiform ecology and phylogeny *204*

3.8.8. The monophyly of suspension-feeding pachycormiforms *207*

3.9. Conclusions 208

4. Constraining the timing of the emergence of the giant bodied suspension-feeding ecology in modern chondrichthyan lineages and the extinction of pachycormiforms 209

4.1. Abstract 209

4.2. Introduction 210

4.2.1. Problems with past interpretations 211

4.2.2. Testing emergence and extinction 213

4.3. Current estimates for extinction and emergence of suspension-feeding lineages ... 214

4.3.1. The fossil record of suspension-feeding pachycormiforms 214

4.3.2. The fossil record of suspension-feeding chondrichthyans 215

4.3.3. Other putative suspension-feeding chondrichthyans 217

4.4. Methods 219

4.4.1. Occurrence data 219

Chondrichthyans. 219

Pachycormiforms. 220

Ages of occurrence records. 220

4.4.2. Estimating extensions on observed ranges 221

4.4.3. Recovery function 223

4.4.4. Bayesian calculations 224

4.5. Results 226

4.5.1. Extinction of suspension-feeding pachycormiforms 226

4.5.2. Emergence of suspension-feeding chondrichthyans 228

4.6. Discussion 229

4.6.1. Extinction of suspension-feeding pachycormiforms 229

4.6.2. Emergence of suspension-feeding chondrichthyans 230

4.6.3. Comparisons to previous estimates 230

4.6.4. Placement of putative suspension-feeding taxa 236

4.6.5. Ecological drivers behind giant bodied suspension-feeder extinction and emergence 243

4.7. Conclusions 246

5. Conclusions and future study **249**

5.1. The morphology of *Martillichthys renwickae* and *Pachycormus macropterus* and implications for pachycormiforms 250

5.2. Pachycormiform interrelationships and divergence estimates, and their broader placement on the teleost stem 253

5.3. Patterns of extinction and emergence of giant bodied suspension-feeders around the K-Pg boundary 256

References 261

Appendix A 311

The known fossil record of pachycormiforms from relevant literature, with specimen numbers, localities and estimates ages given where available 311

Appendix B 334

μCT Scanning Parameters 334

Appendix C 335

μCT Scanning Parameters 335

Specimens analysed for composite taxa 336

Caturus sp. *336*

Euthynotus sp. *336*

Lepidotes sp. *337*

Protosphyraena sp. *337*

Pteronisculus sp. *338*

Character List 339

Character Matrix 357

Character Optimizations 363

PAUP analyses script* *363*

MrBayes analyses code blocks 364

Morphology-only Bayesian analyses *364*

Bayesian analysis including morphological and nuclear data *364*

Fossilized Birth-Death analysis *366*

Stepping stone analysis – Currently accepted relationships *368*

Stepping stone analysis – Alternative relationships hypothesis *369*

Appendix D 371

Occurrence records 371

Suspension-feeding pachycormiform occurrence records *371*

Suspension-feeding chondrichthyan occurrence records *383*

R scripts 390

Pachycormiform extinction *390*

Emergence estimates for suspension-feeding chondrichthyans *396*

Chapter 1

Introduction

Actinopterygii and Teleostei

Actinopterygii — colloquially known as the 'ray-finned fishes' — comprise over half of all extant vertebrate diversity (Nelson *et al.* 2016). The relationships of living taxa in the crown group (the clade united by the last common ancestor of all extant taxa) have been well established through numerous morphological and molecular studies. Current consensus suggests that Actinopterygii is composed of two clades: Cladistia (Polypteriformes: bichirs and ropefish), and Actinopteri, which is further divided into Chondrostei and Neopterygii. Both Cladistia and Chondrostei are freshwater groups of modest diversity, with around 14 species of Polypteriformes in Cladistia (Nelson *et al.* 2016), and 25 species of sturgeon and two species of paddlefish in Chondrostei (Grande & Bemis 1991). Current consensus now recognizes Holostei (comprising the Lepisosteiforms and Amiiformes, the living radiations of which are represented by Ginglymodi and Halecomorphi respectively: Grande 2010; Betancur-R *et al.* 2017), and Teleostei, comprising over 29,500 extant species (Nelson *et al.* 2016).

This hypothesis of neopterygian interrelationships is relatively new. Many earlier cladistic hypotheses supported the halecostome hypothesis of relationships (Teleostei+Halecomorphi to the exclusion of Ginglymodi: Patterson 1973, 1982; Gardiner 1984; Gardiner & Schaeffer 1989; Grande & Bemis 1998; Coates 1999). More recently, molecular and morphological studies have corroborated the holostean arrangement (Halecomorphi+Ginglymodi to the exclusion of Teleostei: Grande 2010; Near *et al.* 2012; Betancur-R *et al.* 2013; Broughton *et al.* 2013; Giles *et al.* 2017; López-Arbarello & Sferco 2018; Ravi & Venkatesh 2018).

Since its diagnosis by Müller (1845), even the name Teleostei has been under immense scrutiny and disagreement among researchers. Before this definition, Agassiz's (1833–1843) classification scheme placed fishes into one of four orders, depending on their scale morphology: Cycloidei (smooth scales), Ctenoidei (toothed scales), Ganoidei (ganoid scales) and Placoidei (pointed scales; Patterson 1977*a*). By contrast, Müller's definition of teleosts was based on a combination of shared traits from across multiple anatomical systems. Its purpose was to unite all fishes sharing "intermuscular bones [epineurals, epiplurals and epicentrals], no muscles on the basal arteria [ventral aorta], and two arterial valves in the cornus arteriosus" (Müller 1845). This classification united the groups Ctenoidei, most of Cycloidei, and some of Ganoidei (the rest of which are split across Holostei, Chondrostei and Actinopterygii more widely). Unfortunately, Müller's diagnosis emphasizes soft tissue traits that limit classification of fossil taxa that either lack these characters or, in case of intermuscular bones, are only found in exceptionally well-preserved specimens. Therefore, Müller and Agassiz concluded that teleosts emerged in the Cretaceous, with Jurassic genera referred to as holostean ganoids due to the enamel on their scales (Patterson 1977*a*).

There are several nomenclatural conventions for the teleost group, each of which have their own limitations or controversies. In traditional cladistics (Hennig 1966), taxa are ordered into monophyletic groups (clades) united by a common ancestor. Work by Jefferies (1979) and Ax (1984; 1985; 1987) established the term "crown" to refer to a clade containing the last common ancestor of all extant taxa plus all of its descendants, both living and fossil. They also use the term "stem" to refer to the paraphyletic group that contains all taxa that fall outside the crown, but are more closely related to the crown than any other living group. This forces a consideration of fossil taxa in the context of the living radiations (the crown) that descend from them, and intimately links the process of inferring relationships among fossils to understanding the sequence of character evolution leading to living clades. It also allows for the acknowledgement of the gradual acquisition of traits through common descent, and upholds the necessity for monophyly to distinguish clearly between groups when considering phylogenetic relationships. The crown group plus its associated stem is known as the total-group (Fig. 1.1).

Within teleosts, De Pinna (1996; Fig. 1.1B) coined a stem-based definition of Teleostei (following Patterson 1977*a*; Patterson & Rosen 1977; Fig. 1.1C; discussed below), that defines the group by the last common ancestor of the stem and includes the crown (i.e. the total-group; Fig. 1.1). However, the base of the teleost clade is poorly resolved due to a combination of uncertainty surrounding which characters should be used to unite teleosts to the exclusion of other groups, and a poor fossil record to map these characters among stem taxa, leading to a huge difference in the amount of detailed phylogenetic and morphological analysis that extant and extinct teleosts have received (De Pinna 1996; Arratia 2015). To

acknowledge this, De Pinna (1996) also suggested a term to refer directly to the crown (or Recent teleosts): Teleocephala, which includes elopomorphs, osteoglossomorphs, clupeocephalans, and euteleosts.

Other researchers, most notably Arratia (1999; 2001; 2004), reject the crown/stem definitions of teleosts, because of the instability of deep branches on the teleost stem, particularly concerning the earliest diverging member of the total-group. Furthermore, Arratia (1999) demonstrates that the putative sister taxon to teleosts, such as *Lepisosteus* and *Amia,* changes depending on the outgroups chosen, highlighting potential ambiguity at the base of the neopterygian tree (Fig. 1.2). Therefore, an apomorphy-based definition of Teleostei has persisted following the original definition by Müller (1945), which encompasses the crown group of teleosts, as well as a number of taxa along the stem that share some derived features of the living radiation but fall outside of it (Fig. 1.1D, E). This apomorphy-based definition was given by Arratia (1999: 323) as:

> "Teleostei is supported at the primitive level by one uniquely derived character (quadrate bearing an elongated posteroventral process) and numerous homoplasies (e.g. mobile premaxilla; articular bone fused with angular and retroarticular bones; neural spine of preural centrum 1 short or rudimentary; pectoral propterygium fused with first pectoral ray; dorsal processes of the bases of the innermost principal caudal rays of the upper lobe present; only ural neural arches modified as uroneurals; symplectic not articulating with lower jaw; posterior myodome extending in basioccipital; frontal bones distinctly broader posteriorly than anteriorly)."

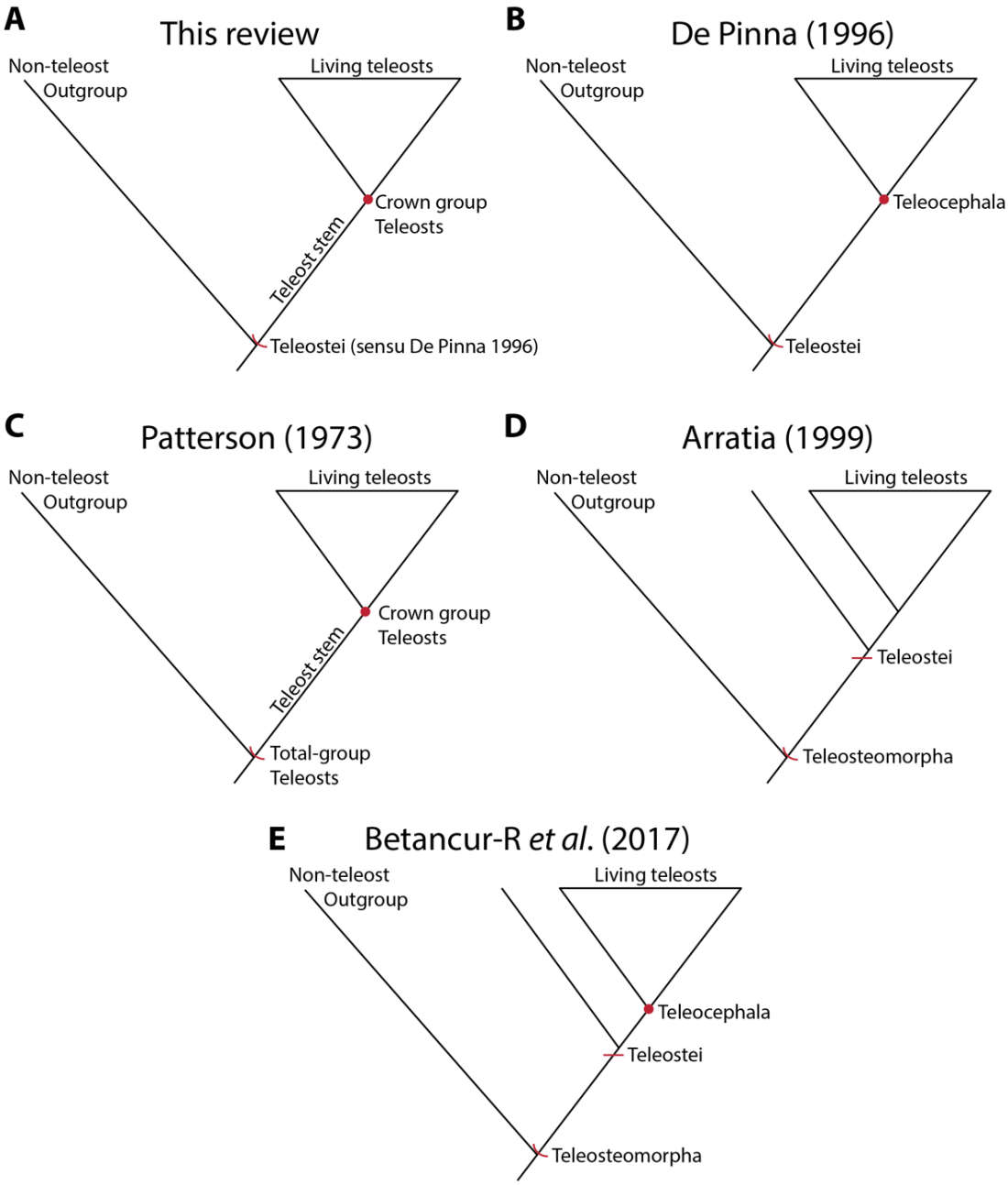

Figure 1.1 – The different naming conventions to refer to the crown, stem and apomorphy-based definitions of teleosts. A) The terminology used in this study. B) The stem-based definition of Teleostei and Teleocephala to refer to the crown group. C) The total-group teleosts (adapted by De Pinna 1996, as also adopted by Patterson & Rosen 1977). D) The apomorphy-based definition (adapted from Müller 1945) with the total-group referred to as Teleosteomorpha. E) The combined use of the apomorphy-based definitions of Teleostei, and the use of Teleosteomorpha and Teleocephala to refer to the stem and crown respectively (also used by Wiley & Johnson 2010).

As such, the most basally-branching teleost under the apomorphy-based definition is designated as *Dorsetichthys bechei* (formerly *Pholidophorus bechei*; Arratia 2013). In the same paper, Arratia (1999) coined the term Teleosteomorpha to refer to the teleost total-group, which includes both the 'true' apomorphy-based teleosts and more distant relatives as identified in other studies (such as aspidorhynchiforms and pachycormiforms; Patterson 1977*a*). The use of this apomorphy-based definition creates a clear view of what taxa are or are not part of the apomorphy-based group. However, depending on the characters used, these apomorphies are not always detectable in taxa that fall along the stem to delimit which taxa fall inside or outside the total-group. In this review, 'teleost' and 'Teleostei' is used to refer to the total-group (*sensu* De Pinna 1996), rather than using the apomorphy (Teleosteomorpha) or crown-based (Teleocephala) definitions (Fig. 1.1A).

Teleost monophyly

The most seminal works in teleost phylogenetics have tried to give a broader overview of classification within the group. Arthur Smith Woodward's *Catalogue of Fossil Fishes in the British Museum (Natural History)* (1889*a*–1901) and Greenwood *et al.* (1966) are arguably the foundations on which most of our understanding of teleost classification stands today, even if some of their specific findings are no longer widely accepted. Woodward (1889*a*–1901) meticulously identified and described thousands of fossil fishes from collections at the Natural History Museum of London (formerly part of the British Museum), while Greenwood *et al.* (1966) proposed the first modern composition of living teleosts using living taxa and a handful of fossils, but both authors avoided becoming embroiled in the debate of the distinction between holosteans and teleosts, and the fossils that distinguish them.

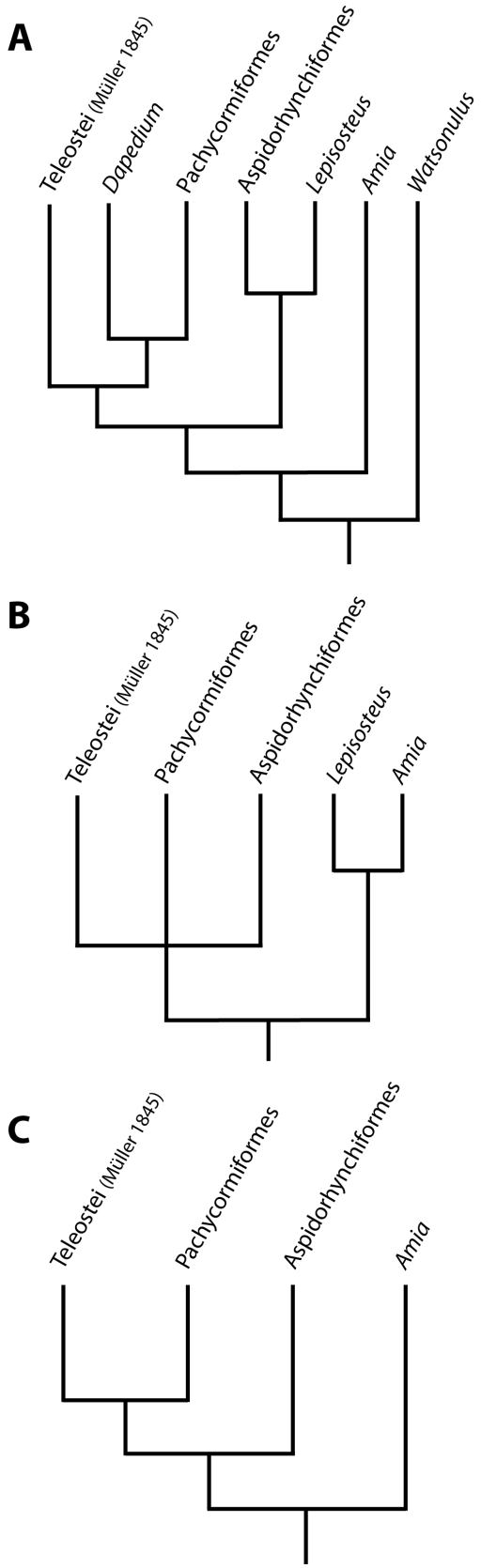

Figure 1.2 – The sister-group of teleosts when A) *Watsonulus*, B) *Amia* and *Lepisoteus* and C) *Amia* are the designated outgroups. In this, Teleostei is defined by the apomorphy-based criteria (*sensu* Müller 1845, Arratia 1999). Adapted from Arratia (1999; figs. 19, 21, 22).

During Woodward's (1889*a*–1901) work, one of the most accepted methods of teleost classification was Agassiz's scale-based orders. However, Woodward (1890) identified a taxon (*Aetholepis mirabilis*) possessing features of both Ganoidei (thick, rectangular ganoid scales anteriorly) and Cycloidei (thin, rounded scales posteriorly). He also noted that thick, double layered, ganoid scales were seen in Carboniferous fishes, but that light, single-layered scales were seen in extant fishes (something he termed "degeneration"; Woodward 1890; Forey 2016), which indicated an evolutionary trend towards lighter scales. In his third volume of the *Catalogue*, Woodward (1895*a*) identified similar scale variation in pholidophorids, which were initially considered to be holosteans. He describes pholidophorid scales to be extremely thin, with a rounded margin (similar to cycloid scales) but that they "for the most part" possess the peg-and-socket articulation of ganoid scales. He therefore redistributed taxa from Agassiz's original scale classification, using characters that become gradually more "specialized" and more similar to modern groups, such as vertebral ossification, and fin and jaw morphology. Woodward recognized the following major groups: Protospondyli (containing Agassiz's Mesozoic ganoids: semionotids, macrosemiids, pycnodontids, eugnathids, amiids, and pachycormids); Aetheospondyli (Aspidorhynchidae and Lepisosteidae, but "recognition of this group is a confession of ignorance"; Woodward 1895*a*: xvii); and Isospondyli (Pholidophoridae, Oligopleuridae and Leptolepidae; Woodward 1895*a*; Patterson 1977*a*; Forey 2016). Although Woodward (1889*a*–1901) did go some way to disentangle teleost and holostean characters in fossils, he eventually concluded (along with Regan 1923; Berg 1940; Bertin & Arambourg 1958; Lehman 1966), that fossil teleosts are inseparable from holosteans, or could only be separated on an arbitrary basis.

Following this, Greenwood *et al.*'s (1966) work provided structure by which to classify and arrange Recent (living) teleosts, which can be analysed using more than just morphological data, including biomechanics, behaviour and molecular data. This was done by identifying specializations that united groups (named "Divisions") of teleosts, which were considered to be independently derived from pholidophorid holosteans. These new classifications also dismantled "basal" teleosts (such as Isospondyli) into three major groups: Elopomorpha; Clupeomorpha; Osteoglossomorpha; and a "division III" which are the euteleosts (Greenwood *et al.* 1967; Patterson 1977*a*). Crucially, these taxa were grouped on the basis of parsimony — the argument that taxa are more likely to be closely related to taxa more similar to them, minimizing the number of evolutionary changes — rather than multiple traits emerging convergently. This reorganization of taxa into groups united by shared specializations, and the relationships of these extant taxa, provided a framework to help interpret the less complete fossil taxa, and Greenwood *et al.* (1966: 347) acknowledged this by writing: "classification of living teleosts must be understood before the fossil record can be interpreted".

As such, the prevailing theory for some time was that teleosts were, in fact, a polyphyletic group, but there was no real consensus on how this would explain the observed evidence. Teleost polyphyly was first suggested by Arambourg (1935*a, b*), who proposed that Clupidae and Chanidae had halecostome ancestors, after comparing the caudal skeletons. Woodward (1942) embraced this idea and suggested several origins of teleosts within holosteans, but some of his suggestions were based on mistaking analogous traits for homologues (e.g. the erroneous homology of the fringing fulcra of the first dorsal and anal rays of *Lepidotes* and

acanthopterygians, the latter of which are now known to lack this trait; Arratia 2015). De Saint-Seine (1949, 1956) outlined two lineages of teleosts with purported halecostome ancestry, while Nyeblin (1961, 1964) proposed three (Fig. 1.3). Arratia (2015: 1006) notes that it is remarkable how many polyphyly hypotheses suggested teleosts as descended from halecostome pholidophorids and points out that pholidophorids themselves are considered a polyphyletic group.

The suggestion that teleosts were descended solely from Jurassic pholidophorids was first proposed by Gross (1964; Arratia 2015). This was supported by Patterson (1967), who wanted to recognise teleostean success as one of the major vertebrate lineages, rivalling that of mammals and birds. He pointed out that teleosts should have a single character or character complex to clearly define them as a distinct taxonomic unit from basal pholidophorids (Patterson 1967: 95) and proposed that living teleosts are monophyletic on the basis of the caudal skeleton, which includes: perichordally ossified vertebral centra; the lower lobe of the caudal fin being supported by two hypurals primitively, and articulating with a single centrum; the ural neural arches being modified into elongate uroneurals; and the anterior uroneurals extending to the preural centra (Patterson 1968: 234).

Patterson later provided a set of characters that united the teleost total-group (Patterson 1973: 262). It is in the same work that he began to build a picture of how teleost relationships are understood today, by naming aspidorhynchiforms as early-diverging stem teleosts and placing pachycormiforms as the sister group to all other teleosts (Fig. 1.4; Patterson 1977*a*).

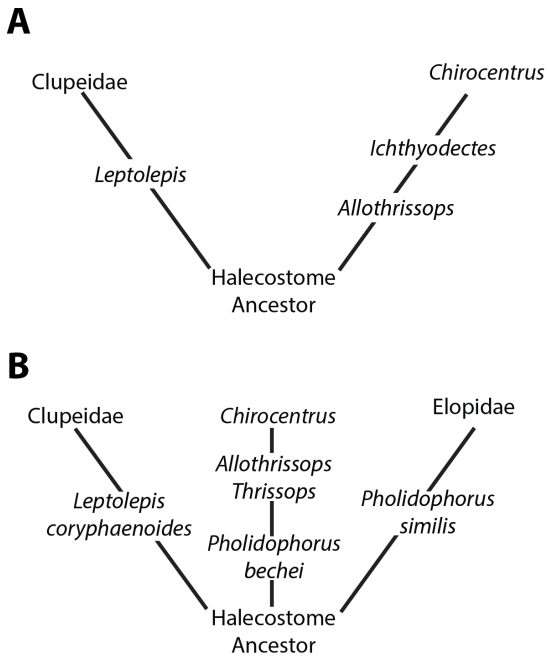

Figure 1.3 – Hypotheses of teleost polyphyly from A) de Saint-Seine (1949, 1956), B) Nyeblin (1961, 1964). Adapted from Arratia (2015; fig. 7).

Patterson's work on the teleost stem

If Teleostei is defined by only apomorphy-based criteria (*sensu* Müller 1845; Arratia 1999), there is a substantial gap between Holostei and Teleostei with no clear framework to show how Teleostei gained the synapomorphies distinguishing them from holosteans. Patterson's (1977*a*; fig. 19) synapomorphy scheme closed that gap with the inclusion of aspidorhynchids and pachycormiforms.

One of the reasons Patterson was able to unravel complex questions surrounding the teleost stem was the recognition of teleostean characters identified by Woodward (1890) in pholidophorids. Pholidophorids had originally been accepted to be halecomorphs because of their ganoid scales, until Woodward (1890) noted that pholidophorids possessed a combination of ganoid and cycloid scales (outlined above) that support their placement

within Isospondyli (and later, teleosts; Patterson 1977*a*). Despite this discovery, most discord still centred around how to draw the line between teleosts and halecomorphs, but the hypothesis of a single pholidophorid origin of teleosts was gaining traction (Gross 1964). This was picked up by Patterson (1973; 1975; 1977*a*; Patterson & Rosen 1977) who placed a handful of pholidophorids in paraphyletic group along the teleost stem (including *Dorsetichthys bechei*, *Pholidophorus higginsi*, *Siemensichthys macrocephalus*, and *P. dorsetensis*; Fig. 1.4) following the construction of a synapomorphy scheme of base to crown teleost characters. While this did transform Pholidophoridae into a grade, this synapomorphy scheme outlined a clear path from stem teleosts to the crown via pachycormiforms, aspidorhynchiforms, and pholidophorids (Patterson 1977*a*; fig. 19).

The sister group to teleosts

Generally, the living sister group to Teleostei has either been resolved as *Amia* (Westoll 1944; Gardiner 1960, 1963; Jollie 1962; Schultze & Wiley 1984), or a clade containing *Amia* and *Lepisosteus* (Nelson 1969; Jessen 1972; Jollie 1984). While both of these scenarios have been supported on the basis of morphological similarities, the latter was also supported by molecular data (Normark *et al.* 1991; Lê *et al.* 1993). Patterson (1973) also tested the placement of *Lepisosteus* as sister group to teleosts, but admitted that this was not a widely hypothesized pattern of relationships at the time, and named *Amia* the sister taxon to Teleostei (supporting Halecostomi over Holostei). However, Olsen (1984) and Olsen and McCune (1991) returned to the *Lepisosteus* sister group hypothesis, although the resolution for these relationships was lost when character polarity was not determined *a priori*.

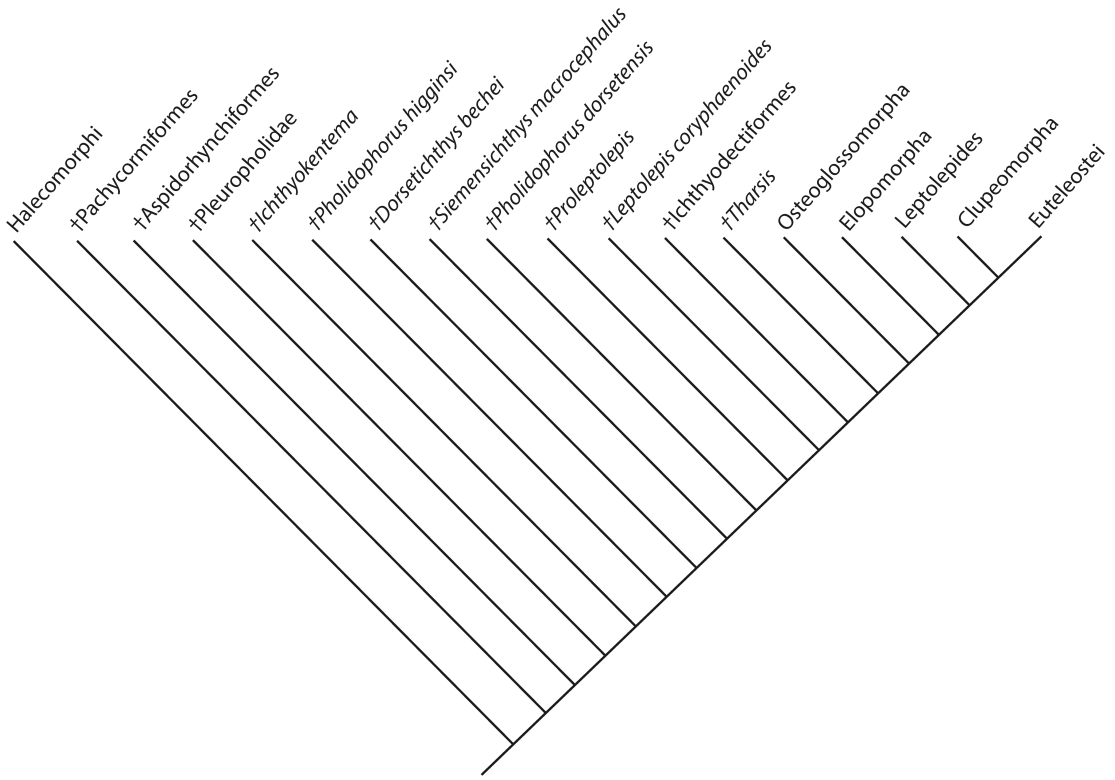

Figure 1.4 – The total-group of teleosts as proposed by Patterson (1977*a*), designating Pachycormiformes as the sister-group to all other teleosts. Adapted from Patterson (1977*a*; fig. 19).

Some of the most influential work regarding the distinction between teleosts and holosteans was by Patterson (1973, 1977*a*), who focussed on delimiting groups by their synapomorphies, rather than grouping them by their symplesiomorphies. Through this approach, Patterson (1973) outlined five characters uniting the teleost total-group (Fig. 1.4) to the exclusion of halecomorphs: (1) ural neural arches modified as uroneurals; (2) small, mobile premaxilla lying lateral to the rostral; (3) internal carotid foramen enclosed in the parasphenoid; (4) pectoral propterygium fused with the first pectoral fin-ray; (5a) seven epurals. He also outlined the synapomorphy scheme that mapped the evolution of modern teleosts from the stem to the crown, starting with pachycormiforms — previously considered halecostomes (Gardiner 1960) — as the earliest diverging group (Patterson 1977*a*; fig. 19; Fig. 1.2).

However, Patterson's (1973, 1977*a*) work was only one of a series to suggest candidates for the teleost stem. Arratia (1999, 2001, 2004) identified pachycormiforms and aspidorhynchids as the sister group to teleosts. On the basis of morphological evidence, other candidates included pycnodonts (Nursall 1996) and a clade containing pycnodonts and *Dapedium* (Gardiner *et al.* 1996; Arratia 1999); dapediids were previously considered incertae sedis between halecomorphs and teleosts. Arratia (1999, 2001, 2004) concluded that morphological evidence of living taxa generally supports an *Amia* sister group, morphological evidence including fossil taxa generally favour a *Lepisosteus* sister group, and molecular evidence supports a holostean (*Lepisosteus* and *Amia*) sister group. She also notes that changing the outgroup taxa in morphological analyses of living and fossil taxa results in an unresolved sister group.

This was, in part, rectified in 2010, when work by Grande (2010; and Grande & Bemis 1998; following Huxley 1860) resurrected Holostei as a group to contain Ginglymodi and Halecomorphi, thereby placing *Amia* and *Lepisosteus* in the same clade. This is a departure from the original definition of Holostei (Müller 1844), but supports the definition suggested by Huxley (1860) because it includes amiids but excludes polypterids. Grande (2010) justifies this by highlighting that the monophyly of Holostei is supported by both morphological and molecular data (Normack *et al.* 1991; Lê *et al.* 1993; also noted by Arratia 2001: 770). The characters Grande (2010; node N; fig. 547) find to support Holostei are:

> "the anterior end of the snout is a simple tube with no internasal lamella (ch. 5); an anterior arm of the antorbital bearing a tubular canal (ch. 12); two vertebral centra fused into condyle during early ontogeny (ch. 27); presence of a pterotic (ch. 29);

presence of paired vomers (ch. 37); mandibular coronoid process composed of more than one bone (ch. 51); presence of a supraangular (ch. 53); neural spines of caudal region both median and paired (ch. 85); branching in all principal rays of the caudal fin (ch. 87); presence of fringing fulcra on the caudal fin (ch. 90); anterior and posterior "clavicle elements" (ch. 96); and four hypobranchials present (ch. 99)."

He also identified several characters of more questionable support (Grande 2010; fig. 547): premaxilla fixed to the braincase (ch. 6); anterior portion of the premaxilla lining the nasal pit and pierced by the olfactory nerve (ch. 8); presence of a small, dermal component of the sphenotic (ch. 23).

By establishing strong morphological and molecular support for holosteans, and their placement as the sister group to teleosts within Neopterygii (as corroborated by subsequent studies: Near *et al.* 2012; Betancur-R *et al.* 2013; Broughton *et al.* 2013; Giles *et al.* 2017; López-Arbarello & Sferco 2018; Ravi & Venkatesh 2018), taxa can be arranged more clearly along the teleost stem. Regarding the teleost total-group, Patterson's (1977*a*) organisation of taxa along the stem is still highly influential, with recent morphological studies such as Arratia (2017) and López-Arbarello & Sferco (2018) resolving a clade that contains aspidorhynchids and pachycormiforms as the sister group to all other teleosts.

Pachycormiformes

The group currently accepted as one of the earliest diverging groups of stem teleosts are the Pachycormiformes. Pachycormiforms are known from the Toarcian (Middle Jurassic) to the Maastrichtian (Late Cretaceous; Cione *et al.* 2018), and have been reported from exclusively

marine sedimentary deposits in Europe, the Americas, and Antarctica (Woodward 1895*b*; Stewart 1988; Kear 2007; Friedman *et al.* 2010; Gouiric-Cavalli 2013; Gouiric-Cavalli & Cione 2015; Wretman *et al.* 2016; Gouiric-Cavalli 2017; Cione *et al.* 2018; Gouiric-Cavalli *et al.* 2019). Please see the Appendix for a list of known pachycormiform fossils recorded in relevant literature (Appendix A), which is restricted to genera accepted in this thesis as pachycormiforms (but see Delsate 1999; Gouiric-Cavalli & Cione 2015, for other putative but understudied candidate pachycormiforms). Furthermore, a number of specimens are preserved in three dimensions, allowing for characters of skeletal morphology to be viewed and recorded *in situ* in a way that flattened or disarticulated fossils do not. Crucially, these three-dimensional fossils allow for a more direct and detailed comparison to extant taxa, providing much needed structural or positional context that would otherwise have been lost.

As well as an abundant fossil record, pachycormiforms are notable for their substantial ecomorphological disparity: from tuna-like predators to giant bodied suspension-feeders (Mainwaring 1978; Lambers 1992; Liston 2006, 2008*a*; Friedman *et al.* 2010; Friedman 2012*a*; Wretman *et al.* 2016). The latter group is particularly intriguing as they may represent pioneers of the giant bodied suspension-feeding ecology that has since disappeared from teleosts and is now only represented in chondrichthyans (such as the whale shark and basking shark; *Rhincodon typus* and *Cetorhinus maximus* respectively) and mysticete whales (such as the blue whale, *Balaeonptera musculus*). Despite such diversity and their hypothesized phylogenetic placement on the teleost stem (discussed below), very little is known about their morphology beyond a handful of studies (Patterson 1975; Mainwaring 1978; Lambers 1992; Friedman *et al.* 2010; Friedman 2012*a*; Wretman *et al.* 2016).

Systematics of pachycormiforms

The first pachycormiform specimens – from the Toarcian (Early Jurassic) deposits of Beaune, Côte-d'Or (Burgundy, France) – were illustrated by D'Argenville (1755) and Faujas De Saint-Fond (1805). Following these illustrations, the first description was by Blainville (1818) who considered them to be similar to *Elops*, and so named the holotype *Elops macropterus*. However, following a re-examination and description of the holotype, Agassiz (1833–1843) reassigned *Elops macropterus* to the new genus *Pachycormus*, but they were still considered to be part of the caturids (Woodward 1895*b*). By allying pachycormiforms with caturids — which were considered to be ancestral relatives of amiids (Woodward 1895*b*; Gardiner 1960, 1967) — they were considered members of the halecomorph clade, the hypothesized sister group to teleosts, rather than teleosts, as later proposed by Patterson (1977*a*)

After Agassiz' work, several more taxa were found and considered by researchers to be clearly closely related to *Pachycormus* and each other (e.g. *Euthynotus*; Wagner 1863; and *Prosauropsis*; Sauvage 1894). Woodward (1895*b*) united these genera in the newly formed family Pachycormidae, along with: *Sauropsis* (Agassiz 1832); *Protosphyraena* (Leidy 1857); *Asthenocormus* (Wagner 1863); *Hypsocormus* (Wagner 1860). He also tentatively included *Leedsichthys* (Woodward 1890), despite poor preservation of material assigned to that genus. In 1896, Woodward also included *Saurostomus* (Agassiz 1833), which he had previously dismissed as a junior synonym of *Pachycormus* (Woodward 1895*b*). Following this, three additional genera were assigned to Pachycormidae in the first half of the 20th Century: *Eugnathides* (Gregory 1923); *Orthocormus* (Weitzel 1930); and *Ohmdenia* (Hauff 1953*a*).

To account for the stark variation between the swordfish-like *Protosphyraena* and other pachycormiforms, *Protosphyraena* was placed within Protosphyraenidae by Berg (1937, 1940), a family defined by: a highly elongate snout; teeth housed in deep sockets; large, sickle-shaped pectoral fins, with unbranched and unjointed rays; and eight radials in the pectoral endoskeleton.

At the same time, Berg (1937, 1940) also erected the order Pachycormiformes to unite Protosphyraenidae and Pachycormidae together, supported by the following mix of derived features and some more general to neopterygians and teleosts: presence of a supraoccipital; presence of large pre-ethmoids; premaxillae separated by a mesethmoid that forms a prominent rostrum (now known as the rostrodermethmoid); presence of a large opisthotic pierced by the vagus nerve foramen; presence of an intercalar; unpaired parietals; presence of an orbitosphenoid; presence of a myodome; numerous branchiostegal rays; the lower caudal lobe supported by a single, expanded haemal arch; and vertebral centra formed of half rings, if present (Berg 1940: 414). Over time, and with the inclusion of newly described taxa such as *Australopachycormus* (Kear 2007) and *Orthocormus* (Weitzel 1930; Lambers 1988; Arratia & Schultze 2013), Pachycormidae has been accepted as the single family represented within Pachycormiformes. As such, Pachycormidae is considered co-extensive with Pachycormiformes.

Pachycormiforms as stem teleosts

The candidacy of pachycormiforms as sister group to teleosts has been proposed on the basis of morphological similarities to other teleosts (Patterson 1973, 1977*a*; Patterson & Rosen

1977; Lauder & Liem 1983; De Pinna 1996) and formal phylogenetic analyses (where they are recovered as sister taxa along with aspidorhynchids; Arratia 1999, 2001, 2004, 2017; López-Arbarello & Sferco 2018). The main problem highlighted within the cladistic analyses is that the placement of pachycormiforms changes depending on the outgroup used (e.g. Arratia 1999). For example, when *Watsonulus* is the outgroup, pachycormiforms (*Pachycormus* and *Hypsocormus*) form a clade with *Dapedium* (Arratia 1999; fig. 19), but when *Lepisosteus* and *Amia* are the outgroup, pachycormiforms (*Pachycormus* and *Hypsocormus*) fall in a polytomy with aspidorhynchids and other teleosts (Arratia 1999; fig. 21). Moreover, when only *Amia* is the outgroup, pachycormiforms are placed as the sister group in exclusion to other teleosts (including aspidorhynchids; Arratia 1999; fig. 22). However, the lack of a consistent sister group to teleosts as reported by Arratia (1999; 2001; 2004) could also be a consequence of outgroup selection, where relationships in the ingroup can depend on the character states of the chosen outgroup, because the outgroup character states are assumed to be primitive (Maddison *et al.* 1984). This can be rectified by using at least two outgroups that share the same primitive character state in order to polarise characters (the first doublet rule; Maddison *et al.* 1984), resulting in parsimony of the entire clade ("global parsimony"; Maddison *et al.* 1984: 103). Despite this, Arratia (1999; 2001; 2004) has suggested that this lack of consistency is a product of a poor understanding of the teleost total-group, most particularly the composition of the teleost stem. This has arguably exacerbated assumptions that some of these sister groups (particularly pachycormiforms) are mysterious and their fossil record is beyond comprehension (Liston 2006, 2010, 2015), rather than being treated systematically to understand the specimens available.

As a result of such limited investigation, the only well described skulls for most of the 20th Century were of *Pachycormus* (Woodward 1908*a*; Lehman 1949; Wenz 1967; Mainwaring 1978), *Hypsocormus* (Woodward 1908*a*), and *Euthynotus* (Wenz 1967), and the only well-described braincase was of *Pachycormus* (Lehman 1949; Mainwaring 1978; Rayner 1948; Patterson 1975). Additionally, the convention of grouping taxa by their primitive similarities rather than identifying their apomorphies meant that pachycormiforms were generally grouped amongst the halecostomes as amioids descended from caturids (Gardiner 1960) due to: presence of median neural spines, a maxilla with peg-like internal head, one supramaxilla, and an interopercular. However, all of the characters listed by Gardiner (1960) are general features of crown neopterygian rather than characters that distinguish pachycormiforms from other groups. Contrary to Patterson's (1973) conclusions, Wenz (1967) proposed that pachycormiforms are an isolated order descended from palaeoniscoids due to their lack of neopterygian characters (Wenz 1967; Patterson 1973: 262). Such characters included the absence of independent premaxillae and a mandibular coronoid process, while retaining a posteriorly inclined suspensorium and post-rostral element fused to the median rostrum. As with Gardiner (1960), the characters suggested by Wenz (1967) to support the relationships between pachycormiform and palaeoniscoids are based on the primitive similarities pachycormiforms share with their proposed relative (caturids or palaeoniscoids; Gardiner 1960; Wenz 1967), rather than the derived characters that they share with neopterygians and other teleosts.

Patterson (1973) rejected the hypothesis proposed by Wenz (1967) by pointing out that independent premaxillae are in fact present in both *Pachycormus* and *Hypsocormus*

(Woodward 1895*b*: pl. 11, figs. 3 & 5; Lehman 1949: pls. 5 & 6), and that no post-rostral is present, but instead that the rostral has fused with the paired, tooth-bearing homologues of the pholidophorid lateral dermethmoids (forming a rostrodermethmoid). As for the absent coronoid process, Patterson (1973) indicated that *Hypsocormus* and *Pachycormus* both have well-developed coronoid processes "of normal holostean and teleostean type" (Patterson 1973: 273). Patterson (1973) added that they display all but one of the neopterygian characters (it was not known if pachycormiforms have pharyngeal dentition; Patterson 1973: 262):

> "Body lobe of tail reduced so that outer principal rays of upper lobe of caudal fin are approximately equal in length to those of lower lobe. Fin-rays equal in number to their endoskeletal supports in dorsal and anal fins. Premaxilla with an internal (nasal) process lining the anterior part of the nasal pit. Vomer differentiated and moulded to underside of ethmoid region. Articular with a coronoid process. Suspensorium vertical or nearly so, preopercular with a narrow dorsal limb. Symplectic developed as an outgrowth of the hyomandibular cartilage. […] Clavicles lost or reduced to one or more plates overlying the postbranchial lamina of the cleithrum."

He goes further to demonstrate that pachycormiforms also possess many teleostean characters: a mobile premaxilla; a toothed median portion of the upper jaw (as in some 'pholidophorids') fused to the rostral (as in leptolepids and higher teleosts); a square-ended symplectic that sits on the medial surface of the quadrate; and uroneurals of a peculiar sort.

Patterson wrote that, while he acknowledged the similarities pachycormiforms share with halecostomes, they do not possess any of that putative clade, and so rejected Gardiner's (1960) hypothesis of a halecomorph identity for pachycormiforms. Therefore, Patterson (1973: 274) concluded that pachycormiforms are more closely related to teleosts than halecomorphs and are best regarded as the sister group to all other teleosts. This conclusion was corroborated by Patterson (1977*a*), Patterson and Rosen (1977), and later by Arratia (1999; 2001; 2004).

Pachycormiform interrelationships

The history of Pachycormiformes

The monophyly of pachycormiforms is 'undoubtable' according to Patterson (1973: 273), who characterized the group by: a median rostrum bearing teeth and containing the ethmoid commissure; large, 'scythe-like' pectoral fins; reduction or loss of the pelvic fins; a highly specialized caudal skeleton and fin; and reduction in segmentation of the fin rays. However, aside from a description of a braincase of *Pachycormus* by Patterson (1975; cited as "in press" in Patterson's 1973 paper), there were still only a handful of pachycormiform descriptions with which to elucidate the interrelationships within pachycormiforms when Patterson evaluated the characters supporting their monophyly (Patterson 1973).

The first detailed appraisal of pachycormiform interrelationships came with the PhD thesis of Mainwaring (1978). To increase the morphological characters available for this analysis, she provided a comprehensive description of the skull of *Pachycormus macropterus*, the type species, building on previous cranium descriptions by Rayner (1948), Lehman (1949), Wenz

(1967) and Patterson (1975). Mainwaring also provided a systematic review of the family following the descriptions by Woodward (1895*b*) and the species described since.

From this review, Mainwaring (1978: 98) redefined Pachycormidae as:

> "shape deeply fusiform to moderately elongate. Premaxillae small, mobile and separated in the mid-line by tooth-bearing lateral dermethmoids which are fused to the rostral. Rostrodermethmoid may or may not be produced anterior to the symphysis of the lower jaw. Nasals separated. Supraorbitals absent; dorsal margin of orbit formed by the dermosphenotic; posterior margin of orbit formed by at least nine rectangular infraorbitals, which meet the two large suborbitals posteriorly. Extrascapular absent; dermopterotic enlarged and containing the supra-temporal commissural sensory canal. Ossification of the notochordal sheath either absent or in the form of hemichordacentra. Pectoral fins scythe-like; pectoral propterygium fused with the first dermal fin ray; dermal fin rays branching only near their extreme ends. Pelvic fins reduced or absent. Caudal fin deeply forked; ural neural arches modified as uroneurals. Squamation of numerous, small, thin, rhombic scales."

Mainwaring hypothesized a series of relationships supported by 20 characters on a hand-drawn cladogram of the six genera considered to be pachycormiforms: *Sauropsis*, *Pachycormus*, *Saurostomus*, *Euthynotus*, *Hypsocormus* and *Protosphyraena*. Mainwaring argued that the monophyly of pachycormiforms is supported by six characters, whose combination is unique to pachycormiforms. Mainwaring's analysis of the wider placement of pachycormiforms disputed the conclusion of Patterson (1973; 1977*a*), that pachycormiforms are the sister group to all other teleosts, because they possess characters 1–7 of the teleost character series established by Patterson (1977*a*; fig. 19: 1, ural neural arches are modified

as uroneurals; 2, small, mobile premaxilla lying lateral to the rostral; 3, internal carotid foramen enclosed in the parasphenoid; 4, pectoral propterygium fused with the first pectoral fin-ray; 5b, six epurals; 6, a median tooth plate covering the basibranchials; 7, a quadratojugal fused with the quadrate as a postero-dorsal process). This contradicts the conclusions drawn by Patterson (1977*a*), who suggested that pachycormiforms only possess characters 1–5a. Based on the identification of these additional characters, Mainwaring (1978) placed pachycormiforms as sister group to *Ichthyokentema* plus all remaining teleosts, with Pleuropholidae and Aspidorhynchiformes forming successively distant clades deeper on the teleost stem.

The next in-depth appraisal of pachycormiform relationships came from the PhD thesis of Lambers (1992), who provided a re-description of *Asthenocormus titanius* and proposed a new pachycormiform genus, *Pseudoasthenocormus*, in the same work. He suggested that Pachycormidae contained nine genera: *Pachycormus*, *Saurostomus*, *Euthynotus*, *Hypsocormus*, *Sauropsis*, *Orthocormus*, *Pseudoasthenocormus*, *Asthenocormus*, and *Protosphyraena*. He also noted five 'problematic' genera due to their poor or incomplete preservation: *Ohmdenia*, which Lambers (1992) suggested is actually *Saurostomus*; *Prosauropsis* (Sauvage 1894), described as being very similar to *Sauropsis*; *Neopachycormus* (Taverne 1977; now recognized as a tselfatiiform: Taverne & Liston 2017), only known from the holotype, a pectoral fin, skull fragments and scales, but hypothesized to be the intermediary taxon between Pachycormidae and Protosphyraenidae (Taverne 1977); *Leedsichthys* (Woodward 1889*a*, *b*), which is highly incomplete but considered a pachycormiform by Martill (1988); and *Eugnathides* (Gregory 1923), whose description lacks

any distinct synapomorphies supporting its placement in pachycormiforms (Schaeffer & Patterson 1984; Lambers 1992).

Once the accepted taxa within pachycormiforms had been established, Lambers (1992) described the formal process for identifying taxa (using *Euthynotus*, *Saurostomus*, *Sauropsis*, *Hypsocormus*, *Pachycormus*, *Orthocormus*, and *Protosphyraena*) and the synapomorphies uniting them, along with an outline of their relationships (Lambers 1992; fig. 15). Unlike Mainwaring (1978), Lambers (1992) was able to run a formal parsimony analysis using the 20 characters provided by Mainwaring (1978). Lambers' (1992) results corroborated Mainwaring's hypothesis, with the only modification being Lambers (1988; 1992) placing the previously excluded taxon *Orthocormus* as the sister-taxon to *Protosphyraena* (Lambers 1992; fig. 23).

He also provided a revised definition of pachycormiforms identifying 15 synapomorphies of the group (Lambers 1992: 255):

> "anterior part of the skull roof formed by a median rostrodermethmoid; dentigerous anterodorsal border of the mouth formed by the rostrodermethmoid, nasals separated by rostrodermethmoid; supramaxilla posterodorsally to maxilla; lower jaw without elevated coronoid process; dorsal border of the lower jaw with an elevation opposite to the premaxilla; lower jaw articulating far behind the orbit; at least six infraorbitals behind the orbit; infraorbitals at the posteroventral corner of the orbit not expanded posteriorly, one infraorbital below the orbit; dermosphenotic forms dorsal border of the orbit; two large, plate-like, posteriorly expanded suborbitals; pectoral fin 'scythe-

like', fin rays of the pectoral fin only segmented distally; pectoral fin rays bifurcating asymmetrically in a y-fashion; uroneurals of a peculiar kind [from Patterson 1973]; hypural plate present; very small, rhombic scales".

Of the proposed definitions of pachycormiforms by Mainwaring (1978) and Lambers (1992), I believe the diagnosis by Lambers to be the most reliable due to its clear description of character states e.g. "nasals separated by the rostrodermethmoid" (Lambers 1992: 255) rather than "nasals separated" (Mainwaring 1978: 98). It should be noted that a small number of characters in Mainwaring's definition (and omitted by Lambers') account for variation seen within the family, such as the rostrodermethmoid forming anterior to the mandibular symphysis, as seen in *Protosphyraena*, *Orthocormus* and *Hypsocormus*. However, such variation is only necessary for distinguishing taxa *within* Pachycormidae, so its omission in Lambers (1992) is not surprising. Nonetheless, there are some characters in Mainwaring's diagnosis that are used commonly in identifying pachycormiforms that have been excluded from Lambers' diagnosis. These include: the reduction/absence of pelvic fins; the absence of supraorbitals; the absence of extrascapulars; the formation of the posterior margin of the orbit by at least nine infraorbitals (reduced to at least six in Lambers 1992); and the separation of the mobile premaxillae by the rostrodermethmoid (defined by Lambers' "dentigerous anterodorsal border of the mouth formed by the rostrodermethmoid"). Another character of note in Mainwaring (1978) is the fusion of the pectoral propterygium to the first pectoral fin ray, but this has since been identified as erroneous because the propterygium of pachycormids is closely bound to the first pectoral ray, but not fused (Arratia & Schultze 2013). Although Mainwaring's (1978) diagnosis has many merits for identifying the shared

characters of pachycormiforms for use in a phylogenetic analysis, Lambers' (1992) diagnosis represents a more refined synapomorphy scheme and an improvement in understanding what characters unite pachycormiforms and the variation between them.

Recent phylogenetic analyses into pachycormiform relationships (Friedman *et al.* 2010; Friedman 2012*a*), using Bayesian and Maximum Parsimony methods, confirmed a number of traits that have been previously been identified as pachycormiforms synapomorphies: a median rostrodermethmoid separating the premaxillary bones (Woodward 1895*b*; Berg 1940; Wenz 1967; Mainwaring 1978; Lambers 1988, 1992; Kear 2007); dermosphenotic forms dorsal margin of orbit (Mainwaring 1978; Lambers 1992); supraorbitals absent (Mainwaring 1978); more than six infraorbitals behind orbit (Lambers 1992); supramaxilla placed posterodorsal to maxilla (Lambers 1992); 'scythe-like' pectoral fins (Wenz 1967, Mainwaring 1978; Lambers 1988; 1992); and pectoral rays with y-type bifurcation (Lambers 1992); hypural plate (Wenz 1967; Patterson 1973; Lambers 1992).

The following characters were also identified to support the monophyly of pachycormiforms (Friedman *et al.* 2010; Friedman 2012*a*), but some of these are homoplastic among other neopterygians, or are poorly known in pachycormiforms: posterior margin of vagal foramen formed by outgrowths of intercalar (coded for 3/14 pachycormiforms; ch. 14, Friedman 2012*a*); anterior myodome absent (only coded for *Pachycormus* and *Orthocormus* sp.; ch. 10, Friedman *et al.* 2010); dorsal and ventral caudal fin ray bases symmetric (a teleost character; Lauder 1989; ch. 78, Friedman *et al.* 2010); pectoral radials with broad posterior radials and narrow anterior stalk (paddle-shaped; ch. 84; Friedman *et al.* 2010); pectoral fin rays without

segmentation (homoplastic within pachycormiforms; ch. 89, Friedman *et al.* 2010); pelvic fin placed anterior to midpoint between anal and pectoral fins (ch. 91, Friedman *et al.* 2010; ch. 118, Friedman 2012*a*).

A number of revisions have been suggested for the character states used in phylogenetic analyses of pachycormiforms. Some revisions were made in Friedman (2012*a*), which is based on the Friedman *et al.* (2010) matrix. For example, character 85 ("scythe-like pectoral fins with lepidotrichia only segmented distally (if segments present)") of Friedman *et al.* (2010 suppl.: 29) is a composite character, referring both to the shape of the pectoral fin and the pattern of lepidotrichial segmentation. This was amended in Friedman (2012*a*) where "scythe-like pectoral fins" is a single character (Friedman 2012*a* suppl.; ch. 113), while characters concerning fin segmentation focus on only the characteristic "Y"-shaped bifurcations of pachycormiforms (Friedman 2012*a* suppl.; chs. 115, 116).

The most thorough analysis of Friedman *et al.*'s (2010) characters come from Arratia and Schultze (2013), who suggested revisions to the coding of *Orthocormus* and pachycormiforms more broadly in the Friedman *et al.* (2010) analysis, most notably: "pachycormiforms should not be coded as having teleostean uroneurals (= modified ural neural arches) because these are preural elements" (Arratia & Schultze 2013: 108). They also indicate that the ossified centra (chordocentra) of some pachycormiforms (*Euthynotus*, *Pachycormus*, *Saurostomus*), as well as those of *Caturus*, *Dorsetichthys bechei* and *Watsonulus*, are not homologous with the ossified centra of other teleosts (autocentra), and so should not be coded as equivalent in a phylogenetic analysis. Another character suggested for revision is the fusion of the first

fin ray to the propterygium. Arratia and Schultze (2013) identify that this fusion is erroneously coded as present in *Pachycormus*, *Hypsocormus*, and *Protosphyraena* in Friedman *et al.* (2010 suppl.; ch. 83), and coded as unknown ("?") in *Elops hawaiiensis*, where fusion is present.

While the corrections suggested by Arratia and Schultze (2013) may not have a considerable bearing on the interrelationships recovered by Friedman *et al.* (2010) and Friedman (2012*a*), acknowledging these suggestions could help to provide a more robust hypothesis of pachycormiform relationships. It would acknowledge hypothesized differences in homology (e.g. the uroneurals, as stated above), without assuming phylogenetic relationships before testing them.

In addition, the distinctive 'scythe-like' pectoral fins often used to identify pachycormiforms has been criticized by Liston and Maltese (2016) as unrepresentative of the true diversity of pachycormiform fin shapes, but nonetheless used uncritically to characterize the long, slender pectoral fins of pachycormiforms. They illustrate that, while pachycormiform fins are distinctive, they are not just restricted to one shape, but have 'scythe' (seen in *Protosphyraena*), 'blade' (seen in *Bonnerichthys* and *Asthenocormus*) and 'sickle' (seen in *Saurostomus*) geometries. While it is clear that there are distinct fin geometries among pachycormiforms, it is unclear how distinctive this variation is compared to non-pachycormiform taxa as no comparative outgroups were used. It seems that the main criticism by Liston and Maltese (2016) is the use of the restrictive terminology "scythe-like" as a pachycormiform synapomorphy. Although "scythe-like" does imply homogenous fin

geometries, this argument makes very little practical difference in phylogenetic analyses to identify trends general in fin morphologies (as in the matrix by Friedman 2012*a*). Nonetheless, Liston and Maltese (2016) are right that this terminology encourages uncritical assumptions of fin morphologies, and this interspecific variation should be acknowledged to avoid inaccuracy. Therefore, I suggest this character should be replaced with "long and slender pectoral fins" rather than "scythe-like" to describe general fin geometries of pachycormiforms.

These authors (Arratia & Schultze 2013; Liston & Maltese 2016) acknowledged that areas of uncertainty or lack of coded characters in Friedman *et al.* (2010) stemmed from a lack of available morphological information, and that many of the characters apparently uniting pachycormiforms are actually unknown for most members of the group. The authors stress the dire need for more thorough analyses of what available material there is, using more contemporary methods, to make the most of what morphological information is available in order to guide us when faced with other poorly preserved specimens.

One such method that has grown in popularity recently is micro-computed tomography (μCT) scanning (Abel *et al.* 2012). Before this, the only methods to examine the internal anatomy of taxa generally involved removing the surrounding matrix from the preserved structures, either mechanically (mechanical preparation) or chemically (acid preparation), but this leaves many structures out of their anatomical context. A way around this involved preparing away thin sections (serial sectioning; Sollas & Sollas 1913; Croft 1950) of the fossil to reveal the internal structures *in situ*, from which drawings or photographs could be taken

(Kermack 1970). Unfortunately, all of these methods generally involve damaging or completely destroying the fossil, which is not practical if the fossil is particularly rare or well-preserved and should be kept intact for future study.

μCT scanning follows the same principle behind serial slicing by using X-rays to generate image slices through the fossil from different perspectives, allowing the fossil to be viewed from different axes. The advantage is that is it non-destructive, but still allows for the fossil to be viewed internally and externally. Virtual reconstructions also provide three-dimensional models of preserved bones that can be viewed either in isolation or in relation to others from any angle. This not only preserves the original fossil, but provides a digital record for future study that can be revisited and re-evaluated if necessary. Since the most notable descriptions of pachycormiforms have been through mechanical preparation and external analysis, the use of μCT scanning could greatly supplement previous descriptions by shedding light on how internal structures articulated with external ones, and how they aided form and function.

Current understanding of pachycormiform interrelationships

Current consensus of pachycormiforms recognizes the following genera within it (Fig. 1.5): *Pachycormus*, *Euthynotus*, *Hypsocormus*, *Orthocormus*, *Protosphyraena*, *Saurostomus*, *Ohmdenia*, *Asthenocormus*, and *Leedsichthys*, with four additional genera added since Lambers (1992): *Martillichthys* (Liston 2006; 'Taxon 13'), *Australopachycormus* (Kear 2007); *Bonnerichthys* (Friedman *et al.* 2010); *Rhinconichthys* (Friedman *et al.* 2010). With the exception of *Australopachycormus*, these recently recognized taxa have joined

Asthenocormus and *Leedsichthys* in a clade now known as the "suspension-feeding pachycormiforms" (Friedman *et al.* 2010: 991; Wretman *et al.* 2016: e1206022-6).

The most recent phylogenetic studies (Friedman *et al.* 2010; Friedman 2012*a*; Wretman *et al.* 2016) have recovered two clades within pachycormiforms with *Euthynotus* as the sister taxon to these two clades, echoing the tree shape shown by Lambers (1988: 389; 1992; fig. 15). The first, named here the 'suspension-feeding' clade (while acknowledging at not all taxa in this clade are suspension-feeders), contains from base to tips: *Pachycormus*, *Saurostomus* and *Ohmdenia* and the giant suspension-feeding pachycormiforms: *Bonnerichthys*, *Rhinconichthys*, *Asthenocormus*, *Leedsichthys* and *Martillichthys*.

The second, named here the 'protosphyraenid' clade contains from base to tips: *Hypsocormus insignis*, *Hypsocormus macrodon*, *Hypsocormus tenuirostris*, and *Orthocormus* (represented at just the genus level in previous analyses), and the large, billfish-like predators ("the macrocarnivores": Wretman *et al.* 2016: e1206022-6) *Australopachycormus* and *Protosphyraena*. Each clade appears to be trending towards distinct ecologies, with the large teeth and pointed snouts (terminating anterior to the mandibular symphysis) of the 'protosphyraenid' clade pointing towards an ecology similar to that of extant billfishes (Juanes *et al.* 2002; Wretman *et al.* 2016). Conversely, the gradual reduction in dentition, increase in body size, and — in some — the evolution of long elaborated gill rakers in the 'suspension-feeding' clade mimics the body plan changes seen in mysticete whales from their predatory relatives (Friedman 2012*a*), with *Ohmdenia* acting as the intermediary taxon that bridges the two ecologies.

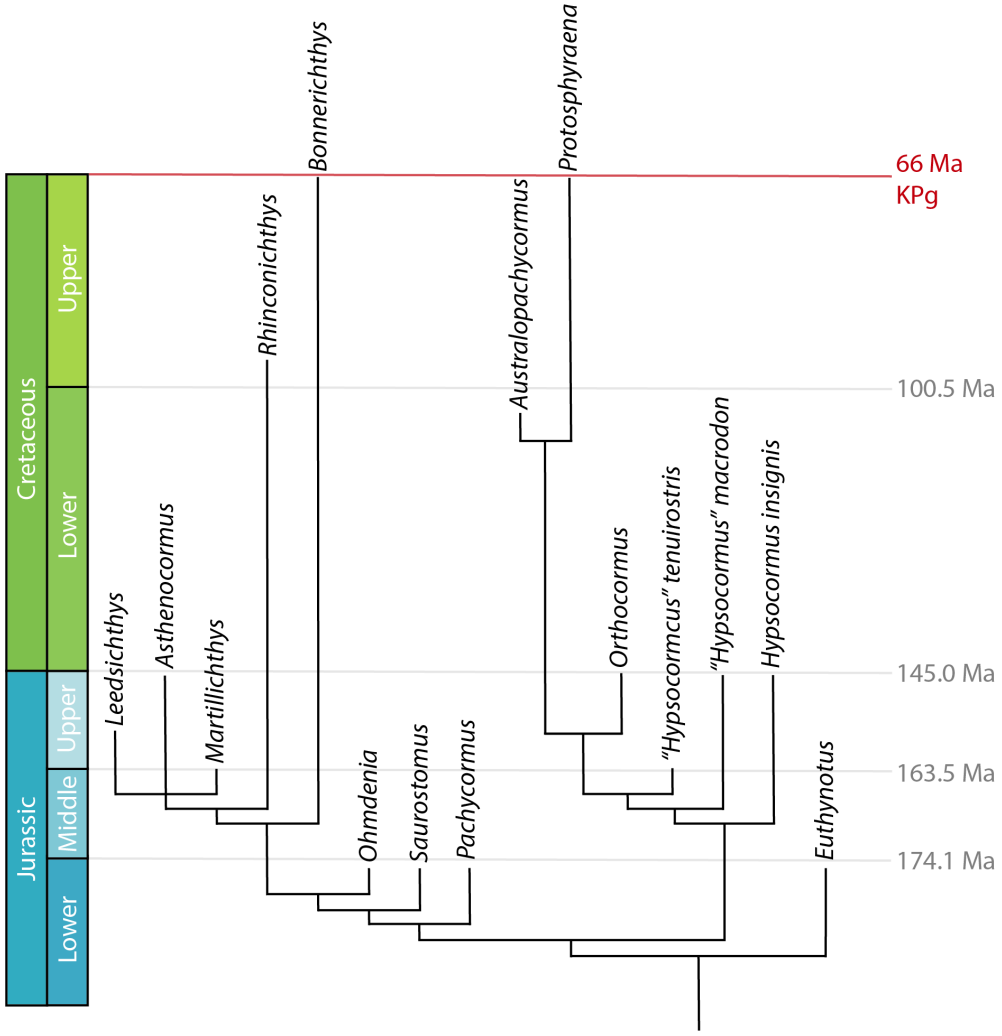

Figure 1.5 – Cladogram of the interrelationships of pachycormiforms from Maximum Parsimony and Bayesian analyses of morphological data and scaled to stratigraphic calibrations. Numbers on the right illustrate the ages of each geological boundary in million years (Ma). The red line denotes the end-Cretaceous mass extinction (KPg). Adapted from Friedman (2012; fig. 2a).

Evolutionary trends of the 'protosphyraenid' clade

For now, the most pressing issue is understanding how traits or ecologies — such as suspension-feeding — emerged and changed over time by improving what available evidence we have with more detailed descriptions of well-preserved specimens. The 'protosphyraenid' clade containing *Hypsocormus*, *Orthocormus*, *Australopachycormus* and *Protosphyraena* (Friedman *et al.* 2010; Friedman 2012*a*; Wretman *et al.* 2016) has received particularly poor

treatment during evaluation of pachycormiform relationships, mainly due to a lack of detailed study beyond a handful of recent studies and descriptions (Lambers 1988, 1992; Kear 2007; Arratia & Schultze 2013). There is only one described braincase, *Orthocormus* (incorrectly identified as *Hypsocormus* by Rayner 1948; Lambers 1992), and many descriptions come from flattened or disarticulated specimens (particularly *Orthocormus*: Weitzel 1930; Lambers 1988; Arratia & Schultze 2013).

Consequently, only a rough outline of the interrelationships within this clade has been proposed (Friedman *et al.* 2010; Friedman 2012*a*), despite many studies stressing the need for further detailed analysis to resolve or review currently accepted relationships (Lambers 1992: 283; 1999: 219; Arratia 1999: 322; 2001: 772; 2004: 279; Kear 2007: 1033; Arratia & Schultze 2013: 117). For example, *Orthocormus*, where a new species was identified as recently as 2013 (*Orthocormus roeperi*; Arratia & Schultze 2013) has only been analysed as a single composite taxon (*Orthocormus* spp.; Friedman *et al.* 2010; Friedman 2012*a*; Wretman *et al.* 2016) rather than being atomized into individual species to test the supposed monophyly of the genus. Additionally, the paraphyly of *Hypsocormus* contradicts cladistic classification whereby genera should represent monophyletic groups. It has therefore been suggested that the species of *Hypsocormus* need re-evaluation, and that *Hypsocormus macrodon* may be better placed within *Orthocormus* (Lambers 1992: 283–284, 1999: 219) due to: inclined premaxillary teeth; a peculiarly shaped pelvic plate; and the "slightly homoplastic" character: a forward projecting temporal boss (Lambers 1992: 283). Similar suggestions have been made regarding the identity of *Hypsocormus tenuirostris* (listed as '*Hypsocormus*' *tenuirostris* in Friedman *et al.* 2010 suppl.: 36), which has an elongated

rostrum and procumbent fangs very similar to those seen in *Orthocormus* (Lambers 1992: 269, 270). Subsequent phylogenetic analyses have placed *H. tenuirostris* as the sister taxon to *Orthocormus* spp. (Friedman *et al.* 2010; Friedman 2012*a*), but the genus *Hypsocormus* remains paraphyletic, and no reassignments of either *H. macrodon* or *H. tenuirostris* have been made.

Evolutionary trends of the 'suspension-feeding' clade

Most recent attention surrounding pachycormiforms has centred on the 'suspension-feeding' clade, and the reasons for the emergence of the suspension-feeding ecology from a group that is most classically considered to be mid-sized fish eaters (Liston 2006, 2008*a*, 2010, 2013, 2016; Friedman *et al.* 2010; Friedman 2012*a*; Liston *et al.* 2013; Schumacher *et al.* 2016; Gouiric-Cavalli 2017; Cione *et al.* 2018; Gouiric-Cavalli *et al.* 2019). These suspension-feeders have been characterized by their large body size — with *Leedsichthys* being estimated as one of the largest fishes ever (Martill 1988; Liston 2006) — and the absence of any teeth. Most notably, they appear to possess elongated gill rakers with 'fimbriations', first reported in *Leedsichthys* (Woodward 1890), or 'needle-teeth' (*sensu* Lambers 1992), first reported *Asthenocormus*. More recent studies have identified similar gill rakers in *Rhinconichthys* (Friedman *et al.* 2010; Schumacher *et al.* 2016), but none have been discovered in *Bonnerichthys* (Friedman *et al.* 2010). As such, the homology of 'fimbriation' or 'needle-teeth' morphology remains unclear (Liston 2013).

In order to better understand the emergence of suspension-feeding taxa, Friedman (2012*a*) carried out a morphospace analysis on pachycormiforms and mysticete whales (for the taxa

examined see Friedman 2012*a* suppl.: 19–20) using eight characters that have been functionally linked to suspension-feeding in previous studies (Sanderson & Wassersug 1993). In the same work, a phylogenetic analysis identified *Ohmdenia multidentata* as the sister-taxon to the giant bodied suspension-feeders because of the presence of a straight-sided hyomandibular and the absence of scales (Friedman 2012*a*). This study also suggested that *Ohmdenia* represents an intermediary stage between the carnivorous and suspension-feeding ecologies based on gradual changes in body plan between carnivorous and suspension-feeding taxa. Crucially, these changes in body plan appear to follow those seen in mysticete whales, which also evolved from classically carnivorous ancestors, in the following steps: (1) alteration to dentition and mandibular morphologies (such as the mandibular aspect ratio and jaw closing mechanical advantage); (2) the loss of dentition; (3) the increase in body size relative to other taxa in the same clade (Friedman 2012*a*; fig. 2b). This study made it clear that, like mysticete whales, these suspension-feeding taxa emerged gradually through a series of changes that may have been driven by ecological opportunity. However, at present, there is little available evidence to document these changes from the 'classic' *Pachycormus* body plan to the giant bodied suspension-feeding morphologies.

Uncertainties surrounding pachycormiform relationships

As noted by previous studies (Lambers 1992, 1999; Arratia 1999, 2001, 2004; Kear 2007; Arratia & Schultze 2013), the description and analysis of more morphological characters within pachycormiforms could vastly improve our understanding of the currently accepted framework of relationships. There are poorly resolved areas of the pachycormiform tree — such as the interrelationships of *Orthocormus*, *Hypsocormus*, and the suspension-feeding

pachycormiforms — and their wider placement among early stem teleosts, that could be improved by the addition of new characters or newly observed character states. This may be done by directly observing characters in well preserved fossils, or indirectly by using these descriptions as a 'Rosetta stone' to compare against poorly preserved or unidentified material of lesser known taxa. The latter might be particularly significant in the case of the poorly preserved suspension-feeders.

Of the predatory pachycormiforms, the best known and best described is *Pachycormus*. Consequently, it has often been used to represent pachycormiforms as a single operational taxonomic unit in analyses of teleost relationships, typically as *Pachycormus* sp. or *Pachycormus macropterus* (e.g. Arratia 2004; López-Arbarello & Sferco 2018). *Pachycormus* is also typically resolved as one of the more primitive pachycormiforms and shows the synapomorphies of pachycormiforms that distinguish them from the rest of the teleost clade (Lambers 1992; Friedman *et al.* 2010; Friedman 2012*a*; Wretman *et al.* 2016). Moreover, a large number of well-preserved *Pachycormus* specimens are known from the Strawberry Bank deposit of Somerset. This deposit is known for its exceptionally three-dimensional fossils (Williams *et al.* 2015), with a number of descriptions of ichthyosaurs. Most notably, some of these ichthyosaurs have preserved soft tissues (Moore 1866), which have been described using μCT scanning (Marek *et al.* 2015). There are also a number of particularly well-preserved crocodylians, including one specimen of *Pelagosaurus* with the remains of a *Leptolepis* skeleton in its ribcage, perhaps indicating its diet (Pierce & Benton 2006). As well as reptiles, Strawberry Bank is known for its fossil fish (reviewed in Woodward 1897), with Rayner (1948) providing a description of *Caturus* from this deposit (BRLSI M1288). Furthermore,

some of the best-preserved specimens are of *Pachycormus*, which are abundant, providing an opportunity to view its internal structures *in situ* using μCT scanning.

The external morphologies of these three-dimensional pachycormiforms have already been described (Woodward 1897; Cawley *et al.* 2018), but it is the internal structures such as the gill skeleton, pectoral girdle and braincase that could provide previously unobserved or unrecorded character states for phylogenetic analysis. The braincase in particular has been cited by Arratia (1999: 282) as a key area for analysis of actinopterygian and teleost evolution because "knowledge about foramina for the passage of nerves and blood vessels seems to be important for understanding the evolution of the actinopterygian cranium". Arratia (1999: 282) also cautions that our current understanding is "limited because the information is available only in few fossil taxa due to poor or incomplete preservation", highlighting again the need for detailed study of well-preserved taxa. This makes the three-dimensional specimens of *Pachycormus* ideal candidates for further study, as both a primitive pachycormiform and a stem teleost, with regards to these poorly understood but crucially important internal structures.

Despite being generally represented as a composite taxon in phylogenetic analyses, *Pachycormus* has long been thought to comprise three nominal species: *Pachycormus macropterus* (Blainville 1818); *Pachycormus bollensis* (Quenstedt 1858); and *Pachycormus curtus* (Agassiz 1843). In addition, *Pachycormus westermani* was originally described by Winkler (1878), but it is considered a junior synonym of *P. bollensis* (Lambers 1992). Wretman *et al.* (2016), consider *P. curtus* to be a junior synonym of *P. macropterus*, and

both Lambers (1992) and Friedman *et al.* (2010) deemed *P. bollensis* too poorly known to be scored in the phylogenetic analysis. Additionally, *P. bollensis* (along with *P. westermani*) has often been synonymized with *Saurostomus esocinus* (Woodward 1895*b*, 1896; Wenz 1967), due to their standard lengths of at least 1 metre (Lambers 1992). The identification of hemichordacentra in *P. bollensis* and *P. westermani* by Lambers (1992), which are absent in *Saurostomus*, justified the placement of *P. bollensis* within *Pachycormus* (with *P. westermani* as a junior synonym). Nonetheless, *P. bollensis* still remains a poorly understood species, with no clear diagnosis or justification for its distinction from other *Pachycormus* species aside from the presence of asymmetrical upper hypaxial caudal rays, where upper rays are shorter than lower ones (Lindkvist 2012: character 78; Cawley *et al.* 2018).

Another reason for such taxonomic ambiguity is that these species are currently diagnosed — if a diagnosis is available — by continuous or vague characters (as in Mainwaring 1978: 98–100 for *P. macropterus* and *P. curtus*), including general patterns in body shape and size. This led to the most recent study into the taxonomy of *Pachycormus* (Wretman *et al.* 2016) to examine whether the proportional variation used to differentiate between these species could be explained by intraspecific variation such as ontogeny, environment and sex (Wretman *et al.* 2016; figs. 2–4) via a morphospace analysis of all three species. The authors concluded that *Pachycormus* is a monotypic genus represented by just *P. macropterus*, while *P. curtus* and *P. bollensis* are junior synonyms. While it seems likely that Wretman *et al.* (2016) are correct that *Pachycormus* is monotypic, there is still some work to be done to understand the complex variation between *Pachycormus* specimens. Despite being best represented in the fossil record, they lack discrete, measurable apomorphies that could clearly

determine the interspecific variation and the true number of species present in *Pachycormus*. These species have also not been compared with aspects of internal morphologies which, as stressed before, could hold far more informative characters for species delimitation.

Similar in-depth analysis, perhaps using μCT scanning, could help resolve other taxonomic uncertainties, such as the composition of *Orthocormus*. Like *Pachycormus*, the three *Orthocormus* species are delimited by a number of continuous characters that are not necessarily informative when used in a phylogenetic analysis, because their undefined ranges means they cannot be used to clearly delimit between species (but see Goloboff *et al.* 2006). Such characters include: the standard length (±1.06 m; ±0.54 m; ±0.43 m), the head length (±21%; ±25%; ±23% of the standard length), approximate number of pectoral (±22; ±37; >30), dorsal (±40; ±48; >52), and caudal (±80; ±93; >100) fin rays for *O. cornutus*, *O. teyleri*, and *O. roeperi* respectively (see Arratia & Schultze 2013; table 1). While the fossil record of *Orthocormus* is poorer than *Pachycormus*, atomizing these taxa and studying them individually could identify any variation between these species that can be measured with existing characters or reveal apomorphies of *Orthocormus* to identify specimens in the future.

Of the giant bodied suspension-feeders, surprisingly little is known about their morphology because of their weakly ossified skeletons. This has resulted in their fossil record being almost exclusively represented by disarticulated fragments of fins and gill skeleton, particularly for *Leedsichthys*, whose morphology is very poorly known (Liston 2006, 2016). While there are some well-preserved skulls and skull fragments (see Friedman *et al.* 2010) of taxa such as *Rhinconichthys* and *Bonnerichthys*, inferences about their morphology have been very

difficult without a 'good' specimen to use as a reference point. Currently, three of the suspension-feeding pachycormiforms — *Asthenocormus*, *Martillichthys* and *Leedsichthys* — are placed in a polytomy. The best-preserved suspension-feeding pachycormiform specimen is the articulated, but very flattened, *Martillichthys renwickae* (NHMUK PV P.61563), the cranium of which may provide new characters to help resolve relationships. Although the external morphology of this specimen has been described (Liston 2008*a*), the lack of description of the internal skeleton has made interpretation of these suspension-feeding pachycormiform specimens challenging. Therefore, a comprehensive description of a well-preserved specimen such as *Martillichthys* using μCT scanning provides opportunity to supplement our current knowledge of the giant bodied suspension-feeding pachycormiforms, and facilitate comparison between species and isolated structures that currently lack any positional context to be informative.

There is also some morphological variation that could have a bearing on ecological function. Within the 'suspension-feeding' clade (*Bonnerichthys*, *Rhinconichthys*, *Asthenocormus*, *Leedsichthys* and *Martillichthys*) itself there are stark variations in morphology despite all these taxa putatively occupying the same ecological role, suggesting there may be some as yet undescribed variation in feeding mechanism among them. There is also suggestion of a long ghost lineage for *Bonnerichthys* and *Rhinconichthys*, which are inferred to emerge in the Middle Jurassic, but do not appear in the fossil record until the Late Cretaceous (Friedman 2012*a*; fig. 2a). This would be consistent with the poor fossil record for marine fishes in the Early Cretaceous and provide ample evolutionary time for apomorphies or — in the case of *Bonnerichthys* — reversals to evolve.

This does also, however, raise the question of whether alternative relationships would explain this variation in morphology between the Jurassic suspension-feeders and *Ohmdenia* compared to *Bonnerichthys* and *Rhinconichthys*. For example, the distal fusion of lepidotrichia along the leading edges of the pectoral fin is currently considered to be convergent between *Bonnerichthys* and *Protosphyraena*. However, it may indicate a closer relationship between these taxa than currently recognized, and a potential secondary origin of suspension-feeding in pachycormiforms. With a better grasp of the morphological variation within pachycormiforms, it would allow us to ask more detailed questions about how their morphology facilitated function, common trends between their hypothesized ecologies, and how their ecology might have been influenced by external factors such as environment, competition and available niches in Mesozoic ecosystems.

Pachycormiform ecology

Within pachycormiforms, the morphological variation between the two clades implies substantial ecological disparity. *Pachycormus* is generally considered to be the 'typical' pachycormiform, both because it is the best-described example and because it is one of the least specialized. Within pachycormiforms, it could be better described as a generalist between two very extreme ecological roles: the large bodied billfish-like macrocarnivores (Wretman *et al.* 2016) and the giant bodied, edentulous suspension-feeders. Many of the inferences made surrounding the ecology of these groups stems from the hypothesized link between jaw morphology and ecological function in fishes more generally, as outlined by Wainwright and Bellwood (2002) and elsewhere. Such analyses facilitate comparison with living taxa exhibiting similar morphologies, where more traits such as biomechanics,

behaviour and diet can be more readily observed, providing some insight into how form influenced function, and the environments in which these diverse taxa lived.

Predatory pachycormiforms

When compared to extant morphological analogues, the jaw morphology of *Pachycormus*, *Saurostomus* and 'protosphyraenids' indicates a highly carnivorous diet. This ecology requires sharp teeth and rapidly closing jaws to catch prey, along with a fusiform, hydrodynamic body for fast swimming (Lambers 1992; Lauder 1995; Wainwright & Bellwood 2002). Possessing sharp teeth alone, however, does not necessarily mean that all predatory pachycormiforms had the same ecological role. The ecological role of the distinctive large procumbent fangs — sometimes paired with paramedial fangs on the rostrodermethmoid — could be interpreted in a number of different ways throughout the gradual morphological shift to the 'billfish' ecology described for *Protosphyraena* and *Australopachycormus* in the 'protosphyraenid' clade (Wretman *et al.* 2016). Interestingly, billfish lack large teeth as adults, possibly because they eat their prey whole (Juenes *et al.* 2002), which *Protosphyraena* and *Australopachycormus* may not have done.

Despite having smaller teeth, the highly fusiform body shape, strong fins and tails, and lightweight scales of *Pachycormus*, *Saurostomus*, *Hypsocormus* and *Orthocormus*, suggest that they were ecological analogues of fast swimming, pelagic predators seen today (Martill 1990; Arratia & Schultze 2013), such as the dogtooth tuna (*Gymnosarda unicolor*).

Ohmdenia

The ecomorphological anomaly among the 'edentulous' pachycormiforms is *Ohmdenia*, due to its placement between the carnivorous pachycormiforms *Pachycormus* and *Saurostomus* and the giant bodied suspension-feeders (Friedman 2012*a*). Its long mandibles will have reduced its bite force relative to other predatory pachycormiforms and, while it has not lost its dentition, its low-crowned teeth arranged in multiple rows suggests a specialism towards holding rather than piercing prey (Friedman 2012*a*). Friedman (2012*a*) highlights that a similar tooth geometry is seen in marine reptiles that target soft-bodied prey, such as cephalopods. The only known specimen of *Ohmdenia* preserves two belemnites (cephalopods) in this gut area, but this is not conclusive evidence of diet due to the highly disrupted nature of the fossil.

Edentulous pachycormiforms

The 'suspension-feeding' clade demonstrates arguably the largest shift in ecomorphology within pachycormiforms. While *Pachycormus* and *Saurostomus* represent tuna-like predators with sharp teeth and a hydrodynamic body for fast swimming, they are phylogenetically resolved within the 'suspension-feeding' clade as successive sister lineages to the giant edentulous pachycormiforms: *Bonnerichthys*, *Rhinconichthys*, *Asthenocormus*, *Leedsichthys*, and *Martillichthys*. To understand the ecology of the giant edentulous pachycormiforms and in the absence of any dentition — another indicator of ecological function — attention has centred on the elaborate gill rakers observed in some taxa. These long gill rakers are a departure from the shorter, more tooth-like rakers seen in carnivorous pachycormiforms (e.g. *Pachycormus* and *Hypsocormus*; Dobson 2016), and it has been hypothesized that these gill

rakers acquired a secondary role in facilitating suspension-feeding by trapping prey items in the oral cavity (Martill 1988; Lambers 1992; Friedman *et al.* 2010; Friedman 2012*a*; Liston 2015). The same feeding mechanism is also seen in extant analogues including whale sharks (Rhincodontidae) and basking sharks (Cetorhinidae; Paig-Tran & Summers 2014). This would make the giant edentulous pachycormiforms the only giant bodied suspension-feeders ever observed in teleosts, with this particular role now only represented in chondrichthyans and mysticete whales (Friedman 2012*a*).

Friedman (2012*a*: 949) outlines similar changes in body plan during the evolution of suspension-feeding ecologies in mysticete whales and giant pachycormiforms, which supports the hypothesized suspension-feeding ecology in pachycormiforms. All of these stages are seen in the 'suspension-feeding' clade of pachycormiforms, but not in the same order. I would argue that increase in body size starts earliest, followed by changes to dentition and mandibular dimensions. Finally, any dentition is lost completely in giant suspension-feeding pachycormiforms. The only additional suspension-feeding trait in the edentulous pachycormiforms is the evolution of long, elaborated gill rakers, also seen in suspension-feeding chondrichthyans (e.g. Paig-Tran & Summers 2014), that direct water and suspended food particles into the oesophagus (Cheer *et al.* 2012).

However, not all of the giant bodied suspension-feeders share the same morphology, despite apparently sharing the same ecological role, indicating variation in feeding modes (as also noted by Schumacher *et al.* 2016: 83). Such variation has been documented in mysticete whales (Sanderson & Wassersug 1993; Hampe & Baszio 2010). However, it is currently

difficult to theorize on potential feeding mode variation within giant bodied suspension-feeding pachycormiforms using the current evidence available.

This is especially true for *Bonnerichthys*, which is well-represented in the Niobrara Formation of the United States (Friedman *et al.* 2013*a*) but shows a curious mix of symplesiomorphic and synapomorphic traits (Friedman *et al.* 2010). Therefore, there are several outstanding questions about how the morphology of *Bonnerichthys* might influence its ecology. For example, *Bonnerichthys* has not been observed with any gill rakers which, if a true absence, hints at a broader ecological question of how taxa without gill rakers suspension-feed. Studies have shown suspension-feeding is not dependent on presence of gill rakers, and that animals have been able to continue suspension-feeding even if their gill rakers have been removed, but it is not clear how (Smith & Sanderson 2013). The question of why there are no gill rakers in *Bonnerichthys* is more a question of whether *Bonnerichthys* secondarily lost them or never had them in the first place, and how that may have impacted its feeding mode or behaviour. Alternatively, some researchers have hypothesized that these rakers were present, but cartilaginous, and so would not appear in the fossil record (Liston; pers. comm.).

There are a number of other uncertainties surrounding the morphology of *Bonnerichthys*, and how that might impact its ecology or even phylogeny. As the earliest diverging giant bodied suspension-feeding pachycormiform, it has a primitively short sphenoid region, which is also seen in *Rhinconichthys*, but appears latest in the fossil record (Friedman *et al.* 2010; Schumacher *et al.* 2016). Additionally, there are a number of autapomorphic traits, such as unsutured skull roofing bones, a fused anterior portion of the pectoral fins is thickened

relative to the rest of the fin and no gill rakers (Friedman *et al.* 2010, 2013*a*). The reason for this variation between *Bonnerichthys* and other suspension-feeding pachycormiforms is unclear, and warrants further study, but it could suggest that our current understanding of pachycormiform relationships does not acknowledge this variation, or different feeding mechanisms for suspension-feeding occur between the giant bodied suspension-feeders.

Mesozoic marine ecosystems

One hypothesis for the considerable ecomorphological disparity within pachycormiforms is that ecological opportunity drove these ecomorphological changes, particularly for the giant bodied suspension-feeders. Although we currently know the basic outlines of pachycormiform relationships, ecologies and evolution, we know very little about why the suspension-feeding ecology in particular evolved, and why suspension-feeding pachycormiforms disappeared at the end of the Cretaceous. Given their disappearance in the fossil record at around the same time as the Cretaceous-Paleogene boundary, it seems likely that they were a victim of the mass extinction, but confidence around the time of their extinction has not been assessed statistically. Investigating the possibility that pachycormiforms survived the K-Pg mass extinction could provide evidence of how the suspension-feeding pachycormiforms fitted into the broader context of the ecosystem in which they inhabited, and how this might have impacted the emergence of modern lineages.

During the Mesozoic, marine ecosystems underwent substantial changes in faunal and floral diversity that are reflected in marine ecosystems today (Hull 2017), dubbed by some as the Mesozoic marine revolution (Vermeij 1977; Ridgewell 2005; Knoll & Follows 2016). The first

recognized indicator of this change was in the shell geometries of marine invertebrates, where shells became narrower and asymmetrically coiled, with ornaments such as spines, to defend against an increase in durophagous predators appearing in Mesozoic marine ecosystems (Vermeij 1977; Sallan 2014). This was also coupled with an increase of infaunal taxa and a decrease in stationary epifauna throughout the late Mesozoic, as invertebrates were forced to find new ways to avoid predation. The increase of durophagous predators and motile invertebrates, along with increases in organismal body sizes, indicates an overall increase in energy use by taxa in the late Mesozoic that allowed for high-energy behaviours (Bush & Bambach 2011). Finnegan *et al.* (2011) estimated that energy use by gastropods increased by at least 150% during the Mesozoic and Cenozoic relative to previous periods (Bush & Bambach 2011: fig. 5*e*).

It is hypothesized that these ecomorphological shifts among Mesozoic fauna point to fundamental changes in ocean chemistry (Bush & Bambach 2011; Knoll & Follows 2016; Hull 2017), with increased nutrients thought to come from the land and submarine volcanism (Bambach 1999; Vermeij 1995). Ridgwell (2005) identified the Cretaceous as a 'warm anomaly' that may have encouraged growth of microfauna and phytoplankton in pelagic waters. The radiation of phytoplankton — including diatoms, coccolithophores and dinoflagellates that could increase nutrient and oxygen in the suspension — permitted an increase in body sizes and motility of consumers that was not previously possible (Bush & Bambach 2011). Perhaps these increases of planktonic and infaunal taxa also improved nutrient cycling and so increased productivity at the primary trophic level (Thayer 1983; Martin 1996; Vermeij 1999). The calcification of plankton also occurred around this time

(150–200 Ma; Hull 2017), which dispersed roughly half of all marine calcium carbonate into deep waters, rather than being restricted to less-stable shallow environments, opening up new foodwebs in the open ocean.

With an increase in infaunal taxa replacing sessile invertebrate suspension-feeders, coupled with an increase in phytoplankton and available nutrients in the water column, the niche for large bodied suspension-feeders may have opened up at this point. This would have also redistributed energy flow through food chains and trophic levels in Mesozoic environments, providing opportunity for other taxa to capitalize on newly available nutrients. Additionally, large body sizes, which were previously restricted by abiotic conditions, could also consume much higher biomasses of phytoplankton and microfauna compared to smaller invertebrate suspension-feeders. Being motile also allowed for giant bodied suspension-feeders — among others — to radiate into pelagic ecosystems that the calcareous plankton had opened up, rather than being restricted to shallow waters.

These changes to marine predation, foodweb structures, and ocean chemistry have persisted in modern marine ecosystems, and arguably the ecological and environmental changes in the Mesozoic set the stage for modern lineages to emerge and occupy these niches (Hull 2017). However, the pioneering giant bodied suspension-feeding pachycormiforms have disappeared. It is possible that this is related to the faunal turnover at the end of the Cretaceous, which resulted in the loss of over 50% of genera and a collapse of primary productivity in pelagic environments (D'Hondt 2005; McCallum 2015; Tajika *et al.* 2018). This collapse included the extinction of nearly all of the pelagic calcareous plankton that pachycormiforms are

hypothesized to have fed on (Bown 2005; fig. 2c; Hull 2017; fig. 2; Tajika *et al.* 2018). It may also be that modern giant bodied suspension-feeding chondrichthyans had already emerged in the Mesozoic and out competed suspension-feeding pachycormiforms when food sources became scarce at the end of the Cretaceous.

Either hypothesis raises several questions about how modern giant bodied suspension-feeding lineages emerged in the wake of pachycormiform (and more broadly the end-Cretaceous) extinction. If suspension-feeding pachycormiforms and chondrichthyans did indeed co-exist at the end of the Cretaceous, how did suspension-feeding chondrichthyans survive when pachycormiforms did not? If they did not co-exist, did chondrichthyans emerge once pachycormiforms had vacated the giant bodied suspension-feeding niche, as hypothesized by Friedman *et al.* (2010)? The fossil record of chondrichthyans, if taken literally, indicates that the modern lineages of giant bodied suspension-feeders began to appear in the fossil record in approximately the mid-late Paleocene. This timing would correspond with the 5–10 Myr evolutionary recovery period generally found for taxa to emerge and occupy newly vacant niches (Kirchner & Weil 2000), and for pelagic calcareous plankton populations to recover (Hull 2017; fig. 2), particularly dinoflagellates, nannoplankton and diatoms. However, even with the dense tooth fossil record of chondrichthyans, it is difficult to place a firm estimate on their emergence based on the fossil record alone. A suspension-feeding ecology evolved several times across several monotypic lineages (including whale sharks and basking sharks; Sanderson & Wassersug 1993), making the emergence of these ecologies fall somewhere between the divergence times (as estimated from molecular analyses) of their respective total-groups from other chondrichthyans and their first appearances in the fossil record.

The same is true for the extinction of pachycormiforms, where the quality of the fossil record means it is unlikely to preserve their true temporal range. While this does not mean that the fossil record is useless (it can provide minima for the timing of taxa extinction and emergence), it does mean that questions surrounding the extinction of pachycormiforms and the emergence of the modern giant suspension-feeders thought to replace them should be tested using statistical analyses that account for the uncertainty of the fossil record (e.g. Strauss & Sadler 1989; Marshall 1990, 1997; Friedman 2012*b*; Capobianco & Friedman 2018). With a clearer picture of the plausible temporal ranges of these major groups, it will be easier to unravel the processes by which pachycormiforms eventually disappeared from Mesozoic oceans, and how the modern giant bodied suspension-feeders took their place.

Outstanding questions

The purpose of this thesis is to address some of the outstanding questions remaining about pachycormiform morphology, ecology and evolution. I aim to provide detailed and informative descriptions of articulated, three-dimensionally preserved crania of both the giant bodied suspension-feeding and the predatory pachycormiform morphologies, using micro-CT (μCT) scanning to view internal and external structures in their structural and positional context.

The first research chapter (Dobson *et al.* 2019; Chapter 2) focusses on re-describing the cranial anatomy of *Martillichthys renwickae* (NHMUK PV P.61563) which, although highly flattened, is the best-preserved skull of the giant bodied suspension-feeders. The external morphology of this specimen has been described previously (Liston 2008*a*) but the internal

structures remain unobserved. Of these internal structures, the braincase can be particularly informative because it is less influenced by the environmental pressures that can affect external morphology, it is character rich, and its synapomorphies are well conserved along lineages making it possible to delineate relationships within neopterygians (Patterson 1975; Olsen 1984; Grande & Bemis 1998; Grande 2010; Giles & Friedman 2014; Giles *et al.* 2015, 2016, 2017). Other works have sometimes disputed the value of the braincase as a source of phylogenetic information (Rauhut 2007; Maddin *et al.* 2012), and though they are correct to argue that braincase should not be considered better than other internal or external structures, these critiques are based on the use of braincase characters in other major groups such as avian theropods (Rauhut 2007) and amphibians (Maddin et al. 2012). In neopterygians, braincases have been comprehensively described for a wealth of taxa (Rayner 1948; Patterson 1975; Olsen 1984; Grande & Bemis 1998; Grande 2010; Giles *et al.* 2015, 2016, 2017; Argyriou *et al.* 2018; Friedman *et al.* 2019) and have been used as evidence to inform interrelationships along teleost and actinopterygian lineages, with internal and external cranial anatomy (including the braincase, dermal skull roofing bones, suspensioria and hyoid arches) sometimes comprising up to 80% of character matrices (Argyriou *et al.* 2018). Therefore, describing the internal cranial anatomy of pachycormiforms will enable comparison with previous descriptions of stem teleosts and holosteans (e.g. Rayner 1948; Patterson 1975), and allow for them to be included in character matrices that include braincase characters to test their placement on the teleost stem.

Therefore, a primary purpose of this description is to provide a model by which to interpret poorly preserved taxa (such as *Leedsichthys*) through comparative anatomy. Therefore, using

this description, I compare the morphologies of the giant bodied suspension-feeding pachycormiforms and discuss how variations in their skull geometries might influence their ecology or phylogeny. I also identify morphological characters that can be added to a pre-existing character matrix (from Friedman 2012*a*) for a phylogenetic analysis into pachycormiform interrelationships in the following chapter.

The second chapter describes the internal and external morphology of a three-dimensionally preserved *Pachycormus* (BRLSI M1361a) from the Strawberry Bank deposit in Somerset. Although the external morphologies of some of these specimens have already been described (Woodward 1897; Cawley *et al.* 2018), μCT scanning has not been used for description or to inform a phylogenetic analysis, despite being a potential source of newly observed or re-described morphologies. The advantage of describing *Pachycormus* is that it is an early diverging, unspecialized pachycormiform, and classically used to represent pachycormiforms in phylogenetic analyses of teleost and neopterygian relationships. Therefore, maximising the morphological information available for *Pachycormus* would improve both analyses into pachycormiform ecology and evolution, and their broader relevance to teleost evolution. Even if some outstanding questions highlighted in this introduction are outside the scope of this thesis, such as the species delimitation of *Pachycormus* spp. (but see Wretman *et al.* 2016), it is hoped that this description will go some way to help subsequent descriptions and analyses.

Following the new descriptions of *Pachycormus* and *Martillichthys*, the second chapter also includes a phylogenetic analysis of pachycormiform interrelationships, using a pre-existing

character matrix (from Friedman 2012*a*). Character states of the taxa already in the matrix are verified through an extensive literature review of available descriptions and previous analyses (i.e. Friedman *et al.* 2010; Wretman *et al.* 2016), acknowledging errors or suggestions for improvement highlighted by other publications (e.g. the homology of uroneurals as noted by Arratia & Schultze 2013; 'scythe-like pectoral fins' as noted by Liston & Maltese 2016). I also aim to improve resolution within the pachycormiform tree by including new characters that could resolve the polytomy between *Asthenocormus*, *Leedsichthys*, and *Martillichthys*. Additionally, I have added new taxa, for example atomizing the composite terminal taxon *Orthocormus* spp. into its constituent species and including aspidorhynchid species to represent an alternative sister group to teleosts.

The phylogenetic analysis itself has several aims which are approached in different ways. The most straight-forward is using this amended matrix to infer the interrelationships of pachycormiforms, and their position on the teleost stem. The matrix from Friedman (2012*a*) already includes some taxa that represent the teleost crown and holostean stem, and the addition of aspidorhynchids serves to evaluate whether aspidorhynchids, pachycormiforms or other stem teleosts are resolved as the most likely sister group to other teleosts. I have employed maximum parsimony and Bayesian methods, and combine morphological and molecular (where available) data to infer relationships and establish their statistical support. As a secondary aim, I have included geological emergence times for a tip-dating analysis using a Fossilized Birth-Death model (Heath *et al.* 2014) to estimate the divergence times for pachycormiforms and the giant bodied 'suspension-feeding' clade. The Fossilized Birth-Death model is a fossil calibration model that allows for extant and extinct taxa to calibrated

individually, which permits co-estimation of tree shape and branch durations through the inclusion of fossil calibrations. Finally, this chapter provides opportunity for analysis of how well supported hypothesized relationships are. This employs a stepping stone analysis to test the support for alternative phylogenies (Xie *et al.* 2010). Specifically, I test the support for a second origin of suspension-feeding in pachycormiforms (as first proposed by Liston & Maltese 2016) compared to the currently accepted pattern of pachycormiform interrelationships.

With a better idea of suspension-feeding pachycormiform anatomy, interrelationships and divergence times, my final chapter aims to put their ecology and evolution in the broader context of how modern lineages emerged following the extinction of pachycormiforms. Taking the fossil record literally, the last suspension-feeding pachycormiforms to become extinct are *Bonnerichthys* and *Rhinconichthys*. However, the fossil record is incomplete, as exemplified by the lack of fossils for these taxa in the Early Cretaceous. Therefore, while the fossil record suggests that these taxa fell victim to the end-Cretaceous mass extinction, it is possible that the fossil record simply does not extend into the Paleogene. I employ Bayesian methods outlined by Strauss and Sadler (1989) and Marshall (1990, 1997) to estimate credible intervals on the occurrence data for *Bonnerichthys* and *Rhinconichthys* and determine how well the timing of edentulous pachycormiform extinction can be constrained given the current palaeontological data.

The same methods are applied to calculate plausible ranges for the emergence of modern analogues to the giant bodied suspension-feeding pachycormiforms: the giant bodied

suspension-feeding chondrichthyans, comprising whale sharks (Rhincodontidae), basking sharks (Cetorhinidae), megamouth sharks (Megachasmidae), and mobulid rays (Mobulidae). For both pachycormiforms and chondrichthyans, I also incorporated an empirical recovery function (*sensu* Marshall 1990, 1997), to account for non-uniform preservation in the fossil record. This removes the assumption of uniform distribution (as in the original Strauss & Sadler 1989 equation), and provides needed flexibility in horizons if preservation potential is low.

The aim of this final chapter is to assess whether suspension-feeding pachycormiforms and chondrichthyans might have co-existed or, as the fossil record suggests and Friedman *et al.* (2010) hypothesized, giant bodied suspension-feeding chondrichthyans emerged in the Cenozoic once pachycormiforms had disappeared entirely. This will help to bring the thesis full circle, where I have asked questions about pachycormiform emergence, evolutionary relationships, ecological role, and extinction. Moreover, it places my research in the broader context of life's history, and how the past has influenced present diversity.

By providing comprehensive descriptions of poorly known taxa, which are resolved along a deep branch of the teleost stem, I hope that they can be used to add much needed context or detail to poorly understood fossils. While the focus of this thesis centres mainly around one group of early diverging teleosts, this work can have a range of benefits. The fossil record itself is not just a tool for building maps of relationships or phylogenies; it is crucial to calibrate molecular clock studies, where the emergence and evolution of traits in the fossil record over time can aid estimations of evolutionary rates in molecular data. Therefore,

descriptions of previously unknown synapomorphies and structures can force a re-evaluation of how traits emerged, and possibly even provide evidence that some modern phenotypes or key synapomorphies emerged earlier than previously thought, which can influence analyses of modern taxa. At a more local level, these descriptions, as mentioned earlier, will be invaluable to interpret poorly preserved fossils that may provide yet more unrecorded variation for a more robust analysis of teleost early relationships. Pachycormiforms in particular represent a considerable range of morphological and ecological variation, and so understanding them can supplement our knowledge of how past ecosystems and environments changed over time, and how that impacted the radiation of modern diversity.

Chapter 2

Cranial osteology of *Martillichthys renwickae* with comments on the evolution and ecology of edentulous pachycormiforms

This chapter has been published as:

DOBSON, C., GILES, S., JOHANSON, Z., LISTON, J. and FRIEDMAN, M. 2019. Cranial osteology of *Martillichthys renwickae* [Neopterygii; Pachycormiformes], and implications for suspension-feeding pachycormids, *Papers in Palaeontology.*

MF and SG contributed with μCT scans, analytical advice and improving drafts of my writing. ZJ and JL provided analytical and editing advice when constructing the manuscript. All other data collection, analyses, and writing were done by CD.

Abstract

Our understanding of the ecology and phylogenetic relationships of Pachycormiformes, a group of Mesozoic stem teleosts including the iconic *Leedsichthys*, has often been hindered by a lack of comprehensive morphological information. Micro-CT scanning of an articulated,

though flattened, cranium of the edentulous *Martillichthys renwickae* from the Middle Jurassic (Callovian) Oxford Clay of the UK reveals previously unknown internal details of the most complete suspension-feeding pachycormiform skull known, including the palate, braincase, and branchial skeleton. The latter preserves gill rakers with elongate, pointed projections similar to those of *Asthenocormus*, in contrast to the finer fimbriations associated with *Leedsichthys*. I also reinterpret some previously described features, including dermal bone patterns of the snout, skull roof, and lower jaw, and the morphology of the ventral hyoid arch. These new anatomical data reinforce the phylogenetic placement of *Martillichthys* as part of the Jurassic clade of edentulous pachycormiforms. The elongated skull geometry of these Jurassic taxa is strikingly similar to that of *Ohmdenia*, the sister taxon to edentulous pachycormiforms, but contrasts sharply with the morphology of the Late Cretaceous edentulous pachycormiform *Bonnerichthys*, raising questions over the phylogenetic relationships among these taxa. Most significantly, *Martillichthys* shows specialized characters with a restricted phylogenetic distribution among suspension-feeding pachycormiforms, including the distinctive gill rakers and a greatly extended occipital stalk. My analysis of *Martillichthys* supports past interpretations of a close relationship with *Asthenocormus*, and provides a model for interpreting the less complete remains of other members of this enigmatic group of fishes.

Introduction

Pachycormiformes is a clade of neopterygian fishes that ranges in age from the Early Jurassic (Toarcian; Lehman 1949) to the end of the Late Cretaceous (Maastrichtian; Friedman 2012*a*; Friedman *et al.* 2013*a*), and represents an early-diverging lineage of stem teleosts (Patterson

1973, 1994; Arratia 2004; Friedman *et al.* 2010; Friedman 2012*a*). Pachycormiform morphology is distinctive, with members of the group united by a number of synapomorphies: a compound bone (rostrodermethmoid) forming the anterodorsal border of the mouth; a reduced coronoid process of the mandible; absence of supraorbitals associated with a dermosphenotic defining the dorsal margin of the orbit; two large, plate-like suborbital bones posterior to the infraorbitals; long, slender pectoral fins (see Liston & Maltese 2016 for a critique of past descriptions of 'scythe-like'); asymmetrical branching of pectoral-fin lepidotrichia; considerable overlap of the hypurals by caudal-fin rays (hypurostegy); and the presence of distinctive uroneural-like ossifications of the caudal-fin endoskeleton (Mainwaring 1978; Lambers 1988, 1992; Arratia & Lambers 1996; Kear 2007; Friedman *et al.* 2010; Friedman 2012*a*; Arratia & Schultze 2013). Pachycormiforms are widely distributed, with abundant material known from Europe and North America (Stewart 1988; Friedman *et al.* 2010; Wretman *et al.* 2016) and rarer remains from South America, Australia, the Middle East, and most recently Antarctica (Woodward 1895*a*; Kear 2007; Gouiric-Cavalli 2013; Gouiric-Cavalli & Cione 2015; Wretman *et al.* 2016; Gouiric-Cavalli 2017; Cione *et al.* 2018; Gouiric-Cavalli *et al.* 2019). Material from Myanmar previously identified as pachycormiform has recently been reinterpreted as a tselfatiiform (Taverne & Liston 2017). Many pachycormiforms are known from well-preserved, articulated or associated specimens, with numerous examples from famous *Lagerstätten* including the Early Jurassic (Toarcian) Posidonia Shale of Germany (Hauff 1953*b*) and Strawberry Bank of the UK (Williams *et al.* 2015; Cawley *et al.* 2018), the Middle Jurassic (Callovian) Oxford Clay of the UK (Martill 1986), the Late Jurassic plattenkalks of Germany and France (Barthel *et al.* 1990; Lambers 1992), and the Late Cretaceous (Coniacian-Campanian) Smoky Hill Chalk of the USA

(Stewart 1988, 1990). Despite this abundance of material, most pachycormiforms remain poorly known, with the clade represented by only a single operational taxonomic unit (generally *Pachycormus macropterus*) in many analyses of neopterygian or teleost relationships (e.g. Arratia 2004; López-Arbarello & Sferco 2018).

The lack of comprehensive morphological information is particularly acute for edentulous pachycormiforms, a presumed clade of large-bodied (> 1 m in total length) taxa interpreted as Mesozoic analogues of mysticete whales and suspension-feeding chondrichthyans (Friedman *et al.* 2010). Its members range in age from the Middle Jurassic to the Late Cretaceous, and currently include five recognized genera: the Jurassic *Asthenocormus* (Quenstedt 1852), *Leedsichthys* (Woodward 1889*a*, *b*, 1895*a*), and *Martillichthys* (Liston 2006, 2008*a*); and the Cretaceous *Bonnerichthys* (Friedman *et al.* 2010, 2013*a*) and *Rhinconichthys* (Friedman *et al.* 2010). Generically indeterminate material has also been associated with this edentulous radiation (Friedman *et al.* 2010; Cione *et al.* 2018), and a variety of unpublished remains are also known. Considerable interest centres on the paleobiology of these giant pachycormiforms and their role in ancient marine ecosystems (Martill 1988; Liston 2006; Friedman *et al.* 2010; Friedman 2012*a*; Liston *et al.* 2013; Ferrón *et al.* 2018; Gouiric-Cavalli *et al.* 2019). Unfortunately, their large size, combined with reduced ossification relative to other pachycormiforms (taken to an extreme in *Leedsichthys* and *Bonnerichthys*), makes them difficult subjects for detailed anatomical study, with even the best-known taxa only described in limited detail. *Rhinconichthys* is known from three incomplete skulls (Friedman *et al.* 2010; Schumacher *et al.* 2016), while *Bonnerichthys* and *Leedsichthys* are represented principally by isolated remains with rare associated but

disarticulated individuals (Friedman *et al.* 2010; Liston 2016). In contrast to the incomplete nature of most edentulous pachycormiform fossils, there is a nearly complete specimen of *Martillichthys* (Liston 2008*a*) and several articulated individuals of *Asthenocormus* (Lambers 1992). These taxa therefore serve an important role in interpreting the more incomplete remains of their close relatives, which is vital to better constraining the evolutionary history and paleobiology of this enigmatic but ecologically significant radiation.

Here I use micro-CT (μCT) scanning to redescribe the cranial anatomy of the holotype of *Martillichthys renwickae* (Fig. 2.1). My study emphasizes concealed aspects of internal structure not accessible by previous, external examinations (Liston 2008*a*), with the principal goals of improving our understanding of *Martillichthys* itself and using this new description to make inferences about the ecology and evolution of both *Martillichthys* and the broader clade of edentulous pachycormiforms. It is my hope that a more detailed account of *Martillichthys* will serve as an anatomical 'Rosetta Stone' for interpreting structure in less complete or more fragmentary remains of its relatives.

Materials and methods

Materials

Pachycormiformes

Bonnerichthys gladius. KUVP 60692, University of Kansas Biodiversity Institute and Natural History Museum. Disarticulated skull, pectoral girdles, and fins from the Coniacian-Santonian Smoky Hill Chalk Member of the Niobrara Formation of Kansas, USA. This

specimen was studied on the basis of uncatalogued casts kept in the University of Michigan Museum of Paleontology.

Leedsichthys problematicus. NHMUK PV P.6921, Natural History Museum, London, UK. The holotype specimen, comprising disarticulated remains of the skull, pectoral girdle, and postcranium. This specimen is from the Callovian Oxford Clay of Peterborough, UK.

Leedsichthys problematicus. NHMUK PV P.10156, Natural History Museum, London, UK. An articulated set of ventral branchial arches plus the left hyomandibula. This specimen is from the Callovian Oxford Clay of Peterborough, UK.

Martillichthys renwickae. NHMUK PV P.61563, Natural History Museum, London, UK. The holotype specimen comprising a nearly complete articulated individual. An additional specimen attributed to *Martillichthys* is housed in the Peterborough Museum (PETMG F161), but this individual is encased in a dense concretion that is likely not amenable to μCT using most laboratory-based machines (pers. obs. MF of similarly preserved fishes from the Oxford Clay Formation). This specimen was μCT scanned in January 2016 (scanning parameters given below and in Appendix B).

Pachycormus macropterus. NHMUK PV OR 32433, Natural History Museum, London, UK. Three-dimensionally preserved skull from the Toarcian of Curcy (Normandy, France). This specimen was μCT scanned in January 2016, and scanning parameters are given in the appendix (Appendix B).

Pachycormus macropterus. BRLSI M1297, Bath Royal Literary and Scientific Institution, Bath, UK. Three-dimensionally preserved cranium and pectoral girdle from the Toarcian deposits of Strawberry Bank *Lagerstätte* in Ilminster (Somerset, UK). This specimen was

μCT scanned in June 2017 and scanning parameters are given in the appendix (Appendix B).

Pachycormus macropterus. BRLSI M1361a, Bath Royal Literary and Scientific Institution, Bath, UK. Three-dimensionally preserved cranium and pectoral girdle from the Toarcian deposits of Strawberry Bank Lagerstätte in Ilminster (Somerset, UK). This specimen was μCT scanned in July 2015 and again in February 2017. Scanning parameters from February 2017 are given in Appendix B.

Protosphyraena sp. FHSM VP-3251, Sternberg Museum of Natural History, Fort Hays State University, Hays, Kansas, USA. Disarticulated specimen comprising incomplete remains of skull and pectoral girdle from the Coniacian-Santonian Smoky Hill Chalk Member of the Niobrara Formation of Kansas, USA.

Figure 2.1 – Skull of *Martillichthys renwickae* NHMUK PV P.61563. A) photograph in ventral view. B) photograph in dorsal view. Anterior to the left in panel A; and to the right in panel B. Scale bar represents 10 cm.

Methods

NHMUK PV P.61563 was scanned using a Nikon Metrology HMX ST 225 CT scanner at the Natural History Museum, London. The X-ray beam was generated with a current of 150 μA and voltage of 190 kV, and a 1 mm copper filter was used. Resolution of the scan was 0.126 mm. The length of the specimen exceeded the maximum field of view for the scanner, so the fossil was imaged in two sections using identical machine settings. Image stacks for these separate scans were then spliced to create a single tomogram stack for segmentation.

The resulting dataset was loaded into Mimics Innovation Suite V.18.0 (http://biomedical.materialise.com/mimics; Materialise, Leuven, Belgium), which was used to segment individual skeletal elements. Data objects were imported into Blender V.2.77a (http://www.blender.org; Blender Institute, Amsterdam, Netherlands) for reconstruction, description and imaging. Limitations arise from damage to or loss of some bones (particularly around the cheek), very close application of adjacent ossifications that obscures their boundaries (particularly the skull roof, braincase and parasphenoid), and difficulties distinguishing bone from matrix in tomograms from some regions of the skull.

Systematic palaeontology

ACTINOPTERYGII Cope, 1887

NEOPTERYGII Regan, 1923

TELEOSTEI Müller, 1845

PACHYCORMIFORMES Berg, 1937

PACHYCORMIDAE Woodward, 1895*a*

Genus *Martillichthys* Liston, 2008*a*

Martillichthys renwickae Liston, 2008*a*

1984 *Asthenocormus* sp. Schaeffer & Patterson, p. 74–75.

1991 *Asthenocormus* sp. Martill, p. 220–222, plate 44.

2008*a* *Martillichthys renwickae* Liston, p. 184–192, figs. 3, 4.

Type specimen. NHMUK PV P.61563, *Martillichthys renwickae.* A nearly complete individual, from Bed 12 of the Oxford Clay Formation at the Dogsthorpe Pit, Peterborough, England (Martill 1986). This corresponds to the Tethyan middle Callovian ammonite zones *Reineckia anceps* to *Erymnoceras coronatum* (Martill 1991, fig 1.2). On this basis, the fossil is assigned an age range of 164.63 Ma to 167.97 Ma (Gradstein *et al.* 2012; table 26.3).

Referred material. PETMG F161, *Martillichthys renwickae*. An unprepared specimen in a concretionary nodule consisting of the cranium and extending to the posterior edge of the base of the pectoral fins.

Diagnosis. The following combination of characters distinguish *Martillichthys* from other edentulous pachycormiforms: canal-bearing rostrodermethmoid; posterior process of rostrodermethmoid extending between frontals; gap between frontals; elongate, pointed gill raker projections; body of gill rakers club-like rather than tapering to a pointed, distal tip; hyomandibula with plate-like rather than cylindrical dorsal head; hyomandibula less than

one third the length of the mandible; elongate preorbital region; elongate occipital stalk; deep groove for the dorsal aorta on the occipital stalk.

Remarks. Previous analyses have been unable to resolve the relationships between *Martillichthys*, *Leedsichthys* and *Asthenocormus*. Liston (2006, 2008*a*) noted many similarities between these taxa, and subsequent cladistic analyses placed the three in an unresolved polytomy (Friedman *et al*. 2010; Friedman 2012*a*). Distinguishing these genera is complicated by a poor understanding of anatomy in *Leedsichthys* and, to a lesser degree, *Asthenocormus*. The most conspicuous difference between *Asthenocormus* and *Martillichthys* concerns the geometry of the contact between the rostrodermethmoid and the frontals. This is depicted as transverse for *Asthenocormus* (Lambers 1992), but is 'v'-shaped in *Martillichthys*. At present, the few aspects of overlapping anatomy in the diagnosis of *Martillichthys* and *Leedsichthys* do not show striking differences with the exception of some aspects of the skull roof and gill rakers (see Liston 2008*a*, fig. 6). More detailed description of *Leedsichthys* will be vital in more clearly differentiating *Martillichthys* from this taxon.

Morphological description

The skull is approximately 484 mm long and measures 142 mm at its widest point. Strong dorsoventral compression has resulted in a maximum specimen depth of only 28 mm (Figs. 2.1, 2.2).

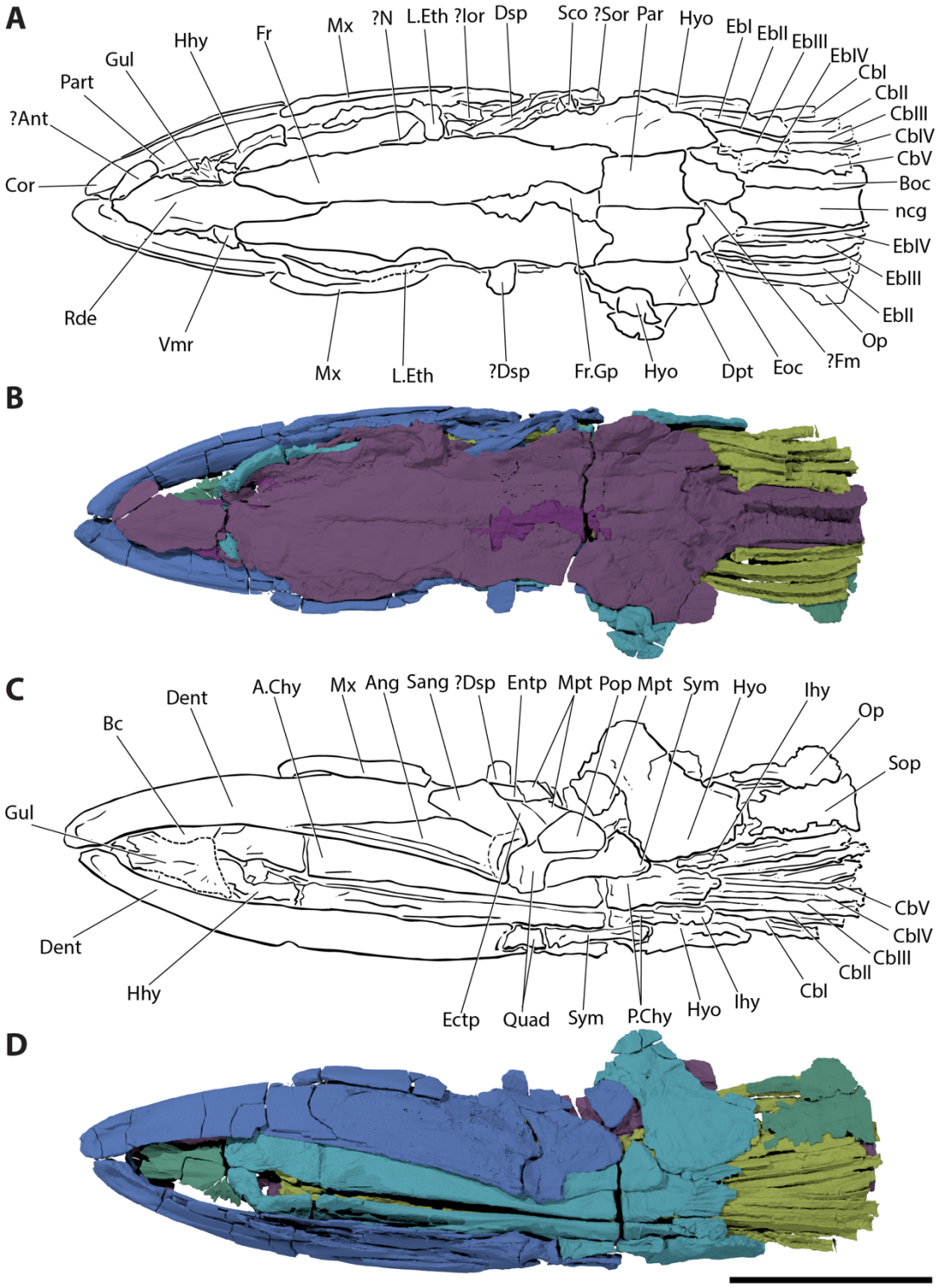

Figure 2.2 – Skull of *Martillichthys renwickae* NHMUK PV P.61563. A) interpretive line drawing of rendered portions of the skull in dorsal view. B) three-dimensional rendering of skull in dorsal view. C) interpretive line drawing of rendered portions of the skull in ventral view. D) three-dimensional rendering of skull in ventral view. Hashed lines indicate areas where margins are uncertain. Anterior to the left. Purple is used to represent the neurocranium; dark blue represents the mandible, upper jaws, palate and orbit; light blue represents the hyoid arch, light green represents the gill basket; and dark green represents the operculogular series. Scale bar represents 10 cm.

Skull roof

Many of the margins between the dermal bones of the skull roof are not discernible in μCT tomograms and divisions are therefore distinguished based on external observation of the fossil. The geometry and position of sutures is approximate, as these show a deeply interdigitating pattern that appears confluent with the fibrous texture of individual bones.

A wedge-shaped bone of uncertain identity is sutured to the right anterolateral margin of the rostrodermethmoid (?Ant, Fig. 2.2*a*, Fig. 2.3*a, b*). The dorsal surface is smooth, and a narrow ridge along the anterior margin of the ventral surface (R, Fig. 2.3*c, d*) closely follows the anterior margin of the tentatively-identified premaxilla. The left posterior corner bears a small notch that aligns with a notch in the rostrodermethmoid (?Nar, Fig. 2.3*a, b*). These notches appear to be present on both sides of the rostrodermethmoid, and presumably frame the anterior naris. This bone shows no obvious indications of grooves or canals, but it is positionally equivalent to the antorbital.

The large rostrodermethmoid is broken into two pieces (Rde, Figs. 2.2*a, b,* 2.4*a, b*); when reconstructed, the complete bone is roughly diamond-shaped, broader anteriorly and gradually tapering to a posterior projection that extends between the frontals (Rde, Figs. 2.2*a, b,* 2.4*a, b*). Two shallow grooves extend along the dorsal surface of the rostrodermethmoid (Su.C, Fig. 2.3*a*), aligned with the long axis of the frontals and converging towards the midline anteriorly but not intersecting. I interpret these as indicating the course of the supraorbital sensory canals, which are ordinarily borne on the nasals. There is no indication of an ethmoid commissure.

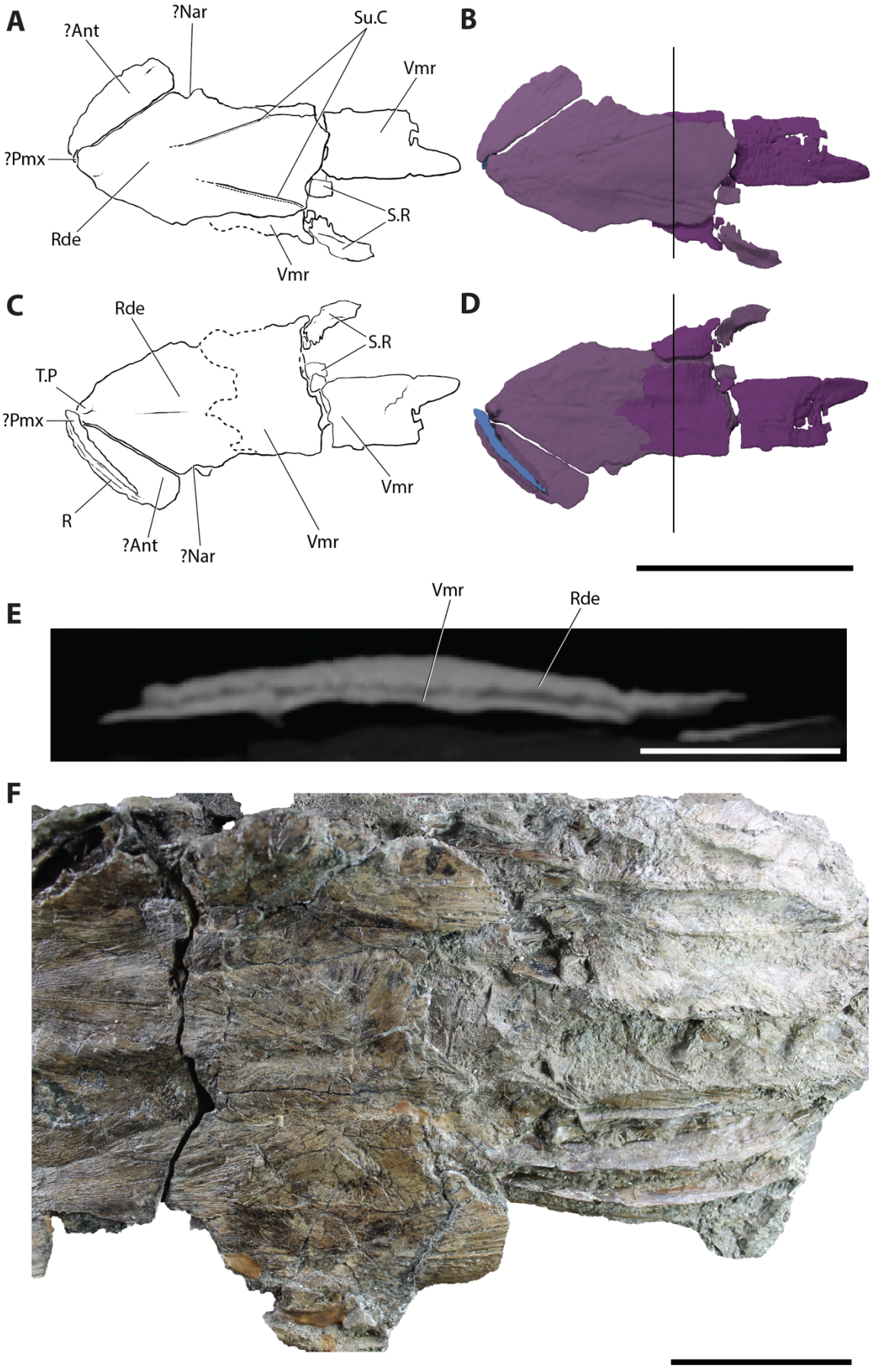

(figure legend on next page)

Figure 2.3 (previous page) – Anterior portion of the rostrodermethmoid and putative vomer and antorbital of *Martillichthys renwickae*, NHMUK PV P.61563. A) interpretive drawing in dorsal view. B) three-dimensional render in dorsal view. C) interpretive drawing in ventral view. D) three-dimensional render in ventral view. E) transverse cross-section through rostrodermethmoid and vomer. F) photograph of the posterior half of the skull roof, and the exposed gill skeleton. Black line in panels B and D indicates position of panel E. Dashed lines indicate where margins are uncertain. Anterior to the left in panels A–D, F. Purple is used to represent the neurocranium; dark blue represents the mandible, upper jaws, palate and orbit; light blue represents the hyoid arch, light green represents the gill basket; and dark green represents the operculogular series. Scale bar represents 5 cm.

The paired frontals are elongate. The mesial margin is straight, and each frontal gradually broadens posteriorly (Fr, Fig. 2.4*a, b*). The frontals are widest at roughly two-thirds of their length, at which point they are separated by a median gap (Fr.Gp, Fig. 2.4*a, b*). This gap extends to the posterior margins of the frontals. The frontals show no traces of sensory canals. A small triangular bone whose mesial margin sutures with the lateral margin of the right frontal might represent a fragment of the nasal, but bears no trace of grooves or a buried canal, making a positive identification difficult (?N, Figs. 2.2, 2.4; see below in 'Cheek, circumorbital bones and sclerotic ossicles').

The parietals are paired, rectangular bones that suture with one another along the midline, and with the frontals anteriorly. They are roughly one third of the length of the frontals (Par, Fig. 2.4*a, b*). The posterior margin of the skull roof has a scalloped margin, with projections formed by the posterolateral corners of the dermopterotics and posteromesial margins of the parietals at the midline (Fig. 2.3*f*). No obvious grooves are present on the dorsal surface of the parietals, which are smooth and unornamented.

Triangular dermopterotics flank the lateral margin of each parietal, and extend anteriorly to contact the posterior third of the lateral margin of each frontal (Dpt, Fig. 2.4*a, b*). The posterolateral corner of each dermopterotic is produced as a small posterior process that forms the lateral prong of the scalloped posterior edge of the skull roof (Fig. 2.4*a, b*).

Braincase, parasphenoid, and associated bones

The braincase is strongly dorsoventrally compressed and cannot be easily distinguished from the overlying skull roof in tomograms. It is similarly difficult to separate the braincase and parasphenoid, although the boundaries between the two are easier to identify in the orbital and ethmoid regions. Sutures between individual ossifications of the braincase are not visible, so only the general morphology of major regions of the braincase can be described. The ethmoid and sphenoid regions of the braincase are largely concealed by the skull roof dorsally, and the broad, spatulate anterior corpus of the parasphenoid ventrally (Fig. 2.4). Flattening of the skull is so severe that anatomy of the braincase can only be described in ventral view.

The anteroposteriorly extensive lateral ethmoids are visible as slender bands of bone extending beyond the lateral margins of the frontals and the parasphenoid (L.Eth, Fig. 2.4). The posterior edge of the lateral ethmoid defines the anterior margin of the orbit (Fig. 2.2*a, b*). There is no clear indication of the median ethmoid ossification, or any of its associated structures (e.g. nasal pits).

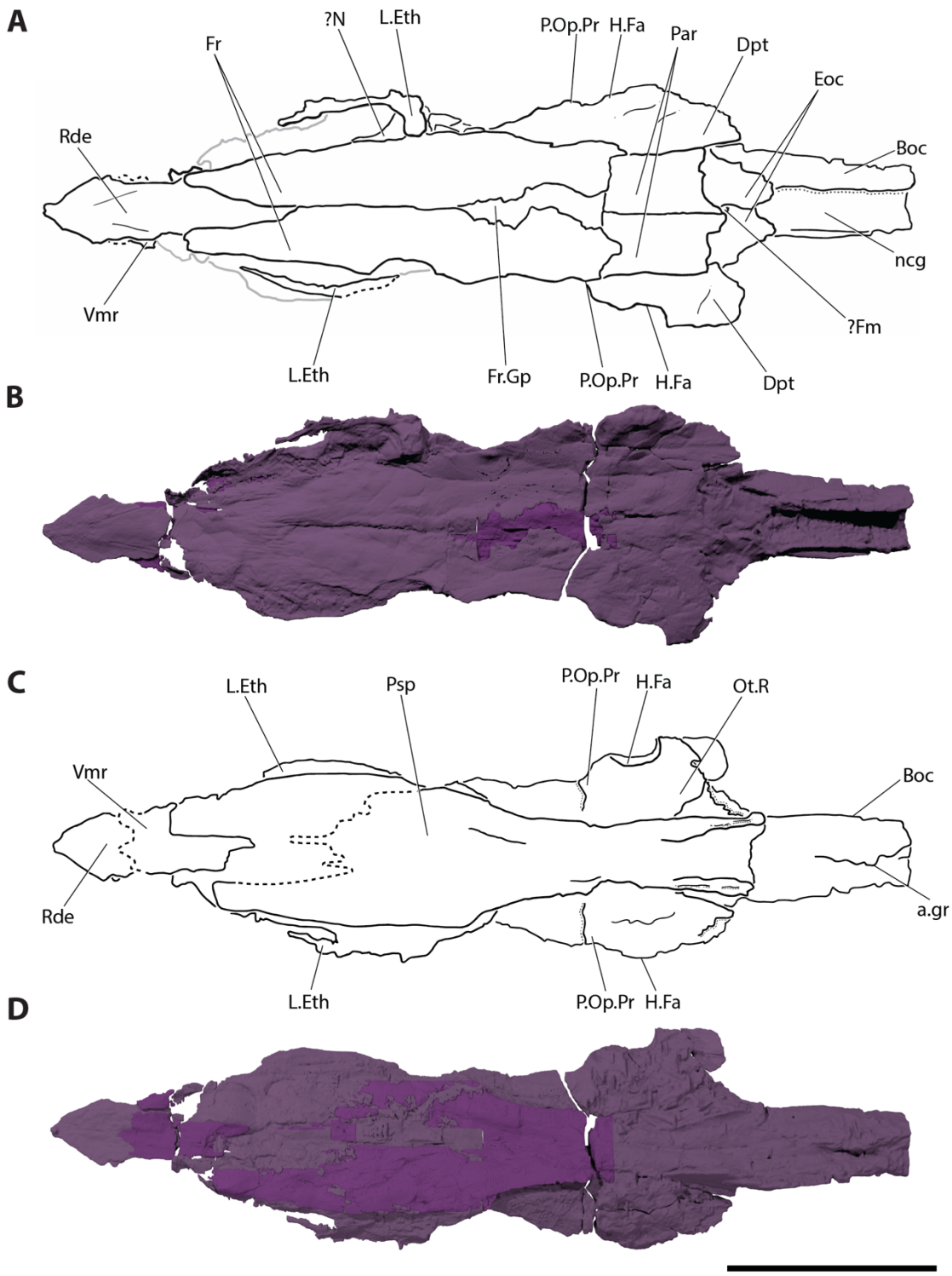

Figure 2.4 – Skull roof and braincase of *Martillichthys renwickae* NHMUK PV P.61563. A) interpretive drawing in dorsal view. B) three-dimensional render in dorsal view. C) interpretive drawing in ventral view. D) three-dimensional render in ventral view. Grey lines represent undefined structures and surrounding matrix. Dashed lines indicate areas where margins are uncertain. Purple is used to represent the neurocranium; dark blue represents the mandible, upper jaws, palate and orbit; light blue represents the hyoid arch, light green represents the gill basket; and dark green represents the operculogular series. Scale bar represents 10 cm for panels A–D and 2 cm for panel E.

The postorbital processes mark the rear margin of the orbit. Their relative position indicates a long preorbital region of the skull, with posteriorly-placed eyes (P.Op.Pr, Fig. 2.4*c, d*). The ventral surface of the otic region shows little detail. This portion of the braincase extends to the lateral edge of the dermopterotics, but has been flattened *post-mortem*. A strap-shaped facet for the articulation of the hyomandibula is visible near the lateral edge of the neurocranium on both sides of the skull (H.Fa, Fig. 2.4*c, d*). The occipital region is the only region of the neurocranium visible in both dorsal and ventral view. It is dominated by a long basioccipital 'stalk' (Boc, Fig. 2.4*a*), which protrudes from the posterior edge of the braincase and extends well beyond the rear margin of the skull roof. The stalk is truncated by breakage at the end of the specimen, and so would have been more extensive. A shallow groove for the dorsal aorta extends along the ventral midline of the stalk (a.gr, Fig. 2.4*c, d*), while its open, gutter-like dorsal surface presumably accommodated the notochord (ncg, Fig. 2.4*a, b*). Exoccipitals are visible dorsally, lying immediately posterior to the rear margin of the skull roof (Eoc, Fig. 2.4*a*, *b*) and flanking the foramen magnum (?Fm, Fig. 2.4*a, b*).

The parasphenoid is long and distinctive in shape. The broad, spatulate anterior corpus of the bone extends at least half of the overall length of the skull, but its anterior margins are not clear. The widest point of the anterior corpus is located at approximately mid-length, where it is equal in width to the frontals, but it is difficult discern the anterior margin of much of the parasphenoid due to the crushed nature of the specimen (Psp, Fig. 2.4*c*, *d*). The corpus becomes medially constricted in the orbital region of the skull. The ventral surface of the anterior corpus bears no obvious teeth or denticles, but is concave, forming an arched roof to the buccal cavity. The posterior stalk of the parasphenoid underlies the otic and

occipital regions of the braincase, although its margins are difficult to discern in μCT data. It appears that the parasphenoid only extends part of the length of the basioccipital stalk, terminating slightly posterior to the dermopterotic processes (Fig. 2.4*c, d*). The ascending process and basipterygoid process of the parasphenoid cannot be identified, nor can the presence or absence of foramina in the bone associated with basicranial circulation be established.

A thin, plate-like ossification lies anterior to the parasphenoid and ventral to the rostrodermethmoid. Although posteriorly distinguishable from the overlying braincase and skull roof (Fig. 2.4*e*), it is impossible to identify a boundary between these ossifications anterior to a point just behind the narial opening. A slight thickening at the anteriormost tip of the flattened skull roof and braincase (T.P., Fig. 2.3*c*, *d*) might be associated with this bone, and the shape of its posterior margin suggests that it may interdigitate with the parasphenoid. Based on its position ventral to the braincase and anterior to and at roughly the same level as the parasphenoid, I tentatively identify it as a median vomer (Vmr, Fig. 2.4*c*, *d*).

Upper jaw

The upper jaw is represented by the maxilla and premaxilla, and there is no indication of a supramaxilla. The maxilla is half the length of the mandible, and roughly three times as long as deep (Mx, Fig. 2.5). The maxilla is rod-like anteriorly, with a circular cross section, but flattens into a concave plate posteriorly, which is applied to the dorsolateral surface of the mandible (Fig. 2.5*a*). In lateral view, the maxilla bears a small prong at its posterodorsal

corner (P.Pr, Fig. 2.5*b-g*), and the anterior tip bears a small articular process (A.Pr, Fig. 2.5*b-g*). The anterodorsal margin has a slightly thickened ridge, which sits slightly above the rest of the dorsal margin of the bone (T.R, Fig. 2.5*b-g*). Due to disarticulation during preservation, it is unclear how the maxilla would have articulated with the rest of the skull (Fig. 2.2*a*, *b*).

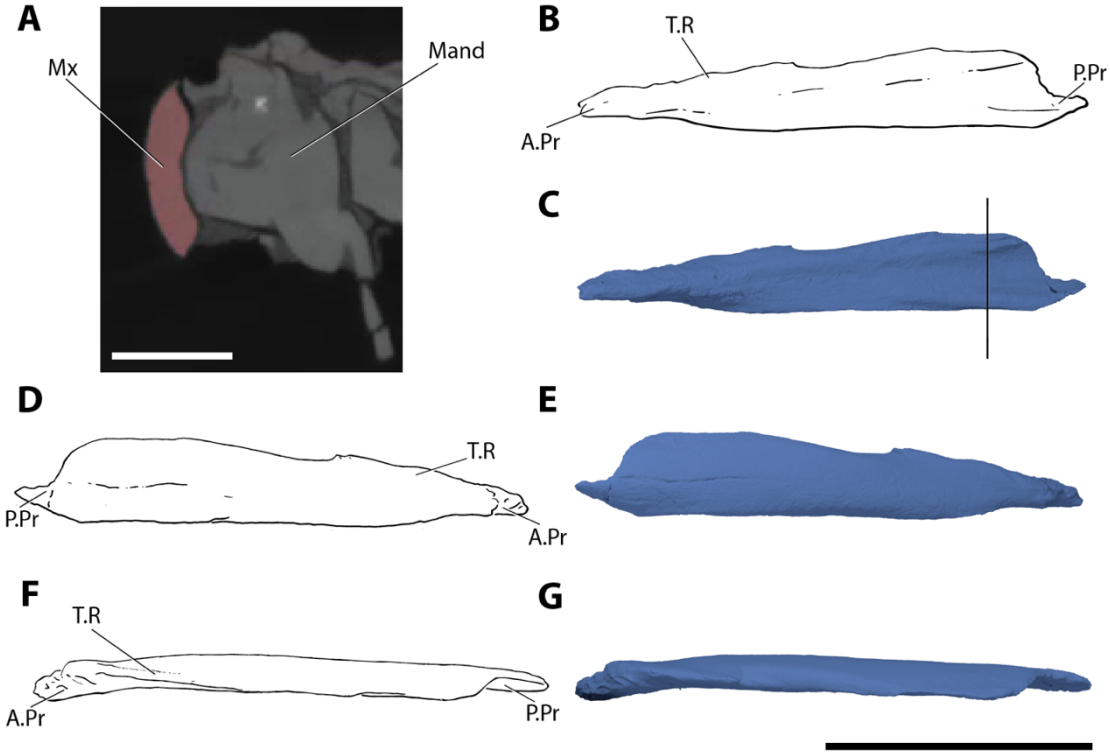

Figure 2.5 – Maxilla of *Martillichthys renwickae* NHMUK PV P.61563. A) transverse cross-section through maxilla. B) interpretive drawing of left maxilla in mesial view. C) three-dimensional render of maxilla in mesial view. D) interpretive drawing of left maxilla in lateral view. E) three-dimensional render of left maxilla in lateral view. F) interpretive drawing of left maxilla in dorsal view. G) three-dimensional render of left maxilla in dorsal view. Black line in panel C indicates position of panel A. Anterior to the left in panels B, C, F and G, and to the right in D and E. Scale represents 10 cm.

A splint-like bone, preserved underneath other dermal bones of the snout on the right side of the fossil, is interpreted as a premaxilla (?Pmx, Fig. 2.3*c, d*). The posterior and medial margins of the bone are incomplete. The preserved fragment is roughly two-thirds of the length of the antorbital, but its true length and width are difficult to discern.

Mandible

Five major bones contribute to the mandible: dentary, angular, surangular, prearticular and articular (Fig. 2.6). These are joined by what is apparently a single coronoid, although sutures between bones are difficult to resolve in tomograms (Fig. 2.6*a-c*).

The dentary is the principal bone on the outer face of the mandible (Dent, Fig. 2.6*d, e*). Each dentary is gently bowed anteriorly, meeting at a rounded symphysis, and a thumb-shaped depression lies near the anterior margin of each. The dentary contributes only a narrow band to the dorsal surface of the mandible, and this oral margin bears no teeth or denticles. The cross-sectional profile of the dentary is 'r'-shaped, with a mesial ridge abutting the lateral margin of the coronoid (Fig. 2.6*b, c*).

Posteriorly, the dentary sutures with the surangular and angular (Sang, Ang, Fig. 2.6*d-g*). In lateral view, the angular is long and wedge-shaped, roughly half the length of the dentary, and tapers to a point halfway along the mandible. The lateral surface of the angular bears two grooves, marking the path of the mandibular sensory canal, which extend parallel to the ventral margin of the jaw and continue on the dentary (MSC, Fig. 2.6*d, e*). The surangular forms the posterodorsal corner of the external surface of the jaw, and sutures with the

dentary anteriorly and the angular ventrally. Midway along the adductor fossa, the dorsal margin of the mandible bears a reduced coronoid process (Cor.Pr, Fig. 2.6*f, g*) composed solely of the surangular.

The wedge-shaped prearticular covers most of the mesial surface of the mandible (Part, Fig. 2.6*f, g*). It defines the anterior margin of the adductor fossa (Ad.F, Fig. 2.6*f, g*), meeting the surangular posterior to the coronoid process, and attaches to the articular posteriorly. The exposed surface of the prearticular is smooth, and free of denticles.

The coronoid series of *Martillichthys* appears to be represented by a single bone, with no visible sutures (Cor, Fig. 2.6*b, c, f, g*). The coronoid can be divided into two principal regions. The more anterior is a bulbous expansion that forms a deeply interdigitated, subvertical suture with the prearticular and a horizontal suture with the inner face of the dentary. The more posterior consists of a long, rod-shaped portion that lies dorsal to the dentary and prearticular, extending from approximately mid-length of the mandible to near the symphysis.

The articular lies at the posterior end of the jaw (Art, Fig. 2.6*d–g*). It is flanked laterally by the surangular and angular, and mesially by the prearticular. The articular defines the posterior margin of the adductor fossa, and bears a well-defined glenoid fossa for the articular condyle of the quadrate (Gl.F, Fig. 2.6*d-g*). The jaw joint is only slightly above the ventral margin of the mandible, and is oriented posteriorly.

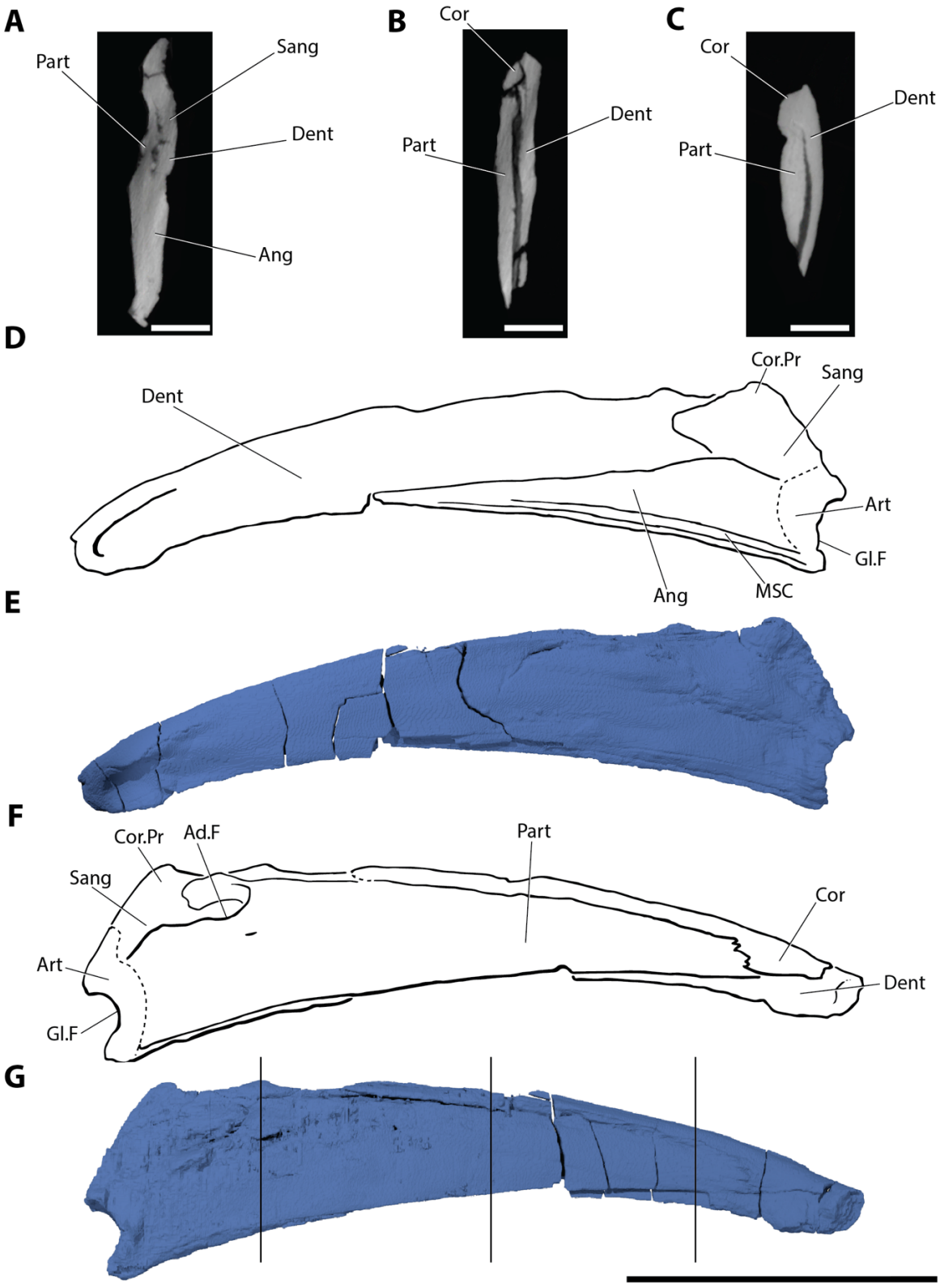

(figure legend on next page)

Figure 2.6 (left) – Mandible of *Martillichthys renwickae* NHMUK PV P.61563. A) transverse cross-section through mandible in the region of the adductor fossa. B) transverse cross-section through mandible at the approximate midpoint. C) transverse cross-section through mandible near anterior margin of coronoid. D) interpretive drawing of left mandible in lateral view. E, three-dimensional render of left mandible in lateral view. F) interpretive drawing of left mandible in mesial view. G) three-dimensional render of left mandible in mesial view. Black lines in panel G indicate position of panels A, B and C from left to right. Anterior to the right in panels F and G; to the left in panels D and E. Dashed lines indicate areas where margins are uncertain. Scale in panels A-C represent 1 cm, and 10 cm in panels D-G.

Gill skeleton

The basibranchials, hypobranchials, and ceratobranchials are preserved (Fig. 2.7*a, b*). Only a single, elongate basibranchial (?BbIII–IV; Fig. 2.7*a*) appears present, but its complex shape and position between multiple hypobranchials suggests that it may represent the fusion of multiple basibranchials.

Mineralized hypobranchials are only apparent for the first two branchial arches (HbI–II, Fig. 2.7*a, b*). Hypobranchial I is largely straight but curves gently towards its antimere, anterior to the basibranchial. The anterior region is expanded into an articular facet, and a ventral, longitudinal groove is visible posterior to this anterior expansion. Hypobranchial II is of a similar length and width to hypobranchial I, although the anterior end is less expanded and the ventral groove less defined.

Five ceratobranchials are present. A gap midway along their length represents a break in the specimen, and the posterior ends are truncated by the end of the block containing the skull

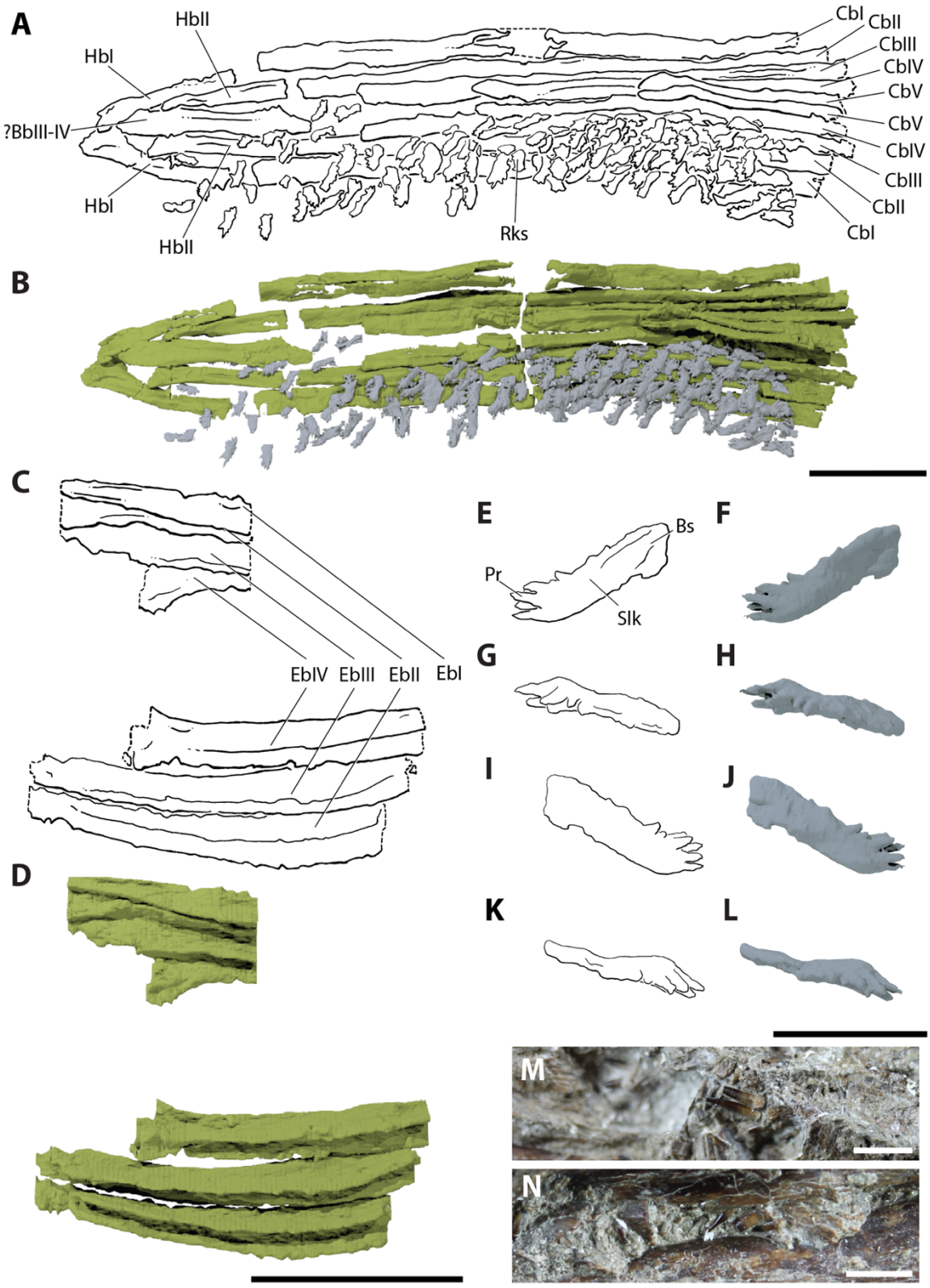

(figure legend on next page)

Figure 2.7 (left) – Dorsal and ventral gill skeleton and associated rakers of *Martillichthys renwickae* NHMUK PV P.61563. A) interpretive line drawing of ventral gill skeleton in dorsal view. B) three-dimensional rendering of ventral gill skeleton in dorsal view. C) interpretive line drawing of dorsal gill skeleton in dorsal view. D) three-dimensional rendering of dorsal gill skeleton in dorsal view. E) interpretive line drawing of raker in dorsal view. F) three-dimensional rendering of raker in dorsal view. G) interpretive line drawing of raker in anterodorsal view. H) three-dimensional rendering of raker in anterodorsal view I) interpretive line drawing of raker in ventral view. J, three-dimensional rendering of raker in ventral view. K) interpretive line drawing of raker in anteroventral view. L) three-dimensional rendering of raker in anteroventral view. M) photograph of gill raker teeth in dorsal view. N) photograph of gill raker teeth in dorsal view. Anterior to the left in panels A–F. Dashed lines indicate areas where margins are uncertain. Purple is used to represent the neurocranium; dark blue represents the mandible, upper jaws, palate and orbit; light blue represents the hyoid arch, light green represents the gill basket; and dark green represents the operculogular series. Scale bars for panels A–D represent 5 cm, 2 cm for panels E–L and 0.5 cm for panels M-N.

(CbI–V, Fig. 2.7*a, b*). Ceratobranchials I and II articulate with hypobranchials I and II respectively. There are substantial gaps between the anterior ends of the remaining ceratobranchials and the basibranchials, indicating that intervening hypobranchials were likely present but unmineralized. The first four ceratobranchials are morphologically similar. Each is a long, thin bone, about three times the length of the basibranchial. The ceratobranchials are 'n'-shaped in cross-section, with a longitudinal groove extending along the ventral side. The fifth ceratobranchials are the shortest of all the series, approximately half the preserved length of the fourth pair and a third of the length of the first (Fig. 2.7*a, b*).

In contrast to the ventral gill skeleton, which is truncated posteriorly, the dorsal gill skeleton appears to be largely complete within the block containing the skull (EbI–IV, Figs. 2.2*a, b*, 2.7*c, d*). Four pairs of epibranchials are present on the right side of the specimen, but only three are preserved on the left (Fig. 2.7*c, d*). However, only the posterior portion can be observed, and as such the presence or absence of uncinate processes cannot be determined. The epibranchials are shorter than the ceratobranchials, and each is shorter than the element anterior to it. Apart from this difference in size, each ceratobranchial shows a broadly similar morphology: slender with a pronounced dorsal groove giving the bone a 'u'-shaped cross-section.

Tooth plates have not been observed in association with the gill skeleton, but numerous elaborate gill rakers are present (Rks, Fig. 2.7*a, b, e–n*). Each raker comprises a long, club-shaped stalk (Liston 2013) that articulates with the gill skeleton, and bears elongate, pointed projections. The length of each projection is understated in μCT renders due to limitations associated with a large (126 μm) voxel size, but the true length — up to 0.5 cm — is apparent from external consideration of the fossil (Fig. 2.7*a, b, e–n*). The rakers are directed anterolaterally, and are oblique to the rest of the gill skeleton (Fig. 2.7*a, b*). They are relatively large, roughly a fifth of the length of the hypobranchials, and extremely numerous: at least 110 are present. The projections extend from the anterior margin of each raker along roughly a quarter of the length (Fig. 2.7*e–m*). Based on the regular spacing between some of the rakers, and their alignment with the ventral ceratobranchials, I estimate that there are approximately 15 rakers per ventral gill arch.

Hyoid arch and palate

The hyoid arch of *Martillichthys* comprises hypohyals, anterior and posterior ceratohyals, interhyals, and hyomandibulae. The hypohyals are laterally flattened, with a rounded profile, and lie close to the midline of the fossil (Hhy, Fig. 2.8*a, b*). Each hypohyal curves gently towards its antimere. Approximately halfway along the ventral edge, a small foramen marks the course of the afferent hyoid artery (AH.A.F, Fig. 2.8*a, b*).

The hypohyals articulate with the elongate anterior ceratohyals posteriorly (A.Chy, Fig. 2.8*a, b*). These are roughly four times the length of the hypohyal and nearly half the length of the entire skull (Fig.2*c, d*). They are straight and laterally compressed, with a medial constriction. A longitudinal groove extending along the posterior half of the lateral face of each ceratohyal indicates the path of the afferent hyoid artery (AH.A.G, Fig. 2.8*a, b*).

The posterior ceratohyals articulate with the anterior ceratohyals (P.Chy, Fig. 2.8*a, b*), and are wedge-shaped, matching the depth of the anterior ceratohyals anteriorly but tapering posteriorly. The longitudinal grooves of the anterior ceratohyals continue on to the posterior ceratohyals.

The trapezoidal interhyals are the smallest bones of the hyoid arch, and lie between the posterior ceratohyal and the ventral portion of the hyomandibula (Ihy, Fig. 2.8*a, b*). The interhyal on the right side appears to be more completely preserved (Fig. 2.2*c, d*).

The following bones of the suspensorium are preserved on the left side of the specimen: the entopterygoid, metapterygoid, ectopterygoid, quadrate and symplectic (Fig. 2.8*c, d*). Only the quadrate, symplectic, and hyomandibula are present on the right side of the skull.

The quadrate (Quad, Fig. 2.8*c*, *d*) is dominated by its well-developed articular head (MQ.J, Fig. 2.8*c, d*). The posteroventral margin of the bone bears a sharp notch approximately a third of the way along its length, into which the rod-like symplectic inserts. The symplectic is approximately the same length as the quadrate but half as wide until the posterior third, which is twice as wide as the rest. Both the right and left symplectic are broken approximately two-thirds of the way along their length (Sym, Fig. 2.8*c, d*).

The toothless ectopterygoid is boomerang-shaped (Ectp, Fig. 2.8*c, d*). The broad posteroventral limb forms a tight sutural connection with the anterodorsal margin of the quadrate. The anterodorsal limb is more slender, and terminates in a pointed tip. The metapterygoid has broken into three pieces: one applied to the quadrate and ectopterygoid; one lateral to the entopterygoid and separated from the more anterior bone by a small crack (Mpt, Fig. 2.8*c*, *d*); and one separated by a further small gap and applied to the anterior margin of the hyomandibula (Fig. 2.2*c, d*). The oval entopterygoid contacts the ectopterygoid ventrally and the metapterygoid posteriorly (Entp, Fig. 2.8*c, d*). The inner surface of the entopterygoid is smooth, with no evidence of denticles.

The hyomandibula is plate-like, roughly rectangular in shape and lies on a slightly diagonal axis relative to the remainder of the skull (Hyo, Figs. 2.2*c, d*, 2.8*a, b*, e–*h*). It is medially

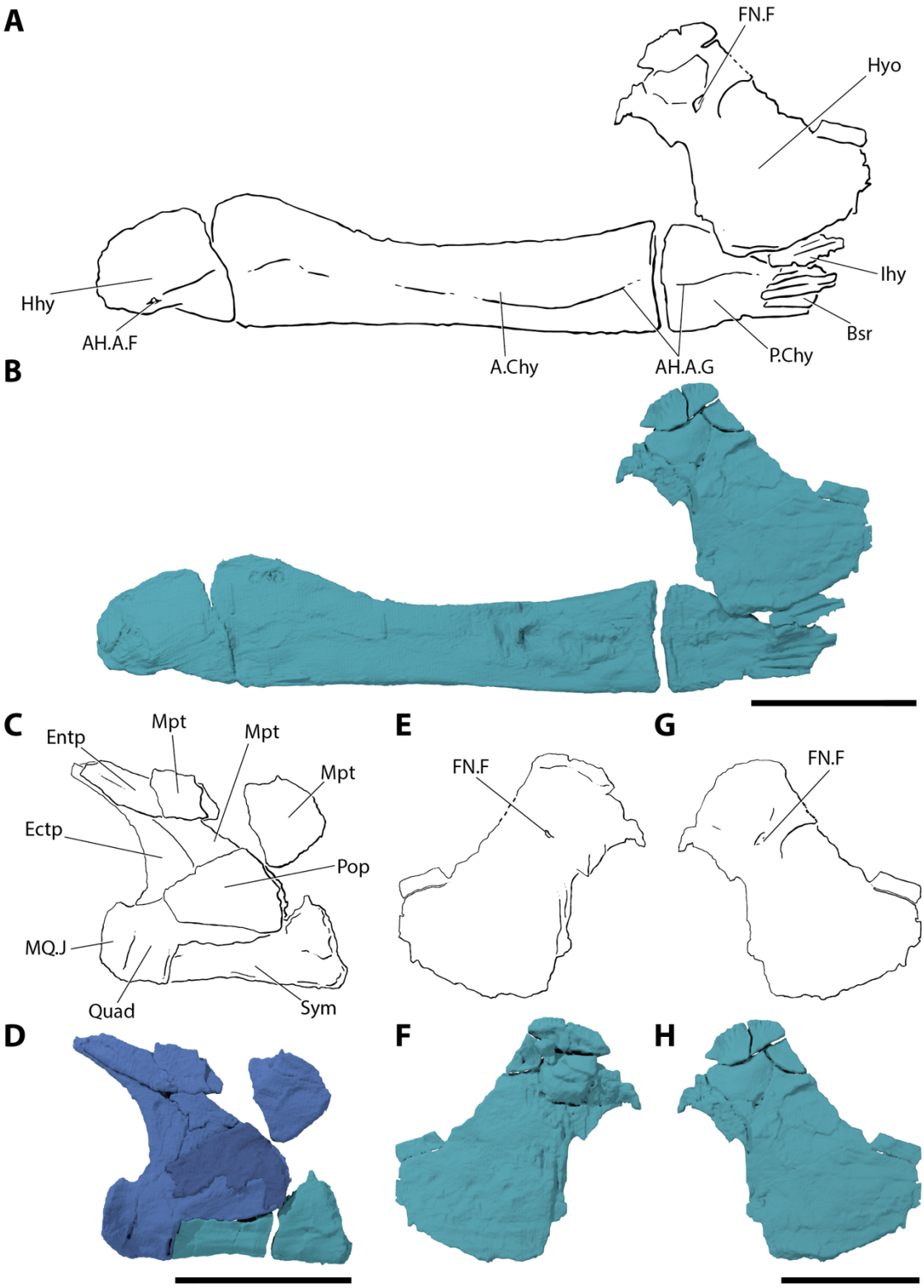

(figure legend on next page)

Figure 2.8 (previous page) – Hyoid arch and palate of *Martillichthys renwickae* NHMUK PV P.61563. A) interpretive line drawing of the left hyoid arch in lateral view. B) three-dimensional rendering of the left hyoid arch in lateral view. C) interpretive line drawing of the left palate in lateral view. D) three-dimensional rendering of the left palate in lateral view. E) interpretive drawing of the left hyomandibula in mesial view. F) three-dimensional render of the left hyomandibula in mesial view. G, interpretive drawing of the left hyomandibula in lateral view. H) three-dimensional render of the left hyomandibula in lateral view. Dashed lines indicate areas where margins are uncertain. Dark blue represents the ectopterygoid, entopterygoid, metapterygoid; navy represents the preoperculum; and light blue represents the hyomandibula, ceratohyals, interhyal and symplectic. Scale bars represent 5 cm.

constricted, with a waisted appearance in lateral view (Fig. 2.8*e*–*h*), and the distal end is expanded to a much greater degree than the proximal head. Although not preserved, a thickened ridge of bone in the posterodorsal portion of the hyomandibula, identified through external analysis, suggests that an opercular process was originally present. A foramen in the upper third of the bone marks the passage of the hyomandibular branch of the facial nerve (FN.F, Fig. 2.8*a*, *b*).

Cheek, circumorbital bones and sclerotic ossicles

Preserved components of the cheek include the infraorbitals, suborbitals, dermosphenotic and preoperculum, as well as fragments of dermal bone that are harder to identify. On the left side of the fossil, midway along the orbit, a square fragment of bone articulates with the lateral margin of the frontal. Comparison to other pachycormids indicates that a dermosphenotic identity is most likely, although the lack of a sensory canal means that a supraorbital identity cannot be discounted (?Dsp, Fig. 2.2). Multiple bones surrounding the orbit are preserved on the right side of the skull, but are displaced from life position (Fig.

2.9). The dermosphenotic is broken into two pieces, but indicates that the complete bone would have framed the posterodorsal and dorsal margins of the orbit (Dsp, Fig. 2.9*a*, *c*-*d*). As preserved, the bone appears triradiate, with a long anterior arm and short posterior and ventral arms; the dorsal margin of the anterior arm closely matches the lateral margin of the skull roof in the orbital region. A portion of the sensory canal is visible on the posterior fragment of the dermosphenotic (S.C., Fig. 2.9*c*-*d*). At least two plate-like bones lie posterior to the orbit, with four more slender ossifications spread across the orbital region. The larger, more posterior bones are interpreted as possible suborbitals (?Sor, Fig. 2.*9b*). Two curved bones in the middle of the orbital region represent an incomplete sclerotic ring. The larger ossicle is approximately one-eighth of the overall skull length (D.Sco, Fig. 2.9). The smaller ossicle appears to be broken (V.Sco, Fig. 2.9). The remaining splint-like bones in the orbital region are likely infraorbitals (?Ior, Fig. 2.9*a, c*-*d*).

A small fragment of the preoperculum is preserved on both sides of the skull (Pop, Fig. 2.8*c, d*). It is thin, closely applied to the lateral surface of the quadrate, and bears a fimbriate posterior margin. No canals or grooves for the preopercular sensory canal are visible.

Operculogular series

The operculogular series consists of the gular plate, branchiostegal rays, operculum and suboperculum. From external analysis, at least 27 branchiostegal rays are present between the hypohyal and anterior ceratohyal, with the series extending along the posterior ceratohyal (Bsr, Figs. 2.1*a*, 2.8*a*, *b*). A total count is not possible, and due to their thinness the branchiostegals are not visible in tomograms or associated renders.

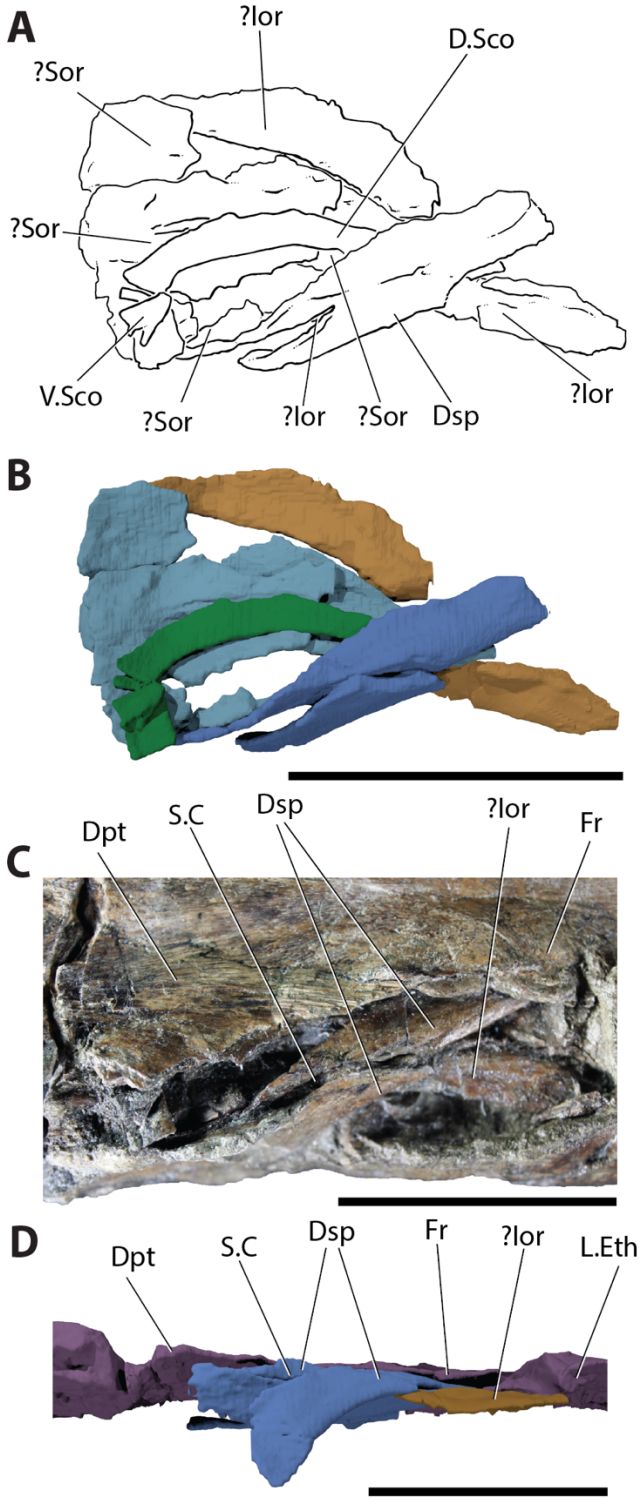

Figure 2.9 – Sclerotic ossicle and circumorbital bones of *Martillichthys renwickae* NHMUK PV P.61563. A, interpretive drawing of right orbital region in dorsal view. B, three-dimensional render of right orbital region in dorsal view. C, photograph of right orbital region in dorsal view. D, three-dimensional render of right orbital region in lateral view. Anterior to the right. Scale bar represents 5 cm.

The gular plate lies immediately posterior to the mandibular symphysis and ventral to the rostrodermethmoid (Gul, Fig. 2.2*c*, *d*). The plate is exceedingly thin near its posterior margin, and terminates with a ragged edge. It is possible that the bone extended further posteriorly, but this weakly mineralised portion was either not preserved or lost during specimen preparation. This posterior region is too thick to be visualized in tomograms, and while visible externally (Fig. 2.1*a*) it is not apparent in renders (Fig. 2.2*c*, *d*) As preserved, it extends approximately half the length of the intermandibular space, covering the hypohyals (Fig. 2.1*a*). By contrast, the thicker region of this bone that is apparent in tomograms is restricted anterior to the hypohyals (Fig. 2.2*c*, *d*). A series of ridges and grooves cover the gular plate, radiating from a smooth region at the center of the ventral surface of the bone (Fig. 2.2*c, d*).

The plate-like operculum and subopercular are preserved on the left side of the fossil, but their margins are incomplete, in addition to being posteriorly truncated (Fig. 2.2*c, d*). The operculum (Op, Fig. 2.2*c, d*) slightly overlaps the dorsal edge of the subopercular. The subopercular terminates posterior to the rounded posterior margin of the hyomandibula (Sop, Fig. 2.2*c, d*). Due to incomplete preservation, little can be said about the relative sizes of these bones.

Discussion

Revisions and additions to previous descriptions

My study of *Martillichthys* provides new information on previously concealed internal anatomy, as well as clarifying some aspects of features only partially exposed at the surface

of the specimen. This permits an update of some anatomical interpretations of *Martillichthys* given in earlier accounts (Martill 1991; Liston 2008*a*).

Skull roof. Re-examination of the specimen permits clarification of several features of the skull roof. I identify a gap between the frontals in *Martillichthys*. A similar opening has been identified between the frontals of the Late Cretaceous pachycormiform *Rhinconichthys taylori* (Schumacher *et al.* 2016), and as either extending between the parietals, or being restricted between the parietals, in *R. uyenoi* and *R. purgatoirensis* respectively (Schumacher *et al.* 2016, fig. 8). Geometry of the frontals suggest that a similar gap might also have been present in *Bonnerichthys* (Friedman *et al.* 2010), although separation between skull roofing bones in this taxon raises questions about equivalence of the condition. Such a gap has not been reported in *Asthenocormus* (Lambers 1992), and is absent in tooth-bearing pachycormiforms. I also find that the rostrodermethmoid of *Martillichthys* is diamond-shaped rather than triangular, and that the dermopterotic extends anterior to the transverse suture between the frontals and parietals rather than terminating at the level of this junction (Liston 2008*a*). This is in broad agreement with conditions in most other pachycormiforms and outgroups.

My interpretation of the identity, geometry, and arrangement of bones contributing to the snout also differs from previous accounts. Liston (2008*a*) interpreted the rostrodermethmoid of *Martillichthys* as a narrow, triangular bone, contacting the frontals via a transverse suture and excluded from the gape by long, slender nasals that contacted one another at the midline. Based on my scan data, I reinterpret the sutures between the rostrodermethmoid and nasals

as grooves for the supraorbital sensory canals, borne entirely on the body of the rostrodermethmoid. This brings the overall geometry of the rostrodermethmoid more into line with that seen in other pachycormiforms, where this bone contacts the upper jaw. Presence of the supraorbital sensory canal on the rostrodermethmoid suggests either migration of this canal from the nasal to the rostrodermethmoid, or fusion of the nasal and its associated canal with the rostrodermethmoid (see below). Among pachycormiforms, a rostrodermethmoid bearing the supraorbital canal is also found in *Bonnerichthys* (Friedman *et al.* 2010), although in that taxon the canal is buried in the bone in a thickened ridge rather than lying superficially. I also find that the rostrodermethmoid bears a long posterior process that extends between the two frontals, rather than meeting those bones along a gently scalloped margin.

The presence of the presumed supraorbital canal on the rostrodermethmoid complicates the interpretation of more lateral bones of the snout. However, based on conditions in other stem teleosts (e.g. *Dorsetichthys bechei*: Rayner 1948; *Pachycormus macropterus*: Lehman 1949; Mainwaring 1978), I agree with Liston (2008*a*) that the ovoid bone on the right side of the snout is a probable antorbital. Much of Liston's (2008*a*) proposed nasals are, according to my revised interpretation, parts of the rostrodermethmoid. I am only able to identify fragments of dermal bone along the margin of the right frontal as a possible nasal.

Paired vomers are known in the tooth-bearing pachycormiforms *Pachycormus* (Lehman 1949, fig. 4; Mainwaring 1978, fig. 7), '*Hypsocormus*' ('*H.*' *tenuirostris*; Martill 1991, fig. 9.6b), *Orthocormus* (reported as *Hypsocormus* in Rayner 1948, fig. 16), and *Protosphyraena* (Felix

1890, pl. 14; Loomis 1900, pl. 14; Hay 1903, fig. 1). In these taxa, the vomers are splint-like, with their long axes oriented anteroposteriorly. The vomers contact along at least part of their length, and are tightly sutured to one another mesially and, in some taxa, to the parasphenoid dorsally. In some cases, the vomers are so intimately bound to one another and the parasphenoid that their margins are difficult to discern. Vomers have not been previously been identified in *Martillichthys* or any other edentulous pachycormiform. While the structure I interpret as a vomer in *Martillichthys* is median, it is possible that it is composed of paired bones that are too tightly joined to be distinguished in my relatively low-resolution scan. The vomer(s) of *Martillichthys* do not appear to have a thickened transverse ridge at the anterior margin of the bone, a feature that is ubiquitous among tooth-bearing pachycormiforms.

Upper jaw. The premaxilla was previously unknown in *Martillichthys*. However, I interpret the incompletely-preserved ossification buried beneath the antorbital and contributing to the oral margin of the upper jaw as representing this bone. The position of the putative premaxilla might also be consistent with a vomer (but see above), but the shape of the bone and its overall proportions broadly match the ventrolateral extension of the rostrodermethmoid of *Bonnerichthys*, interpreted by Friedman *et al.* (2010: 991, fig. 2; pers. obs. of cast of KUVP 60692) as a fused premaxilla. The structure of premaxillae in edentulous pachycormiforms remains poorly known.

As in other pachycormiforms, the maxilla of *Martillichthys* bears an embayment at its posterodorsal corner. This notch marks the position of the supramaxilla in taxa where the

bone is present. I have found no trace of a supramaxilla in *Martillichthys*, but this notch is a persistent feature despite the possible loss of the bone that it accommodates in other pachycormiforms. Apart from the absence of teeth, the most striking difference between the maxilla of *Martillichthys* and most other pachycormiforms is the overall geometry of the bone. The maxillae of *Protosphyraena* (FHSM VP-3251) and *Pachycormus* (NHMUK PV 32433) are more slender than that of *Martillichthys*, and the anterior articular process more spur-like.

Mandible. Previous accounts of external anatomy of the lower jaw are largely accurate, although I disagree with past interpretations of the mandible as being structurally very different from that of other pachycormiforms (Liston 2008*a*: 186). The major exception is the groove reported by Liston (2008*a*) as a suture between the external dermal bones of the mandible and the prearticular, which instead marks the course of the mandibular sensory canal. The prearticular is confined entirely to the mesial surface of the mandible and is not visible in lateral view. μCT data provides the first clear picture of this bone, along with the coronoid and adductor fossa.

Gill skeleton. The most substantial update to the morphology of the branchial arches relates to the anatomy of the gill rakers and their associated projections. Liston (2008*a*, 2013) reported the presence of rakers and fine raker fimbriations in *Martillichthys*, but concluded that tooth-like extensions from the rakers were absent. However, tomograms reveal that elongate, pointed raker projections similar to those reported in *Asthenocormus* (Lambers 1992: 212; questioned by Liston 2013: 137) are present in *Martillichthys* (Pr; Fig. 2.10), rather

than the finer fimbriations or oblique edges associated with *Leedsichthys* (Fim; Fig. 2.10; Liston 2013; Liston 2008*b*; Gouiric-Cavalli 2017, fig. 2). The presence of these tooth-like projections is also apparent from external observation, refuting past claims that such structures belonged to scavengers rather than *Martillichthys* itself (Liston 2008*a*: 191). It is also clear that there is variation between taxa in the geometry of the stalk of the raker (Slk; Fig. 2.10), which is club-like in *Martillichthys* but appears to taper to a point distally in most material attributed to *Leedsichthys* (Liston 2006, figs. 6.1–6.7; Liston 2013, fig 1; Gouiric-Cavalli 2017, fig. 2). While it is possible to determine that the rakers reported in *Asthenocormus* (Lambers 1992, 212, pl. 2*b*) are more morphologically similar to those reported in *Martillichthys* than *Leedsichthys*, they are not complete enough for a more direct comparison.

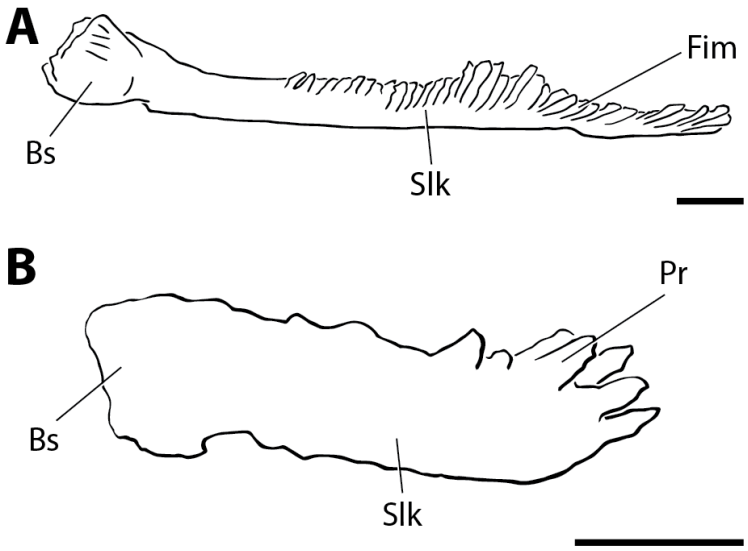

Figure 2.10 – Comparative gill-raker morphology of *Leedsichthys* and *Martillichthys*. A, interpretive drawing of gill rakers found in *Leedsichthys* (modified from Liston 2013, Fig. 1F; NHMUK P.6921) in lateral view. B, interpretive drawing of gill rakers found in *Martillichthys*, NHMUK PV P.61563. Purple represents the neurocranium; light blue represents the suborbitals; orange represents the infraorbitals; dark blue represents the dermosphenotic; and green represents the dorsal and ventral sclerotic ossicles. Scale bars represent 1 cm.

μCT data also adds detail to the gill skeleton, including the presence of a large basibranchial possibly representing the fusion of III and IV (cf. *Pachycormus* as described by Mainwaring 1978, fig. 13). The absence of basibranchial II indicates that it was cartilaginous, as inferred for other pachycormiforms (e.g. Mainwaring 1978). In addition, I find that the fourth epibranchials identified by Liston (2008*a*, fig. 3) instead represent the dorsal margins of the occipital stalk of the braincase.

Hyoid arch and palate. My interpretation of the ventral hyoid arch substantially revises that of Liston (2008*a*), which reported minute hypohyals, short anterior ceratohyals, and exceptionally long posterior ceratohyals, roughly the length of the mandible. Instead, I find that the geometry of the ventral hyoid arch in *Martillichthys* more closely agrees with generalized neopterygian conditions in having short hypohyals and posterior ceratohyals in combination with long anterior ceratohyals (Olsen 1984; Grande and Bemis 1998; Grande 2010). In addition to these updated bone identifications, my scans reveal the presence of an interhyal that is not apparent from external examination.

Cheek, circumorbital bones and sclerotic ossicles. The identity of the disarticulated bones within the orbit requires some discussion. Previous descriptions of *Pachycormus* have identified "at least 10" (Mainwaring 1978: 16) and "at least 11" (Lehman 1949: 10) long, rectangular bones posterior to the orbit as infraorbitals. This arrangement of numerous narrow infraorbitals is generally taken as common to all pachycormiforms, but can only be shown convincingly in a few taxa (e.g. *Euthynotus*: Wenz 1967, fig. 67; *Hypsocormus insignis*: Woodward 1895*a*, fig. 40; '*Hypsocormus*' *macrodon*: Lambers 1992, fig. 17; possibly

Protosphyraena: Felix 1890, pl. 12). By contrast, larger, plate-like bones posterior to the infraorbitals represent suborbitals (Lehman 1949, fig. 2; Mainwaring 1978, fig. 2). Therefore, I interpret the slender, more anteriorly placed orbital bones of *Martillichthys* as infraorbitals (?Ior, Fig. 2.9) and the plate-like bones as suborbitals (?Sor, Fig. 2.9). However, the disruption of their position and the lack of any canals makes these identifications speculative. By contrast, the presence of a sensory canal, combined with the geometry of the bone, clearly establishes the identity of the dermosphenotic. Neither infraorbitals nor suborbitals were identified by Liston (2008*a*), while part of a possible infraorbital was interpreted as a supraorbital (Liston 2008*a*, fig. 3).

Operculogular series. Previously described as having small paired gulars, *Martillichthys* conforms to the general pachycormiform condition in bearing a single large, median gular. The gular commences immediately posterior to the jaw symphysis, encompassing a bone fragment previously interpreted as belonging to the parasphenoid (Liston 2008*a*, fig. 4), and extends posteriorly as a thin, fragmented sheet that covers the anterior half of intramandibular space.

Phylogenetic placement of Martillichthys

Characters resolving Martillichthys *as a pachycormiform.* The monophyly of Pachycormiformes is well-supported by numerous studies that show broad agreement concerning the features uniting the clade (Patterson 1975; Mainwaring 1978; Lambers 1992; Arratia 2004; Liston 2008*a*; Friedman *et al.* 2010; Friedman 2012*a*; Arratia & Schultze 2013; Wretman *et al.* 2016). From this study, I can confirm the following features support the

placement of *Martillichthys* as a pachycormiform (Fig. 2.11; node 1): (1) a compound rostrodermethmoid forming the anterodorsal border of the mouth (*contra* Liston 2008*a*, who interpreted midline contact between the nasals excluding the rostrodermethmoid from the gape); (2) a reduced coronoid process of the mandible; (3) absence of supraorbitals (with the dermosphenotic separating the orbit from the skull roof); and (4) elongate pectoral fins; with (5) distinctive distally bifurcating, asymmetrical, lepidotrichia.

The following features support the placement of *Martillichthys* as an edentulous pachycormiform (Fig 10; node 2): (1) absence of marginal dentition; (2) lack of ornamentation on the dermal bones of the skull; (3) absence of a supramaxilla; (4) broad anterior corpus of the parasphenoid (unlike the narrow corpus reported in *Pachycormus* and most other tooth-bearing pachycormiforms, a broad corpus of the parasphenoid is also seen in *Saurostomus*, which is interpreted as a close relative of edentulous pachycormiforms; Wenz 1967, fig. 65); (5) posterior margin of the parietals form a median projection (unknown in *Bonnerichthys*); (6) absence of a posterior boss on the skull roof (unknown in *Bonnerichthys*); (7) a reduction or loss of scales; and (8) reduction or absence of segmentation in caudal-fin rays (also seen in *Protosphyraena*; McClung 1908; Arratia & Lambers 1996). To this, I add: (9) a gap between the frontals (present in *Rhinconichthys*, equivocal in *Bonnerichthys*, uncertain in *Asthenocormus*; Schumacher *et al.* 2016). A thickened ridge on the lateral surface of the maxilla has previously been cited as a synapomorphy of edentulous pachycormiforms (Friedman *et al.* 2010; Friedman 2012*a*), but this character is highly subjective, and I do not regard it as strong evidence for monophyly of the group.

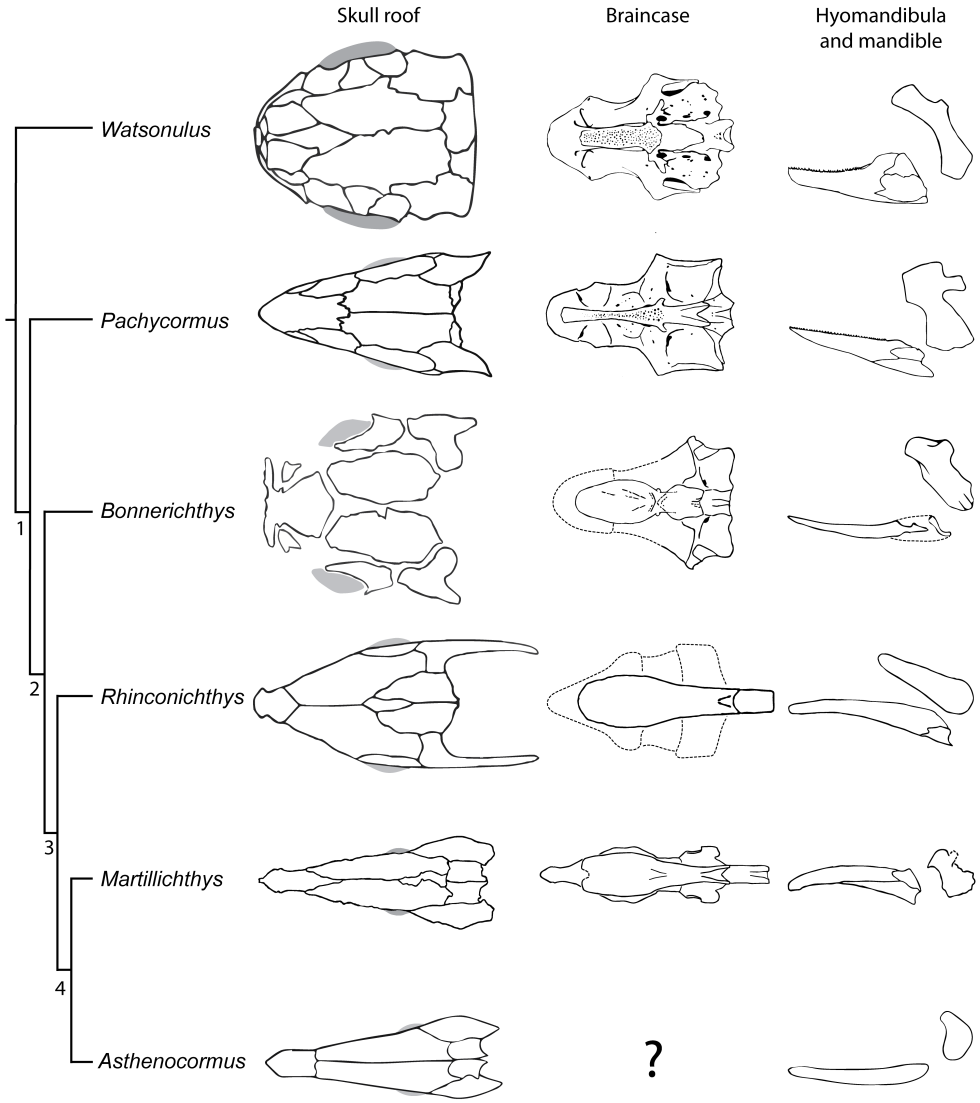

Figure 2.11 – Hand-drawn cladogram showing pachycormiform relationships, with comparisons of major aspects of cranial anatomy. Relationships based on Friedman (2012*a*) and argumentation given in text. Stippling on the parasphenoid indicates extent of the denticle field, if present. Shading indicates placement of eyes. Dashed lines indicate areas where margins are uncertain. Node 1: compound rostrodermethmoid; reduced coronoid process; absence of supraorbitals; elongate pectoral fins; bifurcating, asymmetrical, lepidotrichia. Node 2: absence of marginal dentition; lack of ornamentation on skull bones; absence of a supramaxilla; broad anterior corpus of parasphenoid; posterior margin of parietals form median projection; absence of skull roof posterior boss; reduction/loss of scales; reduction/loss of caudal fin segmentation; gap between frontals. Node 3: elongated occipital stalk; elongated, ornamented gill rakers. Node 4: waisted hyomandibula; highly reduced posterior dermopterotic process; elongated pre-orbital region; and a short hyomandibula. *Asthenocormus* redrawn from Lambers (1992); *Bonnerichthys* redrawn from Friedman *et al.* (2010); *Pachycormus* redrawn from Lehman (1949) and Mainwaring (1978); *Rhinconichthys* redrawn from Friedman *et al.* (2010) and Schumacher *et al.* (2016); *Watsonulus* redrawn from Olsen (1984).

Interrelationships of Martillichthys *and other edentulous pachycormiforms.* Despite limited understanding of most taxa, there are multiple characters that show variable states among edentulous pachycormiforms and might therefore provide clues to their interrelationships. Here I consider the implications of these features, polarizing traits based on conditions observed in proximal (*Pachycormus*: Lehman 1949; Patterson 1975; Mainwaring 1978) and more distal (the early crown neopterygian *Watsonulus*: Olsen 1984) outgroups. I restrict my considerations to edentulous pachycormiforms with the best-known skeletal anatomy: *Asthenocormus* (Lambers 1992), *Bonnerichthys* (Friedman *et al.* 2010), *Martillichthys* (Liston 2008*a*; this study) and *Rhinconichthys* (Friedman *et al.* 2010; Schumacher *et al.* 2016). Less completely known taxa are discussed in the following section.

My study has both corroborated existing (Friedman *et al.* 2010; Friedman 2012*a*; Wretman *et al.* 2016) and suggested additional synapomorphies uniting edentulous pachycormiforms to the exclusion of *Bonnerichthys* (Fig 10; node 3): (1) elongated occipital stalk (uncertain in *Asthenocormus*); and (2) elongated gill rakers possessing ornamentation such as pointed projections or fimbriations.

Friedman (2012*a*) suggested two characters uniting *Asthenocormus* and *Martillichthys* to the exclusion of other edentulous pachycormiforms. First is the presence of (1) a medially-constricted, or waisted, hyomandibula, which contrasts with the more 'slab-sided' hyomandibulae of *Bonnerichthys* and *Rhinconichthys*. However, the reliability of this character is unclear; a waisted hyomandibula is also present in other pachycormiforms, such as *Pachycormus*, and there is a degree of ambiguity in delimiting the contrasting states of

this character. Second, and perhaps more reliably, (2) the posterior process of the dermopterotics is reduced in *Martillichthys* and *Asthenocormus* relative to other pachycormiforms, a condition that contrasts with the extremely long and narrow posterior processes found in *Rhinconichthys* (Fig. 2.11). To these, I add two characters relating to overall skull geometry highlighted in my study of *Martillichthys*: (3) an elongated pre-orbital region (compared with a proportionally shorter pre-orbital region in *Bonnerichthys*, *Rhinconichthys* and outgroups); and (4) a short hyomandibula relative to the mandible, comprising less than one third of the lower jaw length (compared with a hyomandibula greater than one third of the length of the mandible in *Bonnerichthys*, *Rhinconichthys* and outgroups).

Set against these characters suggesting a close relationship between *Martillichthys* and *Asthenocormus*, I note other features shared that could suggest alternative hypotheses. First is the proposal by Schumacher *et al.* (2016) that *Martillichthys* and *Rhinconichthys* might be united by a form of prognathy, with the mandibular symphysis extending beyond the anterior tip of the rostrodermethmoid. I am not convinced that life positions of these structures can be meaningfully assessed in available material of *Martillichthys* and *Rhinconichthys*, as at least some of the apparent prognathy of flattened specimens of these genera may be a result of taphonomic distortion rather than genuine anatomical signal. Second, I note the presence of a supraorbital canal-bearing rostrodermethmoid in *Martillichthys*, seen elsewhere in *Bonnerichthys* (Friedman *et al.* 2010). Although this arrangement is clearly derived relative to outgroups, the rostrodermethmoid of other edentulous pachycormiforms is insufficiently known to evaluate conditions in those taxa.

Conclusions about the phylogenetic relevance of this character awaits additional study of relevant specimens or discovery of more satisfactory material. In summary, I argue that among well-known edentulous pachycormiforms, there appears to be strong support for a close relationship between *Asthenocormus* and *Martillichthys*, with *Rhinconichthys* and *Bonnerichthys* representing more distal outgroups to these sister genera.

Phylogenetic placement of poorly known taxa. Ohmdenia and *Leedsichthys* are two poorly known taxa that are, despite their incompleteness, particularly relevant to understanding the evolution of suspension-feeding pachycormiforms. The Early Jurassic *Ohmdenia*, with its unusual mandibular proportions and dentition, has been placed as the immediate sister lineage to edentulous pachycormiforms (Friedman 2012*a*; Schumacher *et al.* 2016), and thus has a bearing on primitive anatomical conditions of the clade. The Middle-Late Jurassic *Leedsichthys* is probably represented by the greatest amount of fossil material known for any edentulous pachycormiform (Liston 2010), but these remains are often difficult to interpret because of disarticulation and the damage to individual elements, as well as the difficulties posed in handling such quantities of physically large material (Hudson & Martill 1994; Liston 2004; Liston 2016). Nevertheless, *Leedsichthys* has become perhaps the most iconic member of this radiation due to a combination of its great size and anatomical peculiarities (Liston 2004; Liston 2006; Liston *et al.* 2013; Liston 2016).

Ohmdenia, represented by a single associated but badly disrupted individual, presents an unusual combination of characters. It has proportionally elongate mandibles with a distinctive dentition comprising closely-packed, low-crowned teeth in broad bands across the

dorsal margin of the mandible. Friedman (2012*a*) interpreted *Ohmdenia* as the sister lineage of edentulous pachycormiforms on the basis of two unambiguously optimized synapomorphies: the presence of a slab-sided hyomandibula and the apparent absence of scales. However, the phylogenetic hypothesis presented by Friedman (2012*a*) requires reversal to a more conventionally 'waisted' hyomandibula in *Martillichthys*, *Leedsichthys*, and *Asthenocormus*, raising questions about the reliability of this qualitative character. Unfortunately, many key aspects of anatomy with a bearing on placement of this taxon, including much of the skull, remain unknown. Intriguingly, the bone interpreted as the hyomandibula in *Ohmdenia* is very short in comparison to the mandible, broadly corresponding to conditions in *Asthenocormus* and *Martillichthys* rather than to the more generalized pachycormiform proportions characteristic of *Bonnerichthys* and *Rhinconichthys* (Fig. 2.11). Additionally, the presumed hyomandibula appears to lack an opercular process, matching the condition reported in *Rhinconichthys* and *Asthenocormus*. Possible implications of this pattern are considered in the following section, but these hinge upon the uncertain identification of the hyomandibula in *Ohmdenia*.

Leedsichthys, although poorly known, shows some morphological features that support its phylogenetic placement among more completely known edentulous pachycormiforms. First, it possesses elongated gill rakers with oblique edges or fimbriations (Liston 2006, figs. 6.1-6.7; Gouiric-Cavalli 2017, fig. 2). Gill raker anatomy is known for some toothed pachycormiforms such as *Pachycormus* (BRLSI M1297; BRLSI M1361a, pers. obs.), which has small, knob-like rakers that are substantially shorter than the thickness of the supporting bones of the gill arches. These proportions are not dissimilar to what is seen in *Amia* (Grande

& Bemis 1998, fig. 56) and other outgroups, and I regard this as the primitive pachycormiform condition. By contrast, gill rakers are relatively elongate in *Martillichthys*, exceeding the thickness of their supporting gill bones. As very few individual rakers have been described in edentulous pachycormiforms, it is unclear how much they vary within and between individuals and species, limiting inferences made on the basis of observed morphological differences. The only edentulous pachycormiform not known to have elongated rakers is *Bonnerichthys*, which is regarded by this and most other studies as the sister lineage to all remaining edentulous pachycormiforms (Friedman *et al.* 2010; Friedman 2012*a*; Wretman *et al.* 2016). This stands in contrast to the sister group relationship between *Bonnerichthys* and *Leedsichthys* proposed by Schumacher *et al.* (2016, fig. 10). These authors do not report character optimizations for their preferred tree, but propose a lack of connections between the bones of the skull as a synapomorphy of these two genera. While the condition in *Bonnerichthys* is clear, I regard the structure of the skull in *Leedsichthys* as too poorly-known to assess this character, and maintain the hypothesis that *Bonnerichthys* is the sister taxon of all remaining edentulous pachycormiforms.

The most informative material described for *Leedsichthys* is the gill basket NHMUK PV P.10156 (Liston 2008*a*, fig. 7; Liston *et al.* 2013, fig. 4), but the overall structure appears conservative, in line with accounts given for *Pachycormus* (Mainwaring 1978). The hyomandibula of *Leedsichthys* presents two relevant characters. First, it appears to lack an opercular process as in *Rhinconichthys* and (possibly) *Asthenocormus*, although it is possible that the process could have been damaged or lost in available material (cf. *Martillichthys*). Second, and perhaps more informatively, the hyomandibula is short in comparison to

components of the ventral gill skeleton relative to the more generalized conditions in *Pachycormus* (Mainwaring 1978, figs. 11-12; pers. obs. μCT scans of BRLSI M1297) and *Bonnerichthys* (Friedman *et al.* 2010, figs. 2, S7). This suggests that the hyomandibula was also short in comparison to the length of the lower jaw, which can be roughly approximated by the length of the first ventral gill arch. However, the condition in *Leedsichthys* does not appear as extreme as in *Martillichthys* and *Asthenocormus*. Although the illustration of the hyomandibula in *Asthenocormus* given in Lambers (1992, fig. 1*a*) is rudimentary, I am confident that the bone was relatively short given overall cranial geometry, even if more detailed aspects of its anatomy are unclear.

Implications for edentulous pachycormiform evolution and ecology

Previous phylogenetic hypotheses (Friedman *et al.* 2010; Friedman 2012*a*), as well as the arrangement proposed here (Fig. 2.11), highlight some important questions about the evolution of edentulous pachycormiforms. One striking pattern to emerge from these studies is a general incongruence with stratigraphy. The most nested clade of edentulous pachycormiforms—comprising *Asthenocormus*, *Martillichthys*, and probably *Leedsichthys*—is Middle-Late Jurassic in age, and contains the oldest well-known edentulous pachycormiforms. Older material from the Bajocian is too incomplete to identify more precisely than a member of the edentulous pachycormiform clade (Friedman *et al.* 2010; Liston & Gendry 2015). By contrast, the Late Cretaceous *Bonnerichthys* and *Rhinconichthys* belong to earlier-diverging lineages, implying that each has a long unsampled history ranging from Middle Jurassic to Early Cretaceous - an interval of more than 60 million years. Although substantial, such a gap is not entirely unexpected; few diverse faunas of fully

marine fishes are known from the Early Cretaceous. Instead, the most diverse fish localities known from this interval are largely freshwater (e.g. Las Hoyas, Sanz *et al.* 1988) or of mixed influence (e.g. Santana Formation; Martill 2007), with the few rich, but arguably understudied, marine fish faunas concentrated at the very end of the Early Cretaceous (e.g. Toolebuc Formation, Clode 2015; Gault Clay Formation, Forey & Longbottom 2010; Tlayúa Quarry, González-Rodríguez *et al.* 2013). In terms of overall cranial geometry, Late Cretaceous members of these early-diverging edentulous lineages do not closely resemble either well-known Late Jurassic taxa or the putative Early Jurassic sister group of suspension-feeding pachycormiforms, *Ohmdenia*, all of which appear to have relatively narrow crania with shallow suspensoria. By contrast, *Rhinconichthys* and *Bonnerichthys* have skull proportions that more closely resemble those of tooth-bearing pachycormiforms like *Pachycormus*. This hints at possibilities of a more complex evolutionary history of suspension-feeding pachycormiforms that should be tested by more detailed study of key taxa and revised phylogenetic analyses incorporating new anatomical observations.

In particular, *Bonnerichthys* presents a curious combination of characters relative to other edentulous pachycormiforms. Gill rakers are not known for this taxon despite nearly complete but disarticulated branchial arches, and an opercular process of the hyomandibula is retained; the latter feature is only known in *Martillichthys* among edentulous taxa, and even appears to be lost in *Ohmdenia*. Among edentulous pachycormiforms for which the condition can be assessed, *Bonnerichthys* is also an outlier in retaining a primitive geometry of the occiput. Set against these primitive features are peculiar derived traits of *Bonnerichthys* unique to that genus or otherwise only known in pachycormiforms in apparently distantly-

related lineages. Among the latter, the most striking is distal fusion of individual lepidotrichia along the leading edges of the fin, which is characteristic of *Protosphyraena* (Dollo 1893; Friedman 2012*a*) and its probable junior synonym *Australopachycormus* (not reported in original description by Kear 2007, but apparent in undescribed pectoral fin NHMUK PV P73611, also from the Toolebuc Formation of Australia and presumably attributable to the genus). This peculiar arrangement is regarded as convergent between the two groups, and is known to occur sporadically among other pachycormiforms (e.g. an isolated caudal fin from the Toarcian Beacon Limestone Formation of Strawberry Bank, UK, BRLSI M1393, likely attributable to *Pachycormus*). Such an incongruous distribution of characters raises some questions concerning the strength of support for the edentulous pachycormiform clade; many of the characters uniting these taxa relate to modifications associated with suspension-feeding, and therefore might not be independent of each other. Critical appraisal of the evolutionary history of edentulous pachycormiforms will also require a more detailed understanding of the anatomy of toothed members of the broader pachycormiform radiation. Although the balance of evidence at present appears to support the monophyly of edentulous pachycormiforms, I provide past studies of suspension-feeding lamniform sharks as a cautionary note. Early morphological studies of *Megachasma* argued for a sister group relationship between this genus and *Cetorhinus*, with much of the supporting evidence deriving from anatomical features plausibly linked to suspension-feeding (Maisey 1985). Subsequent studies, including molecular analyses, reject the sister group relationship between cetorhinids and megachasmids (Martin & Naylor 1997; Motta 2004), but highlight the challenges presented by convergence upon broadly similar feeding modes by closely-related lineages.

Regardless of the phylogenetic implications of structural variations across edentulous pachycormiforms, it seems probable that major differences in head proportions point to important — but as yet undetermined — differences in feeding ecology. Cranial patterns among edentulous pachycormiforms range from the long, slender heads of *Martillichthys* and *Asthenocormus*, to the conventionally-proportioned head of *Rhinconichthys* associated with a slender hyomandibula, to the stout, large-eyed head of *Bonnerichthys*. Among living suspension feeders, the considerable variation in skull shape in closely related lineages appears linked to differences in feeding mode. Mysticete whales show substantial differences in overall cranial geometry (Sanderson & Wassersug 1993; Hampe & Baszio 2010), with morphologically distinctive lineages characterized by particular feeding modes: benthic suction feeding in grey whales (Eschrichtiidae); continuous ram feeding in bowhead and right whales (Balaenidae); and ram feeding in rorqual whales (Balaenopteridae; Goldbogen *et al.* 2007). Likewise, the independent radiations of mobulid, rhincodontid, megachasmid, and cetorhinid chondrichthyans have contrasting skull geometries associated with divergent approaches to suspension feeding (Moss 1977; Compagno 1990; Motta 2004; Motta *et al.* 2010; Paig-Tran & Summers 2014). It seems possible that the variation in cranial shape apparent in the suspension-feeding pachycormiforms could have some bearing on their feeding mechanisms. However, current treatments of the paleoecology of edentulous pachycormiforms are either quantitative but coarse (e.g. Friedman 2012*a*) or qualitative and limited to specific taxa (e.g. Schumacher *et al.* 2016), limiting any further inferences or comparisons to patterns of variation in living taxa. Additional information on the cranial anatomy of edentulous pachycormiforms will also help to better establish ecological diversity within this assemblage.

Conclusions

Re-examination of the skull of the Middle Jurassic (Callovian) *Martillichthys renwickae*, combined with μCT examination of previously concealed morphology, provides the most detailed account of cranial structure in edentulous pachycormiforms. This group has attracted considerable paleobiological and paleoecological interest, but even major aspects of their anatomy remain poorly understood for most of its members. Reinterpretation of external details of the skull, including the snout, skull roof, cheek, lower jaw, operculogular series, and ventral hyoid arch brings the anatomy of *Martillichthys* more into line with conditions described in other pachycormiforms. μCT scanning reveals a premaxilla, portions of the braincase including a long, trough-like occipital stalk, a parasphenoid with a broad, paddle-like corpus, and an intact branchial skeleton. The latter preserves numerous club-shaped rakers, each bearing elongate, pointed projections. These rakers are found *in situ*, as with the gill basket specimen of *Leedsichthys*, representing the most complete picture yet available of the deployment of rakers across the gill skeleton in an edentulous pachycormiform.

Collectively, these observations reinforce past interpretations of *Martillichthys* as highly nested within the monophyletic edentulous pachycormiforms. In particular, the unusual cranial geometry of *Martillichthys*, characterized by a greatly elongated preorbital region of the skull and short hyomandibula, strongly supports a close relationship with the Late Jurassic *Asthenocormus*. Long ghost lineages leading to the Late Cretaceous *Rhinconichthys* and *Bonnerichthys* are inferred here as in most other studies of edentulous pachycormiforms. This is consistent with a poor Early Cretaceous record of marine fishes. However, the very

generalized morphology of *Bonnerichthys* compared to both other edentulous pachycormiforms and the Early Jurassic *Ohmdenia* remains striking, and suggests that more exhaustive phylogenetic analyses of the group are necessary following more comprehensive documentation of anatomy in major pachycormiform lineages. Regardless of their exact patterns of interrelationships, a diversity of cranial geometries in edentulous pachycormiforms suggests a diversity of suspension-feeding strategies in this group, consistent with modern mysticete whales and planktivorous chondrichthyans.

.

Chapter 3

Cranial osteology of *Pachycormus*, relationships and divergence times among pachycormiforms

This chapter has been prepared in the style of the Journal of Systematic Palaeontology for submission. MF and SG contributed μCT scans, analytical advice, and improving drafts of my writing. All other data collection, analyses, and writing have been done by CD.

Abstract

Pachycormiformes, a group of early diverging stem teleosts, show stark ecological and morphological disparity, from tuna-like predators to giant-bodied suspension feeders. Despite this, and a number of well-preserved fossils from Jurassic and Cretaceous deposits around the world, they have received little detailed attention. This study employs μCT scanning to provide a description of an early pachycormiform taxon, *Pachycormus*, on the basis of a three-dimensionally preserved specimen from the Toarcian Strawberry Bank deposit of Ilminster, Somerset, UK. I supplement previous descriptions by reinterpreting poorly understood structures, such as the pectoral endoskeleton, and identify new features, including

a urohyal, a branched metapterygium-like posterior pectoral radial, and large fangs on the anteriormost coronoid toothplates of the mandible. I then use this description to inform morphology-only and combined phylogenetic analyses, the latter including 12 nuclear gene sequences, in order to build a clearer picture of pachycormiform evolution. My results corroborate patterns of pachycormiform interrelationships recovered in previous analyses, and estimate that the group emerged in the Carnian (Late Triassic; 231.82 Ma, 95% HPD = 213.08–250.92 Ma), with the giant bodied suspension-feeders emerging in the Toarcian (Early Jurassic; 172.45 Ma, 95% HPD = 164.59–184.27 Ma). I also use Bayes factors to test for multiple origins of suspension feeding in pachycormiforms, but find that this hypothesis is poorly supported. I identify a number of characters that are widespread across early actinopterygians, such as the anterodorsal projection of the suboperculum, or restricted to a subset of taxa within pachycormiforms, such as the broad anterior corpus of the parasphenoid seen only a number of pachycormiforms. From this description, I hope that other early neopterygians can be interpreted, to improve our understanding of teleost evolution.

Introduction

Teleosts are the largest group of fishes within Actinopterygii — ray-finned fishes — accounting for over 30,000 species and representing over half of all vertebrates (Nelson *et al.* 2016). As such, teleosts were dubbed the third major vertebrate clade alongside mammals and birds (Patterson 1967), but unlike them, we have a very poor understanding of teleost early evolutionary history and relationships (e.g. Zhou 2004; Kemp 2005; Luo 2007; Brusatte *et al.* 2015; Close *et al.* 2015; Chatterjee 2015). This is, in part, due to discord over the definition of Teleostei following its original apomorphy-based definition (Müller 1845), and

which taxa fall inside or just outside of this group (Arratia 1999, 2001, 2004, 2015). This uncertainty has been exacerbated by a poorly studied fossil record in proportion to the amount of available material, particularly concerning anatomically complex and thus phylogenetically informative internal structures such as the braincase, gill skeleton and pectoral girdle. Consequently, this has restricted the number of morphological characters available for phylogenetic analysis, contributing to a poorly resolved teleost stem. However, understanding the stem can build a clearer picture of how extant teleosts arose, and how the gradual acquisition of traits has influenced function, behaviour and ecology in modern ecosystems. Therefore, thorough analyses of well-preserved examples of early groups are key for improving the resolution of teleost relationships as a whole.

One of the most contentious areas of teleost relationships is the distinction between earliest-diverging teleosts and their holostean sister group. Previous studies placed *Amia* as the sister taxon to teleosts (Patterson 1967, 1973, 1977*a*; Patterson & Rosen 1977; De Pinna 1996; Arratia 1999, 2001, 2004), but this taxon is now placed in Holostei with *Lepisosteus* (gar; following Huxley 1860; Grande 2010; Faircloth *et al.* 2013; Sallan 2014; fig. 1). Many of the groups suggested to branch from the teleost stem, such as aspidorhynchids, pachycormiforms, dapediids and pycnodonts, have suffered from a lack of detailed analysis into the characters observable in the fossil record, and subsequent analyses have failed to rigorously analyse these group when considering their placement of taxa along the teleost stem (e.g. De Pinna 1996; who did not confirm the presence of characters recorded by Patterson 1977*a* in fossil taxa). The lack of well-recorded characters also influences the arrangement of taxa on the stem, where changing the outgroup affects polarity of character states and which taxon is

resolved as the sister group to other teleosts (as demonstrated by Arratia 1999; figs. 19–22). However, this is also a consequence of using only one outgroup, rather than using multiple outgroups to establish global parsimony (Maddison *et al.* 1984). Current consensus places Pachycormiformes as one of the earliest-diverging teleosts groups (Patterson 1973, 1977*a*; Patterson & Rosen 1977; Lauder & Liem 1983; De Pinna 1996; Arratia 1999, 2001, 2004), but this is largely from an acceptance of the original synapomorphy scheme laid out by Patterson (1973) that identified them as such, rather than a robust analysis of alternative hypotheses of the teleost stem. Pachycormiforms ranged from the Early Jurassic (Toarcian) to the end of the Late Cretaceous (Maastrichtian; Cione *et al.* 2018) and are known from marine deposits of Europe, the Americas, Australia and Antarctica (Woodward 1895*a*; Stewart 1988; Kear 2007; Friedman *et al.* 2010; Gouiric-Cavalli 2013; Gouiric-Cavalli & Cione 2015; Wretman *et al.* 2016; Gouiric-Cavalli 2017; Cione *et al.* 2018; Gouiric-Cavalli *et al.* 2019).

Despite their relative abundance, pachycormiforms have also suffered from scant analysis of their morphology and systematic relationships. The early to mid-late 20th Century provided a handful of detailed descriptions for the skulls of *Pachycormus* (Lehman 1949; Wenz 1967; Mainwaring 1978), *Euthynotus* (Wenz 1967), *Hypsocormus* (Woodward 1908*a*), and *Protosphyraena* (Loomis 1900; Hay 1903), and the braincases of *Pachycormus* (Rayner 1948; Lehman 1949; Patterson 1975; Mainwaring 1978) and *Orthocormus* (incorrectly identified as *Hypsocormus* by Rayner 1948; Lambers 1992). Following these descriptions came a number of appraisals of the phylogenetic placement of pachycormiforms, with particular focus on *Pachycormus* as the best-known taxon (Patterson 1973, 1977*a*; Patterson & Rosen 1977).

These were the first studies to show robust support for pachycormiform monophyly, and ally them with the teleosts (Patterson 1973, 1977*a*; fig. 19) rather than among caturids (Woodward 1895*a*; Gardiner 1960; Patterson 1973, fig. 13).

Since then, our understanding of pachycormiforms has increased substantially, with a number of phylogenetic analyses providing a clearer insight into pachycormiform interrelationships. The description of *Pachycormus* by Mainwaring (1978) united a suite of novel and previously described morphological characters for phylogenetic analysis, and outlined a basic synapomorphy scheme and framework of pachycormiform relationships (Mainwaring 1978; fig. 30). These synapomorphies were reappraised by Lambers (1992) and Liston (2006) following the descriptions of *Asthenocormus* (Lambers 1992), *Leedsichthys* (Martill 1986, 1988, 1991, Liston 2006), *Martillichthys* (Liston 2006, 'Taxon 13') and *Orthocormus teyleri* (Lambers 1988). Since these analysis, there have been a number of new and improved descriptions, some representing new taxa, that could inform a phylogenetic analysis of the group: *Orthocormus roeperi* (Arratia & Schultze 2013), *Australopachycormus* (Kear 2007), *Ohmdenia* (Hauff 1953*a*; Friedman 2012*a*); *Bonnerichthys* (Friedman *et al.* 2010); *Rhinconichthys* (Friedman *et al.* 2010; Schumacher *et al.* 2016); *Asthenocormus* (Lambers 1992); and *Martillichthys* (Liston 2008*a*; Dobson *et al.* 2019; Chapter 2).

These recent descriptions, along with new analyses into pachycormiform interrelationships (Friedman *et al.* 2010; Friedman 2012*a*; Wretman *et al.* 2016), confirmed the presence of two distinct clades within pachycormiforms. These major clades are characterized by two distinct ecologies: one containing the giant suspension-feeding pachycormiforms (*Asthenocormus*,

Bonnerichthys, *Leedsichthys*, *Martillichthys* and *Rhinconichthys*), and the other containing billfish-like macrocarnivores (*Australopachycormus* and *Protosphyraena*; Friedman 2012*a*; fig. 2; Wretman *et al.* 2016; fig. 4a), with more generalized piscivores falling between these extreme ecologies (e.g. *Pachycormus*, *Hypsocormus* and *Orthocormus*). Despite this, pachycormiform phylogeny is still poorly resolved (Arratia & Schultze 2013), as is their broader placement on the teleost stem, and it is unclear when they diverged from the rest of the teleost clade. The uncertainty surrounding pachycormiform divergence is made worse by studies describing the earliest holostean fossils from Olenekian (250 Ma; Early Triassic; Olsen 1984), providing a minimum date for teleost and holostean divergence. However, the earliest pachycormiforms appear approximately 67 Ma later (Toarcian; Rayner 1948; Lehman 1949; Patterson 1975; Mainwaring 1978), creating a ghost lineage requiring explanation.

A possible problem is that many pachycormiform descriptions are based on flattened or disarticulated fossils, limiting most observations to the visible, external characters. In particular, the giant bodied suspension-feeders have a poorly ossified skeleton, leading to very few complete or articulated fossils being found. One advantage of this has been that many internal characters, such as the hyoid arch and gill skeleton of these suspension-feeders have been observed and described (Friedman et al. 2010; Liston 2013), but they lack comparative material from the generally better-preserved predatory pachycormiforms. Additionally, any internal characters of complete or well-preserved specimens are often accessed through destructive methods such as acid or mechanical preparation (e.g. Mainwaring 1978), which removes the positional context of structure articulation within the organism. Therefore, no matter how comprehensive the character matrix, many inferences

about pachycormiform ecology and evolution have been limited by the lack of available information (e.g. *Leedsichthys*; Liston 2006; and *Ohmdenia*; Hauff 1953*a*; Friedman 2012*a*). Work on improving morphological data from well-preserved pachycormiform specimens has already begun, with a revised description of *Martillichthys,* a poorly understood taxon (Dobson *et al.* 2019; Chapter 2). This study analysed the external and — previously inaccessible — internal characters of a flattened but articulated cranium and associated gill arches via micro-CT (μCT) scanning. An alternative phylogeny is also suggested, whereby morphological similarities between the giant bodied suspension-feeder *Bonnerichthys* and *Protosphyraena* may indicate a second origin of suspension-feeding within pachycormiforms.

This study expands on Dobson *et al.* (2019; Chapter 2) by describing the cranium of a predatory pachycormiform, *Pachycormus macropterus*. This species is an ideal candidate for study, as other specimens have been described before, providing strong groundwork to build on. Its internal anatomy was described by Mainwaring (1978) using acid and mechanical preparation methods, leaving unresolved areas of uncertainty such as the morphology of the braincase, gill basket and pectoral endoskeleton. As a generalized pachycormiform, it is easily comparable to non-pachycormiform outgroups and is often chosen to represent the clade in broader phylogenetic analyses (e.g. Gardiner *et al.* 1996; Arratia 1999, 2001, 2004; Hurley *et al.* 2007; Lopéz-Arbarello & Sferco 2018). Most crucially, many *Pachycormus* specimens have been found at the Toarcian Strawberry Bank deposit in Ilminster, Somerset, but have only been described based on their external anatomy (Woodward 1897; Cawley *et al.* 2018). This deposit is renowned for its well preserved, three-dimensional fossils (Williams *et al.* 2015), some of which preserve soft tissue characters (Moore 1866), and μCT scanning has proved a

useful tool for describing crocodilians (Pierce & Benton 2006) and ichthyosaurs (Marek *et al.* 2015) from this site. Therefore, these *Pachycormus* specimens are promising candidates for μCT scanning to view their internal anatomy in their positional context, and provide a comprehensive description of *Pachycormus*.

Therefore the objectives of this study are fourfold: (1) to describe the internal anatomy of *Pachycormus* based on μCT scans of Strawberry Bank specimens, namely specimen BRLSI M.1361a; (2) to use this description, and that of *Martillichthys renwickae* (Dobson *et al.* (2019; Chapter 2), to identify pre-existing and novel characters for maximum parsimony and Bayesian phylogenetic analyses of pachycormiform interrelationships; (3) to estimate the evolutionary timescale of pachycormiforms using a Bayesian Fossilized Birth-Death framework (Heath *et al.* 2014); (4) to test support for the hypothesis of multiple origins of suspension-feeding in pachycormiforms.

Methods

Materials

Pachycormus macropterus. BRLSI M1361a, Bath Royal Literary and Scientific Institution, Bath, UK. Three-dimensionally preserved cranium and pectoral endoskeleton and fins from the Toarcian of Strawberry Bank in Ilminster (Somerset, UK). This specimen was μCT scanned most recently in November 2016. Scan parameters are given below and in the appendix (Appendix C).

Pachycormus macropterus. NHMUK PV P.24410, Natural History Museum, London, UK. Three-dimensionally preserved braincase from the Toarcian of Curcy (Normandy, France), and the specimen described by Patterson (1975), Mainwaring (1978) and Wenz (1967).

Pachycormus macropterus. NHMUK PV OR 32433, Three-dimensionally preserved skull from the Toarcian of Curcy (Normandy, France), and the specimen described by Rayner (1948), Patterson (1975) and Mainwaring (1978). This specimen was μCT scanned in January 2016 and scanning parameters are given in the appendix (Appendix C).

Pachycormus macropterus. NHMUK PV P.32438, Three-dimensionally preserved braincase from the Toarcian of Curcy (Normandy, France), and described by Mainwaring (1978).

Pachycormus macropterus. BRLSI M1297, Three-dimensionally preserved cranium, pectoral endoskeleton and fin from the Toarcian of Strawberry Bank in Ilminster (Somerset, UK). This specimen was μCT scanned in June 2017 and scanning parameters are given in the appendix (Appendix C).

Pachycormus macropterus. BRLSI M1311, Three-dimensionally preserved cranium from the Toarcian of Strawberry Bank in Ilminster (Somerset, UK). This specimen was μCT scanned in February 2017 and scanning parameters are given in the appendix (Appendix C).

Pachycormus macropterus. BRLSI M1395, Three-dimensionally preserved cranium and pectoral endoskeleton and fin from the Toarcian of Strawberry Bank in Ilminster (Somerset, UK). This specimen was μCT scanned in February 2017 and scanning parameters are given in the appendix (Appendix C).

Hypsocormus tenuirostris. NHMUK PV P.10579, Natural History Museum, London, UK. Articulated cranium from the Callovian Oxford Clay of Peterborough. This specimen was μCT scanned in January 2016. Scanning parameters are in the appendix (Appendix C).

Martillichthys renwickae. NHMUK PV P.61563 (holotype), Natural History Museum, London, UK. Articulated but dorso-ventrally flattened specimen from the Callovian Oxford Clay of Dogsthorpe Pit (Peterborough, UK). This specimen was μCT scanned in January 2016, and scanning parameters are given in the appendix (Appendix C).

Pachycormidae gen. et sp. indet. NHMUK PV P.41669, Natural History Museum, London, UK. Three-dimensionally preserved incomplete skull from the top of the Bajocian (Middle Jurassic) Inferior Oolite of Dorset, UK, partially described by Friedman *et al.* (2010).

X-ray computed tomography scanning

M1361a was scanned using a Nikon XT H 225 ST μCT scanner at the Life Sciences Department of the University of Bristol. The specimen was scanned in two stacks, both using identical scan settings: a voltage of 225 kV, a current of 176 μA, an exposure of 1.41 s, and using a 2 mm copper filter. In total, the scan produced 3141 projections, with 8 frames per projection and a voxel size of 0.047613 mm. After scanning, the image stacks for both scans were stacked together to create a single tomographic series for segmentation.

The tomograms were loaded into Mimics Innovation Suite V.19.0 (http://biomedical.materialise.com/mimics; Materialise, Leuven, Belgium), to segment individual skeletal elements. The resulting models were imported into Blender V.2.79b (http://www.blender.org; Blender Institute, Amsterdam, Netherlands) for reconstruction, description and imaging.

Systematic palaeontology

Class **Actinopterygii** Cope, 1887

Subclass **Neopterygii** Regan, 1923

Infraclass **Teleostei** Müller, 1845

Order **Pachycormiformes** Berg, 1940

Family **Pachycormidae** Woodward, 1895*a*

Diagnosis (emended from Lehman 1949; Wenz 1967; Mainwaring 1978; Lambers 1992; Arratia 2004; Kear 2007; Cawley et al. 2018). The following morphological traits diagnose Pachycormidae: premaxillae and nasals separated on the mid-line by the rostrodermethmoid; presence of teeth on the rostrodermethmoid; presence of a compound rostrodermethmoid; absence of supraorbitals; dermosphenotic forming the dorsal margin of the orbit; at least nine rectangular infraorbitals; presence of two large, plate-like suborbitals; presence of an enlarged dermopterotic that houses the supra-temporal commissural sensory canal; long, slender pectoral fins (previously 'scythe-like pectoral fins', but see Liston & Maltese 2016 for a critique on this); asymmetrical 'Y'-bifurcating fin-rays; presence of small, rhombic scales.

Genus ***Pachycormus*** Agassiz, 1833

Type and only species. Pachycormus macropterus (Blainville 1818), initially described as *Elops macropterus*. The holotype is MNHN-F-JRE 50 (formerly MNHN 10529-10530), which is a complete specimen preserved as part and counterpart, from the Toarcian (Early Jurassic) deposits of Beaune, Côte-d'Or (Burgundy, France; Brignon 2017).

Diagnosis (emended from Mainwaring 1978). The following morphological characters diagnose *Pachycormus macropterus*: rostrodermethmoid not produced anterior to symphysis of mandibles; dermal skull roof raised posteriorly into a pronounced frontoparietal boss; mandible with a single row of marginal teeth; and post-supracleithrum present.

Occurrence. This *Pachycormus* specimen is from the Strawberry Bank deposit of Ilminster, Somerset, which is part of the Beacon Limestone Formation. Vertebrate fossils from this deposit are renowned for their exceptional preservation, often in three dimensions, and include fish, ichthyosaurs and crocodilians (Williams *et al.* 2015). Fish fossils are known from the 'Reptile Bed' of Strawberry Bank, which corresponds to the *Harpoceras falciferum* ammonite zone, giving an age of c. 183 Ma (Gradstein *et al.* 2012; Williams *et al.* 2015).

Remarks. The genus *Pachycormus* includes three nominal species: the type species, *P. macropterus* Blainville 1818; and two referred species, *P. curtus* Agassiz 1833 and *P. bollensis* Quenstedt 1858, which are diagnosed on the basis of skeletal dimension variation, such as pre-orbital length to head length ratios (see Mainwaring 1978). A morphospace distribution analysis between these species by Wretman *et al.* (2016; fig. 2) showed considerable morphospace overlap between species, and concluded that variation in proportional dimensions was due to ontogenetic variation and sexual dimorphism, as seen in other actinopterygians (Parker 1992), or postmortem distortion. This led to the conclusion that *Pachycormus* is, in fact a monospecific genus: *P. macropterus*. For the purpose of this study, *Pachycormus* is accepted as a monospecific genus containing *P. macropterus*.

Morphological description

General observations

M1361a is a complete, three-dimensionally preserved cranium and pectoral girdle of *Pachycormus*, with both pectoral fins present (Fig. 3.1). Either during mechanical preparation or when the specimen was removed from its concretion, most of the dermal bone of the skull was removed, leaving only their impressions. However, in places, this has exposed some of the endoskeletal bone, such as the hyomandibula (Fig. 3.1). Additionally, the anteriormost tip of the snout has either been partially prepared away or broken in concretion, resulting in some of the rostrodermethmoid dentition and the anteriormost tip of the mandibles being lost. Squamation is clearly visible posterior to the pectoral fins. Externally, there is very little evidence of post-mortem distortion. The right side of the fossil is displaced slightly above the left, and there is some lateral compression of the body posterior to the pectoral fins, but most structures remain in articulation and *in vivo* arrangement.

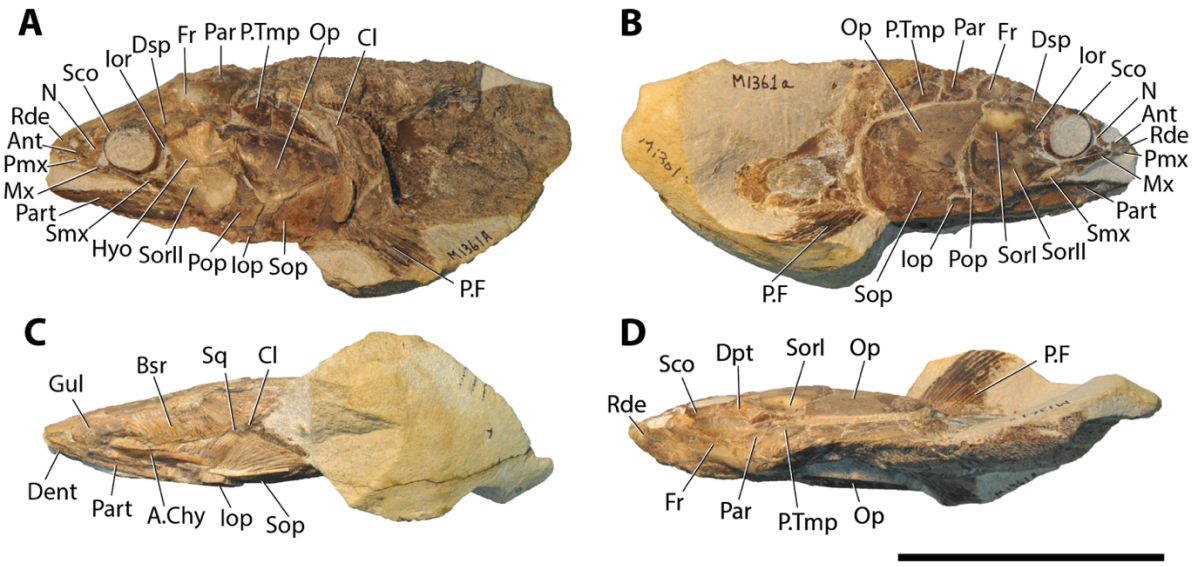

Figure 3.1 – Photographs of M1361a, showing the dermal bones present in A) left lateral view, B) right lateral view, C) ventral view, D) dorsal view. Scale bar represents 5 cm.

The maximum length of the fossil is roughly 160 mm; and maximum width, including the pectoral fins, is 56 mm. Maximum skull length, from nose tip to the posterior margin of the suborbitals, is 85 mm; maximum skull depth is 53 mm; and maximum skull width is 33 mm.

External dermal skeleton

The external structures of specimens of *Pachycormus* from Strawberry Bank (excluding M1361a) have recently been described in detail by Cawley *et al.* (2018), so this description will focus less on this anatomy. External examination of M1361a identifies the following features (Figs. 3.1–3.3): rostrodermethmoid (Rde), with dentition contributing to the oral margin of the upper jaw (Rde.T); nasal (N); plate-like antorbital (Ant); frontal (Fr); parietal (Par); a frontoparietal boss; dermal ornament on the skull-roofing bones; dermosphenotic (Dsp), contributing to over half of the dorsal margin of the orbit; dermopterotic (Dpt); premaxilla (Pmx); maxilla (Mx); supramaxilla (Smx); dentary (Dent); prearticular (Part); angular (Ang); surangular (Sang); sclerotic ossicle (Sco); at least nine infraorbitals (Ior); two suborbitals (Sor); preoperculum (Pop); interoperculum (Iop); operculum (Op); suboperculum (Sop); at least 40 branchiostegal rays (Bsr); gular (Gul); post-temporal (P.Tmp); supracleithrum (S.Cl); cleithrum (Cl); and dorsal and ventral post-cleithra (P.Cl).

Braincase and parasphenoid

While the braincase (Bc) is well-preserved, some of it was cartilaginous is life and has therefore not fossilised (Figs. 3.2–3.4). This has resulted in ossifications collapsing relative to their life position, making them difficult to identify confidently. The postorbital region of the braincase is largely complete, originating posterior to the ascending processes of the

parasphenoid (Fig. 3.4). Examination of μCT scans of better-preserved braincases in BRLSI M1361a, BRLSI M1311 and NHMUK PV P.24410 shows that the following structures are observable in BRLSI M1361a: orbitosphenoid; sphenotic; pterotic, prootic, opisthotic, otoccipital fissure; intercalar and basioccipital.

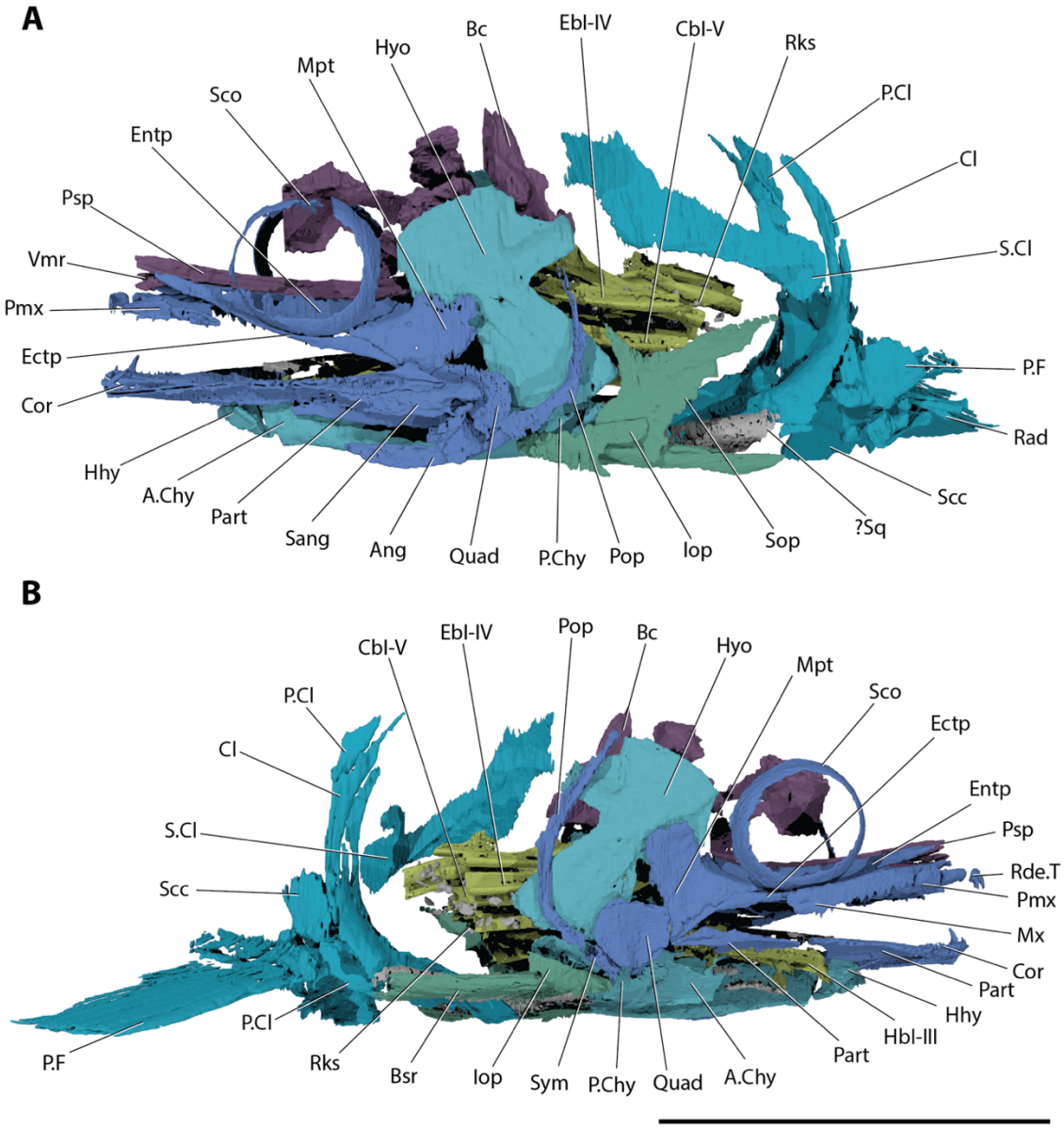

Figure 3.2 – Three-dimensional renders of all structures present in the μCT scan of M1361a in A) left lateral view, B) right lateral view. Purple is used to represent the neurocranium; dark blue represents the mandible, upper jaws, palate and orbit; light blue represents the hyoid arch, light green represents the gill basket; dark green represents the operculogular series; turquoise represents the pectoral girdle; and grey represents unidentified structures. Scale bars represent 5 cm.

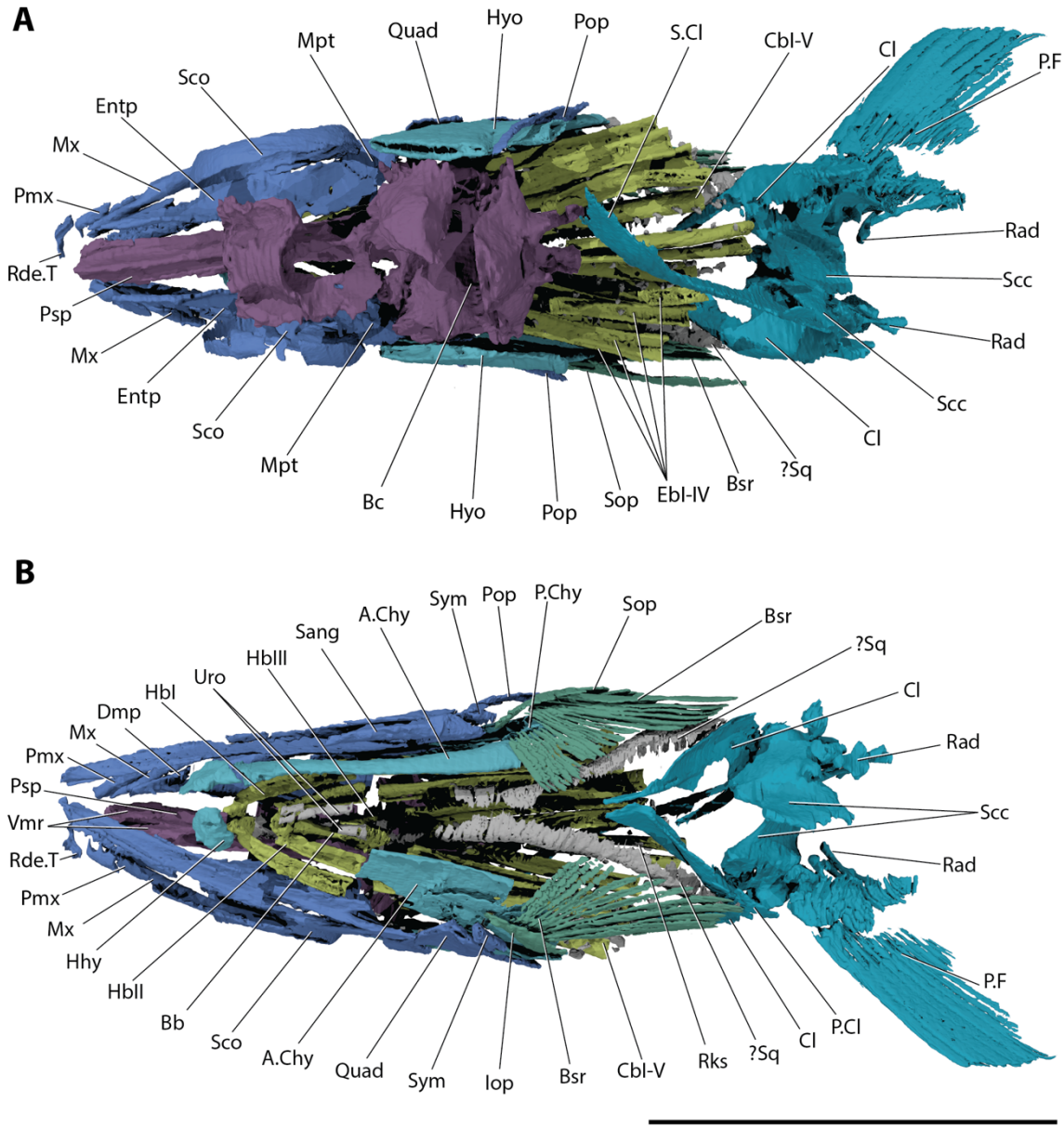

Figure 3.3 – Three-dimensional renders of all structures present in the μCT scan of M1361a in A) in dorsal view, B) ventral view. Purple is used to represent the neurocranium; dark blue represents the mandible, upper jaws, palate and orbit; light blue represents the hyoid arch, light green represents the gill basket; dark green represents the operculogular series; turquoise represents the pectoral girdle; and grey represents unidentified structures. Scale bars represent 5 cm.

The orbitosphenoid is a midline ossification and the anteriormost section of the braincase as preserved (Obsp; Fig. 3.4B). In dorsal view, it is roughly rectangular, with a slightly concave posterior margin, but it is unclear if this is due to incomplete preservation. It contributes to

the orbital septum (ospt) and the roof of the orbit and terminates anterior to the prootic (Pro) and sphenotic (Sph). The sphenotic is only partially preserved on the right side, and has become disarticulated when the roof of the skull caved in. What remains is trapezoidal, and forms part of the roof of the orbital region of the braincase. Posteriorly, it would meet the anterior of the pterotic (Pto) in life, but sits ventral to the pterotic in this specimen.

The immediate postorbital region is composed of the pterotic, prootic and opisthotic (Opso). The boundary between the prootic and opisthotic is not clear, but together they border the pterotic ventrally, sitting beneath the facet for the hyomandibula (H.Fa). Examination of other specimens (BRLSI M1311; NHMUK PV P.24410) also shows that the suture starts at or just anterior the glossopharyngeal foramen and extends posterodorsally up to the hyomandibular facet (H.Fa; fig. 4; Patterson 1975; fig. 106; Mainwaring 1978; fig. 22). The pterotic has also been partially displaced, where the left side has been pushed into the brain cavity. Its margins are difficult to determine as it is incompletely ossified, but its ventral margin forms the dorsal edge of the hyomandibular facet. The prootic forms the posterior wall of the orbit and it is pierced by several foramina. The largest opening accommodated the jugular canal (jc), which sits halfway along the anterior margin of the prootic and leads to the orbit. Within the cavity for the jugular canal, and posterior to it, lie two more foramina for the branches of the facial nerve: the palatine branch (VII.pal) and the hyomandibular branch (VII.hym; Fig. 3.4A, E). The anteroventral margin of the opisthotic and the part of the ventral margin of the prootic form the vestibular fontanelle (v.fn), which flanks the lateral margin of the parasphenoid (Psp) behind the ascending processes (asp). On the postero-lateral corner of the opisthotic is the foramen for the vagus nerve (X) and the

intercalar (Ic), which is separated from the opisthotic by the branches of the vagus nerve that bifurcate within the vagus nerve foramen and the foramen for the subsidiary branch of the vagus nerve (fs.X).

The posterior braincase is composed of the basioccipital (Boc), which is the most complete neurocranial structure present in BRLSI M1361a. The otoccipital fissure (oc.f) separates the basioccipital from the opisthotic and pterotic. The otoccipital fissure is continuous with a basal fissure (b.fs) that delineates the anterior margin of the basioccipital. The fissure is continuous, and is intercepted by the vagus nerve as it extends posterior to the intercalar and ventrally to meet the vestibular fontanelle ventrally. Due to the roof of the braincase being unossified, it is unclear whether a posterior dorsal fontanelle was present and continuous with the otoccipital fissure, though previous descriptions do not describe one (Patterson 1975; Mainwaring 1978).

The foramina present on the basioccipital are for the occipital artery and the foramen magnum (Fm). The foramen for the occipital artery (foca) is ventral to the vagus nerve and lateral to the forked posterior margin of the parasphenoid, and the occipital nerve pierces the braincase via a foramen lateral to the foramen magnum. The foramen magnum is transversely oval, and sits just above the midpoint of the braincase. Beneath it is the notochordal pit (ncp), which is conical, and tapers to a small pit deep inside the braincase. Its lateral and ventral edges are formed by the basioccipital, which possesses a deeply forked ventral process that forms the pronounced groove for the dorsal aorta (a.gr).

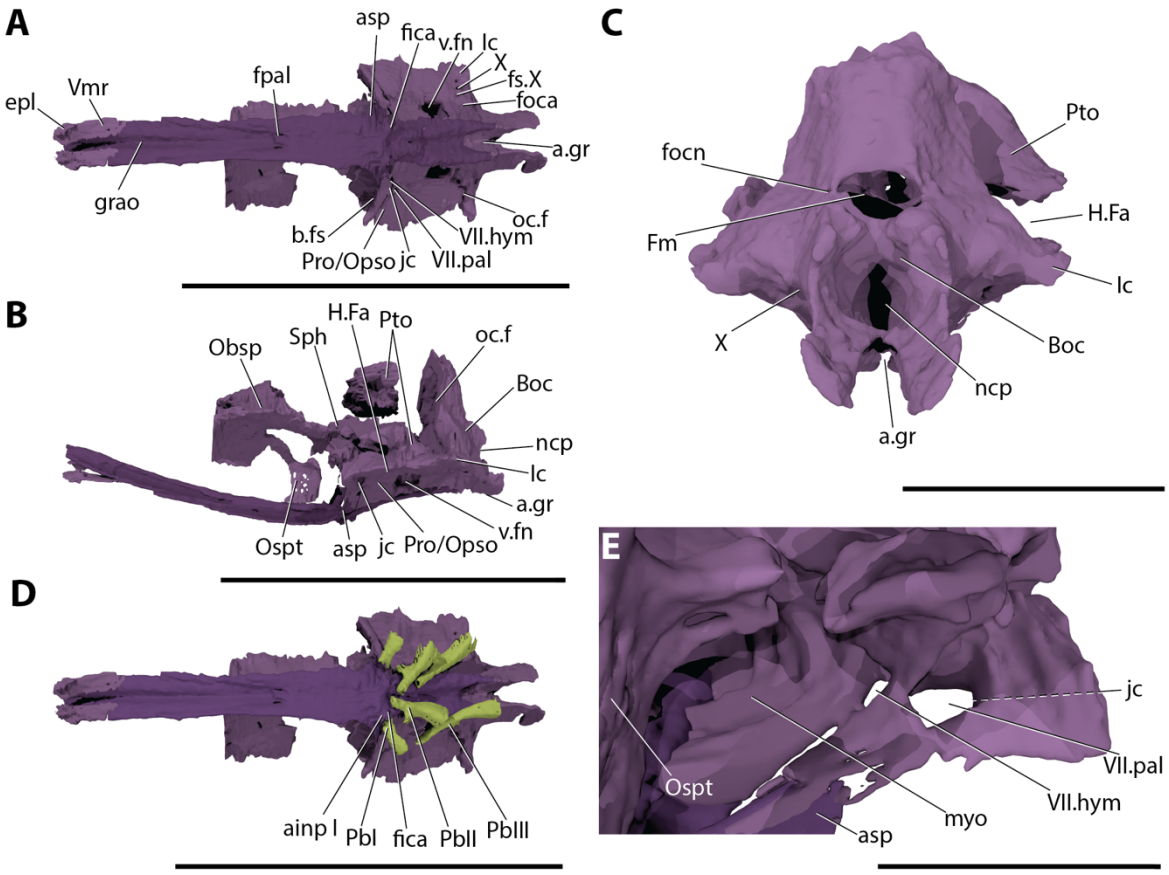

Figure 3.4 – Three-dimensional renders of the braincase and parasphenoid of M1361a in A) ventral view, B) left lateral view, C) three-dimensional render in posterior view, D) ventral view showing articulation of the infrapharyngobranchials with the braincase and parasphenoid, E) anterior view of the interior of the orbital region. Purple is used to represent the braincase, parasphenoid and vomers; and light green represents the pharyngobranchial series. For clarity between neurocranial structures, a slightly darker shade of purple is used for the parasphenoid. A dotted line indicates labels that lead behind the structure shown. Scale bars represent 5 cm for panels A, B and D, 2 cm for panel C; and 1 cm for panel E.

The parasphenoid is completely preserved. It is approximately 2/3 the length of the cranium and forms the floor of the ethmoid region (Figs. 3.3A, 3.4A, B, D, 3.5). There is no evidence of any dentition, though this is due to the resolution of the scan, as dentition is described on other specimens (e.g. Lehman 1949; Mainwaring 1978). The anterior corpus is curved dorsally, and is narrow and of constant width until it reaches the ascending processes, which project dorso-posteriorly roughly two-thirds of the way along the parasphenoid to bridge the

basal fissure (Fig. 3.5). Anterior to the ascending processes are two shallow notches on the lateral edges of the parasphenoid, which allowed the efferent pseudobranchial arteries to enter the braincase ventrally (fpsa). Just posterior to the ascending processes, where their posterior margins meet the body of the parasphenoid, are two foramina for the internal carotid arteries (fica). On the ventral surface, the medial margins of the internal carotid artery foramina are bracketed by a small ventral process. This ventral process acts as an articular facet (ainp I) for the anterior processes of the infrapharyngobranchials I (PbI) and, medially, a small excavation houses the subcephalic muscles (rscm). Posterior to this site is another deep ventral groove, and the posterior margin is deeply forked, to accommodate the dorsal aorta (Figs. 3.4A–D, 3.5A, B). Anterior to this forked posterior margin, the dorsal aorta likely bifurcates posterior to the excavation for the subcephalic muscles (rscm). The dorsal aorta then travels externally lateral to the articular facets for the pharyngobranchials (ainp I), and extends anteriorly along a median groove on the ventral surface of the anterior corpus of the parasphenoid (grao). This groove starts at the foramen for the palatine nerves (fpal) and terminates at the anterior tip of the parasphenoid. Lateral to the aortic groove, two shallower grooves (gpal) direct the palatine nerves anteriorly along the ventral surface.

On its dorsal surface, the parasphenoid has a pronounced dorsal median ridge (dmr) that terminates as a crest (smc) between the ascending processes. This median ridge also contributes in part to the interorbital septum of the braincase, and the floor of the myodome (myo). This dorsal ridge separates the palatine nerves as they move onto the ventral surface via two foramina that flank the dorsal median groove at the longitudinal midpoint of this dorsal ridge (fpal; Figs. 3.4, 3.5).

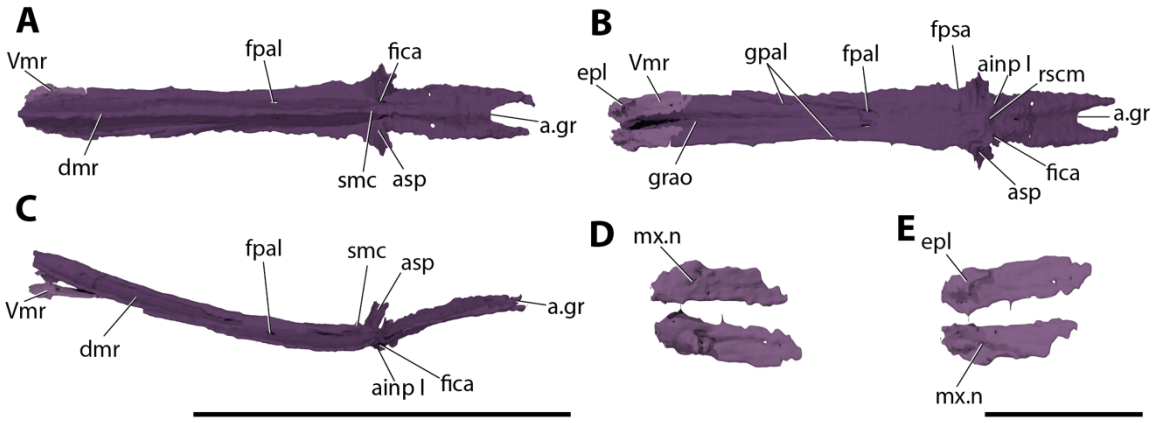

Figure 3.5 – Three-dimensional renders and interpretive drawings of the parasphenoid M1361a in A) dorsal view, B) ventral view, C) left lateral view; and the vomers in D) dorsal view, E) ventral view. For clarity between neurocranial structures, a slightly darker shade of purple is used for the parasphenoid. Scale bars represent 5 cm for panels A–C; and 1 cm for panels D and E.

Beneath the anterior part of the parasphenoid are the paired vomers (Vmr; Fig. 3.5), which are roughly four times longer than their width, and approximately one sixth the length of the parasphenoid. Their posterior margins contact the parasphenoid, but the anterior margins do not (Fig. 3.5C). The antero-ventral margin of each vomer is slightly thickened, named the transverse 'vomerine head' by Mainwaring (1978: 25), creating an attachment site for the ethmopalatine ligaments (epl) on the lateral margin, and posterior to this ridge is a small foramen for the maxillary nerve (mx.n).

Upper jaw

The upper jaw is composed of the maxilla (Mx), premaxilla (Pmx), and the teeth of the rostrodermethmoid (Rde.T; Figs. 3.2, 3.6). The supramaxilla is not visible in tomograms, but it has been identified externally (Smx; Fig. 3.1A-D).

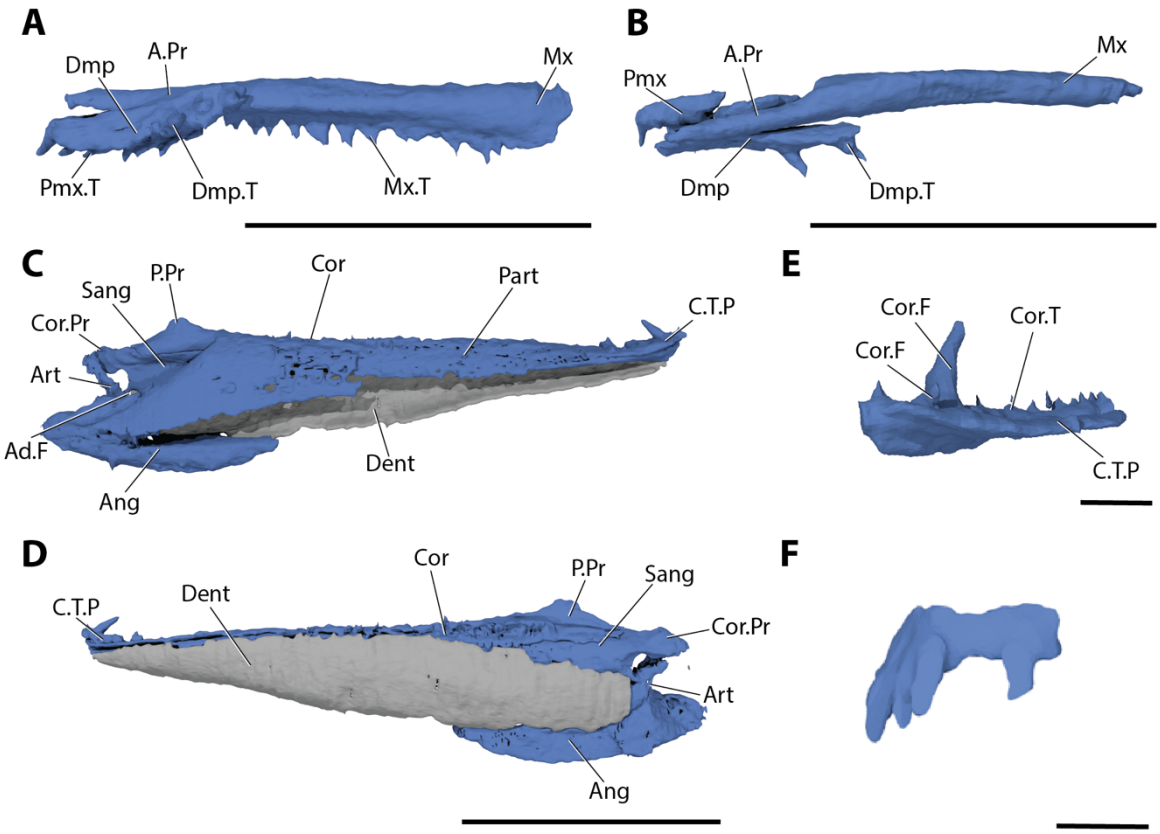

Figure 3.6 – Three-dimensional renders and interpretive drawings of the upper jaw, dermopalatine and mandible of M1361a. A) the maxilla, premaxilla and dermopalatine in medial view, B) the maxilla, premaxilla and dermopalatine in dorsal view, C) left mandible in medial view, D) the left mandible in lateral view with the dentary reconstructed, E) the coronoid tooth plate and enlarged fang in medial view, F) three-dimensional render of the rostrodermethmoid dentition in anterior view. Dark blue is used to represent the mandible and upper jaws; and grey is used to represent the reconstructed dentary. Scale bars represent 2 cm for panels A–D, and 0.1 cm for panels E and F.

The maxilla is best preserved on the right side of the skull, but incomplete in the scan due to preparation (Fig. 3.2A). It is ¾ the length of the mandible, and lies ventral to the antorbital and the sclerotic ossicle, and postero-ventral to the rostrodermethmoid (Figs. 3.1, 3.2). It terminates beneath the infraorbitals, posterior to the orbit (Fig. 3.1). There is a single row of 13 small, needle-like teeth (Mx.T) along most of the ventral margin that are approximately 2–3 mm tall. The anterior maxilla forms a long anterior process (A.Pr). This

anterior process appears to be an extension of the thickened dorsal ridge seen on the medial surface of the maxilla, and articulates between the premaxilla and dermopalatine (Dmp; Fig. 3.6). The antero-posterior margin of the maxilla is deeply excavated to house the supramaxilla, though this is only visible on the left side of the fossil (Fig. 3.1).

The premaxilla is positioned anterior to the maxilla. It is present on both sides of the skull, but the right has broken into two pieces (Figs. 3.2, 3.6A, B). It is a dorso-ventrally compressed rectangle in shape, about a quarter of the length of the maxilla, and sits ventral to the edentulous anterior process of the maxilla and antorbital. The ventral margin of the premaxilla bears six teeth of similar size to the maxilla (Pmx.T; Figs. 3.1, 3.6A, B). The posterodorsal margin bears a prominent notch for articulation with the maxilla.

The most anterior structure present is the rostrodermethmoid, which has four teeth preserved (Rde.T; Figs. 3.2, 3.3, 3.6F). While the body of the rostrodermethmoid is not apparent in the scan, viewing the fossil shows it to be confluent with these teeth. This dentition is not complete due to damage during preservation, and possibly mechanical preparation, but three teeth matching those seen on the premaxilla are visible on the right side of the rostrodermethmoid (Fig. 3.6F).

Mandible

The mandible consists of the prearticular (Part), angular (Ang), surangular (Sang), articular (Art) and coronoid (Cor; Fig. 3.6C–E). The dentary (Dent) is not fully preserved but the impression of its inner surface is visible in the specimen, allowing for reconstruction.

The largest completely preserved bone present is the prearticular, which forms the mesial surface of the mandible (Fig. 3.6C, D). It is triangular, with a deep excavation on the posterior margin for the adductor fossa (Ad.F). Above this excavation is a posterodorsal projection (P.Pr) which forms a raised process on the dorsal surface of the mandible, but is not the coronoid process due to its position anterior to the adductor fossa. The coronoid process (Cor.Pr) is found posterior to this process, above the adductor fossa, and is formed by the surangular. The posteriormost quarter of the prearticular sutures with the dorsal margin of the surangular. There is no evidence of any dentition on the prearticular, which is likely due to scan resolution.

Based on viewing the fossil and the impression of the prepared dentary, the dentary makes up almost the entire lateral surface of the mandible (Fig. 3.6D). Dorsally, the dentary meets the coronoid series, which bridges the gaps between the dorsal margins of the dentary and prearticular, and the posterior margin of the dentary slots between the ventral margin of the surangular and the dorsal margin of the angular, terminating anterior to the jaw joint. However, it is unclear if these are the true margins between the angular, surangular and dentary due to the dentary being prepared away. These margins are also unclear externally on the specimen, due to cracks and breaks on the exposed right side of the fossil.

External analysis of this specimen does appear to show that the coronoid region is composed of multiple plates, but it is unclear if these are real divisions, or breaks due to damage, so the number present cannot be confirmed beyond at least two coronoids (C.T.P; Fig. 3.6C–E), which sit at the anteriormost tip of the mandible. These bones bear small, regularly

spaced, conical teeth along the lateral margin (Cor.T), that continue onto the anterior margin of the coronoid (Fig. 3.6C–E). In addition, the plate bears two large, conical fangs (Cor.F; Fig. 3.6E) that are two to three times larger than other teeth, and are not repeated on the rest of the mandible, maxilla, premaxilla, rostrodermethmoid or dermopalatine. (Figs. 3.2, 3.6). On the right toothplate, the more anterior of these fangs is small and more medially orientated, while the more posterior is larger and vertically orientated. It presumed the orientation of the anteriormost fang is slightly distorted. Presence of an empty socket on the left toothplate indicates that this tooth was lost, but the more medially orientated fang is present. Beyond these tooth plates, the coronoid extends posteriorly and terminates ventral to the posterodorsal projection of the prearticular.

The angular and surangular are present on the posterior portion of the mandible, but both are incomplete due to preparation (Fig. 3.6C, D). From external analysis of the right side, the angular forms the postero-ventral corner of the lateral portion of the mandible, and most of the mandibular-quadrate joint, by which the articulation of the mandible with the upper jaw. It possesses a large anterior process that is the same length as the surangular and a third of the length of the mandible. Only the posterodorsal corner contacts the ventral posterior margin of the surangular.

The surangular forms the dorsal corner of posterior margin of the mandible and is half the height of the angular (Fig. 3.6C, D). It is also triangular, with the dorsal margin meeting with the coronoid and lying lateral to the posterior portion of the prearticular. The posterior corner of the dorsal margin is slightly raised, forming a reduced coronoid process. Beneath

the coronoid process, the ventral margin slopes downwards, following the posterodorsal margin of the dentary.

The posteriormost structure of the mandible is the articular, which bears a large facet for articulation with the quadrate. The articular is splint-like, with its postero-ventral surface forming the ventral half of the mandibular-quadrate joint, which is positioned on the dorsal half of the posterior margin of the lower jaw. Between the prearticular and the angular is a small cavity, the adductor fossa, which represents where the adductor mandibularis muscle attaches to the mandible.

Palate

The palate consists of the ectopterygoid (Ectp), entopterygoid (Entp), dermopalatine (Dmp), metapterygoid (Mpt), and quadrate (Quad; Figs. 3.2, 3.7).

The entopterygoid is triangular in shape, and its dorsal surface is slightly concave to follow the shape of the parasphenoid (Figs. 3.2, 3.7). Anteriorly, the entopterygoid starts as a narrow anterior process that articulates with the dermopalatine. From there it widens as it passes under the sclerotic ossicle, where its posterior margin sutures with the anterior margin of the metapterygoid. Its lateral edge sutures with the anterior half of the ectopterygoid, and the mesial edge flanks, but does not touch, the anterior corpus of the parasphenoid. There is no indication of any teeth, which is due to scan resolution.

Flanking the entopterygoid mesially, and beneath the sclerotic ossicle, is the ectopterygoid (Figs. 3.2, 3.7). This is a narrow structure that starts roughly one third of the way along the entopterygoid and extends back to meet the vertical portion of metapterygoid along its ventral margin. From this point, it slopes downward sharply, following the ventral margin of the metapterygoid, and terminates at the anterior margin of the quadrate. Due to the ectopterygoid being preserved internally, the presence of dentition could not be confirmed through external analysis, and low resolution could not confirm their presence in the tomograms.

The dermopalatine sits mesial to the premaxilla and maxilla (Fig. 3.6A, B). It is antero-medial to the entopterygoid (Fig. 3.7), but does not suture with it, and is lateral to the vomers (Fig. 3.3B). Its antero-lateral margin has a shallow groove that sits dorsal to the anterior process of the maxilla. It is approximately the same length as the anterior process of the maxilla, and its posterior half bears two large, conical teeth (Dmp.T; Fig. 3.6). These teeth also appear to project laterally, at a perpendicular angle to the maxillary teeth, which is due to the orientation of the dermopalatine shifting during preservation. If the dermopalatine is twisted to position the teeth vertically, the lateral groove would run along the dorsal surface, as described in Mainwaring (1978: 30), and would be overlain by the anterior process of the maxilla.

The metapterygoid comprises two sections (Fig. 3.7), and primarily links the hyomandibula to the palate. There is a rectangular, vertical plate, where the posteroventral corner meets the anterodorsal corner of the quadrate and overlaps the lateral surface of the hyomandibula.

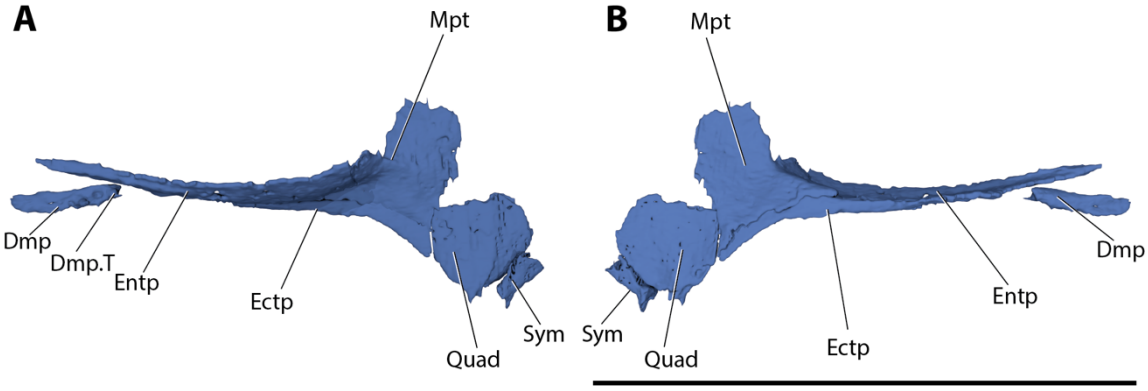

Figure 3.7 – Three-dimensional renders of the right palate of M1361a in A) medial view, B) lateral view. Scale bar represents 5 cm.

The anteroventral corner extends forward to form a triangular anterior process, where the horizontal portion extends mesially from the dorsal margin. The horizontal plate is roughly triangular, and it meets the posterior margin of the entopterygoid anteriorly. There is a shallow notch on the dorso-lateral corner of the horizontal plate where it meets the vertical plate, which accommodates the mandibular branch of the trigeminal nerve (Fig. 3.7).

Ventral to the metapterygoid is the quadrate, which is approximately trapezoid in shape, and tilted forwards at a 45° angle (Figs. 3.2, 3.7). The anterodorsal corner meets the metapterygoid posteriorly, and its posterior margin is lateral to the ventral corner of the hyomandibula. Its anterior margin is mesial to the dorsal half of the mandible, but postero-lateral to its ventral half, including the angular and articular. On the mesial surface of the anteroventral corner, there is a slightly thickened ridge that extends from the ventralmost corner towards the dorsal margin, forming a facet for the symplectic. The anterior margin of the quadrate is thickened, and is slightly concave, forming a condyle for articulation with the articular of the mandible. There is no evidence of a quadratojugal. To articulate with

the mandible, the quadrate is orientated diagonally dorso-ventrally, where the dorsal half is aligned with the internal surface of the mandible, nearly sitting inside the adductor fossa, and the ventral half is aligned with the external surface. However, the right side is not complete enough for comparison, so it is unclear if the position of the quadrate described here is distorted.

Sclerotic ossicle, circumorbital bones and cheek

The sclerotic ossicle (Sco) comprises two semi-circular plates, and sits above the posterior half of the maxilla, and half way along the mandible (Figs. 3.1, 3.2, 3.8). The plates meet at the ventralmost point, halfway along the entopterygoid, and at the dorsalmost point, where they have separated slightly during preservation (Figs. 3.2, 3.8). No orbital bones have been identified in the scan, but external analysis of the fossil confirms the presence of two large suborbitals (Sor), nine small, rectangular infraorbitals (Ior) bordering the posterior margin of the orbit, an elongated infraorbital at the anteroventral corner of the orbit, and an antorbital (Ant) that forms the ventral margin of the anterior nostril (Fig. 3.1). There is no evidence of any supraorbitals between the dorsal margin of the orbit and the dermosphenotic (Dsp; Fig. 3.1).

The nine posterior infraorbitals form the posterior margin of the orbit, and separate the orbit from the suborbitals. A gap along the posteroventral corner of orbit beneath the infraorbital series indicates that more infraorbitals may have been present, but these could not be identified (Fig. 3.1).

The anterior infraorbital is triangular and borders the mid-dorsal margin of the maxilla ventrally, and defines the anteroposterior corner of the orbit. Anteriorly, it contacts the posterior margin of the antorbital, and its anterodorsal margin briefly contacts the posteroventral corner of the nasal (N; Fig. 3.1). No canals are visible on this structure in the tomogram or through external analysis.

The suborbitals are large plate-like bones that anteriorly contact the posterior margins of the infraorbital series and the supramaxilla and maxilla. The ventral suborbital is largest, roughly 1.5 times the size of the dorsal suborbital, and both are trapezoid. Posteriorly, their margins slightly overlie the anterior margin of the preoperculum.

The preoperculum is not completely preserved in the tomogram but is visible externally. It is trapezoid shaped, with a crescent shaped anterior margin that is slightly overlain by the suborbitals anteriorly. The anteroventral corner starts posterior to the quadrate and symplectic, and ventral to the posterior margin of the hyomandibula (Fig. 3.2). The ventral half is broad, flanking the ventral suborbital anteriorly, and the suboperculum (Sop) and interoperculum (Iop) posteriorly (Figs. 3.1, 3.2). As it extends dorsally, it tapers to a point between the operculum and dorsal suborbital, forming a narrow dorsal limb. There is no evidence of a canal in the tomogram.

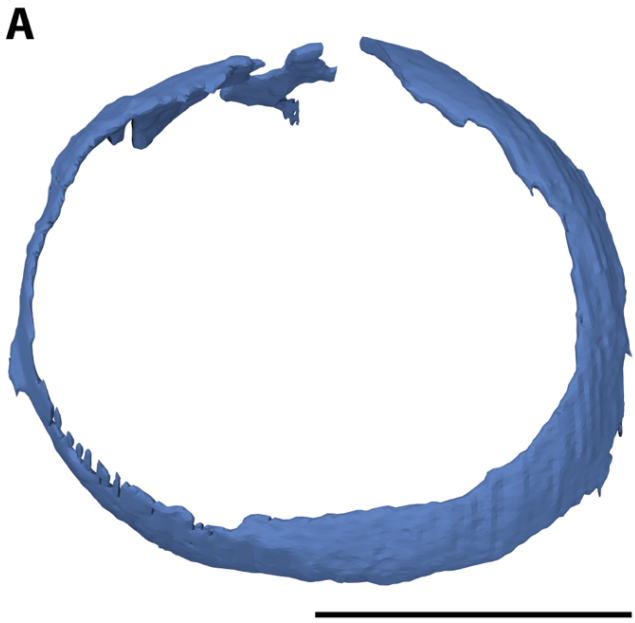

Figure 3.8 – Three-dimensional render of the left sclerotic ossicle of M1361a in lateral view. Scale bar represents 1 cm.

Dorsal gill skeleton

I identified four pairs of epibranchials (EbI–IV) and three pairs of pharyngobranchials (PbI–III; Figs. 3.2, 3.3, 3.9A). The epibranchials are approximately 'u'-shaped in cross-section and possess an uncinate process on the dorsal lateral margins, which are most strongly developed on epibranchials III and IV. Each epibranchial is straight, and they direct inward towards the midline anteriorly. The longest is epibranchial I, and each subsequent epibranchial being shorter than the previous.

Each of the infrapharyngobranchials has unique morphologies. The shortest is pharyngobranchial I, which is tubular, and sits almost oblique to the rest of the gill skeleton, and its anterior margin articulates with the parasphenoid lateral to the foramen for the internal carotid arteries (ainp I; Fig. 3.4D). Pharyngobranchial II is twice the length of the first, and a similar shape, but bears a cylindrical uncinate process on the lateral margin,

roughly a quarter of the way back from the anterior. From this process, pharyngobranchial II widens gradually and terminates at a square end. The anterior margin of pharyngobranchial II articulates with the parasphenoid posteromedial to the foramen for the carotid artery. Pharyngobranchial III is three times the length of the first and also tubular, but slightly laterally compressed. It curves outwards laterally and bears an uncinate process halfway along the lateral margin. Pharyngobranchial III has been displaced during preservation and so does not articulate with the braincase. Both pharyngobranchials II and III are directed medio-anteriorly at a similar angle to the epibranchials (Fig. 3.9A).

Ventral gill skeleton

The gill basket is the best-preserved internal structure (Fig. 3.9B–D). Of the ventral gill skeleton, at least one basibranchial (Bb), three pairs of hypobranchials (HbI–III), five pairs of ceratobranchials (CbI–V) and associated rakers (Rks) are present.

The anteriormost structures are the hypobranchials. Hypobranchials I and II are morphologically similar, with hypobranchial II sitting medial to hypobranchial I. Hypobranchial II is roughly two-thirds the length of hypobranchial I. Both are straight but angle medio-anteriorly. The anteriormost portion of both also has a small articular process which curves inwards to almost meet along the midline. Hypobranchial III is posterior to hypobranchial II and flanks the posterior half of the basibranchial. The right hypobranchial III has become slightly displaced so sits ventral to the rest of gill skeleton. Each is triangular, and medial anterior margin bears an uncinate process directed towards the midline.

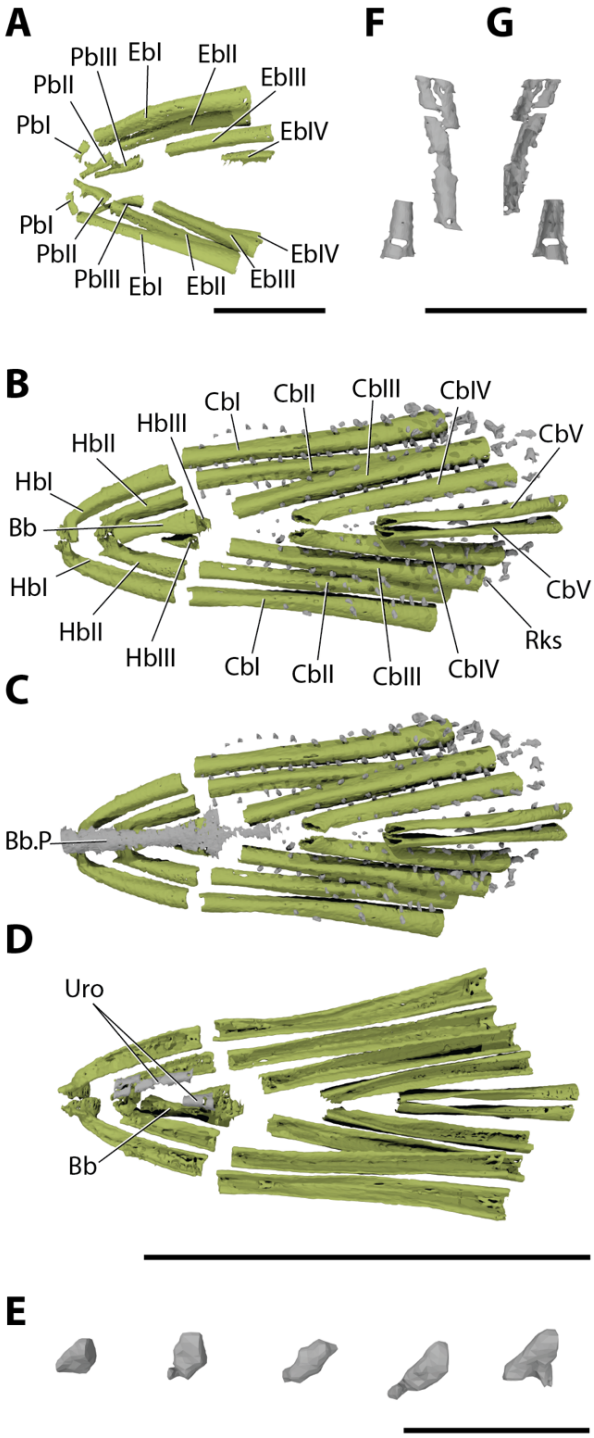

Figure 3.9 – Three-dimensional renders of the gill skeleton and gill rakers of M1361a. A) the dorsal gill skeleton in ventral view, B) interpretative drawing of the dorsal gill skeleton in ventral view, B) the ventral gill skeleton in dorsal view showing the gill rakers, C) the ventral gill skeleton in dorsal view showing the gill rakers and basibranchial tooth plate, D) the ventral gill skeleton in ventral view showing the urohyal *in situ*, E) the gill rakers in lateral view, F) the urohyal in dorsal view, G) the urohyal in ventral view. Light green is used to represent the gill basket; and grey is used to show the basibranchial toothplate, urohyal and gill rakers. Scale bar represents 2 cm for panels A; 5 cm for panels B–D; and 1 cm for panel E–G.

At least one basibranchial sits along the longitudinal midline just posterior to the origin of hypobranchial II (Fig. 3.9D). It is straight, tubular in cross-section, with a slight medial constriction. On the midpoint of the ventral surface, there is an uncinate process that angles posteriorly at a 45° angle.

There is also a large, single tooth plate associated with the basibranchial (Fig. 3.9C; Bb.P), which sits anterodorsal to the hypobranchials and basibranchial, and terminates between the third ceratobranchials. Due to incomplete preservation, its true shape is difficult to determine, but it appears to be the same width as the basibranchial, and has a pair of lateral projections approximately two-thirds posteriorly along the tooth plate, covering the third hypobranchials. Due to the resolution of the scan, no dentition could be observed.

There are five ceratobranchials present, and each originates posteromesial to the one preceding it (Fig. 3.9B–D). The longest are ceratobranchials I–III, which are all 'n'-shaped in cross-section and approximately all the same length. The anterior margins of ceratobranchials I–III align with the posterior margins of hypobranchials I–III respectively, with a small gap separating them. Ceratobranchial IV is also 'n'-shaped in cross-section, but anteriorly it becomes strongly laterally compressed, forming a medially concave articulation area. Ceratobranchial V is the only ceratobranchial to sit parallel to the midline, rather than being directed inwards anteriorly. It bears the same articulation site as described in ceratobranchial IV, but its cross-section is ovoid rather than 'n'-shaped. This shape is not constant throughout: the ventral midsection of the bone is highly laterally compressed, creating a semi-circular arch between the anterior and posterior margins. It also has a twisted

appearance anteroposteriorly, caused by the ventro-medial anterior margin moving to become the ventrolateral posterior margin.

The space between the dorsal and ventral gill arches is littered with small gill rakers (Fig. 3.9C, D). The rakers are short, rounded projections that are evenly spaced along the edges of the ceratobranchials and epibranchials. Both the dorsal and ventral rakers are present, but some have become displaced during preservation. Each raker is tooth-like and slightly ovoid, and the anteriormost rakers are approximately 2 mm tall but gradually increase in height, until the posteriormost rakers are double the height of the anteriormost rakers (Fig. 3.9E). Approximately 15 evenly spaced rakers are associated with each ceratobranchial and ten associated with each epibranchial. There are no rakers associated with the basibranchial, hypobranchials, or pharyngobranchials.

A median structure lies ventral to the basibranchial of the ventral gill skeleton (Uro; Figs. 3.3B, 3.9F, G). It is poorly preserved but appears to be 'u'-shaped in cross-section, similar to the epibranchials (Fig. 3.9). There appear to be three pieces, but it is unclear if they represent separate structures or if a single structure has been broken. The middle fragment is the longest, which is flanked laterally by a fragment roughly a third of its length, and both sit beneath the left hypobranchial II. The final fragment is postero-lateral to the largest fragment and sits beneath the basibranchial and left third hypobranchial, and between the hypobranchial IIs. Its anterior margin is the same width as the middle fragment's posterior margin but gradually widens to twice its width by the time the posterior margin is reached. I identify this structure as a urohyal.

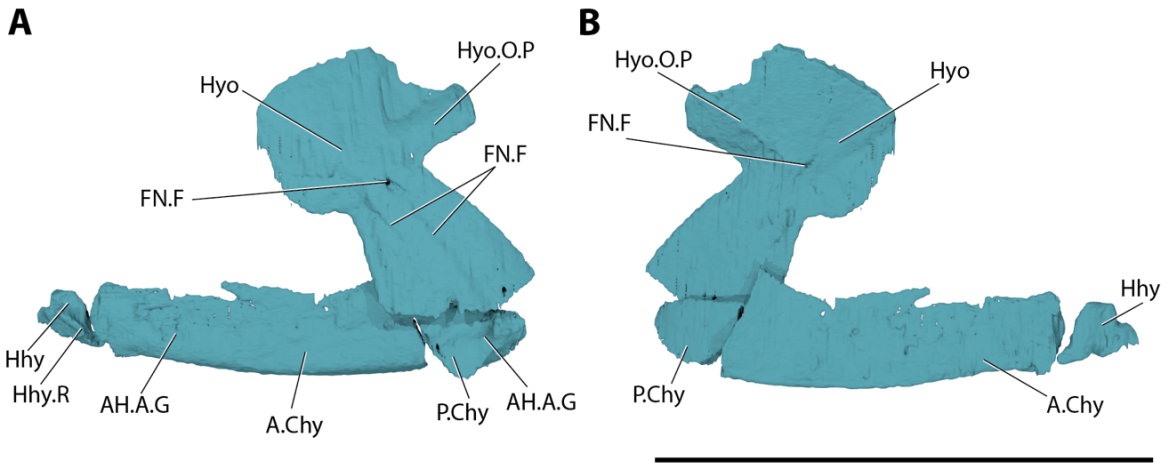

Figure 3.10 – Three-dimensional renders of the left hyoid arch of M1361a in A) lateral view, B) medial view. Scale bar represents 5 cm.

Hyoid arch

The hyoid arch consists of the hypohyals (Hhy), anterior (A.Chy) and posterior (P.Chy) ceratohyals, hyomandibula (Hyo; Fig. 3.10), and symplectic (Sym; Fig. 3.7). No interhyals were identified.

The hypohyal articulates with the anterior ceratohyal (Figs. 3.3B, 3.10). It is roughly the same size as the posterior ceratohyal and approximately trapezoidal (Fig. 3.10). A ridge extends anteroposteriorly along the middle of the lateral surface at a 20° angle (Hhy.R; Fig. 3.10).

Of the ceratohyals, those from the left side are best preserved (Figs. 3.2, 3.10). The anterior ceratohyal is approximately ¾ the length of the mandible, and starts directly ventral to the anterior of the sclerotic ossicle, and ventro-lateral to the gill skeleton. It is laterally flattened, and has slightly concave dorsal and convex ventral margins. The posterior margin terminates mesial to the hyomandibula and mandibular-quadrate joint, as a squared end. A groove for

the afferent hyoid artery extends along the upper third of the lateral side for most of its length, but sweeps up sharply to meet the dorsal margin just behind the anterior margin (AH.A.G; Fig. 3.10).

The posterior ceratohyal is about a fifth of the length of the anterior ceratohyal and sits ventral and mesial to the hyomandibula. The overall shape is roughly triangular, but all margins are rounded slightly. Its dorsal margin is straightest and follows the same angle as the ventral margin of the hyomandibula, but they do not contact. Both the anterior and posterior ventral margins are thickened relative to the dorsal margin, forming a shallow groove that extends between the mesial and lateral sides, from the posteroventral margin to the anteroventral margin. Near the posterior margin of the lateral surface, there is a deep excavation, which appears to be a continuation of the groove for the afferent hyoid artery that is seen on the anterior ceratohyal (AH.A.G; Fig. 3.10).

The hyomandibula is separated into two portions by a pronounced waist (Fig. 3.10). The anterior half of the dorsal portion is roughly circular, with the opercular process (Hyo.O.P; Fig. 3.10) extending from the posterior margin at approximately 45°. Anteriorly, the dorsal portion meets the posterior margin of the metapterygoid (Fig. 3.2). The ventral portion is trapezoid and inclines anteriorly (at about 60°) and makes up roughly half of the full height of the hyomandibula. The lateral surface bears two parallel grooves that extend up the centre of the ventral portion and terminate approximately halfway up the bone (FN.Gr; Fig. 3.10). The foramen for the facial nerve pierces both lateral and mesial sides in approximately the centre of the bone (FN.F; Fig. 3.10).

The symplectic is ventral to the hyomandibula, and slots between the ventral margin of the quadrate along its mesial surface. It is about half the length of the quadrate, and is cylindrical in cross-section, with the posterior half gradually increasing in size before terminating with a square edge (Fig. 3.7). The posteroventral corner of the mandibular-quadrate joint of the mandible does not form a secondary articulation with the symplectic.

Operculogular series

This series consists of the branchiostegal rays (Bsr; Fig. 3.3B), the interoperculum (Iop), operculum (Op) and the suboperculum (Sop; Figs. 3.1, 3.2, 3.11). The operculum is not present in the scan, but is seen externally on the fossil. The gular plate is only visible externally as a plate between the anterior quarter of the mandibles (Gul; Fig. 3.1E–F).

Of the opercular series, the best-preserved examples are on the left side (Figs. 3.2A, 3.11A). The interoperculum is anteroventral to the suboperculum, and ventral to the preoperculum and hyomandibula. The dorsal corner of the interoperculum overlaps the ventral margin of the suboperculum, and posteroventral corner of the operculum. The interoperculum starts just posterior to the jaw joint and symplectic, and external analysis shows it was trapezoid rather than the triradiate structure indicated in the model reconstructed from tomograms.

The suboperculum is dorsal to the interoperculum and posterior to the hyomandibula and preoperculum. The main body is trapezoid, but the anterodorsal corner bears a long dorsal process that extends dorsally between the preoperculum and the anterior margin of the operculum (Sop.Pr; Figs. 3.1, 3.2, 3.11A).

The ventralmost structures of the skull are the branchiostegal rays, of which between 15–21 are visible in the tomogram but at least 40 are visible externally (Figs. 3.1C, 3.3B, 3.11B). They articulate with the ventromedial margin of the interoperculum and the ventrolateral margin of the posterior ceratohyal. From this origin, they fan outwards as they extend posteriorly, terminating just anterior to the cleithrum (Figs. 3.2A, 3.3B).

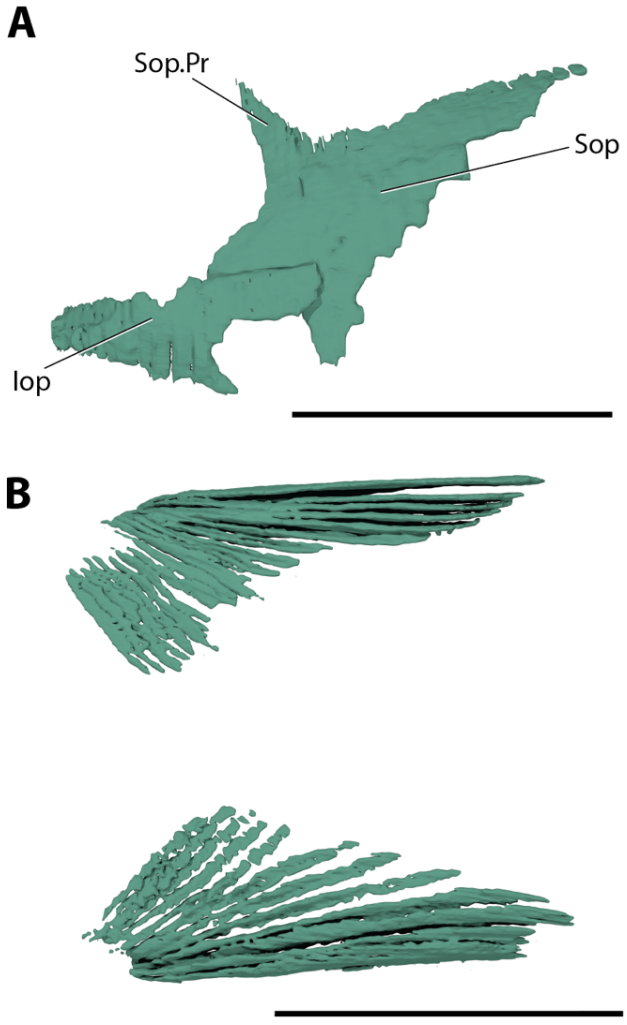

Figure 3.11 – Three-dimensional renders of the operculogular system of M1361a. A) the interoperculum and suboperculum in lateral view, B) the branchiostegal rays in ventral view. Scale bars represent 2 cm.

Pectoral girdle

The pectoral girdle is composed of the cleithrum (Cl), dorsal and ventral postcleithra (P.Cl; Figs. 3.2, 3.12), and supracleithrum (S.Cl; Fig. 3.2), the scapulocoracoid (Scc; Figs. 3.2, 3.12, 3.13), and fin radials (Rad; Figs. 3.12, 3.14). The fins are also present, which are described below (P.F; Figs. 3.1–3.3, 3.12, 3.15).

The cleithrum forms a crescent shape similar to the preoperculum (Figs. 3.2, 3.12). It has a thickened ventral half that forms a vertically orientated, triangular base with a short, anterior limb, and thin dorsal half that forms a long dorsal limb. This dorsal limb extends upwards and curves forward in a comparable shape to the preoperculum. The anteroventral corners of the anterior limb almost meet along the longitudinal midline, just posterior to the last pair of ceratobranchials, then curve outwards laterally to flank the lateral edges of the scapulocoracoids. These anteroventral corners also bear a lateral groove that follows the dorsal margin of the anterior limb. This groove disappears at the broad, middle section of the cleithrum, where the lateral surface inclines medially to become an almost horizontal shelf.

Posterior to the cleithrum are the dorsal and ventral post-cleithra (Fig. 3.12). The dorsal post-cleithrum is a small, plate-like, triangular bone that aligns with the posterodorsal margin cleithrum. The ventral postcleithrum sits behind the posteroventral corner of the cleithrum, but it is incomplete, making its shape unclear.

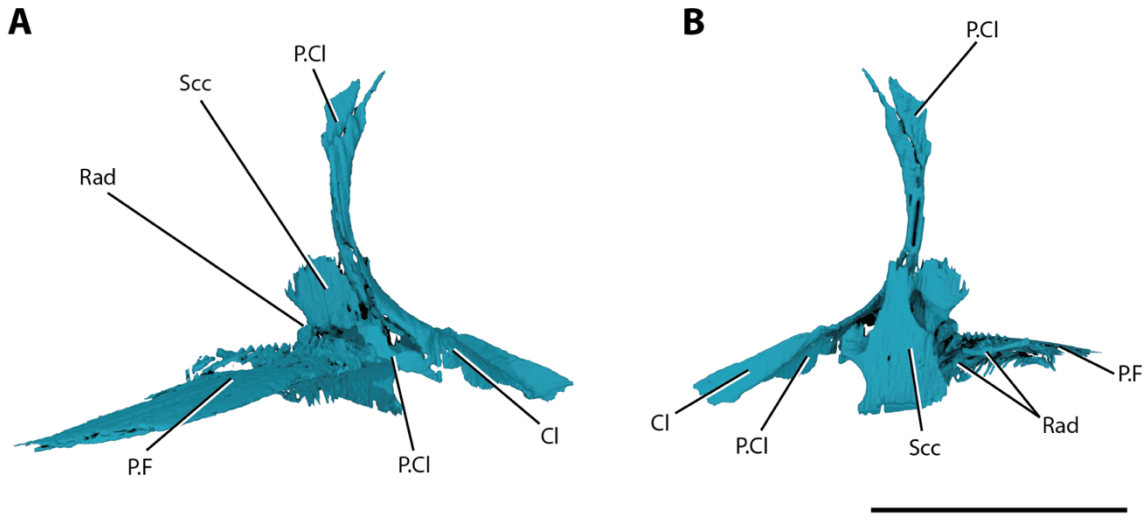

Figure 3.12 – Three-dimensional renders of the right pectoral endoskeleton of M1361a in A) lateral view, B) in medial view. Scale bar represents 3 cm.

The supracleithrum is mostly complete, but possesses a slightly uneven dorsal margin, indicating damage (Fig. 3.2B). However, the ventral margin appears complete and possesses a kink, or elbow, approximately halfway along its length. It is a slender structure, positioned anterior to the cleithrum and extends above the space for the operculum, terminating just posterior to the opercular process of the hyomandibula.

The scapulocoracoid is tripartite, and consists of the scapula, the mesocoracoid, and the coracoid as a single ossification (Fig. 3.13). The scapula (Scp) is the large, dorso-lateral portion, which contacts the posterior surface of the dorsal limb of the cleithrum along its anterior margin. Medial to the scapula is the mesocoracoid (MCor), which forms a horizontal arch around the dorsal muscle canal (dmc) and braces against the medial surface of the coracoid (Crr).

The mesocoracoid also bears a short anterior process that extends slightly beyond the anterior margin of the scapulocoracoid itself. The corner between the scapula and mesocoracoid arch forms a small foramen for the diazonal nerve (fdn).

The coracoid is the broad, plate-like ventral projection on the mesial side, which has a concave anterior margin to form the ventral muscle canal (vmc) between the ventral process of the coracoid and the anterior limb of the cleithrum. The coracoid also possesses an anterior (A.C.Pr) and posterior process (P.C.Pr; Fig. 3.13). While both scapulocoracoids are present, the left has become slightly displaced, but the right is in situ.

The posterior margin of the scapulocoracoid bears a number of shallow facets, the glenoid fossae (Gl.F; Fig. 3.13), for the articulation of the radials. The lateralmost facet is convex and marks the corner between the scapula and the mesocoracoid arch, which is where the dorsomedial corner of the propterygium articulates with the scapulocoracoid. The second facet is deepest for the concave anterior margin of the second radial. It is unclear how many more facets there are but at least two more radials articulate directly with scapulocoracoid in this specimen. One contacts a facet that is ventro-lateral to the second radial, and the other inserts into a deep crater-like facet (R.Fa; Fig. 3.13) that marks the junction between the mesocoracoid arch and the ventral process of the coracoid.

Six fin radials are present in the pectoral fin (Fig. 3.14), and articulate with the posterior surface of the pectoral girdle (Fig. 3.12). The propterygium (Ptg; Fig. 3.14) is the anteriormost radial which is medial to, but not fused with, the proximal lepidotrichia and

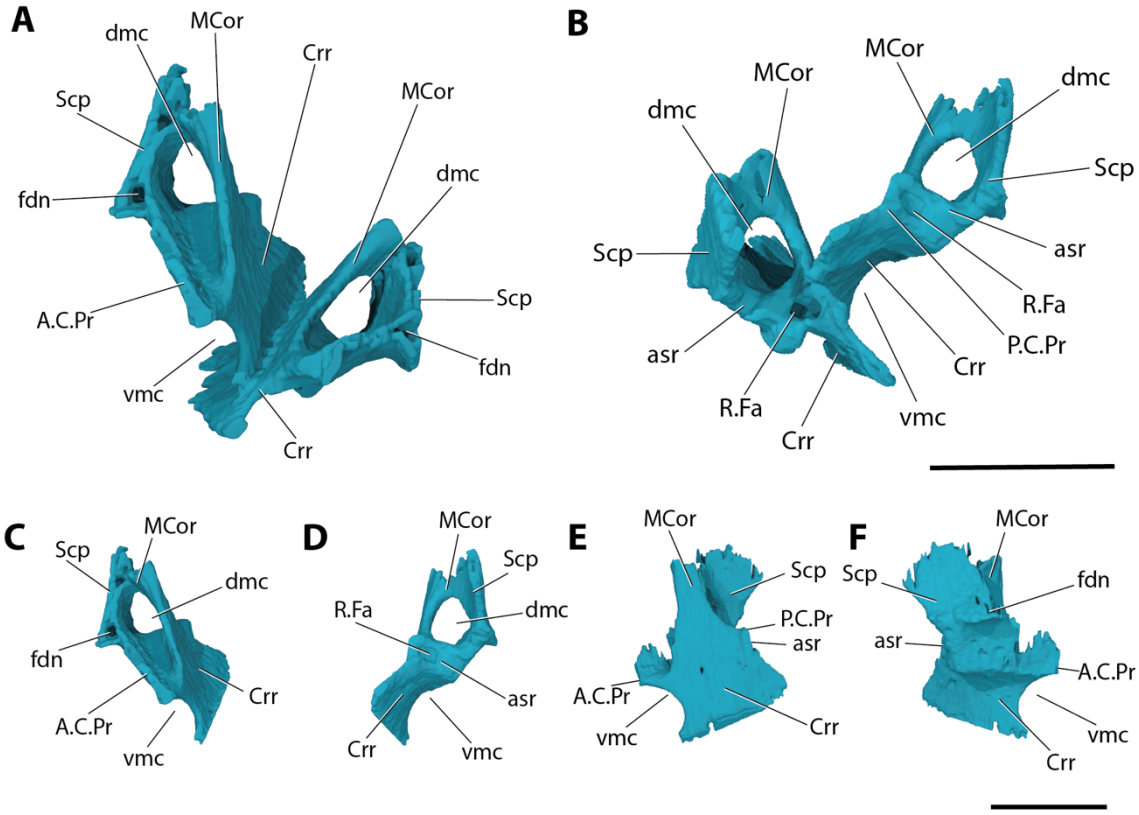

Figure 3.13 – Three-dimensional renders of the scapulocoracoid of M1361a. A) both scapulocoracoids in anterior view, B) both scapulocoracoids in posterior view, C) the right scapulocoracoid in anterior view, D) the right scapulocoracoid in posterior view, E) the right scapulocoracoid in medial view, F) the right scapulocoracoid in lateral view. Scale bar represents 2 cm in panels A and B; and 1 cm in panels C–F.

instead is braced by other lepidotrichia. It is roughly trapezoid, with a small ventral process that projects ventrolaterally from the bone at a 45° angle. The ventral margin, medial to the ventral process, is pierced by the propterygial canal anterodorsally. The second radial (II; Fig. 3.14) is largest and roughly square, with a concave anterior margin, orientated vertically. The two radials following the second radial have a paddle-shaped anterior head, and rod-like posterior portion (III–IV; Fig. 3.14). The fifth radial is long and skinny, with a slight medial constriction, and a laterally expanded head posteriorly to articulate with the fin rays (V; Fig. 3.14).

There is a final radial that matches that in Jessen's (1972) mechanically prepared specimen of *Pachycormus* (Jessen 1972; pl. 24.1), with a forked distal bifurcation that leads me to identify it as a metapterygium (Mtg; Fig. 3.14). This metapterygium is situated close to the posterior margin of the scapulocoracoid, but it is unclear if it articulated directly with the scapulocoracoid.

Both of the distinctive, slender pectoral fins are visible from external analysis, but only one has been rendered in the tomogram (Figs. 3.2A, 3.3). It is lateral to the scapulocoracoid and radials, and posterior to the cleithrum (Fig. 3.12). There are at least 20 fin rays (FRs), which have distal 'Y'-shaped bifurcations that occur independently of the ray joints (bf; Fig. 3.15).

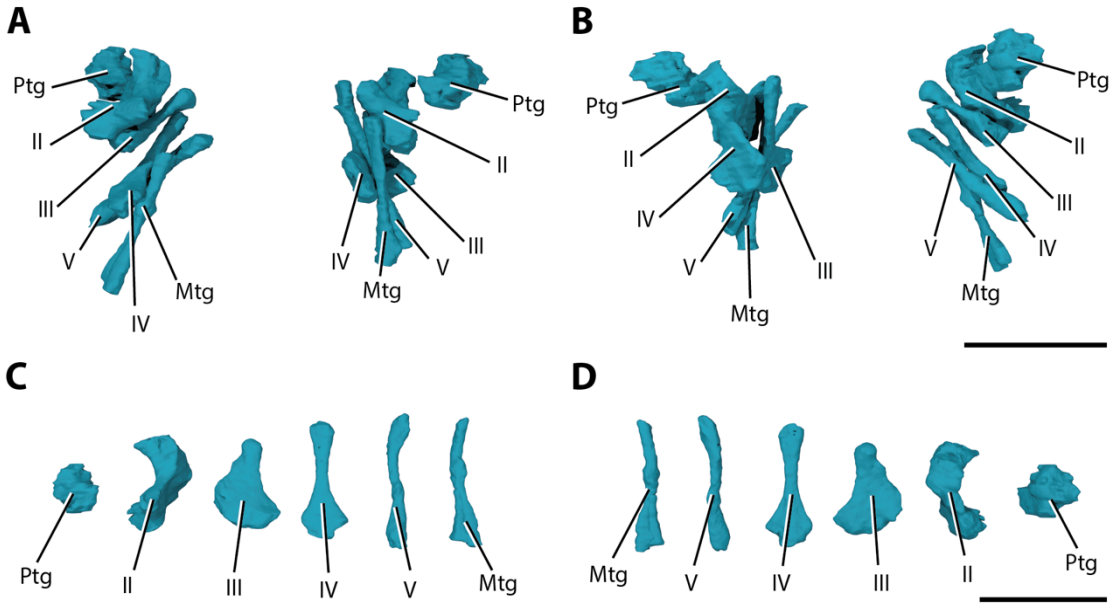

Figure 3.14 – Three-dimensional renders of the fin radials of M1361a. A) the radials arranged *in situ* in dorsal view, B) the radials arranged *in situ* in ventral view, C) the radials arranged individually in dorsal view, D) the radials arranged individually in ventral view. Scale bar represents 1 cm.

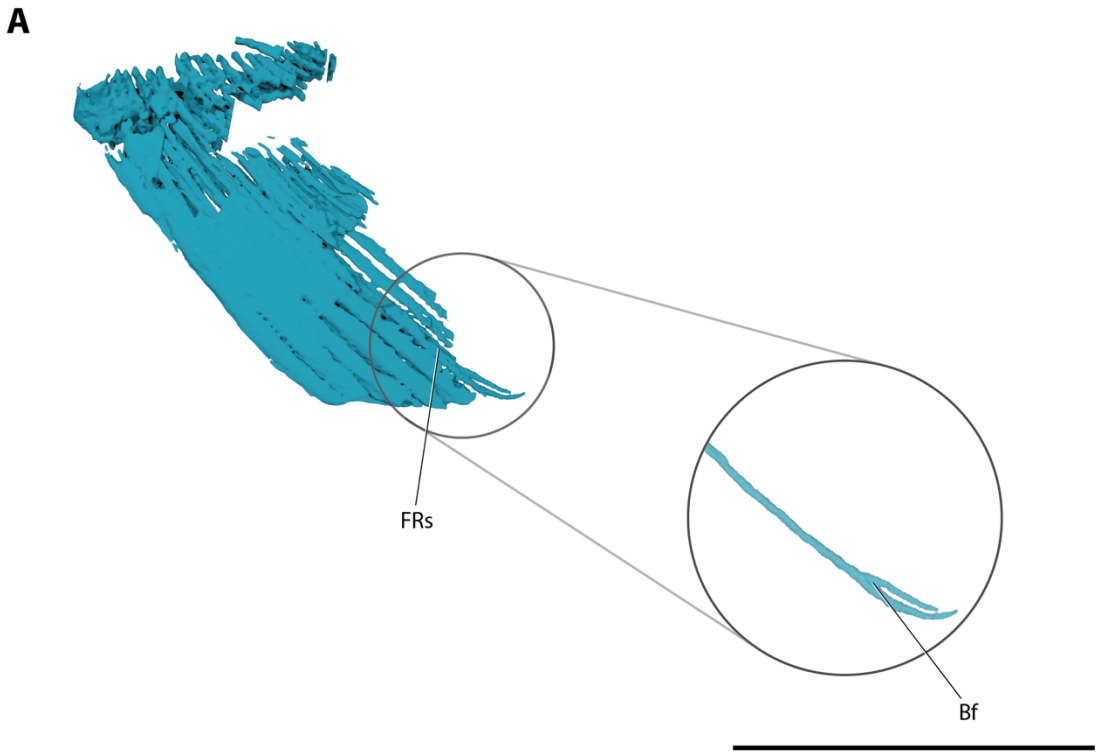

Figure 3.15 – Three-dimensional renders of the left pectoral fin and fin ray bifurcation of M1361a in dorsal view. Scale bar represents 5 cm.

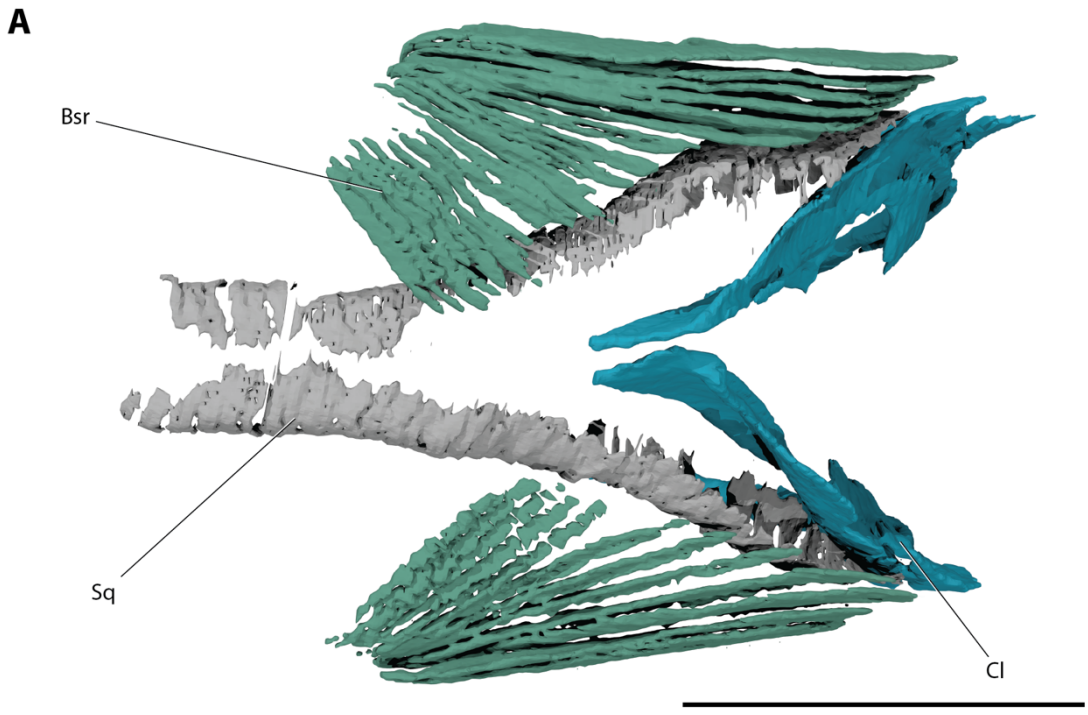

Figure 3.16 – Three-dimensional renders of the branchiostegal rays, the cleithra, and squamation flanking the cleithra of M1361a in ventral view. Dark green is used to represent the branchiostegal rays; turquoise is used to represent the cleithra; and grey is used to represent the 'hair-like' embedded squamation that sits in a similar topological position to the clavicle or serrated appendage. Scale bar represents 2 cm.

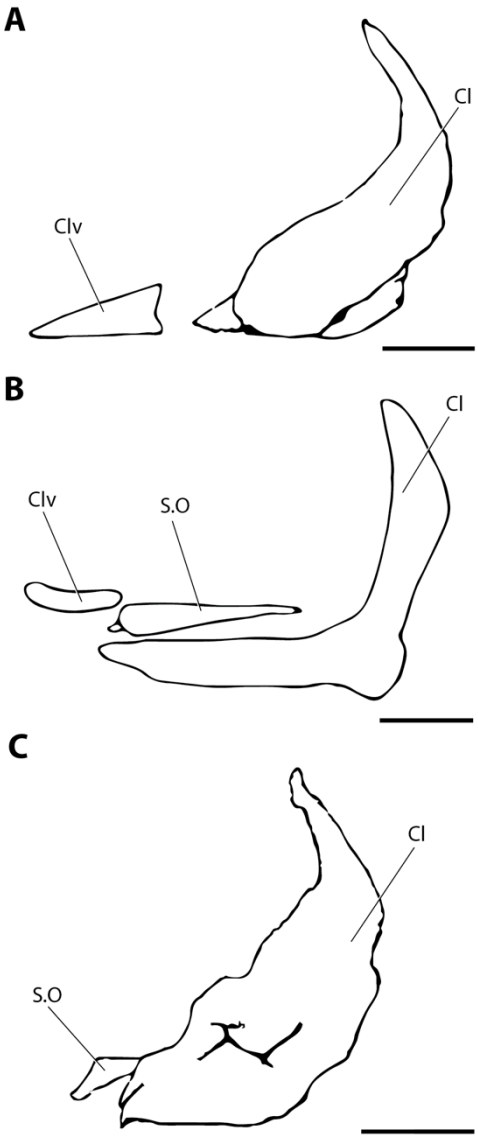

Figure 3.17 – Interpretive drawings of the clavicle or serrated appendage of A) *Watsonulus* (interpreted from Olsen 1984; fig. 16), B) *Amia* (interpreted from Grande & Bemis 1998; fig. 89), C) *Semionotus* (Olsen & McCune 1991; fig. 11). Scale bars represent 1 cm.

Previously unknown structure

Between the branchiostegal rays and ventral skeleton, and anteroventral to the cleithra, is a paired structure of uncertain identity (Sq; Figs. 3.3B, 3.16). Each structure is semi-circular in cross-section, and seems to be composed of many 'hair-like' structures, being long and slim and arranged sequentially. Anteriorly, they originate close to the midline, ventral to ceratobranchials IV and V, and then move laterally to flank the ventrolateral edge of the

cleithra, forming a sigmoid shape in ventral view. It is possible that these are a series of scales that have become embedded dorsal to the branchiostegal rays. If not squamation, the position relative to the cleithra suggests two other possibilities: either a serrated appendage or clavicle, but the morphology of the structures differs from these (compare Sq, Fig. 3.16, with Clv or S.O, Fig. 3.17). Therefore, I interpret these paired structures as squamation embedded between the branchiostegal rays and the ventral gill basket.

Phylogenetic analyses

Matrix construction and coding

The morphology-only dataset is based on the matrix produced by Friedman (2012*a*), which included characters derived from previous analyses of pachycormiform relationships including the characters from Mainwaring (1978) that were formalized by Lambers (1992) and Liston (2006). It was edited in Mesquite V.3.5 (Maddison & Maddison 2018), and has been expanded to include three species of aspidorhynchids, which have previously been suggested as closely related to pachycormids (Brito 1997; Arratia 1999): *Aspidorhynchus acutirostris*, *Belonostomus tenuirostris*, and *Vinctifer comptoni*. Codings for *Pachycormus* were updated in light of the description below, and *Martillichthys renwickae* was recoded in light of the description by Dobson *et al.* (2019; Chapter 2). The genus *Orthocormus* was also atomized so all three currently recognized species (*O. cornutus* Weitzel 1930; *O. roeperi* Arratia & Schultze 2013; *O. teyleri* Lambers 1988) were represented. While *Caturus*, *Euthynotus*, *Lepidotes*, *Protosphyraena* and *Pteronisculus* are also represented by multiple species each, however, unlike other genera that contain multiple species, I have not coded these as individual species. This is because some of the specimens analysed, for example *Caturus* and

Lepidotes, are not identified to a species level, or individual species are too poorly known to be informative on their own. Additionally, the species of *Euthynotus* are poorly known and described (Wenz 1967), and *Protosphyraena* type material is fragmentary material such as teeth and fins (e.g. Woodward 1895*a*, *b*, 1908). The specimens and literature descriptions used to code these composite taxa are listed in the appendix (Appendix C).

All taxa were updated with respect to the corrections highlighted in Arratia and Schultze (2013), and a review of the relevant literature. Twelve additional characters (both novel and from the literature) were also added; see the Character List in the appendix (Appendix C) for full details and references. Due to incomplete coding, *Discoserra pectinodon* was removed, and several characters from the original matrix (Friedman 2012*a*) are modified or excluded: vertebrate fused into adult occipital condyle (ch. 23; present/absent); the shape of the posterior margin of the skull roof (ch. 37; 'W'-shaped/straight or concave); marginal dentition (ch. 56; present/absent); maxilla length relative to skull length (ch. 64; long, extends beneath orbit/short); position of orbit relative to the maxilla (ch. 65; centred over maxilla/restricted to the posterior half of the maxilla); position of jaw joint (ch. 76; well behind orbit/below or anterior to orbit); uroneurals (ch. 101; absent/present); and the clavicle (ch. 105; present/absent). Character 23 was removed because it can only properly be assessed in taxa where ontogeny can be observed, and therefore any codings of fossil taxa would be on the basis of preconceived assumptions of homology. Character 37 has now been split into two characters: the free, elongate posterior process of the dermopterotics (ch. 38, absent/present) and median projection of the parietal posterior margin (ch. 122, present/absent); this allows additional morphological information to be captured. Character

56 is changed to measure dentary rather than marginal dentition. This allows the extent of dentition to be more accurately analysed through measuring dentary dentition (this character), prearticular dentition (ch. 88) and the new character: maxillae dentition (ch. 131; absent/present). Character 64 is expanded to measure more variation in maxilla length in terms of relative skull length rather than orbit position (as measured in ch. 65). The new character states for character 64 are as follows: one third or less/between one and two thirds/over two thirds. Character 65 is expanded to distinguish between taxa with orbits placed fully posterior to the maxilla (indicating a long sphenoid region) or those with orbits slightly behind the midpoint of the maxilla by using the following character states: centred over the maxilla/restricted to the posterior half of the maxilla/fully posterior to maxilla. Character 76 is coded reliably for many taxa in the matrix, but it is too similar to character 65 (outlined above). Keeping both of these characters would double the signal strength of what is essentially a question about skull dimensions, with a focus on the length of the ethmoid region. Therefore, as character 65 had more character states (allowing for more subtle variation to be captured), this character was retained while character 76 was removed. Character 101 was expanded to account for the differences in homology of uroneurals as raised by Arratia and Schultze (2013), who point out that pachycormiform uroneurals are composed of preural, not ural elements. Therefore, the character states are now as follows: absent/composed of ural elements/composed of preural elements. Character 105 (clavicle present/absent) was deleted and modified into character 133 (paired ossification anterior to the cleithrum) which removed the assumptions of homology that would come with identifying a clavicle or a serrated appendage in the taxa analysed.

The final morphological dataset comprises 129 morphological characters and 33 taxa. A molecular dataset (with DNA sequences of 12 nuclear genes; Broughton *et al.* 2013) was then combined with this dataset, and extinct taxa were calibrated to their stratigraphic ranges (from Gradstein *et al.* 2012). Of the 33 taxa coded, four had both morphological and molecular data coded, and two were coded from more than one species following Giles *et al.* (2017). These used morphological data taken from *Elops hawaiiensis* and *Lepisosteus platostomus*, and nuclear gene data from *Elops saurus* and *Lepisosteus osseus* respectively. *Amia calva* and *Hiodon alosoides* were coded for both morphological and molecular data. For analyses containing all taxa, the Triassic stem neopterygian *Pteronisculus* sp. was the designated outgroup (López-Arbarello & Sferco 2018).

Pachycormiform-only matrix

I used a reduced dataset containing only pachycormiforms in order to test an alternative hypothesis for pachycormiform interrelationships. As previous analyses have resolved *Euthynotus* spp. as the sister taxon to all other pachycormiforms (Friedman 2012*a*; Wretman *et al.* 2016), this was designated as the outgroup. As no molecular data are available for these taxa, only morphological and stratigraphic data were included for the pachycormiform-only analyses. This pachycormiform-only matrix was not used as a tool for inferring pachycormiform relationships but rather as a restricted dataset to test alternative hypotheses for the origin of suspension-feeding pachycormiforms (see stepping stone analysis section below).

Phylogenetic analyses

Maximum parsimony. Parsimony analyses were run in PAUP* 4.0a163 (Swofford 2003) for both the complete dataset and the pachycormiform-only subset. Only the 129 morphological characters were used for this analysis. I conducted an equally weighted parsimony analysis with random stepwise addition, five trees held at each step, and maxtrees set to 35000 and 500 replicates. Bootstrap values were calculated using a heuristic search with 500 replicates, and 5 trees held at each step. Bremer decay support was calculated using a heuristic search that increased the length of the shortest trees by one until all the nodes completely collapsed and were unresolved.

Bayesian analyses. The following analyses were conducted in MrBayes 3.2.6 (Ronquist *et al.* 2012): a morphology-only analysis to compare against the parsimony analysis, and a tip-dating analysis using a Fossilized Birth-Death (FBD; Heath *et al.* 2014) model. Both these analyses were conducted using the complete dataset only. The pachycormiform-only dataset was used only for the stepping stone analysis (see below).

To conduct the morphology-only analysis, any genetic or stratigraphic data were removed from the datasets. This analysis used the Markov chain Monte-Carlo model, with the rates prior set to a gamma distribution. There were 4 chains used for 2 runs with samples taken every 100 steps, and 50% of each run was discarded as burn-in.

The analyses employed the Fossilized Birth-Death model (Heath *et al.* 2014) included morphological, genetic (where available), and stratigraphic data for the complete dataset. I

partitioned the dataset to use an inverse-gamma (6-category) distribution of rates for genetic data, and a gamma distribution rate for morphological data. For stratigraphic data, extinct taxa were assigned a uniform range (constrained by estimates provided by ammonite zones from Gradstein *et al.* 2012) and fixed to 0 if they are extant. For taxa spanning long intervals (e.g. *Protosphyraena* and *Bonnerichthys*), stratigraphic ranges were set to the shortest time interval of their first occurrence record. The sample stratigraphy (samplestrat) prior used 'diversity' assumptions but was split into 4 regimes to account for preservation heterogeneity in the fossil record (Wright 2017*a*). These regimes were set to represent the Toarcian–Bathonian (Mid-Jurassic; 182.7–161.1 Ma), Callovian–Tithonian (Late Jurassic; 166.1–145 Ma), Berriasian-Aptian (Early–late Early Cretaceous; 145–113 Ma), and Albian–present (late Early–present; 113 Ma–present). These partitions were chosen to account for the heterogeneity of preservation between them, with the Early Cretaceous in particular having a poor fossil record for marine actinopterygians, while other intervals are characterized by numerous well-studied and well-preserved marine fish faunas (e.g. Oxford Clay, Cerin, Solnhofen in the case of the Callovian–Tithonian interval; Barthel *et al.* 1990; Martill 1990; Bernier *et al.* 1991).

I used a fossilization clock (in order to run an FBD analysis), which assumes an exponential speciation prior, and designated an instantaneous branching rate of 0.05 per lineage-million years as my prior ("speciationpr=exp(20)"). The extinction and fossilization priors were set to beta(1,1), which assumes a uniform (flat) prior for chance of extinction/fossilization, and is the default in MrBayes. The sample probability was 0.00013 (as only a tiny subset of living neopterygians was sampled), and the clock rate prior was given a gamma(1,2) distribution.

For all Bayesian analyses, a Markov chain Monte-Carlo model was set to run until the standard deviation of split frequencies was below 0.01 and the effective sample size given in Tracer v.1.7.1 (Rambaut *et al.* 2018) was greater than 250, indicating run convergence.

Resulting consensus trees from the parsimony and Bayesian analyses were viewed in FigTree v.1.4.3 (http://tree.bio.ed.ac.uk/software/figtree/). Changes in morphological character states were traced and a final optimisation tree for the maximum parsimony analysis was constructed MacClade (v.4.08; Maddison & Maddison 2005). For the Fossilized Birth-Death Model, tip dates and their credible intervals were also viewed in FigTree.

Stepping stone analysis. To test statistical support for the alternative hypothesis of a second origin of suspension feeding compared to the currently accepted relationships (Friedman 2012*a*; Wretman *et al.* 2016), the morphological and stratigraphic data of the pachycormiform-only subset was used.

I used the same priors as the FBD model analysis, but used the assumption that the latest occurring pachycormiforms (*Bonnerichthys* and *Protosphyraena*) are still extant, setting their calibration priors to 'fixed(0)' because current implementation is not optimized for analyses without some extant tips (see Wright 2017*b*). All other ages were adjusted accordingly, and set relative to the midpoint of the stratigraphic range of *Bonnerichthys* and *Protosphyraena* records from the Western Interior seaway (86.15 Ma; Gradstein *et al.* 2012; Friedman *et al.* 2013*a*; Stewart 1988). Sampling regimes were removed due to analyses failing

to converge. The sampling probability prior was also altered to 0.117 (2/17) as both *Bonnerichthys* and *Protosphyraena* represent living taxa in this analysis.

Two analyses were conducted: one with a constraint applied to group *Bonnerichthys* with the other suspension-feeding pachycormiforms (*Leedsichthys problematicus*; *Asthenocormus titanius*; *Martillichthys renwickae*; and *Rhinconichthys taylori*) to represent the currently accepted hypothesis of relationships (see Friedman 2012*a*; Wretman *et al.* 2016). No constraints were added to the relationships within this clade. The alternative topology constrained a grouping of *Bonnerichthys* with the toothed-pachycormiforms *Australopachycormus hurleyi* and *Protosphyraena* spp. to test the support for the two origins of suspension-feeding hypothesis (Liston & Maltese 2016; Dobson *et al.* 2019; Chapter 2).

These analyses used stepping stone ('ss'), with a burins prior of -1, and were run for 150,000,000 generations (Xie *et al.* 2010). The mean marginal likelihoods (expressed as natural logarithms, *ln*). These estimates of marginal likelihoods can be used to compare models through Bayes factors (Kass & Raferty 1995; Nylander *et al.* 2004; table 1). The Bayes factor (BF) is simply the ratio of marginal likelihoods for two models ($L1$ and $L2$):

$$BF = \frac{L1}{L2}$$

Since marginal likelihoods from stepping stone analyses are reported as natural logarithms, the expression for Bayes factor must be modified accordingly:

$$BF = e^{lnL1 - lnL2}$$

Strong support for a given topology is indicated by a Bayes factor exceeding 10 (Kass & Raftery 1995; Nylander *et al.* 2004; table 1).

Results

Phylogenetic analyses

The phylogenetic analyses are in broad agreement with the most recent studies of pachycormiform relationships (Friedman 2012*a*; Wretman *et al.* 2016), but some differences are outlined below.

Maximum parsimony analysis. The teleost clade (Fig. 3.18; node A) is united by three characters, two of which are unambiguous (parasphenoid pierced by the internal carotid artery, ch. 27; and an unpaired, midline ossification ventral to the basibranchial, ch. 132), and contains pachycormiforms, aspidorhynchids, *Dorsetichthys*, and the teleost crown (nodes B, Q and R respectively). Aspidorhynchids, *Dorsetichthys* and the teleost crown form a clade (node P) united by four characters, of which one is unambiguous: a median vomer (ch. 24), but Bootstrap support is weak (65%; Fig. 3.18). Pachycormiforms (node B) are resolved as the sister group to the aspidorhynchid and crown teleost clade, and their monophyly is supported by high Bootstrap support (97%; Fig. 3.18), and three homoplastic (presence of a posterior boss on the skull roof, ch. 36; the dermosphenotic contributes to more than half of dorsal margin of orbit, ch. 42; pelvic fins anterior to the midpoint between the anal and pectoral fins, ch. 118) and four unambiguous characters: contribution of the rostral bone to the oral margin (ch. 31); hypural plate present (ch. 102); long, slender pectoral fins (ch. 113); bifurcations of lepidotrichia occurring independently of joints (ch. 116). *Euthynotus* is resolved as sister taxon to all other pachycormiforms. Two unambiguous characters support the pachycormiform clade excluding *Euthynotus* (node C): absence of

independent extrascapulars (ch. 39); presence of greatly expanded urodermals forming prominent caudal keels (ch. 100), but Bootstrap support is very poor (54%; Fig. 3.18).

Pachycormiforms apart from *Euthynotus* fall into two groups, called here the 'protosphyraenid' (Nicholson & Lydekker 1889) and the 'suspension-feeding' clades (nodes D and J respectively), however Bootstrap support for these two clades is extremely weak (<50%; Fig. 3.18). Aside from within the giant bodied suspension-feeders (*Bonnerichthys*, *Rhinconichthys*, *Asthenocormus*, *Leedsichthys* and *Martillichthys*), Bootstrap support for pachycormiform interrelationships is very weak and does not pass above 60% (Fig. 3.18).

The 'protosphyraenid' clade (node D) is supported by a single unambiguous character: presence of paramedial fangs on the rostrodermethmoid (ch. 34). Node E excludes *Hypsocormus insignis* based on a single, unambiguous character: presence of procumbent fangs on the dentary (ch. 82) supporting the rest of the clade. *Hypsocormus macrodon* is excluded from the clade above node F, which is united by one unambiguous character (the rostrodermethmoid extending beyond the mandibular symphysis, ch. 32), one homoplastic character (premaxillary dentition enlarged relative to maxillary teeth, ch. 60) and Bootstrap support of 61% (Fig. 3.18). Node G is united by a single unambiguous character: absence of marginal teeth on the rostrodermethmoid (ch. 33), and so excludes *Hypsocormus tenuirostris*. The species of *Orthocormus* form a clade with unresolved internal relationships (node H) united by only one homoplastic character: presence of a sphenoid region that contributes to over ½ the overall skull length (ch. 127), but this has extremely poor Bootstrap support. The sister clade to node H (node I) contains *Protosphyraena* spp. and

Australopachycormus, and is supported by one homoplastic (absence of bifurcations of the pectoral fin-rays, ch. 115) and two unambiguous characters (parietals fused into a single midline ossification, ch. 35; and carinae extending the length of the teeth, ch. 57).

The 'suspension-feeding' clade (node J) is united by three homoplastic (presence of a narrow ascending limb of the preoperculum, ch. 55; a splint-like supracleithrum, ch. 107; absence of pelvic fins, ch. 117) and one unambiguous character (a prominent kink in the long axis of the supracleithrum, ch. 108; only coded for three taxa in the 'suspension-feeding' clade: *Ohmdenia*; *Pachycormus*; *Saurostomus*). *Pachycormus* is placed as the earliest diverging taxon within the 'suspension-feeding' clade, but bootstrap support for this placement is below 50%. The monophyly of all remaining members of this group to the exclusion of *Pachycormus* is supported by three characters, two of which are unambiguous (a broad anterior corpus of the parasphenoid, ch. 25; and the length of vertical axis of the hypural greatly exceeds the horizontal axis, ch. 103), and one is homoplastic (presence of free, elongate posterior processes of the dermopterotics, ch. 38). Node L unites members of the 'suspension-feeding' clade to the exclusion of *Saurostomus* and *Pachycormus*, and is supported by two homoplastic characters: straight anterior and posterior margins of the hyomandibula (ch. 70) and the absence of scales (ch. 119). The giant suspension-feeding pachycormiforms (node M) have one of the highest Bootstrap support values (78%; Fig. 3.18), but this support is still only moderately strong. The group is united by three synapomorphies, the only unambiguous one being the lack of dentary dentition (ch. 56). The two homoplastic characters are: absence of ornamentation on skull roofing bones (ch. 29) and absence of maxillary dentition (ch. 131).

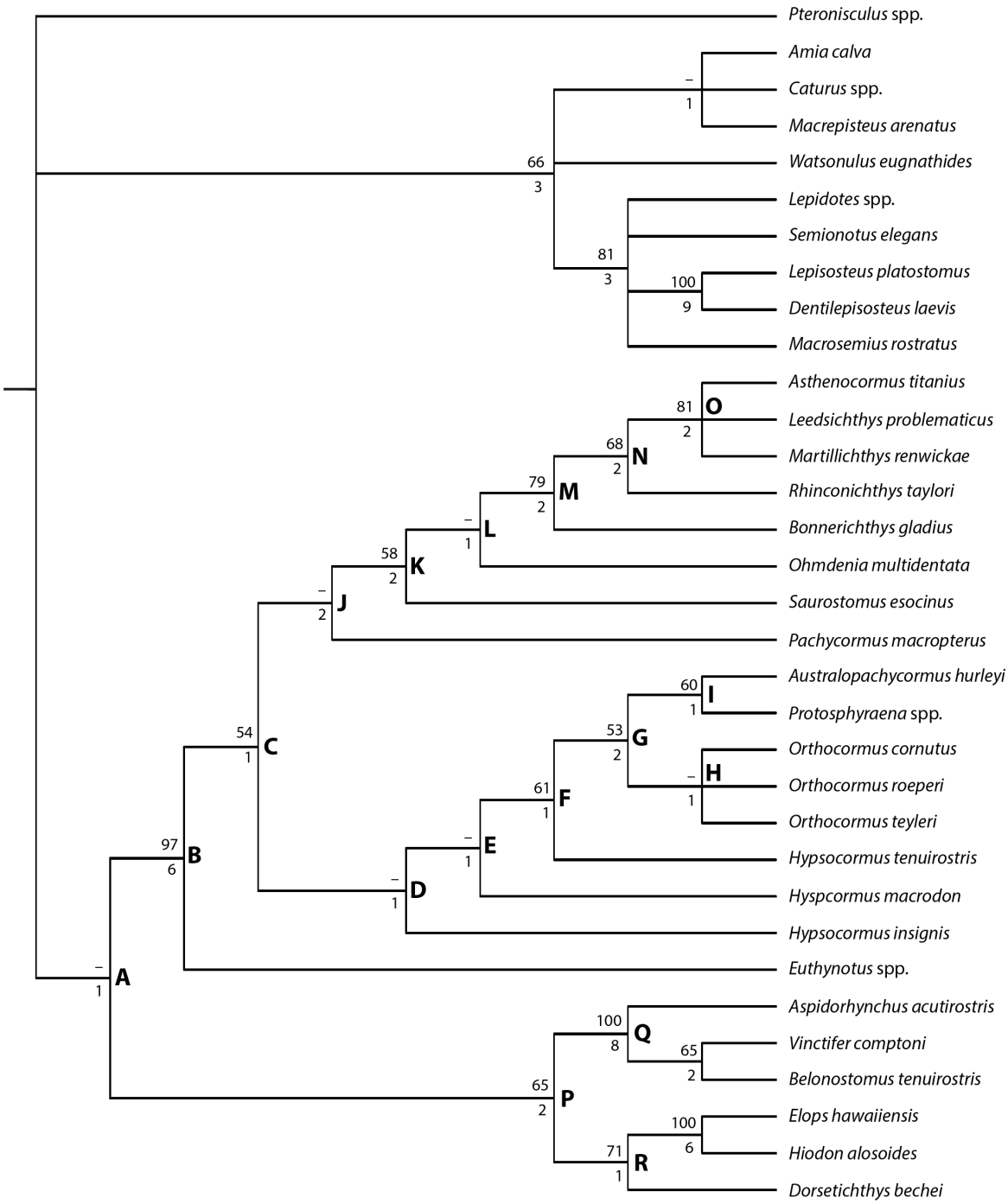

Figure 3.18 – Strict consensus tree of the morphology-only maximum parsimony analysis, with Bootstrap support values above each node, and Bremer Decay values below each node. Nodes denoted with a "–" represent nodes with less than 50% Bootstrap support. Major nodes are represented by A: Teleosts, B: Pachycormiforms, D: 'Protosphyraenid' pachycormiforms, J: 'Suspension-feeding' pachycormiforms, M: Suspension-feeding pachycormiforms, O: 'Jurassic' suspension-feeding pachycormiforms Q: Aspidorhynchids, R: Crown teleosts.

Of the giant suspension-feeders, *Bonnerichthys gladius* is placed as the earliest-diverging, while the clade including all other giant suspension feeders (node N) is supported by one unambiguous character (occiput extends far beyond posterior margin of the skull roof, ch. 130), and one homoplastic character (dorsal aorta housed in a shallow depression, ch. 22). Bootstrap support for the placement of *Bonnerichthys* to the exclusion of other giant bodied suspension-feeding pachycormiforms is relatively weak (68%; Fig 3.18).

Asthenocormus titanius, *Martillichthys renwickae* and *Leedsichthys problematicus* are resolved in a polytomy, to the exclusion of *Rhinconichthys taylori*, and are united by five homoplastic characters: maxilla length one third or less of relative to skull length (ch. 64); orbit fully posterior to the maxilla (ch. 65); a strongly waisted hyomandibula (ch. 70); presence of raker ornamentation (ch. 127); and hyomandibula height less than one third of the mandible length (ch. 128). This pattern of relationships is moderately well-supported and the best supported node within the pachycormiforms (81; Fig. 3.18). The absence of free, elongate posterior processes of the dermopterotics (ch. 38) represents a reversal in the lineage leading to *Asthenocormus*.

Bremer decay. Bremer decay support is weak overall in the tree, with most nodes collapsing after 1 or 2 steps, particularly within the pachycormiform clade (Fig. 3.18). However, the strongest supported nodes are for the clades containing pachycormiforms (node B; Bremer decay = 6; Fig. 3.18); the crown teleosts *Elops hawaiiensis* and *Hiodon alosoides* (Bremer decay = 6); aspidorhynchids (node Q; Bremer decay = 8); and the lepisosteiforms *Lepisosteus platostomus* and *Dentilepisosteus laevis*; (Bremer decay = 9).

Bayesian analysis. The results of the morphology-only Bayesian analysis (Fig. 3.19) are in agreement with the parsimony analysis (Fig. 3.18), with the exception of some relationships within holosteans in the Bayesian analysis: *Watsonulus* is placed as the sister taxon to all other holosteans; *Macrosemius* is placed as sister taxon to the clade containing *Lepidotes*, *Semionotus*, *Lepisosteus* and *Dentilepisosteus*; and *Amia*, *Caturus* and *Macrepisteus* are placed as a polytomy with the clade containing *Macrosemius*, *Lepidotes*, *Semionotus*, *Lepisosteus* and *Dentilepisosteus* (i.e. Ginglymodi; Fig. 3.19). Pachycormiform monophyly is strongly supported (BPP=0.99). Outside of the 'protosphyraenid' clade, posterior probability values are generally high, particularly within the 'suspension-feeding' pachycormiform clade (BPP >0.95, Fig. 3.19). However, the node including all pachycormiforms except *Euthynotus* only receives moderate support (BPP=0.78, Fig. 3.19).

Inclusion of nuclear genes for extant taxa has little effect on topology outside the holostean total-group and the placement of *Hiodon* among aspidorhynchids, but this is very poorly supported (BPP=0.51; node P; Fig. 3.20). Support for teleost monophyly (node A) increases marginally compared to the morphology-only Bayesian analysis (BPP=0.74, Fig. 3.19; BPP=0.8, Fig. 3.20) but is still not very strong.

Support also increases for the node uniting the 'protosphyraenid' and 'suspension-feeding' clades (node C; BPP=0.78, Fig. 3.19; BPP=0.83, Fig. 3.20), but support within these clades is largely unchanged. The least supported pachycormiform node is that subtending the 'protosphyraenid' clade (node D; BPP=0.53, Fig. 3.19; BPP=0.57, Fig. 3.20). The group uniting *Orthocormus*, *Australopachycormus*, and *Protosphyraena* is also weakly supported

(node G; BPP=0.64, Fig. 3.19; BPP=0.65, Fig. 3.20), with the species of *Orthocormus* not recovered as a clade.

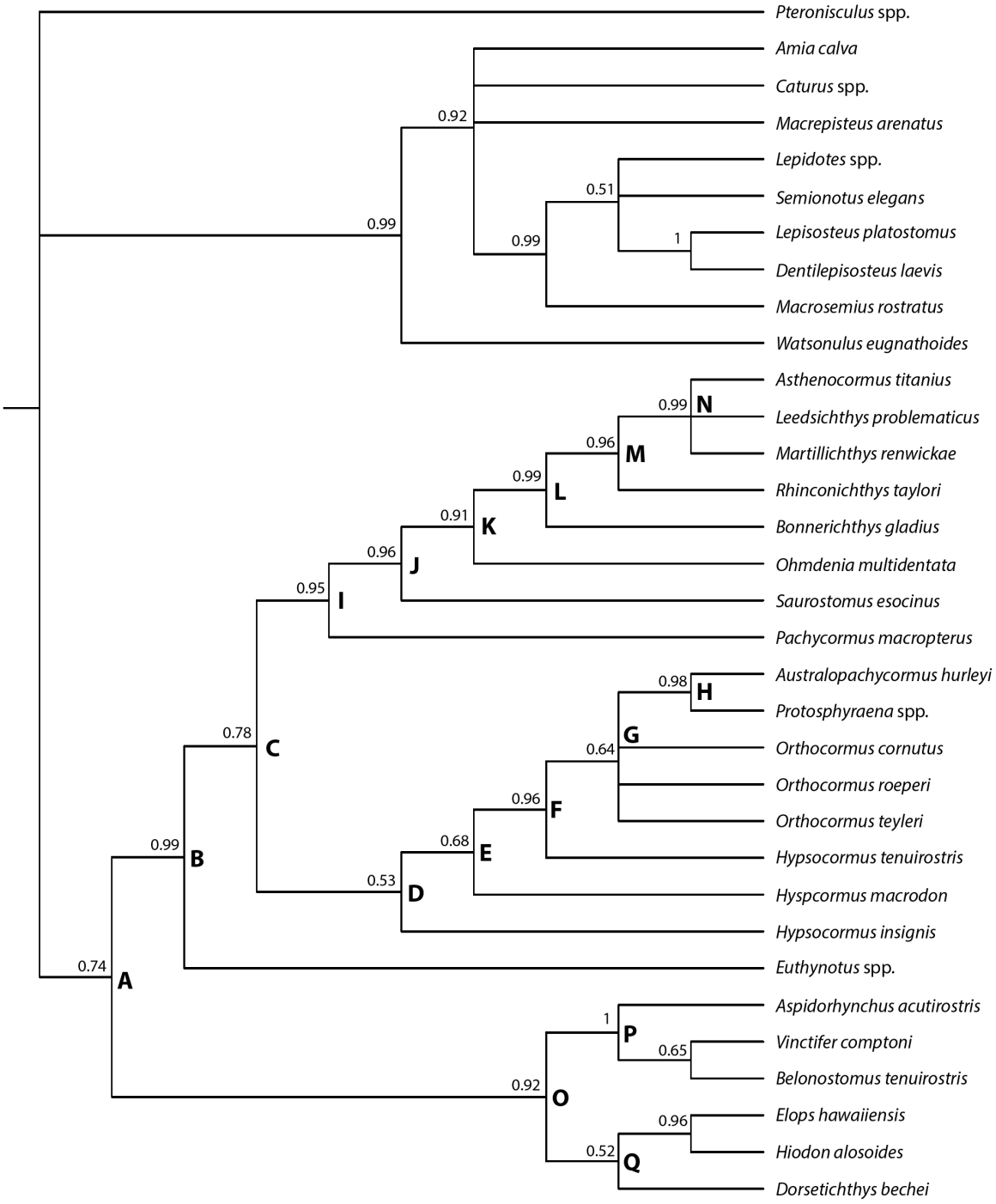

Figure 3.19 – Phylogenetic hypothesis of the morphology-only Bayesian analysis, with Bayesian support values shown at each node. Major nodes are represented by A: Teleosts, B: Pachycormiforms, D: 'Protosphyraenid' pachycormiforms, I: 'Suspension-feeding' pachycormiforms, L: Suspension-feeding pachycormiforms, N: 'Jurassic' suspension-feeding pachycormiforms P: Aspidorhynchids, Q: Crown teleosts.

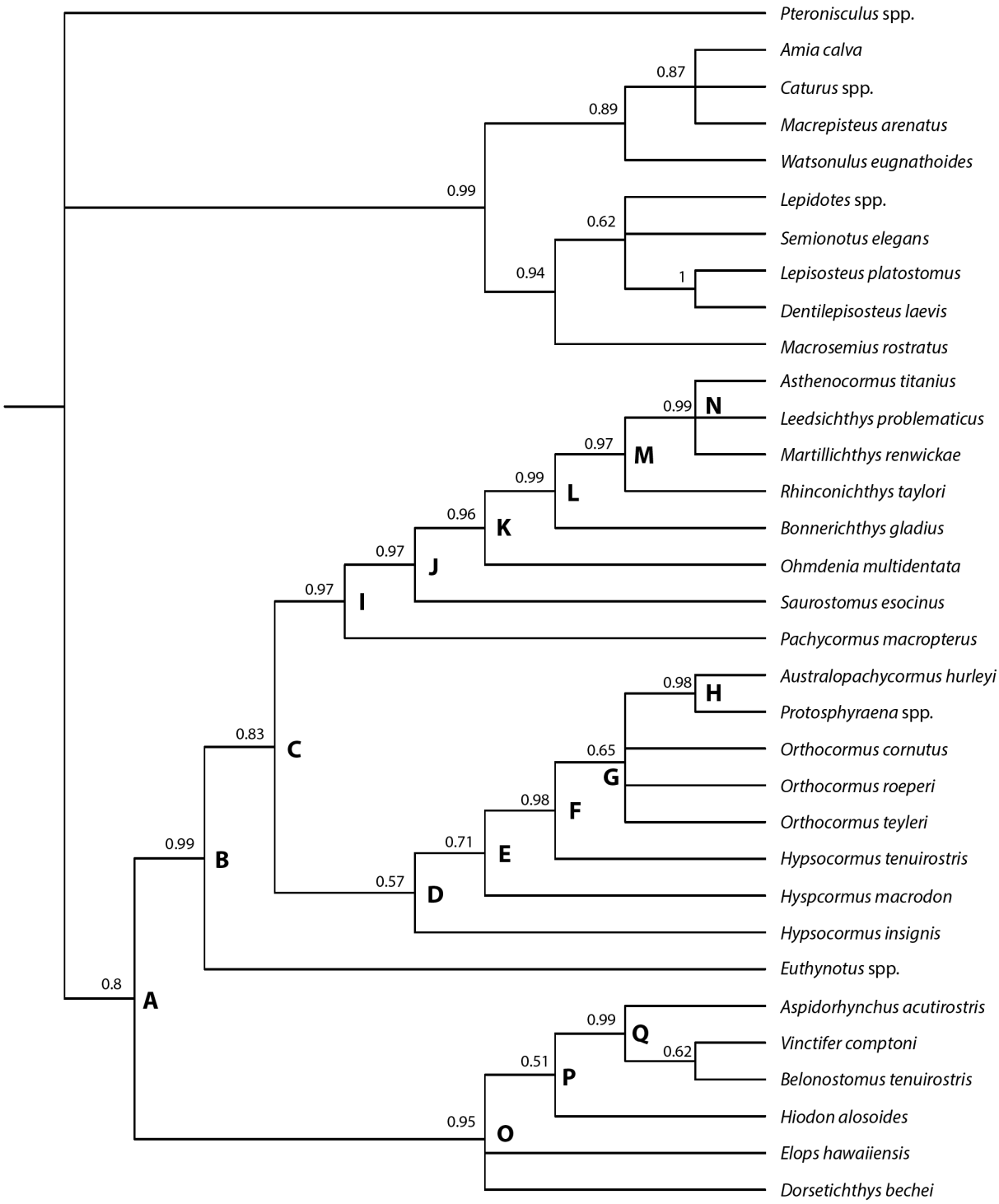

Figure 3.20 – Phylogenetic hypothesis of the Bayesian analysis including morphological and molecular data, with Bayesian support values shown at each node. Major nodes are represented by A: Teleosts, B: Pachycormiforms, D: 'Protosphyraenid' pachycormiforms, I: 'Suspension-feeding' pachycormiforms, L: Suspension-feeding pachycormiforms, N: 'Jurassic' suspension-feeding pachycormiforms, O: Aspidorhynchids and crown teleosts, Q: Aspidorhynchids.

Fossilized Birth-Death model analysis. Relationships recovered in the FBD analysis are less resolved than either the parsimony or Bayesian analyses excluding stratigraphic data (Fig. 3.21). The most notable changes to previous phylogenies are: *Amia* as sister taxon of *Lepisosteus* plus *Dentilepisosteus* to the exclusion of other holosteans (including 'semionotids' *sensu lato*); the giant-bodied suspension-feeders as the sister group to all other pachycormiforms; and *Euthynotus* as the sister group to the clade containing *Hypsocormus* spp., *Orthocormus* spp., *Australopachycormus* and *Protosphyraena*. The remaining pachycormiforms — *Pachycormus*, *Saurostomus* and *Ohmdenia* — also form a clade that is sister group to a clade containing *Euthynotus*, *Hypsocormus*, *Orthocormus*, *Australopachycormus* and *Protosphyraena*.

Inferred divergence times within the tree span the latest Paleozoic to the late Mesozoic. Total-group teleosts are estimated to have diverged at approximately 264.52 Ma (Capitanian, Permian), although an earliest Triassic origin cannot be excluded (95% HPD = 250.5–279.06 Ma). The age of the last common ancestor of pachycormiform clade is estimated as 231.82 Ma (Carnian, Upper Triassic; 95% HPD = 213.08–250.92 Ma). The giant bodied suspension-feeders also diverge with the node uniting *Asthenocormus*, *Leedsichthys*, *Martillichthys*, and all later edentulous pachycormiforms dated as 172.45 Ma (95% HPB = 164.59–184.27 Ma), which equates to the Toarcian (Early Jurassic). Divergence between *Bonnerichthys* and *Rhinconichthys* is estimated as 104.78 Ma (95% HPD = 98.99–111.75 Ma), which places their emergence in the Albian (Early Cretaceous). The age of the clade uniting all remaining pachycormiforms is placed at 217.1 Ma (Norian, Upper Triassic; 95%

HPD = 203.22–231.68 Ma), in a phylogenetic framework that loosely resembles the two pachycormiform clades recovered in the Bayesian and parsimony analyses.

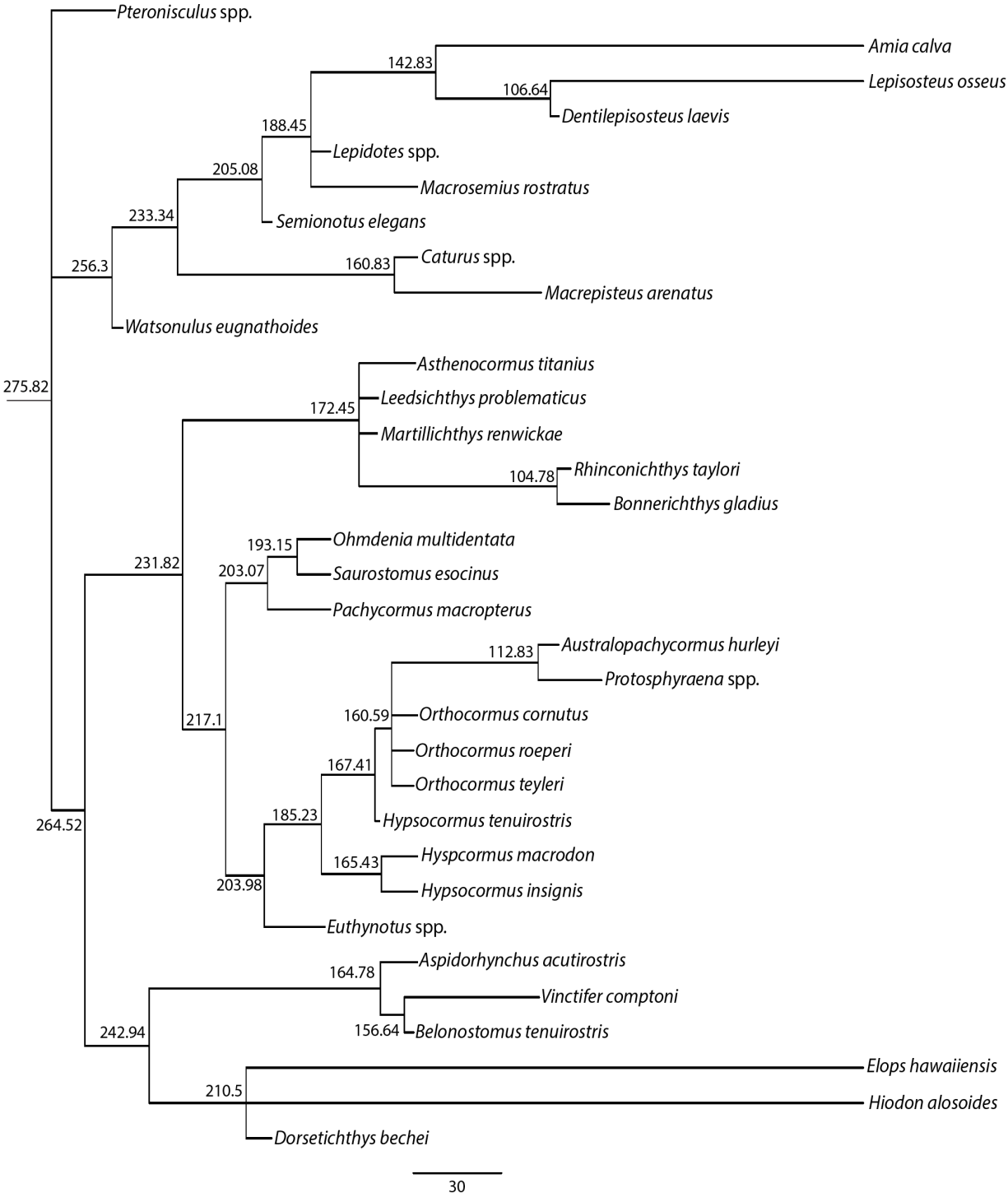

Figure 3.21 – Timescaled phylogenetic hypothesis from the Fossilized Birth-Death model analysis including morphological, genetic and stratigraphic data, with estimated node ages shown at each node. Scale bar represents 30 Myr.

Stepping stone analysis. The topologically unconstrained phylogenetic hypothesis, which supports the monophyly of giant suspension feeders, has mean marginal log likelihood of 839.65. The alternative hypothesis of two origins of suspension-feeding has a mean marginal log likelihood of 604.65. Using equation 1 outlined above, this means that the Bayes factor for this comparison is $\sim 1.14 \cdot 10^{102}$. This is many orders of magnitude higher than the guide threshold of 10 required to show strong support for one hypothesis over another given by Nylander *et al.* (2004), meaning there is very strong support for the more orthodox phylogeny over the alternative set of hypothesized relationships.

Discussion

Revisions to past descriptions and comparisons to other taxa

External analysis. The structures identified through external analysis (Fig. 3.1) corroborate those identified by Cawley *et al.* (2018). However, alterations to this and previous descriptions (Rayner 1948; Lehman 1949; Wenz 1967; Patterson 1975; Mainwaring 1978) are discussed below.

Braincase and parasphenoid. The structure of the braincase is in agreement with past accounts, and I corroborate Mainwaring's (1978) description of a curved prootic-opisthotic suture, rather than the vertical suture described by Patterson (1975).

The only other reasonably well-described pachycormiform braincases are those of *Protosphyraena* (Loomis 1900; pl. 19) and *Orthocormus* (referred to as *Hypsocormus* in Rayner 1948), which Rayner indicates is very similar to that of *Pachycormus* (Rayner 1948:

312). The main difference is the presence of two paramedial fangs in the rostral region, which sit anterior to the vomers but posterior to the anterior most tip of the skull (the elongate rostrum of *Orthocormus* and *Hypsocormus*), as well as the presence of an extended rostrum. *Pachycormus* also lacks the elongate occipital stalk described in *Martillichthys* and *Rhinconichthys* (Schumacher *et al.* 2016; Dobson *et al.* 2019; figs. 4, 10; Chapter 2).

Upper jaw. In agreement with Cawley *et al.* (2018), I describe the maxilla as a dorsoventrally compressed ovoid, rather than the triangular ossification described by Mainwaring (1978). I also find that Rayner (1948; fig. 17) has misidentified the premaxilla as the supramaxilla.

The edentulous anterior process forms a substantial part of the maxilla in *Pachycormus*; however, its relative size is much smaller in the maxilla of *Hypsocormus* (Woodward 1895*a*: pl. XI, fig. 3), and *Australopachycormus* (Kear 2007: 1035), but larger than that in *Protosphyraena* (Hay 1903: fig. 9; Woodward 1908*a*: pl. XXXI, fig. 4, 4A). Lambers (1992: 236) notes that this process is absent in *Euthynotus*, because (contrary to Wenz 1967) he suggests that the maxilla and premaxilla are fused.

Mandible. Due to the poor preservation of the lower jaw, particularly the dentary, very few morphological characters could be investigated. A reduced coronoid process is present, contrary to previous descriptions, which was misidentified as composed of the articular bone by Mainwaring (1978: 21), and considered absent by Wenz (1967: 118). Conversely, Patterson (1973: 274) describes both *Hypsocormus leedsi* (Woodward 1895*a*: BMNH P.6833) and *Pachycormus* as having a "well developed coronoid process" that is "of normal holostean

and teleostean type" (as pictured in Lehman 1949; pl. 9). This study found that the reduced coronoid process is composed of the surangular, and sits dorsal to the mandibular-quadrate joint. This would match the placement and composition of the reduced coronoid process seen in *Martillichthys* (Dobson *et al.* 2019, fig. 6; Chapter 2).

The most notable revision to the morphology of the lower jaw of *Pachycormus* relates to the presence of large fangs on the anteriormost coronoid plates. Previously unknown, these are similar to but smaller than the procumbent fangs associated with the 'protosphyraenid' clade taxa such as *Orthocormus* and *Protosphyraena* (Hay 1903; fig. 3; Lambers 1988; fig. 2; pl. 2B; Arratia & Schultze 2013; fig. 4). This is the first time these fangs have been described outside the 'protosphyraenid' clade, and their condition has not been assessed in the sister-taxon of all other pachycormiforms, *Euthynotus* (Wenz 1967). They were also unreported in previous descriptions of *Pachycormus* (Lehman 1949; Wenz 1967; Mainwaring 1978), which may be due to the anteriormost tip of the mandible being missing in the specimens or these not being visible in other specimens.

Palate. The presence of an independent quadratojugal, as reported by Mainwaring (1978), could not be corroborated. Patterson (1973) postulated that a thickened ridge on the postero-ventral margin of the quadrate represents a fused quadratojugal. However, no such ridge is present in this specimen, ruling out this interpretation. A thickened ridge on the medial surface of the quadrate most likely represents a contact surface for the symplectic. A quadratojugal (ch. 71) is not reported in other pachycormiforms included in this analysis (*Bonnerichthys*; *Euthynotus*; *Martillichthys*; *Protosphyraena*).

Sclerotic ossicle and circumorbital bones. This analysis corroborates the identification of at least 10 infraorbitals in *Pachycormus* (Mainwaring 1978: 16). However, the suggestion by Lehman (1949) and Wenz (1967) of up to 13 infraorbitals being present cannot be discounted. Other pachycormiforms have been described with a similar number of infraorbitals. *Hypsocormus macrodon* possesses nine infraorbitals according to Woodward (1895*a*; fig. 17) and seven according to Lambers (1992: 260). There are only six infraorbitals in *H. insignis* (Lambers 1992: 260) and 'six or seven small' infraorbitals in *Euthynotus* (Wenz 1967: 148; fig. 67). In contrast, Mainwaring (1978) counted nine in *Euthynotus* and *Hypsocormus*, leading her to designate "at least nine rectangular infraorbitals forming the posterior margin of the orbit' as a diagnostic character of Pachycormiformes (Mainwaring 1978: 112). In light of this, Lambers (1992: 255) revised this to "at least six infraorbitals behind the orbit" but, despite its plasticity, Mainwaring's (1978) diagnosis still appears in subsequent studies (e.g. Kear 2007). This study also confirms the presence of two suborbitals, and agrees with the conclusion that the third suborbital identified in *P. curtus* by Wenz (1967, fig. 53) is an individual anomaly.

Dorsal gill skeleton. The absence of suprapharyngobranchials concurs with previous descriptions and patterns of teleost evolution (Lehman 1949: 24, fig. 9; Nelson 1969; Mainwaring 1978; Hilton 2011: 441–442, fig. 7), as does my description of the infrapharyngobranchial and epibranchial series. The fourth epibranchials described by Mainwaring (1978: 38, fig. 16) appear to have been described upside down in comparison to the epibranchials found here (Fig. 3.9). This is probably due to her material being studied after acid preparation, when information about life orientation had been lost.

The position and orientation of the fourth epibranchials found in this specimen more closely matches the description of Lehman (1949: 24, fig. 9), but I do not find the fourth epibranchial to be "less developed" than the first (Lehman 1949: 24). I find the epibranchial morphologies described by Mainwaring (1978: 38) are more accurate, provided that the fourth epibranchial is rotated as described above.

Ventral gill skeleton. These are the best-preserved structures in the tomogram, and most of the structures identified here agree with those described by Mainwaring (1978) and Lehman (1949). However, I found no evidence of the fused basibranchial described by Mainwaring (1949), and my observations agree with the basibranchial description by Lehman (1949). Given the position of the basibranchial in relation to the second hypobranchials, structure described here is at least the third basibranchial.

I also found very few toothplates, compared to the higher number described by Mainwaring (1978). I describe one overlying the basibranchial, which Mainwaring also identified, but the 'small toothplates' littering the ceratobranchial series are identified here as gill rakers rather than toothplates. More gill rakers are present than those figured (Fig. 3.9) but the resolution of the scan limited the number that could be segmented.

These short, unornamented gill rakers are simple compared to the long, ornamented gill rakers of the giant suspension-feeders, or the short rakers bearing large teeth seen in *Hypsocormus* (Dobson 2016; fig. 3). They are also the most similar to those in outgroups such as *Amia* and *Lepisosteus* (Grande & Bemis 1998; figs. 53–54; Grande 2010; fig. 68),

suggesting that the raker morphology in *Pachycormus* is primitive for pachycormiforms, with the obvious caveat that conditions in other taxa — most critically *Euthynotus* — remain unclear. Gill rakers within pachycormiforms are highly varied and appear closely linked to diet and ecology (Friedman 2012*a*; Liston 2013; Dobson *et al.* 2019; Chapter 2), the most characteristic being those of the giant-bodied edentulous forms. All of these taxa apart from *Bonnerichthys* have extremely elongate, ornamented gill rakers (Liston 2013; fig. 1; Dobson *et al.* 2019; fig. 7; Chapter 2) that are hypothesized to serve a role in suspension feeding, comparable to modern planktivorous chondrichthyans (Liston 2013; Paig-Tran & Summers 2014).

I also report a median structure ventral to the basibranchial and hypobranchials of the gill skeleton. This structure is also seen in tomograms of other *Pachycormus* specimens (BRLSI M1297; BRLSI M1311; NHMUK PV OR 32433). It was observed previously by Mainwaring (1978: 42–43), who suggested that it is either a urohyal, or a median ventral toothplate, but concluded that 'its identity remains a mystery'. I reject the hypothesis of this structure being a median toothplate, due to its topology, which is beneath, and thus outside, the oral chamber.

Mainwaring's (1978) uncertainty in identifying this bone is due to comparison to the typical morphology and composition of urohyals reported in some 'pholidophorids' (Patterson 1977*b*): '*Pholidophorus' germanicus* and *Siemenichthys microcephalus* (formerly *Pholidophorus macrocephalus*; Arratia 2013), which are now considered to be stem teleosts (Patterson 1977*a*; fig. 19; Arratia 2013; fig. 95). In these taxa, the urohyal comprises ventral

and dorsal plates, joined so as to form a bone with a cross section resembling an inverted 'T'. Patterson (1977*b*) argued this structure represents a skeletal composite, consisting of fusion between the interclavicle (dermal bone) and the endoskeletal dorsal plate.

There were two reasons that Mainwaring (1978: 43–44) rejected the identification of a urohyal, both of which relate to a specific aspect of its appearance: (1) the urohyal in *Pachycormus* curved downwards, not upwards as in 'pholidophorids'; and (2) the denticles on the structure in *Pachycormus* were not multicuspid like those on the pholidophorid urohyal. However, I find that the structure in *Pachycormus* does curve upwards, adding support to its identification, and there is some indication that the bone is cylindrical in other *Pachycormus* specimens (Fig. 3.22A, B). I also find that this bone is dermal, like the horizontal, ventral plate of the 'pholidophorid' urohyal (Patterson 1977*b*). However, the *Pachycormus* urohyal does not have an inverted 'T' cross-section, or the multicuspid denticles described by Mainwaring (1978), which are both considered unique to 'pholidophorids' by Arratia and Schultze (1990). Although, teeth similar to those described by Mainwaring (1978) on the structure in *Pachycormus* have also been found on the uncontroversial urohyal of *Leptolepis coryphaenoides* (Arratia & Schultze 1990; fig. 10E).

More generally, identification of this structure as a urohyal draws support from its position and function. In living teleosts, the urohyal represents an ossified tendon that anchors ligaments of the hypohyals anteriorly and lies ventral to the basibranchials (de Beer 1937; Patterson 1977*b*). Outside teleosts, a urohyal is also known in *Polypterus*, where it ossifies as three separate structures (Fig. 3.23; Arratia & Schultze 1990), but this is not homologous

with the teleostean urohyal (Arratia & Schultze 1990: 278). The topology of the urohyals in teleosts and *Polypterus* match that of the urohyal seen in *Pachycormus*, supporting its identification. The anterior head of the structure in *Pachycormus* also appears to bifurcate in a similar way to the articular head of urohyals described in 'pholidophorids', such as '*Pholidophorus' germanicus* (Fig. 3.23; Patterson 1977*b*; fig. 5A–C; 106) and crownward stem teleosts such as *L. coryphaenoides* (Fig. 3.23; Arratia & Schultze 1990; fig. 10A), indicated by there being two fragments of this structure that sit parallel to each other. However, a junction between these two parallel structures is not obvious in *Pachycormus*. This bifurcated head is sometimes seen in extant teleosts such as *Hiodon alosoides* (Arratia & Schultze 1990; fig. 11) but its absence in other specimens (Fig. 3.23; Hilton 2002; fig. 59) suggests there may be some plasticity in urohyal shape depending on which parts of the tendon mineralize.

The plasticity of urohyal ossification within teleosts may explain the variation in morphology between specimens of *Pachycormus* (Fig. 3.22), where the bone is cylindrical in some specimens and 'u'-shaped in others, but this may also be explained by incomplete preservation. If this bone is a teleostean urohyal (Arratia & Schultze 1990), it is expected to be in articulation with the ventral hypohyals, and lack of contact between the urohyal and hypohyals is considered to be a sarcopterygian trait (Arratia & Schultze 1990). At present, it is unclear what the structure in *Pachycormus* articulated with, beyond it terminating anteriorly beneath the second hypobranchials. This is largely due to the lack of well-preserved examples of this bone, and because the example in M1361a appears to have been slightly displaced during preservation, with the posterior most fragment overlapping slightly with

the fragment anterior to it. Analysis of other specimens shows that this structure is most commonly placed ventral to the basibranchial and hypobranchials (Figs. 3.9D, 3.22C) and medial to the anterior ceratohyals, but its anterior limits are yet to be fully determined. The potential ossification plasticity of this bone may also influence its placement relative to the hypohyals. As such, while I am unsure of the "true" placement of the structure in *Pachycormus*, its placement and morphology closely resembles other examples of the urohyal in teleosts, and the uncertainty around its exact topology is not significant enough to warrant reidentification.

If the bone in *Pachycormus* is not the urohyal, the only other potential identification is as an interclavicle, which is known in primitive actinopterygians but has never been described in neopterygians (Gardiner 1984; Arratia & Schultze 1990), making it unlikely to be present in *Pachycormus*. Patterson (1977*b*) homologized the interclavicle with the horizontal plate of the pholidophorid urohyal (Arratia & Schultze 1990) and Arratia and Schultze (1990) concluded that the presence of a teleost urohyal (as opposed to the urohyal seen in sarcopterygians or *Polypterus*) outside the teleost clade is 'doubtful'. However, it is not clear whether this includes pachycormiforms, given that their apomorphy-based definition of Teleostei excludes members of the teleost stem (Arratia 1999; 2001; 2004; 2015). If we are to adhere to the most parsimonious explanation, the structure seen in *Pachycormus* is most likely to be a teleostean urohyal (Arratia & Schultze 1990), and possibly the earliest example of the urohyal in teleosts, rather than an interclavicle that has yet to be described in neopterygians (Gardiner 1984; Arratia & Schultze 1990).

Therefore, topology and morphology of the structure in BRLSI M1361a leaves little doubt that this is the same as the structure described by Mainwaring (1978: pl. 13, 14, 19) from NHMUK PV P.24410 and P.32438, and the same structure is seen in NHMUK PV OR 32433, BRLSI M1297, and BRLSI M1311 (Fig. 3.22). However, I disagree with Mainwaring's (1978) conclusion of it being a ventral toothplate and so identify this structure as a urohyal based on its position and anatomical correspondence to that structure in other teleosts.

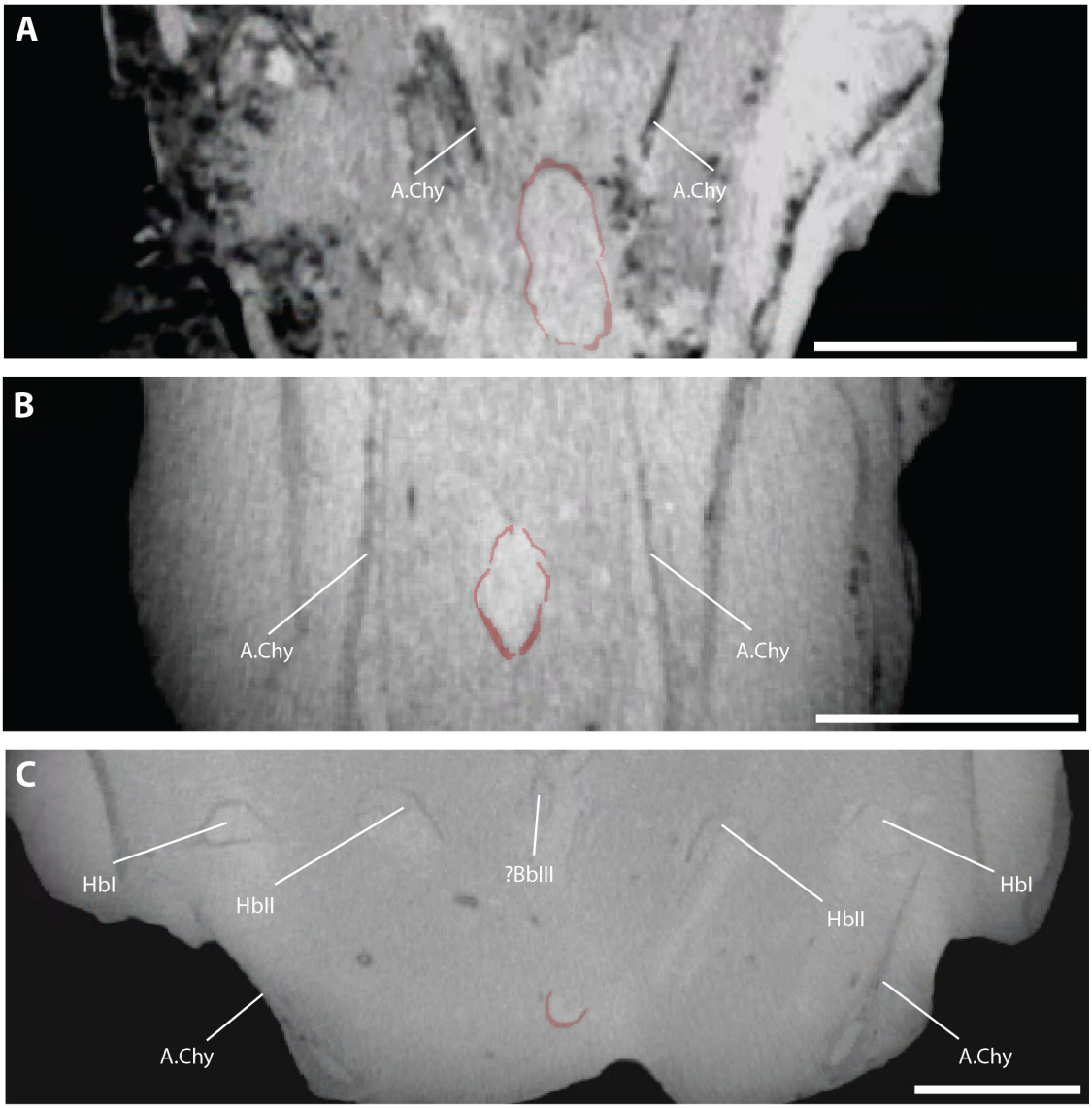

Figure 3.22 – μCT images of the urohyal seen in other *Pachycormus* specimens in coronal view: A) NHMUK PV OR 32433 B) BRLSI M1311; C) BRSLI M1297. For clarity, the shape of the urohyal is highlighted in red. Scale bar represents 1 cm.

Hyoid arch. I found no evidence of any toothplates covering the mesial surface of the anterior ceratohyals, as found during the preparation of some specimens by Mainwaring (1978: 33), although she does clarify that it is unclear if these toothplates are associated with the ceratohyals or have become displaced. It is extremely unlikely that any toothplates would be found ventral to the gill basket, since they would sit underneath the mouth, so I consider the toothplates described by Mainwaring (1978: 33) to be displaced rather than associated with the hyoid arch. Additionally, I found no evidence of an interhyal, which was reported above the posterior ceratohyal in NHMUK P.24410 (Mainwaring 1978; fig. 11), but this is the only specimen in which it has been recorded, so its absence in the specimen examined here is not surprising. Although this is a primitively present trait in actinopterygians (Patterson 1982; Giles *et al.* 2017), the interhyal may not ossify in *Pachycormus*, as with living holosteans (e.g. *Amia*, *Lepisosteus*; Grande & Bemis 1998; Grande 2010), or may be extremely reduced (e.g. *Watsonulus*, *Semionotus*; Olsen 1984; Olsen & McCune 1991) and easily missed.

Operculogular series. My description of the operculum, suboperculum and the interoperculum agree with the morphologies and margins of previous accounts (Lehman 1949: 13, fig. 2; Wenz 1967; 117–118, fig. 53; Mainwaring 1978: 17–18, fig. 2).

Pectoral endoskeleton. This is one of the structures most revised from previous descriptions because, until now, the pectoral endoskeletons of pachycormiforms have been poorly known. The most comprehensive descriptions have come from Hay (1903), Woodward (1908*b*); Wenz (1967), Jessen (1972) and Mainwaring (1978), the final three of which focus on the pectoral

girdle of *Pachycormus*. I agree with the observation by Jessen (1972), that the overall morphology of the scapulocorarcoid of *Pachycormus* is very similar to *Elops* and *Salmo* (Jessen 1972: 75). However, this study found a number of differences from previous descriptions.

I found a much larger scapular foramen beneath the mesocoracoid arch of the scapulocoracoid than the one described by Mainwaring (1978: 82), or that of *Protosphyraena* (Woodward 1909; fig. 44), and of those seen in other neopterygian taxa surveyed (e.g. *Lepisosteus*, Jessen 1972; pl. 3.6; *Amia*, Jessen 1972; pl. 12). However, the ventral process of *Protosphyraena* appears larger relative to the scapulocoracoid than the one described here (Woodward 1909; fig. 44). In addition, the coracoid of *Pachycormus* possesses an anterior process, which is seen in other teleosts and *Acipenser* (Jessen 1972; Patterson 1973).

Pachycormus also possesses a posterior process on the coracoid, which is seen in some ontogenetic stages of *Elops* and *Salmo*, but this is not listed as a teleost or neopterygian character by Jessen (1972). Neither of these processes have been previously described in the scapulocoracoid of *Pachycormus* (Wenz 1967; Mainwaring 1978) or *Orthocormus* (misidentified as *Hypsocormus* and representing the same individual described by Rayner 1948; Jessen 1972; pl. 25.2).

I also found six proximal radials, rather than the four previously described (Jessen 1972; Mainwaring 1978), and no ossified distal radials. I found that the propterygium does not fuse with the first fin rays, but I found only one canal on the anterior surface (two canals have

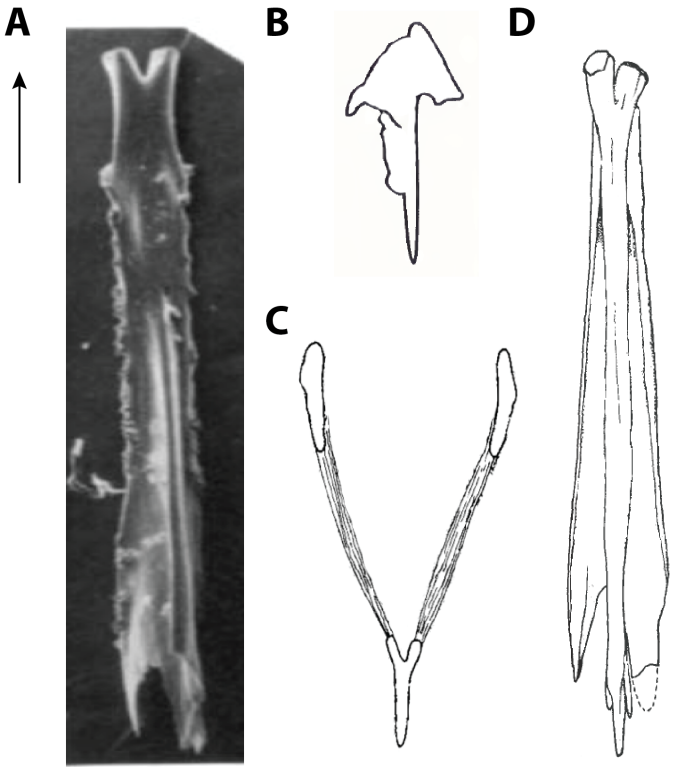

Figure 3.23 – Interpretive drawings of the urohyal of A) *Leptolepis coryphaenoides* (photograph from Arratia & Schultze 1990; fig. 10A); B) *Hiodon alosoides* (interpreted from Hilton 2002; fig. 59D); C) *Polypterus* (interpreted from Arratia & Schultze 1990; fig. 1); D) '*Pholidophorus' germanicus* (interpreted from Patterson 1977*b*; fig. 5C). Hashed lines on panel C indicate adjoining muscle. Arrow indicates the direction to the anterior.

been described by Jessen 1972). I describe a lateral process on the propterygium, but it is unclear if this is the same as the posterior process reported for *Elops* and *Salmo* (Jessen 1972: 88). I have also described the same "hourglass shaped" intermediate radials, and that the final two radials (what would be radials VI and VII) have fused proximally into a single radial (Mtg; Fig. 3.14) with a slightly forked distal element. In overall morphology, this branching element corresponds positionally and structurally to the forked radial seen in *Atractosteus* sp. (mtg; Fig. 3.24; Grande 2010; fig. 296), though this is not interpreted as a metapterygium (Grande 2010: 402). Presence of a metapterygium is a character known in non-teleost actinopterygians (Coates 1994; Hilton 2011) and gnathostomes more generally,

but its presence is also figured in *Pachycormus* by Jessen (1972; pl. 24.1, 24.2). A similar, but non-bifurcated structure is seen in the holostean *Amia calva*, which is only partially ossified from a larger metapterygium that is pre-formed in cartilage (Mtgo; Fig. 3.24), for the articulation with the distal radials. Its preservation in *Pachycormus* suggests that it is endoskeletal. In *Pteronisculus* sp., the bifurcated distal ends are unfused, individual radials (radials IV–V; Fig. 3.24) which each articulate with distal radials separately (Fig. 3.24; Jessen 1972; fig. 10).

I also note that radials II and III (Fig. 3.14) are much more square (radial II) or paddle-shaped (radials III–IV) than those described in Jessen (1972), also not noted by Mainwaring (1978). A "C"-shaped second radial, and "paddle-shaped" subsequent radials are also described in *Protosphyraena* (Woodward 1909: 150–151; fig. 44) and *Bonnerichthys* (Friedman *et al.* 2010: 991; figs. S8–10). Unlike the "hourglass"-like radial V (Fig. 3.14), radial II is curved laterally and cups the scapulocoracoid with a concave anterior margin, rather than articulating with an anterior head.

Radial III has more of an hourglass shape but its distal margin is flared into a large paddle (this is also present but less exaggerated in radial IV), while the anterior head resembles those of radials VI–V. The morphologies of radials II and III are not comparable to that described for the radials of *Pachycormus* (pl. 24.1, 24.2) or *Orthocormus* (pl. 25.2) in Jessen's (1972) description, nor other neopterygians (e.g. *Amia*; Jessen 1972; Grande & Bemis 1998; *Elops*; Jessen 1972; *Lepisosteus*; Jessen 1972; Grande 2010; *Salmo*; Jessen 1972; *Watsonulus*; Olsen 1984).

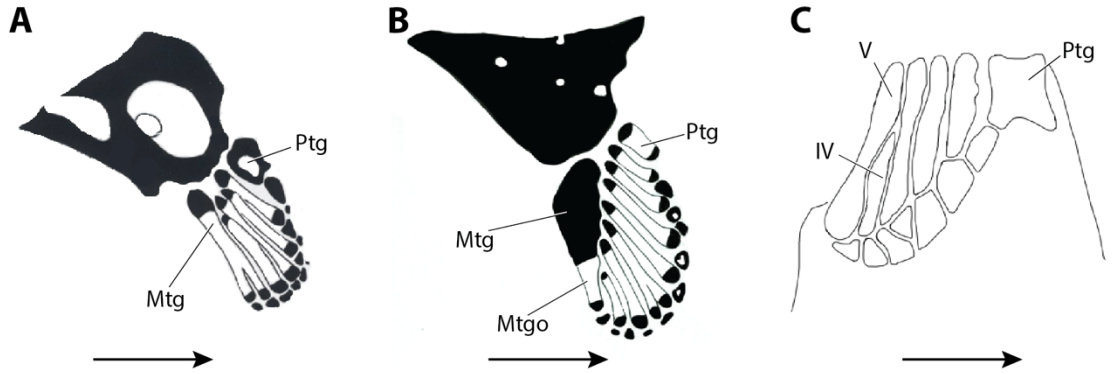

Figure 3.24 – Interpretive drawings of the metapterygium of A) *Atractosteus* sp. (interpreted from Grande 2010; fig. 296); B) *Amia calva* (interpreted from Grande & Bemis 1998; fig. 90); C) *Pteronisculus* sp. (interpreted from Jessen 1972; fig. 10). Arrow indicates direction of the anterior.

Embedded squamation. The squamation reported in the topological position of the clavicle or serrated appendage has never been described before in *Pachycormus*. The structure described here, while anterior to the cleithrum, does not form a cap, nor sit dorsal to the anterior limb of the cleithrum. It is also extremely elongate and extends far more anteriorly than in previous descriptions of a clavicle or serrated appendage.

This structure is not unique to this specimen: it has been observed in the same place, with the same 'hair-like' morphology in cross section, in μCT scans of other *Pachycormus* specimens (BRLSI M1311; BRLSI M1395; NHMUK PV OR 32433), and is visible externally on BRLSI M1297 flanking the antero-ventral corners of the cleithra. The latter also shows scale-like patterning, adding support to its identification as squamation between the branchiostegal rays and the gill basket. Given these considerations, I interpret this structure as embedded squamation and not a clavicle or serrated appendage.

Characters diagnosing Pachycormus *as a pachycormiform*

Previous studies (Mainwaring 1978; Friedman 2012*a*; Wretman *et al.* 2016; Cawley *et al.* 2018) identified the several synapomorphies defining *Pachycormus* as a pachycormiform (see Systematic Palaeontology; above). From the analyses for this study, I found that some characters from the diagnosis of *Pachycormus*, such as 'long, slender pectoral fins' (node B, ch. 113) are seen to support pachycormiforms more broadly in my results (as in previous diagnoses; Mainwaring 1978; Friedman 2012*a*; Wretman *et al.* 2016; Cawley *et al.* 2018), whereas others, such as 'at least nine infraorbitals posterior to the orbit' (ch. 51) suffer from a lack of coding within pachycormiforms (5/17 pachycormiforms are coded for this character: *Hypsocormus insignis*; *H. macrodon*; *H. tenuirostris*; *Orthocormus roeperi*; *Pachycormus*). Additionally, the independence of extrascapulars (node C, ch. 39) support the monophyly of pachycormiforms to the exclusion of *Euthynotus* and therefore is not a pachycormiform synapomorphy.

The monophyly of Orthocormus and Hypsocormus

Orthocormus and *Hypsocormus* are of questionable monophyly (Lambers 1992: 283–284, 1999: 219), the latter being consistently resolved as paraphyletic (Lambers 1992; fig. 23; Lambers 1999: 219; Friedman *et al.* 2010 suppl.; fig. S12; Friedman 2012*a*; fig. 2a). The characters diagnosing *Orthocormus* were first presented by Weitzel (1930), a number of which were included in this analysis because they are also present in other pachycormiform genera: rostrodermethmoid produced anterior to symphysis of the lower jaw (ch. 32); pronounced, anteriorly directed frontal boss (ch. 36); large, laterally compressed teeth on the rostrodermethmoid, directed obliquely forward (chs. 33, 34 and 57); larger teeth on the

premaxilla than the maxilla (ch. 60); large, procumbent coronoid teeth (chs. 56 and 82); pelvic fin originating nearer to the pectoral fin than the anal fin (ch. 118); dorsal fin completely in advance of the anal fin base (ch. 94). There are also a number of characters that are continuous and difficult to code as discrete states for a phylogenetic analysis, such as: trunk elongate and fusiform; large pelvic fin; and more than 40 caudal rays. Lambers (1988) presented an amended diagnosis: premaxilla with only one large tooth in its posterior half (ch. 60); dentary with large, conical teeth (ch. 82); a pair of large, procumbent, anterior teeth on the dentary (chs. 56, 82); fulcra absent on all fins (ch. 114); head length 21% of standard length (SL); prepelvic length 36% of SL; preanal length 64% of SL; predorsal length 57% of SL; fin-ray counts: pectoral fin ± 22; pelvic fin ± 22; anal fin ± 60; caudal fin (both lobes) ± 40; dorsal fin ± 40.

Woodward (1895*a*) defined the genus *Hypsocormus* with the following: fusiform shape and laterally compressed trunk; a small head, less deep than the trunk; a rostrodermethmoid that is produced beyond the mandible symphysis (ch. 32); long, slender maxillae; large, triangular premaxillae, with larger teeth than those on maxilla (ch. 60); powerful, conical dentition (chs. 34, 57) in incomplete sockets; teeth on the maxilla, premaxilla and dentary are widely spaced medially, and flanked laterally by minute clustered teeth (ch. 81); large vomerine and prearticular teeth and small, granular pterygoid teeth; gular plate present (ch. 91); absence of notochordal sheath ossifications; short and slender ribs; minute or absent fin-fulcra (ch. 114); pectoral fins large and sickle-shaped (ch. 113), but the first three or four fin rays do not branch distally (ch. 115); small pelvic fins present (ch. 117); dorsal fin partially or completely anterior to the anal fin (ch. 94); anal fin base greatly extended; caudal fin deeply

forked; small, rhombic scales (chs. 119, 121); lateral line inconspicuous. Woodward (1895*a*) also noted similarities between the suborbital and circumorbital bones (chs. 46, 47, 48, 51, 53), sclerotic ossicle, and supramaxilla (chs. 68, 69) of *Hypsocormus* and *Pachycormus* but these are similarities also shared with *Orthocormus* in my character matrix. Mainwaring (1978) introduced some additional characters, some of which conflict with Woodward (1895*a*): rostrodermethmoid does not extend anterior to the symphysis of the lower jaw (ch. 32); presence of a frontoparietal boss (ch. 36); dorsal and anal fins opposed (contra Woodward 1895*a*), or dorsal slightly in advance of anal (ch. 94); and anal fin base extended.

These conflicting definitions are reinforced by the heterogeneity between characters meant to define *Hypsocormus*, but instead appear to show the discrete changes in body plan between *H. insignis* and the *Protosphyraena* and *Australopachycormus* clade. The elongate rostrum only appears in *H. tenuirostris*, as do the large premaxillary teeth (both absent in *H. insignis* and *H. macrodon*). The dentary teeth do not protrude from the mouth (ch. 2) in *H. insignis*; and the dorsal and anal fins are opposed in *H. macrodon* (ch. 118; Mainwaring 1978). Aside from these interspecific changes in *Hypsocormus*, the only character difference between *Hypsocormus* and *Orthocormus* in my matrix is the partial overlap of the dorsal and anal fin bases in *Hypsocormus* (ch. 94, unknown in *H. tentuirostris*; dorsal fin anterior in *Orthocormus*; Lambers 1988; pl. 1; Arratia & Schultze 2013; fig. 6). This character state is not unique to *Orthocormus* (also present in *Pachycormus*, *Elops hawaiiensis* and *Dorsetichthys bechei*), and its coding is somewhat arbitrary. The fins as seen in *Orthocormus*, particularly *O. roeperi* (Arratia & Schultze 2013; fig. 6) could be considered to be

overlapping, involving the posterior tip of the dorsal fin and the anterior of the anal fin, although whether this represents a clear overlap is equivocal.

In both the parsimony and Bayesian analyses, and in agreement with previous phylogenetic analyses (Lambers 1992, 1999; Friedman 2012*a*; Wretman *et al.* 2016), the three *Hypsocormus* species are resolved as successive sister taxa to remaining 'protosphyraenid' pachycormiforms rather than a clade. Combined with low support for a relationship between *Hypsocormus insignis* and *H. macrodon* (node D; Bootstrap=<50; Fig. 3.18; BPP=0.53–0.57; Figs. 3.20, 3.21), this strongly indicates that the monophyly of *Hypsocormus* spp. can be rejected. Contrary to Lambers' (1992, 1999) suggestion, I do not find *H. macrodon* to have strong association with *Orthocormus*, and do not agree that this taxon belongs within *Orthocormus*.

The strong support for the clade containing *H. tenuirostris*, the polytomy containing *Orthocormus* spp., *Australopachycormus hurleyi* and *Protosphyraena* sp. would support the hypothesis that *H. tenuirostris* is more similar to *Orthocormus* and 'protosphyraenids' (Nicholson & Lydekker 1889) than *H. insignis* (Lambers 1992: 238). *H. tenuirostris* also shares the elongate rostrum and protruding dentition of *Orthocormus* and the 'protosphyraenids'.

However, I caution that *Orthocormus* does not form a clade in either Bayesian analyses, and only a single, highly subjective character supports the *Orthocormus* clade (ch. 127, a sphenoid region contributing to over half of the overall skull length) in the parsimony

analysis. Therefore, while I cannot confirm the monophyly of *Orthocormus*, their polytomy in these results mean there is currently no definitive proof to reject the monophyly of *Orthocormus* either.

'Protosphyraenid' vs. 'suspension-feeding' pachycormiforms

In agreement with previous analyses (Friedman 2012*a*; Wretman *et al.* 2016), my parsimony and Bayesian analyses show that pachycormiforms (excluding *Euthynotus*) form two clades (Figs. 3.19–3.21), although this is distorted when stratigraphy is included (Fig. 3.21). Each clade is supported by one unambiguous character: paramedial fangs on the rostrodermethmoid for the 'protosphyraenid' clade (ch. 34); and a prominent elbow on the long axis of the supracleithrum for the 'suspension-feeding' clade (ch. 108). However, the Bayesian support value for the 'protosphyraenid' clade is extremely low (BPP=0.53–0.57; Figs. 3.20, 3.21), especially when compared to the high support seen for the 'suspension-feeding' clade (node I; BPP=0.95–0.97; Figs. 3.20, 3.21). There is also much lower resolution in this clade compared to the 'suspension-feeding' clade, which further impacts the posterior support calculated during the Bayesian analysis.

This disparity in resolution and statistical support between the two pachycormiform clades is a testament to how little is known about the 'protosphyraenid' clade compared to the 'suspension-feeding' clade, and how little is still known about pachycormiforms as a whole. The low resolution may be the result of a lack of morphological data, for example of the braincase (only documented for *Protosphyraena* spp. by Loomis 1900; and *Orthocormus* sp. by Rayner 1948) for 'protosphyraenid' clade taxa.

Pachycormiform monophyly and the teleost stem

As with previous efforts (Friedman *et al.* 2010; Friedman 2012*a*; Wretman *et al.* 2016), my study resolved pachycormiforms as a monophyletic group with moderate support (node B; BPP=0.99; Figs. 3.20, 3.21). However, only a small number of the characters that support the monophyly of pachycormiforms here are the same as the characters that are typically used to support the clade: contribution of rostral bone to oral margin (ch. 31; unambiguous); the dermosphenotic contributes to more than half of dorsal margin of orbit (ch. 42; this is absent in *O. roeperi*); long, slender pectoral fins (ch. 113; unambiguous); and fin ray bifurcations occur independently of joints (ch. 116; unambiguous).

It is worth noting that many of the characters used to diagnose pachycormiforms are not unique to the group, such as bifurcation of the pectoral fin-rays (ch. 115) and small, rhombic scales (ch. 119). There are also a number of characters in the pachycormiform diagnosis (Mainwaring 1978) that are not present in all pachycormiforms, such as the contribution of the dermosphenotic to over half of the dorsal margin of the orbit (ch. 42; absent in *O. roeperi*), and the absence of independent extrascapulars (39; present in *Euthynotus*). This does not necessarily mean that these characters are invalid, particularly for the reversal of character 42 in *O. roeperi*, where the proportion of the dermosphenotic contributing to the dorsal margin of the orbit is only just below half, but it does illustrate that caution should be taken when comparing results here to diagnoses from the literature.

There are also three characters found to support pachycormiform monophyly here that do not traditionally appear in the synapomorphic characters for pachycormiforms. As with some

of the other characters mentioned here, two of them have an inconsistent distribution within pachycormiforms, or a wider distribution elsewhere. The first is the presence of a posterior boss on the skull roof (ch. 36), which is absent in *Australopachycormus* (Kear 2007), *Martillichthys* (Dobson *et al.* 2019; Chapter 2), and *Rhinconichthys* (Friedman *et al.* 2010; Schumacher *et al.* 2016) and unknown for *Bonnerichthys*, *Leedsichthys* or *Ohmdenia*, but clearly recorded as absent in taxa outside pachycormiforms. However, an inclined skull roof resembling a posterior boss is also reported on the skull roof in pycnodonts and dapediids, (Kriwet 2005; Theis & Waschkewtiz 2016) which were recently resolved as stem neopterygians and stem holosteans respectively (Latimer & Giles 2018). Similarly to early classifications of pachycormiforms, dapediids and pycnodonts have been assigned to a number of major groups, with dapediids being classed as 'semionotids', holosteans, stem holosteans and stem teleosts (Patterson 1973; Bermúdez-Rochas & Poyato-Ariza 2015; Giles *et al.* 2017; Lopez-Arbarello & Sferco 2018), and pycnodonts have been previously affiliated with teleosts, but support for this is tenuous (Poyato-Ariza 2015). Arratia (1999) also resolved *Dapedium* as the sister-taxon to pachycormiforms, but this was not on the basis of skull morphology.

The second character with inconsistent distribution among pachycormiforms is the placement of the pelvic fins anterior to the midpoint between the anal and pectoral fins (ch. 118), which is present in *Euthynotus*, *H. insignis*, *O. cornutus*, *O. roeperi*, *O. teyleri*, and *Protosphyraena*, but at or posterior to the midpoint in *H. macrodon* and unknown or inapplicable in all other pachycormiforms. Unlike the posterior boss on the skull roof, I consider this second character is too poorly known within pachycormiforms to be diagnostic.

The final character, which is unambiguous, is the presence of a hypural plate within pachycormiforms (ch. 102). While consistently absent in all taxa outside of the pachycormiforms in this matrix, it is recorded as present in 10 of the 17 pachycormiform taxa in this analysis, (and unknown for the other pachycormiforms) and may be a diagnostic character for pachycormiforms.

More broadly, pachycormiforms are also resolved within teleosts (node A) as a sister group to the aspidorhynchids and crown teleosts clade (node P). I would like to add note of caution about the strength of support here (node P), as two of the characters supporting this clade (ch. 28, presence of foramen for the efferent pseudobranchials; ch. 73, a slender, split-like symplectic) are more broadly distributed throughout the neopterygian tree. Because other crownward stem teleosts (such as Pleuropholidae; Patterson 1977*a*; fig. 19) are not included in this study, there is insufficient taxon sampling to determine whether aspidorhynchids are the sister group to crown teleosts. It is more likely that these two groups have been united by more broadly distributed characters (e.g. chs. 28 and 73, as noted above; and ch. 133, absence of a paired ossification anterior to the cleithra).

The age of pachycormiforms

The FBD analysis provided a mean age of pachycormiform divergence within the Carnian (Late Triassic), and the emergence of the giant bodied suspension-feeding pachycormiforms within the Aelenian (Middle Jurassic; Fig. 3.21). The first estimate is approximately 54 Myr earlier than the records of the earliest pachycormiforms (Toarcian, Early Jurassic; Hauff 1953*a*; Wenz 1967; Mainwaring 1978; López-Arbarello 2012; Friedman 2012*a*). But this date

seems quite late if pachycormiforms are — as hypothesized — one of the earliest diverging groups of teleosts. The estimates here are influenced by the taxa chosen in this analysis, due to their stratigraphic range. Of the teleost taxa included in this analysis, only *Dorsetichthys* appears earlier in the fossil record than pachycormiforms (Early Jurassic; Hettangian; Arratia 2013), despite diverging crownward of them. We know from previous studies that the fossils chosen to calibrate internal node ages can hugely influence divergence estimates in a node-dating analysis (e.g. Hurley *et al.* 2007; Near *et al.* 2012; Giles *et al.* 2017), and the neopterygian tree is infamous for a 70–100 Myr temporal gap between molecular estimates of divergence and the first appearance in the fossil record of (Near *et al.* 2012; Broughton *et al.* 2013).

This "teleost gap" was reduced in a recent study by Giles *et al.* (2017), which estimates an earliest Permian divergence between Teleostei and Holostei (mean: 298.4 Ma (Asselian: Cisurialian); 95% HPD: 278.4–318.4 Ma; Giles *et al.* 2017). However, the minimum age of crown neopterygians according to the fossil record is 250 Ma (Olenekian; Early Triassic; Giles *et al.* 2017), as constrained in this study by *Watsonulus* (Olenekian; Olsen 1984), but other Triassic crown neopterygians could have been included (such as the teleost *Prohalecites* or the holostean *Sangiorgioichthys*; Friedman 2015; fig. 2K–L) to better constrain divergence estimates of the neopterygian crown. There are also other putative crown neopterygians that could be included in this analysis such as *Acentrophorus* (Gill 1923; but this needs more rigorous study before it can be considered a crown neopterygian; Friedman 2015). Therefore, it is possible that the divergence dates provided here hint at wider problems of early teleost evolutionary history; failure to recognize early neopterygian taxa (Friedman 2015); their

rarity in the fossil record and lack of inclusion in phylogenetic analyses (Sallan 2014); and absence of preserved material in older deposits (Hurley *et al.* 2007).

From my results, the divergence time estimated for the giant bodied suspension-feeders is plausible given their fossil record, with specimens of *Asthenocormus*, *Leedsichthys* and *Martillichthys* appearing in the Callovian (Middle Jurassic; Lambers 1992; Liston 2006, 2008*a*; Dobson *et al.* 2019; Chapter 2), and an unidentified edentulous pachycormiform known from the Bajocian (Middle Jurassic) Inferior Oolite of Dorset (NHMUK PV P.41669; Friedman *et al.* 2010), although not included in this analysis.

Notably, however, the inclusion of stratigraphic data results in different patterns of relationships and a general loss of resolution compared to previous analyses (Figs. 3.19–3.21; Friedman 2012*a*; Wretman *et al.* 2016). This is not to say that one phylogeny is 'more correct' than another, but merely that morphology and stratigraphy provide conflicting signals for some relationships, particularly concerning the giant bodied suspension-feeders as sister group to all other pachycormiforms and the placement of *Rhinconichthys* and *Bonnerichthys* therein. *Bonnerichthys* and *Rhinconichthys* are resolved as the earliest diverging giant bodied suspension-feeding pachycormiforms in the parsimony and Bayesian analyses, with *Bonnerichthys* possessing primitive characters (Friedman 2012*a*) despite only being known from the Late Cretaceous fossil record (Friedman *et al.* 2013*a*). This has previously been resolved as an extremely long ghost lineage, with no fossils attributed to the *Bonnerichthys* or *Rhinconichthys* lineages throughout the Early Cretaceous and Late Jurassic. This would be consistent with the poor marine actinopterygian fossil record for the

Early Cretaceous (Chapter 4; fig. 4.2), and would allow time for character reversal in *Bonnerichthys* and *Rhinconichthys* from the character states seen in *Ohmdenia* and the Jurassic suspension-feeders, such as the elongate sphenoid region. However, the inclusion of stratigraphy reverses suspension-feeding pachycormiform relationships, with *Rhinconichthys* and *Bonnerichthys* emerging as a clade in the Albian at the earliest — as suggested by their fossil record — and *Asthenocormus*, *Leedsichthys* and *Martillichthys* emerging in the Aelenian (Fig. 3.21).

Suspension-feeding pachycormiforms more broadly are resolved as sister group to the two clades that typically seen in pachycormiforms in parsimony and Bayesian analyses (Figs. 3.19–3.21; Friedman 2012*a*; Wretman *et al.* 2016), rather than placing them with *Pachycormus*, *Saurostomus* and *Ohmdenia* (Fig. 3.21). Resolution within the 'protosphyraenid' clade resolution stays largely the same as in the parsimony and Bayesian analyses, but *Euthynotus* is resolved the sister-taxon to this clade only, rather than to pachycormiforms as a whole. This suggests that stratigraphy is the strongest phylogenetic signal in this analysis, leading to some taxa being grouped by similar stratigraphic ranges (e.g. the grouping of *Euthynotus* and the 'protosphyraenid' clade, and the Callovian giant bodied suspension-feeders) rather than by similar morphologies. However, some morphological characters still have enough phylogenetic signal to override stratigraphy and roughly outline some of the relationships seen in the parsimony and Bayesian analyses, such as: placing *Bonnerichthys* and *Rhinconichthys* with the other suspension-feeders (albeit with a different topology); and the clade containing *Pachycormus*, *Saurostomus* and *Ohmdenia*

remaining separate from the 'protosphyraenid' clade, which is also similar to the relationships in other analyses (Friedman *et al.* 2010; Friedman 2012; Wretman *et al.* 2016).

As such, while there are some similarities between the phylogeny produced in the FBD analysis (Fig. 3.21) and the phylogenies produced using Bayesian and maximum parsimony methods (Figs. 3.18–3.20), the inclusion of stratigraphy distorts the patterns of relationships that is consistent across the other analyses conducted in this study. This includes the rearrangement or loss of some clades that are strongly supported in the maximum parsimony and Bayesian analyses, such as the succession of clades within the 'protosphyraenid' (Nodes I–N; Figs. 3.19, 3.20) that collectively have a minimum Bayesian support of 0.91 (Node K; Fig. 3.19) or 0.96 (Node K; Fig. 3.20). Similar relationship distortion is seen in the well supported holostean clades, where *Amia calva* is moved to a clade containing the lepisosteiforms, despite the Bayesian analyses placing *Amia* outside the clade containing lepisosteiforms, *Macrosemius*, *Lepidotes* and *Semionotus* with a support of 0.99 and 0.94 (Figs. 3.19 and 3.20 respectively).

This supports the suggestion made earlier that the influence of stratigraphy on the resultant phylogeny is stronger than the influence of character states in many instances. However, many taxa (most notably *Bonnerichthys* and *Rhinconichthys*) are not necessarily reliably represented in the fossil record, and their stratigraphic ranges are limited to only their known range regardless of their hypothesized ghost lineages or relationships that are well supported by morphological and molecular evidence (e.g. Figs. 3.18–3.20).

Therefore, while the relationships outlined by the FBD analysis are not necessarily incorrect, they override strongly supported relationships seen in other analyses and need to be considered in the light of how their recorded stratigraphic ranges are limited by their fossil record. While the inclusion of other early neopterygians (such as *Prohalecites* or *Sangiorgioichthys*; Friedman 2015) could better constrain divergence times of early holostean and teleost taxa, the inclusion of stratigraphic information in this analysis will always be constrained by the quality of the known fossil record of the taxa studied. Until more fossils of the taxa included in this study are reported from new locations (outside their current stratigraphic range), the hypothesis of relationships given in the Bayesian and maximum parsimony analyses are the most likely given the observed morphological and molecular evidence.

Notes on pachycormiform ecology and phylogeny

As with previous descriptions (Wenz 1967; Mainwaring 1978), I agree that the general jaw morphology of sharp, needle-like teeth in *Pachycormus* indicates a predatory ecology (after Bellwood & Hoey 2004) which is supported by the presence of cephalopod remains in the stomach of a *Pachycormus* specimen from the Posidonia Shale, Germany (Přikryl *et al.* 2012). Within the gill basket and jaw morphologies of pachycormiforms, there are also a number of features that vary between species that could reveal more sequential evolutionary changes within the 'protosphyraenid' and 'suspension-feeding' clades.

For instance, a character that has received attention recently concerns pachycormiform gill raker morphology (e.g. Liston 2013; Gouiric-Cavalli 2017). The Jurassic members of the giant

bodied suspension-feeders (*Asthenocormus*, *Leedsichthys* and *Martillichthys*) are characterized by elongate, elaborate gill rakers that are presumably strongly linked to ecological function (Lambers 1992; pl. 2; Liston 2006, 2008*a*; 2013; fig. 1; Dobson *et al.* 2019; fig. 7; Chapter 2). This analysis included findings of a new raker morphology in *Hypsocormus tenuirostris*, which has the short, toothlike rakers seen in *Pachycormus*, but up to three raker teeth associated with each raker (Dobson 2016; fig. 3). The role of these short but toothed rakers may be associated with helping to grasp and hold larger prey items in the mouth to swallow them whole (Vanderwalle *et al.* 1994). However, several studies have noted that gill raker morphology is highly plastic and dependant on various pressures including ontogeny and environment (June & Carlson 1971; Sanderson & Wassersug 1993; Hjelm & Johansson 2003), making strong inferences about their role in the ecology of *Hypsocormus* challenging. If the primary role of these rakers is protection, this may result in some plasticity because this role can be performed by numerous morphologies, unlike the role of the rakers in the giant suspension-feeders. Analysis of more rakers within the 'protosphyraenid' clade of pachycormiforms would give a clearer indication of whether this raker morphology is linked to ecological role, or if it is plastic among taxa depending on life history and ontogeny.

The maxilla morphology is typical of those described in other predatory taxa, with a distinctive toothed, ventral margin, and an edentulous anterior process to articulate with the premaxilla. While the size of this anterior process varies between taxa, it serves an important role in facilitating articulation between the maxilla and premaxilla, via the maxillary-premaxillary ligament, for jaw protrusion and movement during prey capture (Westneat 2005). Without knowing for certain the diet choice of different pachycormiform

taxa (beyond perhaps cephalopods; Přikryl *et al.* 2012), it is not possible compare jaw mobility and diet choice of pachycormiforms with extant analogues, but it suggests that some degree of upper jaw movement was possible in the tuna-like *Pachycormus* and *Hypsocormus*. Conversely, the reduction of this process in the billfish-like *Protosphyraena* and *Australopachycormus* (Hay 1903; fig. 9; Woodward 1908*a*; pl. XXXI fig. 4, 4A; Lambers 1992; fig. 13; Kear 2007: 1035), and even the lack of an articular process in *Euthynotus* (due to the fusion of the maxilla and premaxilla in this taxon: Wenz 1967; Lambers 1992: 236) may indicate a limited upper jaw mobility due to a ram feeding lifestyle.

Another newly described character in *Pachycormus* is the presence of large fangs on the anteriormost coronoid plate. These are also seen in the tomograms of other *Pachycormus* specimens: BRLSI M1297; BRLSI M1311; BRLSI M1395; NHMUK PV OR 32433. Morphologically, they seem to be similar — but less exaggerated — to the large fangs at the anterior of the mandible in *Hypsocormus*, *Orthocormus*, *Australopachycormus* and *Protosphyraena*, although the fangs in *Pachycormus* do not protrude forwards out of the mouth. These fangs have also never been described in other predatory taxa such as *Euthynotus*, *Saurostomus* (Wenz 1967) and *Ohmdenia* (Friedman 2012*a*), but their absence in these forms cannot be confirmed. However, it does tell us that these fangs are more broadly distributed than just the 'protosphyraenid' clade, but are lost at some point between *Pachycormus* and *Ohmdenia* during the shift to the suspension-feeding ecology.

The loss of these fangs between *Pachycormus* and *Ohmdenia* would corroborate an analysis conducted by Friedman (2012*a*) that identified *Ohmdenia* as the sister group of the giant

bodied suspension-feeding pachycormiforms, and an intermediary taxon between the predatory and suspension-feeding ecologies. Friedman (2012*a*) showed that *Ohmdenia* and the giant bodied suspension-feeders possessed a number of sequential changes in jaw morphology and geometry that have also characterised the evolution of suspension-feeding in mysticete whales (Sanderson & Wassersug 1993; Hampe & Baszio 2010). As well as the increase in mandibular length noted in *Ohmdenia* and the Jurassic clade of suspension-feeders (Dobson *et al.* 2019; Chapter 2), and a reduction of marginal dentition, suspension-feeders also exhibit an increase in gape size made possible by an elongate rostrum and the placement of the mandibular-quadrate joint on the postero-ventral corner of the mandible (Dobson *et al.* 2019; fig. 6; Chapter 2).

The monophyly of suspension-feeding pachycormiforms

The stark difference in skull geometries between *Bonnerichthys*, *Rhinconichthys* and *Ohmdenia* and the Jurassic suspension-feeding pachycormiforms is reinforced by some derived features shared between *Bonnerichthys* and *Protosphyraena*. These include: the fusion of distal lepidotrichia along the leading edges of the pectoral fins; the "C"-shaped second radial allowing for two independent articulations with the shoulder girdle; and a series of "paddle-shaped" radials (the latter two are also similar to the pectoral girdle of *Orthocormus*; Friedman *et al.* 2010; and now also in *Pachycormus*; Fig. 3.14). This led Liston and Maltese (2016) and Dobson *et al.* (2019; Chapter 2) to query the monophyly of the suspension-feeders, and postulate a second origin of suspension-feeding within the 'protosphyraenid' clade. This alternative hypothesis was tested here using stepping stone analysis, which found stronger support for a single origin of suspension-feeding

pachycormiforms. This shows that the gap in stratigraphic occurrences between the 'Jurassic' (*Asthenocormus*, *Leedsichthys* and *Martillichthys*) and 'Cretaceous' (*Bonnerichthys* and *Rhinconichthys*) suspension-feeding pachycormiforms is not enough to override the signal of their similar morphologies, and that the relationships estimated in the phylogenetic analyses are the best supported relationships explained by the data available. Therefore, for now, I reject the hypothesis suggested by Liston & Maltese (2016) and Dobson *et al.* (2019; Chapter 2) of multiple origins of suspension-feeding, and accept the phylogeny produced by this and other phylogenetic analyses (Friedman *et al.* 2010; Friedman 2012*a*; Wretman *et al.* 2016).

Conclusions

This analysis has revealed previously poorly described structures, such as the pectoral endoskeleton, and undescribed characters, such as the presence of a metapterygium-like branching radial, a urohyal, and the large fangs of the anterior coronoid. It has also corroborated previous hypotheses of phylogenetic relationships, and highlighted areas where morphological variation could provide insight into ecological function, such as the gill raker morphology. This description of an early diverging pachycormiform gives a deeper insight into teleost synapomorphies that can now be used to help elucidate the broader relationships of the early teleosts, such as the origin of the teleost urohyal deep within the teleost stem. Despite this, the inferences that can be made from this analysis are still limited by the lack of specimens, particularly for the long ghost-lineage of *Rhinconichthys* and *Bonnerichthys* that could help to resolve the origin of the giant suspension-feeding ecology. It is hoped that this description and analysis can be used for future comparisons to specimens to improve the observable characters in some of the lesser known predatory pachycormiform species.

Chapter 4

Constraining the timing of the emergence of the giant bodied suspension-feeding ecology in modern chondrichthyan lineages and the extinction of pachycormiforms

This chapter has been prepared in the style of a manuscript for publication, but a target journal has not yet been chosen. MF and SG contributed with analytical advice and improving drafts of my writing. All other data collection, analyses, and writing have been done by CD.

Abstract

The giant bodied suspension-feeding ecology has evolved numerous times in chondrichthyans, with four independent lineages in modern fauna. Previous studies have hypothesized that these groups emerged in the Cenozoic following the extinction of the giant suspension-feeding pachycormiforms that occupied this ecology throughout the Mesozoic, but disappeared from

the fossil record towards the end of the Cretaceous. This study aims to estimate credible time intervals for the extinction of suspension-feeding pachycormiforms, and the emergence of modern suspension-feeding chondrichthyan lineages based on the density of their observed fossil record over time. I apply a method that accounts for heterogeneity of the fossil record over time by calculating the proportion of geological units with potential to preserve the focal groups within the range studied. Results indicate that extinction of suspension-feeding pachycormiforms in the early Cenozoic cannot be excluded (point estimate = 59 Ma; 95% CIs = 47.6–65.9 Ma). I find that cetorhinids likely emerged in the middle Eocene (46.3 Ma; 42–55.3 Ma), but the oldest credible interval for megachasmids makes it impossible to rule out a Mesozoic origin (44 Ma; 35.1–73.1 Ma). I also find that rhincodontid (71.1 Ma; 57.1–118.3 Ma) and mobulid (66 Ma; 57.1–76.5 Ma) suspension-feeders may have emerged in the Mesozoic, with credible intervals extending into the Cenomanian, potentially overlapping with the suspension-feeding pachycormiforms (from the fossil record of the Late Cretaceous). There are also some putative suspension-feeding chondrichthyans known from the Cretaceous, which are not related to living radiations or known in the Cenozoic fossil record. This may indicate a shift in diversity patterns during the faunal turnover of the end Cretaceous mass extinction, where the loss of planktonic foraminifera and vulnerability of large bodied taxa to extinction events led to the extinction of Cretaceous suspension-feeders but allowed modern radiations to emerge.

Introduction

Marine environments are characterized by substantial biodiversity (Norris 2000), including the largest marine vertebrates: obligate suspension-feeders. In modern ecosystems, this

ecological role is filled by four independent lineages of chondrichthyans (the basking shark, *Cetorhinus maximus*; whale shark, *Rhincodon typus*; megamouth shark, *Megachasma pelagios*; and manta and devil rays, Mobulidae) and mysticete whales (Mysticeti). Although suspension-feeding is not an ecology unique to these giant taxa, the ecomorphological shift from moderately to large bodied pelagic predators to giant bodied suspension-feeders is a trend that has been noted in previous studies (Freedman & Noakes 2002; Maisey *et al.* 2004; Deméré & Berta 2008; Friedman 2012*a*; Pimiento *et al.* 2019). The giant bodied suspension-feeding stem teleosts of the Jurassic and Cretaceous (Friedman *et al.* 2010; Liston 2010; Friedman 2012*a*) appear to represent another example of this pattern. These taxa form a clade within a group more typically containing tuna and billfish-like predators and billfishes (e.g. *Pachycormus* and *Protosphyraena*; Mainwaring 1978; Hay 1903; Wretman *et al.* 2016), known as the pachycormiforms. It has been hypothesized that the giant suspension-feeding taxa of modern ecosystems emerged following the extinction of giant bodied suspension-feeding teleosts that disappear from the fossil record before the Cretaceous-Paleogene (K-Pg) boundary (Friedman *et al.* 2010). This study seeks to test this hypothesis.

Problems with past interpretations

A literal reading of the fossil record gives the impression that there is an approximately seven million year gap between the extinction of suspension-feeding pachycormiforms (at the K-Pg boundary; 66 Ma) and the emergence of the first, modern suspension-feeding chondrichthyans (Thanetian; 59.2 Ma; Noubhani & Cappetta 1997), with toothless mysticetes radiating in the Oligocene (33.9–23.03 Ma; Peredo *et al.* 2018). Because they are well-represented in the fossil record (54–59% of living genera are preserved; Quental &

Marshall 2010), estimates for the emergence of mysticete suspension-feeders are relatively well constrained both by fossils (e.g. Deméré *et al.* 2005; Deméré *et al.* 2008; Uhen 2010; Geisler *et al.* 2017) and molecular clocks (Sasaki et al. 2005; Jackson *et al.* 2009; Marx & Fordyce 2015), and undoubtedly postdate the K-Pg extinction by many millions of years. However, because three of the four modern suspension-feeding chondrichthyan lineages are monotypic, molecular clock estimates only provide a maximum bound for their emergence by estimating the divergence of their total-groups, rather than when the ecology itself emerged. By contrast, the presence of suspension-feeding chondrichthyans in the fossil record provides a minimum bound on the emergence of their ecology, with the actual origin falling between these two dates. Additionally, we know that the fossil record is, by nature, incomplete, and does not always record the first occurrences of a group. While the fossil record of suspension-feeding chondrichthyans is dense, it is restricted to teeth and the occasional gill raker, which can limit identification. Therefore, it is possible that suspension-feeding chondrichthyans appeared in marine ecosystems before they appear in the fossil record. Similarly, it is also possible that pachycormiforms existed in the Paleogene, but this needs to be tested in a quantitative way, using an approach that acknowledges incompleteness of the fossil record to provide a range within which groups might have plausibly gone extinct or originated. Using this approach, I will evaluate the hypothesis proposed by Friedman *et al.* (2010), namely that the origins of modern chondrichthyan suspension feeders postdate the extinction of suspension-feeding pachycormiforms, and are possibly attributable to ecological opportunities presented by the disappearance of that group.

Testing emergence and extinction

To test this hypothesis, this study aims to estimate a plausible time range for the extinction of suspension-feeding pachycormiforms and the emergence of giant suspension-feeding in modern lineages of chondrichthyans based on the distribution of fossils of these groups. Molecular clock analyses can only time the maximum divergence of these taxa from their predatory relatives, and the fossil record the minimum estimate for when suspension-feeding ecologies emerged in these monotypic lineages. Therefore, the actual emergence of this ecology will be some point after the suspension-feeders divergence from their sister taxa but before the ecology appears in the fossil record, which is what I will be testing. I will also be controlling for the quality of the fossil record, as the preservation of fossils for these focal groups are not uniform over time. This is based on work by Strauss and Sadler (1989), who first proposed a way of using Bayesian probability to infer confidence intervals for extension of taxonomic ranges beyond those observed in the fossil record. I further account for heterogeneity of fossil preservation based on work by Marshall (1997).

A combination of the approaches of Strauss and Sadler (1989) and Marshall (1990; 1997) was presented by Friedman *et al.* (2013*b*) and Capobianco and Friedman (2019). The original method was designed to identify a credible time range in which a group of taxa may have disappeared given their density in the fossil record (Strauss & Sadler 1989). However, this method, along with Marshall (1990), works on the assumption that fossils are randomly distributed through time, and have an equal probability of appearing in any horizon within the given temporal range of the first and last known fossils. This assumption is constantly violated by the fossil record, which is characterized by considerable variability in the

preservation of fossils over time. The work by Marshall (1997) presented a method to account for preservation heterogeneity by calculating a potential of fossil recovery within each predefined time frame, which can then be used to inform the confidence interval analysis by relaxing or contracting the confidence intervals calculated accordingly. This allows for horizons with a poor potential of yielding fossils to be identified, and reduces the weight that these absences have on overall analysis, compared to high potential fossil yielding horizons that still lack a record of the focal taxon. Therefore, the estimates produced by combining these methods (as in Friedman *et al.* 2013*b*; Capobianco & Friedman 2019) are more realistic regarding the quality and preservation potential of the fossil record over time.

There are two aims for this study: (1) estimate the plausible span of range extensions for each of the focal groups (i.e. the chondrichthyan groups Cetorhinidae, Megachasmidae, Mobulidae, Rhincodontidae; and the giant suspension-feeding pachycormiforms); (2) explore what patterns in ocean ecosystems may have led to the extinction of pachycormiforms and the emergence of suspension-feeding chondrichthyans. In doing so, I hope to shed more light on how the events in Earth's history set the stage for modern lineages of giant bodied suspension-feeders to emerge.

Current estimates for extinction and emergence of suspension-feeding lineages

The fossil record of suspension-feeding pachycormiforms

Fossils of giant bodied suspension-feeding pachycormiforms are known from the Middle Jurassic–Late Cretaceous, with specimens described from Europe, Asia, the Americas and Antarctica (Lambers 1992; Liston 2006, 2008*a*, 2010; Friedman *et al.* 2010, 2013*a*; Gouiric-

Cavalli 2017; Schumacher *et al.* 2016; Cione *et al.* 2018; Gouiric-Cavalli *et al.* 2019; Dobson *et al.* 2019) and represent the only known example of the giant suspension-feeding ecology in teleosts. As with chondrichthyans, the fossil record of giant bodied suspension-feeding pachycormiforms suffers from being composed of poorly preserved or disarticulated material, and is exacerbated by a poorly ossified skeleton. No fossils of suspension feeders are reported from the Early Cretaceous. Nonetheless, they are relatively abundant in the Late Cretaceous, but this has only recently been recognized (Friedman *et al.* 2010, 2013*a*). Genera within this giant bodied suspension-feeding clade include: *Asthenocormus*, *Bonnerichthys*, *Martillichthys*, *Rhinconichthys* and — most famously — the largest fish to have ever lived: *Leedsichthys* (Liston 2004, 2010; Liston *et al.* 2013). By the end of the Cretaceous only *Bonnerichthys* is present in the fossil record. However, this taxon is known from a range of geographically widespread deposits from multiple stratigraphic horizons (Stewart 1988; Parris *et al.* 2007; Friedman *et al.* 2010; Grandstaff *et al.* 2011; Friedman 2012*a*; Friedman *et al.* 2013*a*; Schumacher *et al.* 2016; but see Cione *et al.* 2018). There are also two specimens identified as Pachycormidae indet.: an incomplete, edentulous skull of a pachycormiform from the Bajocian (Middle Jurassic) Inferior Oolite of Dorset, UK (Friedman *et al.* 2010) and a large, isolated fin attributed to a suspension-feeding pachycormiform from the latest Maastrichtian (Late Cretaceous; for details of identification, see Cione *et al.* 2018). This is the last known occurrence of suspension-feeding pachycormiforms.

The fossil record of suspension-feeding chondrichthyans

Mobulidae. The suspension-feeding rays, mobulids, are a family within Myliobatiformes, but their composition and relationships have been contested, with some authors treating the

group as a sub-family (i.e. Mobulinae; Adnet *et al.* 2012). Following Cappetta (2012), Adnet *et al.* (2012) and Enault *et al.* (2013), I restrict mobulids to the following taxa: *Burnhamia* Cappetta 1976; *Eomanta* Pfeil 1981; *Eoplinthicus* Cappetta & Stringer 2002; *Mobula* Rafinesque 1810; *Manta* Bancroft 1829; *Oromobula* Adnet *et al.* 2012; and *Plinthicus* Cope 1869. Of these, *Burnhamia*, *Eomanta*, *Eoplinthicus*, *Oromobula* and *Plinthicus* are known only as fossils.

Lamniformes. Cetorhinids and megachasmids are separate families of lamniform sharks, each of which is monotypic in the present day. It was originally hypothesized that cetorhinids and megachasmids formed a clade (Maisey 1985; fig. 2) to the exclusion of other lamniform lineages. However, molecular data separate the two groups, thereby indicating that suspension-feeding evolved convergently between them (Martin & Naylor 1997; Sorenson *et al.* 2014). Both the fossil record and molecular clock analyses support the emergence of lamniforms during the Late Jurassic (Underwood 2006; Sorenson *et al.* 2014), followed by diversification in the Cretaceous thought by some to be an adaptive radiation event (Cappetta 1987; Martin & Naylor 1997; Naylor *et al.* 1997).

Cetorhinidae. The earliest definitive examples of cetorhinids are Eocene in age. There are currently three recognized species: the extinct *Cetorhinus parvus* (=*Keasius parvus*) and *Keasius taylori*, representing the stem, and the extant *Cetorhinus maximus*, representing the crown. Traditionally fossils found in the Eocene are assigned to *K. taylori*, early Miocene and Oligocene are considered *C. parvus* (or *K. parvus*) and younger fossils are considered *C. maximus* (Welton 2013*a*), but their origin and interrelationships remain unresolved.

Megachasmidae. Fossils, and even contemporary records, of megachasmids are particularly rare, with only a handful of tooth records to represent stem megachasmids (*Megachasma applegatei* and *M. alisonae*; Shimada *et al.* 2014; Shimada & Ward 2016 respectively), and only 100 recorded sightings of the extant *M. pelagios* (Taylor *et al.* 1983). This has often made it difficult to attribute fossil teeth to a taxonomic ranking beyond "*Megachasma* sp." (Shimada *et al.* 2014). This lack of fossil evidence has made the origin and interrelationships of megachasmids very difficult to elucidate, and their origin remains unclear (Shimada & Ward 2016). However, a Mesozoic origin for the megachasmid total-group has been hypothesized before by Shirai (1996; fig. 4) and corroborated by molecular studies (90–104 Ma; Martin *et al.* 2002; 73–139 Ma; Heinicke *et al.* 2009). The earliest fossil occurrence of a probable suspension-feeding megachasmid is *Megachasma applegatei* is from the Priabonian (late Eocene; Shimada & Ward 2016).

Rhincodontidae. Rhincodontids are also poorly known in the fossil record, and suspension-feeding genera in this family are the extinct *Palaeorhincodon* and the extant *Rhincodon typus* (Cappetta 2012). The earliest known fossils of these suspension-feeding rhincodontids are known from the Thanetian (late Paleocene; Noubhani & Cappetta 1997). A molecular clock analysis suggests a Santonian divergence for total-group rhincodontids (Sorenson *et al.* 2014; fig. 1).

Other putative suspension-feeding chondrichthyans

Triassic suspension-feeders. Another species that was attributed to cetorhinids, *Pseudocetorhinus pickfordi* has been described from the Late Triassic (Rhaetian) deposits of

Devon (Duffin 1998), with a substantial stratigraphic gap between it and uncontested basking shark fossils, all of which are Cenozoic in age. Cetorhinid affinity was further disputed due to the lack of similarity between the homodont teeth of *Cetorhinus* and the heterodont teeth of *Pseudocetorhinus* (Andreev & Cuny 2012). Hence, *Pseudocetorhinus* is considered to be more likely a stem selachimorph than cetorhinid or even lamniform (Andreev & Cuny 2012), and unlikely to be a suspension-feeder due to its tooth morphology not matching those of modern suspension-feeding chondrichthyans (Cappetta 2012; fig. 320; Shimada *et al.* 2015).

Cretaceous suspension-feeders. Cretomanta Case *et al.* 1990, is known from the Cenomanian (Shimada *et al.* 2006; Underwood & Cumbaa 2010). As its name suggests it has been proposed as a relative of mobulids. However, tooth morphology of *Cretomanta* is now generally considered to be convergent to mobulids. Its placement is, however, unclear, with some suggesting affinities with lamniforms (Noubhani & Cappetta 1997; Cappetta 2006), or as an unidentified group within batoids (Underwood & Cumbaa 2010).

In addition to *Cretomanta*, *Platylithophycus cretaceus* (Bronson & Maisey 2018) is represented by a partial gill skeleton from the Coniacian–Santonian (Late Cretaceous) of Niobrara Formation of Kansas. Uncertainty over how to interpret the remains resulted in it being misidentified as green algae (*Platylithophycus cretaceum*; Johnson & Howell 1948: 632; pl. 93; figs. 1, 2), and as a sepiid cephalopod (Miller & Walker 1968: 181; pls. 2, 3). Bronson & Maisey (2018) suggest that *Platylithophycus* may be a Cretaceous relative of mobulids based on gill raker morphology. It is also possible that *Platylithophycus* is a relative of

Cretomanta (also known from the Coniacian; Case *et al.* 1990; Shimada *et al.* 2006; Underwood & Cumbaa 2010), but there is no overlapping material between the two taxa. Finally, the suspension-feeding genera *Archaeomanta* and *Eomobula* are not included in this analysis due to Adnet *et al.* (2012) identifying them as suspension-feeding myliobatids that are unrelated to the mobulid radiation.

Among sharks, Shimada (2007) described the Cenomanian remains of a taxon identified as *Megachasma comanchensis*. However, this was later placed in the new genus *Pseudomegachasma comanchensis*, due to its tooth morphology being considered convergent with that found in the other species of *Megachasma* (Shimada *et al.* 2015). Shimada *et al.* (2015) also moved *Pseudomegachasma* to Odontaspididae, as a close relative of the piscivorous *Johnlongia* and the other Cretaceous suspension-feeder *Pseudomegachasma casei* (formerly *Eorhincodon casei*; Nessov 1999; Shimada 2007; Shimada *et al.* 2015) based on their similar tooth morphologies.

Methods

Occurrence data

Chondrichthyans. Occurrences were considered at the family level (Cetorhinidae, Megachasmidae, Mobulidae, Rhincodontidae; Fig. 4.1), based on a survey of the literature beginning with Cappetta (2012). The following genera are considered valid members of the modern clades of suspension-feeding chondrichthyans: *Keasius*, *Cetorhinus* (Cetorhinidae); *Rhincodon, Palaeorhincodon* (Rhincodontidae); *Burnhamia*, *Eomanta*, *Eoplinthicus*, *Manta*, *Mobula*, *Oromobula*, *Plinthicus* (Mobulidae; following Cappetta 2012 and Adnet *et al.* 2012);

and *Megachasma* (Megachasmidae). Other putative suspension-feeding taxa (e.g. *Pseudocetorhinus*, *Pseudomegachasma* and *Cretomanta*) were excluded from the occurrence records due to them not being considered members of the focal modern lineages (Adnet *et al.* 2012; Korneisel *et al.* 2015; Shimada *et al.* 2015; Frederickson *et al.* 2016).

Pachycormiforms. Occurrence records of pachycormiforms were recorded from a literature review. The following genera were included in this dataset (Fig. 4.1): *Asthenocormus*, *Bonnerichthys*, *Leedsichthys*, *Martillichthys*, *Rhinconichthys*, and the Pachycormidae indet. specimens (see above). For comparison, a second dataset was composed containing only records of *Bonnerichthys*, which is last occurring pachycormiform and known from the most horizons of the Cretaceous pachycormiforms (*Bonnerichthys*; *Rhinconichthys*; Pachycormidae indet.).

Ages of occurrence records. Age ranges of the occurrence record stratigraphic horizons (formations and/or localities) were constrained as much as possible using age estimates from the relevant literature (generally formation age, which was verified against Gradstein *et al.* 2012). Boundary ages between stages were taken from the International Chronostratigraphic Chart (Cohen *et al.* 2013). Repeats of occurrences from the same horizon (at formation level) were removed, leaving only one occurrence record for each horizon. However, if there were occurrences from many stages within the same formation — such as the Niobrara Formation — these were broken down into individual horizons representing each stage (e.g. “Niobrara Santonian”, “Niobrara Campanian”) to prevent occurrences of very different ages in the same temporally extensive formation from being discounted.

Estimating extensions on observed ranges

The calculations given in Strauss and Sadler (1989) are used with the assumption of uniform distribution of fossils through time, but the fossil record is known to be non-uniform (Benton *et al.* 2000). Therefore, I applied the framework set out by Marshall (1997) to use preservation and recovery potential functions to relax the credible intervals if fossil recovery is non-uniform. This was done by sorting data into 1-million-year bins, where each bin is assigned a value representing the proportion of focal group fossils present in that bin. Therefore, a uniform distribution of fossils was only assumed at each sampling bin (the sampling opportunity) rather than over time, allowing for non-uniform fossil preservation overall (Friedman *et al.* 2013*b*; Capobianco & Friedman 2019).

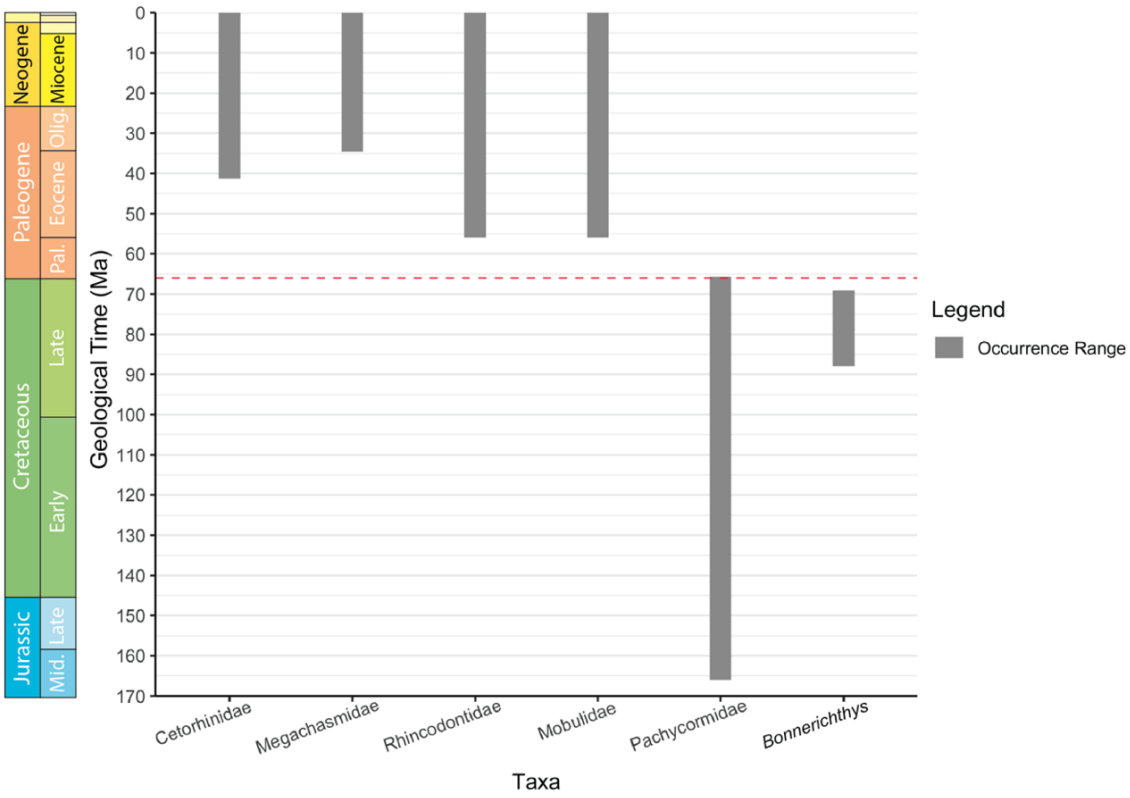

Figure 4.1 – The fossil record of modern suspension-feeding chondrichthyans and pachycormiforms used for this study. The Cretaceous-Paleogene boundary is marked by a dashed red line.

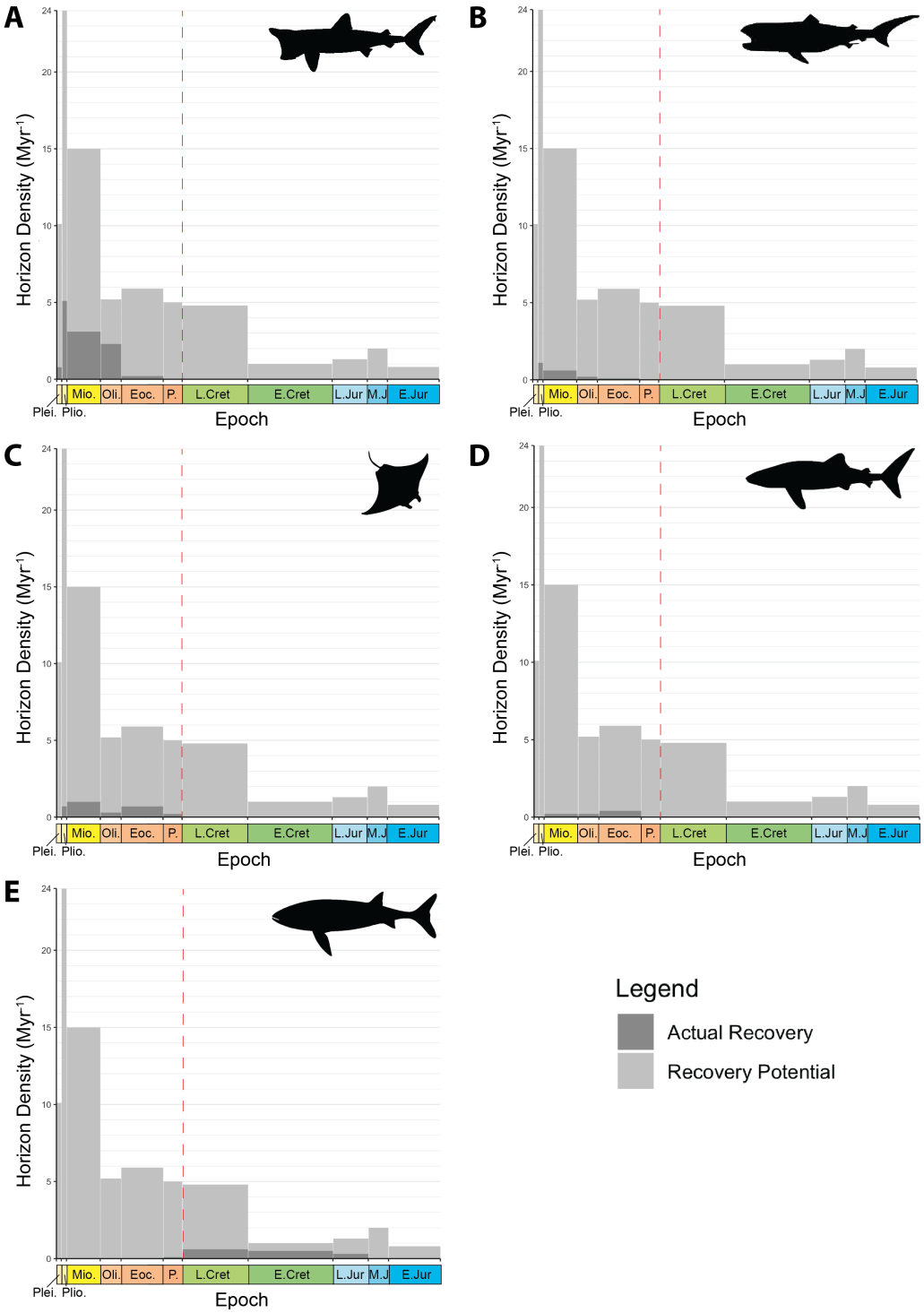

Figure 4.2 – The recovery potential of fossils in each epoch for each focal lineage: A) Cetorhinidae; B) Megachasmidae; C) Mobulidae; D) Rhincodontidae; E) Pachycormiformes. The dark grey bars indicate the proportion of fossils collected for each focal lineage, while the light grey bars represent the proportion of fossil recorded in the Paleobiology Database for chondrichthyans or actinopterygians (for pachycormiforms) within each epoch searched. Abbreviations for geological epochs are as follows: Plei. – Pleistocene; Plio – Pliocene; Mio. – Miocene; Oli. – Oligocene; Eoc. – Eocene; P. – Paleocene; L.Cret. – Late Cretaceous; E.Cret. – Early Cretaceous; L.Jur – Late Jurassic; M.J – Middle Jurassic; E.Jur – Early Jurassic. No occurrences were recorded for the Holocene.

Recovery function

The recovery function is used to infer preservation potential, based on whether horizons have yielded taphonomic analogues, but not the focal group (therefore more likely to be a true absence of the focal group), or if neither the focal group nor the taphonomic analogues are present (more likely to be a false absence due to lack of preservation). As such, I can statistically account for non-uniform preservation of the fossil record, and assess the likelihood of fossils of interest being found in these horizons. A list of horizons that might possibly yield groups of interest was compiled using the Paleobiology Database (paleobiodb.org). The age range of horizons collected spanned from is 201.3 Ma to 0 Ma, to include potential horizons that might bear fossils of the focal group beyond their observed fossil records (Fig. 4.2). The decision to designate the end of the Triassic (201.3 Ma) as an oldest bound reflects strong evidence that modern lineages of suspension-feeding chondrichthyans are substantially younger. The fossil record for modern sharks (Neoselachii) begins at the Late Triassic–Early Jurassic (Maisey *et al.* 2004; Benton 2015: 179; Nelson *et al.* 2016). Molecular analyses have shown a late Carboniferous (306 Ma; Renz *et al.* 2013) to late Permian origin estimated for the divergence between sharks (Selachimorpha) and rays (Batoidea) within neoselachians (minimum 250 Ma; Klug 2010; Inoue *et al.* 2010), and no molecular or fossil evidence of any modern suspension-feeding chondrichthyans appears before the Cretaceous (145 Ma; see above).

For the chondrichthyan suspension-feeders, my recovery function was based on all marine deposits that had been reported to yield chondrichthyans, resulting in approximately 8400 records. For pachycormiforms, I only collected marine deposits bearing actinopterygians,

resulting in 6500 records. From these lists, I only kept those that had a formation name recorded, or enough locality information to allow me to find the corresponding formation from the literature. Minimum and maximum age constraints were then checked against the literature for accuracy, and any repeat records of the same formation were removed. I also added any formations that were present in the focal group occurrence data that had been missing from the PBDB dataset. This resulted in 595 formations for chondrichthyans, and 579 formations for actinopterygians.

Bayesian calculations

The analysis was conducted in R v. 3.5.2 (R Core Team 2018), using a script modified from Capobianco & Friedman (2019). This script included calculations for extension of lineage emergence or extinction based on the density of their fossil record, using Strauss and Sadler's (1989) equation 26. This calculates maximum posterior density endpoint (θ) of a stratigraphic range, given the occurrence data (x), from which two-tailed 95% oldest and youngest credible intervals, and the one-tailed 95% credible interval can be calculated:

$$h(\theta|x) = \frac{(n-2)[(\theta - y) - \theta^{-n+1}]}{u_n} \qquad \text{if } z < \theta < 1 \tag{1}$$

where y is the last recorded fossil appearance of the group of interest, n is the number of horizons yielding fossils of the group of interest, and u_n (Strauss & Sadler 1989; equation 25) is calculated by:

$$u_n = (z-y)^{-n+2} - (1-y)^{-n+2} - z^{-n+2} + 1 \tag{2}$$

where z is the first recorded fossil appearance. In these equations, θ, y and z are rescaled to set the prior upper bound to 1, and assumes a uniform distribution of fossils. Because this assumption is always violated by the fossil record, I employed the recovery function explained above, which allows for non-uniform fossil distributions through time by breaking the dataset up into sampling bins that assume a uniform distribution individually, but allow variation across the dataset as a whole. The Bayesian point estimate of θ is calculated by Strauss & Sadler's (1989) equation 27 (equation 3 here), which is the mean of their equation 26 (equation 1 here, shown above):

$$\frac{(n-2)u_n - 1}{(n-3)u_n} + \frac{y[(z-y)^{-n+2} - (1-y)^{-n+2}]}{u_n} \quad (3)$$

To assign a precise age of each occurrence, fossils were randomly placed in a 1-million-year bin within the constrained age from which they were recovered (e.g. Chattian). To account for uncertainty of these randomly generated ages, the analysis was repeated 1000 times, each time assigned to a new bin for each occurrence. For each replicate, the point estimate (equation 3), the youngest credible interval (youngest CI; the 2.5% quantile of equation 1), the oldest credible interval (oldest CI; the 97.5% quantile of equation 1) and the one-tailed 95% credible interval (equivalent to the 90% quantile of equation 1) are calculated. Of these 1000 replicates, the result is obtained by taking the median point estimate, youngest CI, oldest CI and the one-tailed 95% CI, and the 95% confidence intervals (the 2.5% and 97.5% quantiles of the point estimate, youngest and oldest CIs, and one-tailed 95% oldest CI) are calculated. This produces 12 values in all: the median point estimate (±95%), the median youngest CI (±95%), the median oldest CI (±95%), and the median one-tailed 95% CI

(±95%). The results reported here are the median point estimate, plus the maximum confidence of the oldest CI and minimum confidence interval of the youngest CI calculated around the point estimate.

Results

Extinction of suspension-feeding pachycormiforms

I found that the credible extinction range (two-tailed 95% CIs) for pachycormiforms spans the Lutetian–Danian (47.6–65.9 Ma; Fig. 4.3; Table 1), with a point estimate in the Thanetian (59 Ma), and a one-tailed 95% CI of 53.8 Ma (Ypresian; Fig. 4.4; Table 1).

Table 1 – The point estimates, two-tailed 95% credible intervals (CIs), and one-tailed credible intervals for each focal group, estimating a plausible range of suspension-feeding chondrichthyan emergence and suspension-feeding pachycormiform extinction.

Taxa	Point Estimate (Ma)	Youngest 95% CI (Ma)	Oldest 95%CI (Ma)	One-tailed 95% CI (Ma)
Cetorhinidae	46.3	42	55.3	47.9
Megachasmidae	44	35.1	73.2	54.7
Mobulidae	66	57.1	76.5	69.4
Rhincodontidae	71.1	57.1	118.3	81.7
Pachycormiformes	59	47.6	65.9	53.8
Bonnerichthys	60.6	40.5	69	50.8

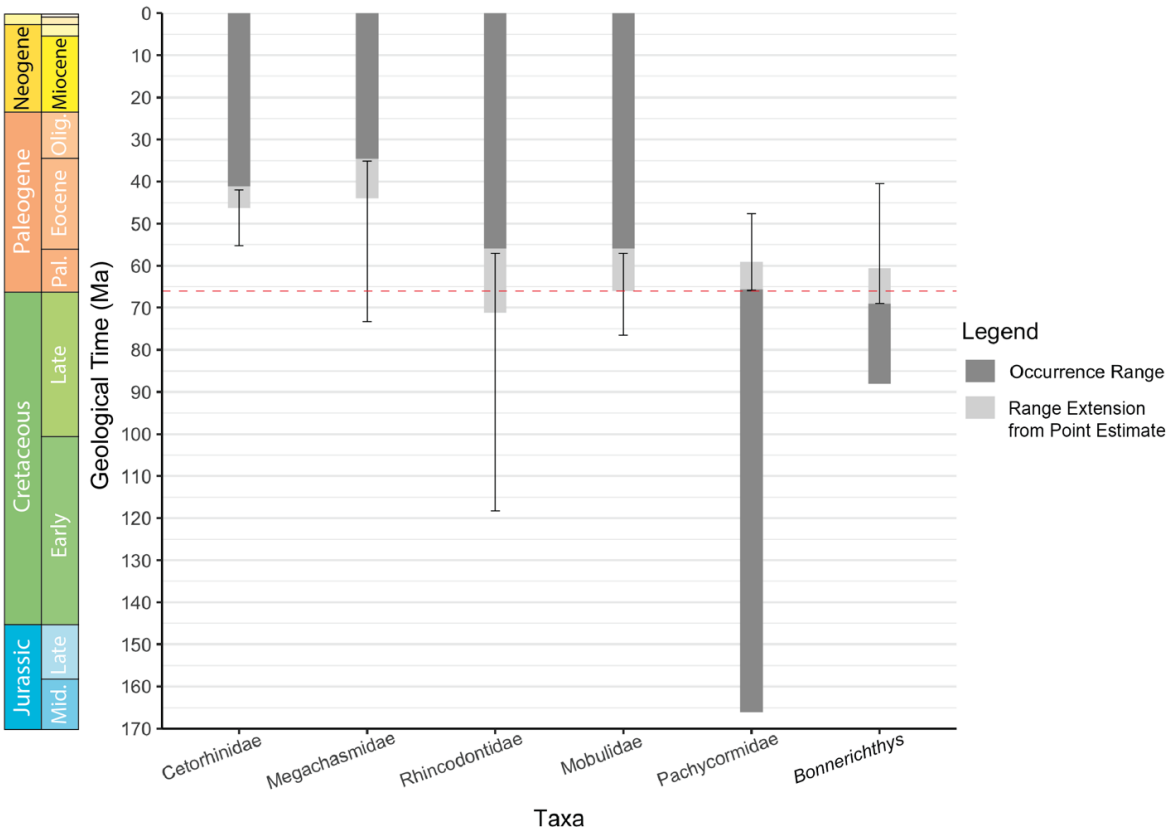

Figure 4.3 – The extension of the fossil record using the point estimate calculated in this study, with the two-tailed 95% credible intervals. The dark grey bars indicate the original fossil record for each lineage while the light grey bars mark the estimated extension on this range (the point estimate). Whiskers show the maximum and minimum two-tailed 95% credible intervals of around the point estimate, when considering the density of the fossil record and relative recovery function. The Cretaceous-Paleogene boundary is marked by a dashed red line.

Limiting this analysis to records of *Bonnerichthys* does make the point estimate of pachycormiform extinction younger, but only mildly, to 60.6 Ma (still within the Thanetian). The two-tailed CI range of 40.5–69 Ma (Bartonian–Maastrichtian; Fig. 4.3), and a one-tailed 95% CI of 50.8 (Ypresian; Fig. 4.4), means I cannot rule out an extinction at the end-Cretaceous. While the hypothesis of extinction at the K-Pg cannot be excluded, neither can survival into the Cenozoic.

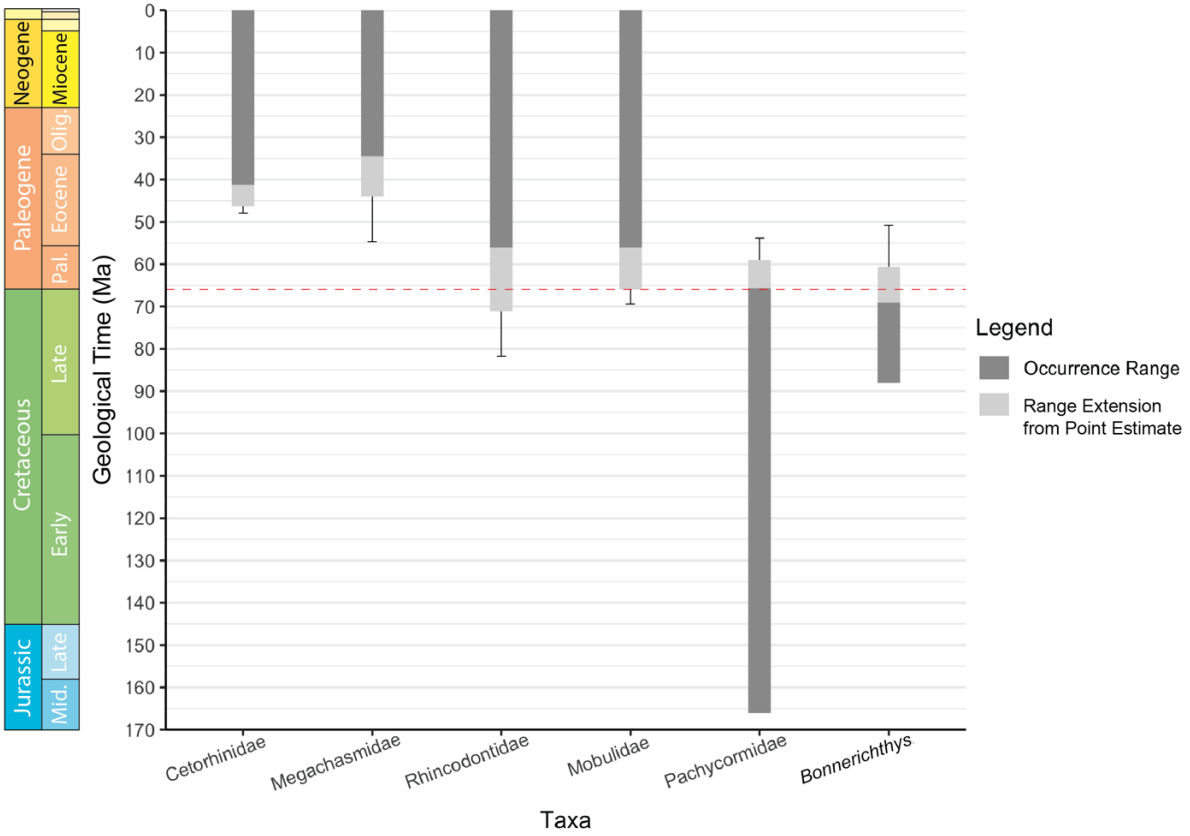

Figure 4.4 – The extension of the fossil record using the point estimate calculated in this study, with the one-tailed 95% credible interval. The dark grey bars indicate the original fossil record for each lineage while the light grey bars mark the estimated extension on this range (the point estimate). Whiskers show the maximum one-tailed 95% credible interval of the point estimate, when considering the density of the fossil record and relative recovery function. The Cretaceous-Paleogene boundary is marked by a dashed red line.

Emergence of suspension-feeding chondrichthyans

The oldest and youngest credible range for emergence of all the chondrichthyan groups fall between 35.1–118.3 Ma (Priabonian–Aptian; Table 1). The credible interval for the origin of rhincodontids is broad, between the Thanetian–Aptian (two-tailed 95% CI = 57.1–118.3 Ma; one-tailed 95% CI = 81.7 Ma; Table 1), with a point estimate of 71.1 Ma (Maastrichtian). The origin of mobulids spans between the Thanetian–Campanian (57.1–76.5 Ma; one-tailed 95% CI = 69.4 Ma; Table 1), closely bracketing the K-Pg boundary at 66 Ma (Fig. 4.3). The

point estimate of mobulids is approximately at the K-Pg boundary itself (Table 1; Figs. 4.3, 4.4). The credible intervals for the origin of cetorhinids and megachasmids are Lutetian–Ypresian (42–55.3 Ma; one-tailed 95% CI = 47.9 Ma; Table 1) and Priabonian–Campanian (35.1–73.1 Ma; one-tailed 95% CI = 54.7 Ma) respectively.

Discussion

Extinction of suspension-feeding pachycormiforms

My results cannot exclude the possibility that suspension-feeding pachycormiforms did survive into the early Cenozoic, with both the dataset containing all suspension-feeding pachycormiforms and the *Bonnerichthys* only dataset suggesting extinction anywhere within the Lutetian–Danian and Bartonian–Maastrichtian intervals respectively; Figs. 4.3, 4.4). However, these ranges are also consistent with the hypothesis that the group went extinct at the end of the Cretaceous.

Previous studies (e.g. Marshall 1995; Marshall & Ward 1996) have shown that mass extinction events can be identified using confidence interval methods for multiple lineages. This is based on identifying instances of the Signor-Lipps effect, where the incompleteness of the fossil record results in groups of taxa that disappeared simultaneously appearing to disappear more gradually (and vice versa; Signor & Lipps 1982). In the case of a cohort of extinction victims, 50% confidence intervals for individual lineages should fall in equal proportion above and below the extinction event (Marshall 1995; Marshall & Ward 1996). However, because *Bonnerichthys* and a single indeterminate pachycormiform are the only

examples of pachycormiforms from the end of the Cretaceous, these methods cannot be applied here.

Emergence of suspension-feeding chondrichthyans

These results support the hypothesis of a Cenozoic origin for cetorhinids. There is also support for megachasmids emerging in the Cenozoic, but the oldest of the megachasmid credible intervals stretches into the Mesozoic (73.4 Ma; Campanian), so a Mesozoic origin cannot be rejected for this lineage. Similarly, because the oldest CI of mobulid emergence is in the Campanian (76.5 Ma), I cannot reject a Cretaceous origin of mobulids. A Cretaceous origin is also estimated for rhincodontids, although these credible intervals are so broad that an early Paleogene origin cannot be ruled out (57.1–118.3 Ma; Fig. 4.3; 4.4).

Among the suspension-feeding chondrichthyan lineages, only cetorhinids can be confidently interpreted as emerging within the Cenozoic. All other groups have broad credible intervals that span wide intervals of the Late Cretaceous and Paleogene. Therefore, the hypothesis of this study — that there would be no overlap between the extinction of pachycormiforms and the emergence of suspension-feeding chondrichthyans — cannot be accepted at this time.

Comparisons to previous estimates

It is currently hypothesised that modern lineages of suspension-feeding chondrichthyans emerged following the K-Pg mass extinction (Cione & Reguero 1998; Friedman *et al.* 2010; Paig-Tran & Summers 2014). The results presented here cannot reject the possibility of a Mesozoic origin of suspension-feeding for all of the modern chondrichthyan groups other than

cetorhinids. However, my inferred times of origin for suspension feeding within these groups do generally fall after the divergence times given by molecular clock estimates for the total-groups. These should represent semi-independent estimates of the oldest bound on the timing of origin for suspension feeding in these groups (cetorhinids; megachasmids; mobulids; rhincodontids; Fig. 4.5).

Lamniformes.

Cetorhinidae. (Total-group divergence: 142–83 Ma; Heinicke *et al*. 2009; 121–81 Ma; Sorenson *et al*. 2014). Molecular clock analyses show total-group cetorhinids appearing to form part of the Cretaceous radiation of lamniforms (Fig. 4.5; Heinicke *et al*. 2009; Sorenson *et al*. 2014; fig. S2b). Cetorhinids are the most densely sampled taxon in this study, with my results suggesting that the suspension-feeding ecology emerged between the Ypresian and Lutetian (Figs. 4.3–4.5), approximately 60 Myr after cetorhinids diverged from other lamniforms (Fig. 4.5). This suggests a long evolutionary history of the cetorhinid total-group predating the origin of suspension-feeding. It is, of course, also possible that the delayed emergence of the suspension-feeding ecology is due to a lack of recognized cetorhinid fossils from earlier horizons. However, given the comprehensive fossil record of cetorhinids after the Lutetian, and the high scientific interest in deposits from around the K-Pg boundary, this seems unlikely.

Megachasmidae. (Total-group divergence: 139–73 Ma; Heinicke *et al*. 2009; 106–99 Ma; Sorenson *et al*. 2014). The poor fossil record and subsequently wide CIs of megachasmids places their emergence between the Priabonian and the Campanian. Molecular clock

estimates for the age of the megachasmid total-group fall within the Mesozoic. Heinicke *et al.* (2009) provide an estimate of 104 Ma (95% CI: 139–73 Ma), while Sorenson *et al.* (2014) infer megachasmid emergence at 99 Ma (99 Ma; Sorenson *et al.* 2014; fig. S2b), with narrower credible intervals than Heinike *et al.* (2009). However, while the older credible interval falls in the Albian (106 Ma; Fig. 4.5; Sorenson *et al.* 2014), the younger CI is obscured in the figure (Sorenson *et al.* 2014; fig. S2b), though it does not extend beyond ~90 Ma. Only the oldest CI and point estimate are shown in Figure 4.5. As with cetorhinids, this result implies a substantial history of the megachasmid total-group predating the origin of suspension-feeding. However, the slight overlap between the youngest credible interval of Heinicke *et al.* (2009; 73 Ma) and the oldest credible interval of my results (73.2 Ma; Fig. 4.5) means that a shorter interval between divergence of the total-group and emergence of this feeding mode cannot be ruled out.

Mobulidae. (Total-group divergence: 32.3–14.2 Ma; Aschliman *et al.* 2012; 34.88–25.33 Ma; Poortvliet *et al.* 2015; 40–26.2 Ma; Bertozzi *et al.* 2016. Crown-group divergence: 25.33–19.20 Ma; Poortvliet *et al.* 2015). Current molecular studies have largely focussed on the divergence of total-group mobulids from their sister group rhinopterids (Aschliman *et al.* 2012; Bertozzi *et al.* 2016). These studies report similar estimates, with mobulids and rhinopterids diverging in approximately the Oligocene–early Miocene. Aschliman *et al.* (2012) estimate that this divergence happened at approximately 22.6 Ma (32.3–14.2 Ma; Fig. 4.5; Aschliman *et al.* 2012; table 4). Bertozzi *et al.* (2016) estimated that mobulids diversified between 40–26.2 Ma, depending on whether both mitochondrial and nuclear or just nuclear data are used (Bertozzi *et al.* 2016; table 2). Poortvliet *et al.* (2015) found a similar estimates to Aschliman

et *al.* (2012) and Bertozzi *et al.* (2016), with the total-group emerging an Oligocene (30.12 Ma), and credible intervals extending back into the late Eocene (Priabonian; 34.88–25.33 Ma). Poortvliet *et al.* (2015) also provides an estimate of crown mobulid divergence at in the late Chattian (22.27 Ma), with credible intervals spanning from the mid-Chattian to the late Aquitanian (25.33–19.20; Poortvliet *et al.* 2015; fig. 4; node 3).

However, all of these estimates are much later than the first appearance of stem mobulids (*Burnhamia*; Adnet *et al.* 2012; Cappetta 2012; Enault *et al.* 2013; Underwood *et al.* 2015) in the fossil record, and are therefore not a true estimate of the emergence of the mobulid total-group. These estimates are also not a true reflection of the crown radiation of mobulids either, as they are only represented by a single node (as with the monotypic suspension-feeding chondrichthyan lineages), and so only provide an oldest bound for mobulid divergence. The only recent study to account for stem taxa (*Burnhamia*, *Eomanta*, *Eoplinthicus*, *Oromobula*, and *Plinthicus*) when estimating mobulid divergence has been Adnet *et al.* (2012), which places the emergence of suspension-feeding in mobulids around the Thanetian–Ypresian boundary (Adnet *et al.* 2012; fig. 9, node C). This estimate is a later origin than the point estimate given here (65.4 Ma; Table 1), because the occurrence records taken by Adnet *et al.* (2012) were taken directly from the fossil record rather than being used to empirically estimate divergence dates.

The lack of stem mobulids in molecular clock studies such as Aschliman *et al.* (2012) is acknowledged by Aschliman (2014: 976), who indicates that the divergence estimate of mobulids and rhinopterids is likely an underestimate due to poor modelling of branch lengths

in Aschliman *et al.* (2012). Aschliman (2014) goes on to acknowledge that the hypothesis of relationships and divergences proposed by Adnet *et al.* (2012) is the most likely because it best fits the fossil record and minimises the number of ghost lineages. I find my results to be in agreement with Adnet *et al.* (2012), who uses fossil record occurrences only, rather than a molecular clock analysis. I also consider that the temporal extended range suggested in my results does not seem implausible given the fossil record or the divergence of mobulids from myliobatids in these studies.

Rhincodontidae. (Total-group divergence: 162–106 Ma; Heinicke *et al.* 2009; 124–54 Ma; Sorenson *et al.* 2014). Similar to megachasmids, rhincodontids are poorly sampled from the fossil record, and so have wide CIs that span from the Thanetian to the Aptian (a range of 61.2 Ma; Figs. 4.3, 4.4). These overlap closely with the divergence estimate for total-group Rhincodontidae from other orectolobiforms at 88 Ma (95% CI: 124–54 Ma; Fig. 4.5; Sorenson *et al.* 2014).

They also overlap with the divergence estimates given by Heinicke *et al.* (2009), but these estimate the divergence of Hemiscyliidae from the Ginglymostomatidae+Stegosomatidae clade (Heinicke *et al.* 2009; node 38, fig. 2), to which Rhincodontidae is the sister lineage (Sorenson *et al.* 2014; fig. 1). Therefore, the date from Heinicke *et al.*'s (2009) should be older than the origin of the rhincodontid total-group, but it nevertheless provides a useful upper bound complementing that derived from Sorenson *et al.* (2014).

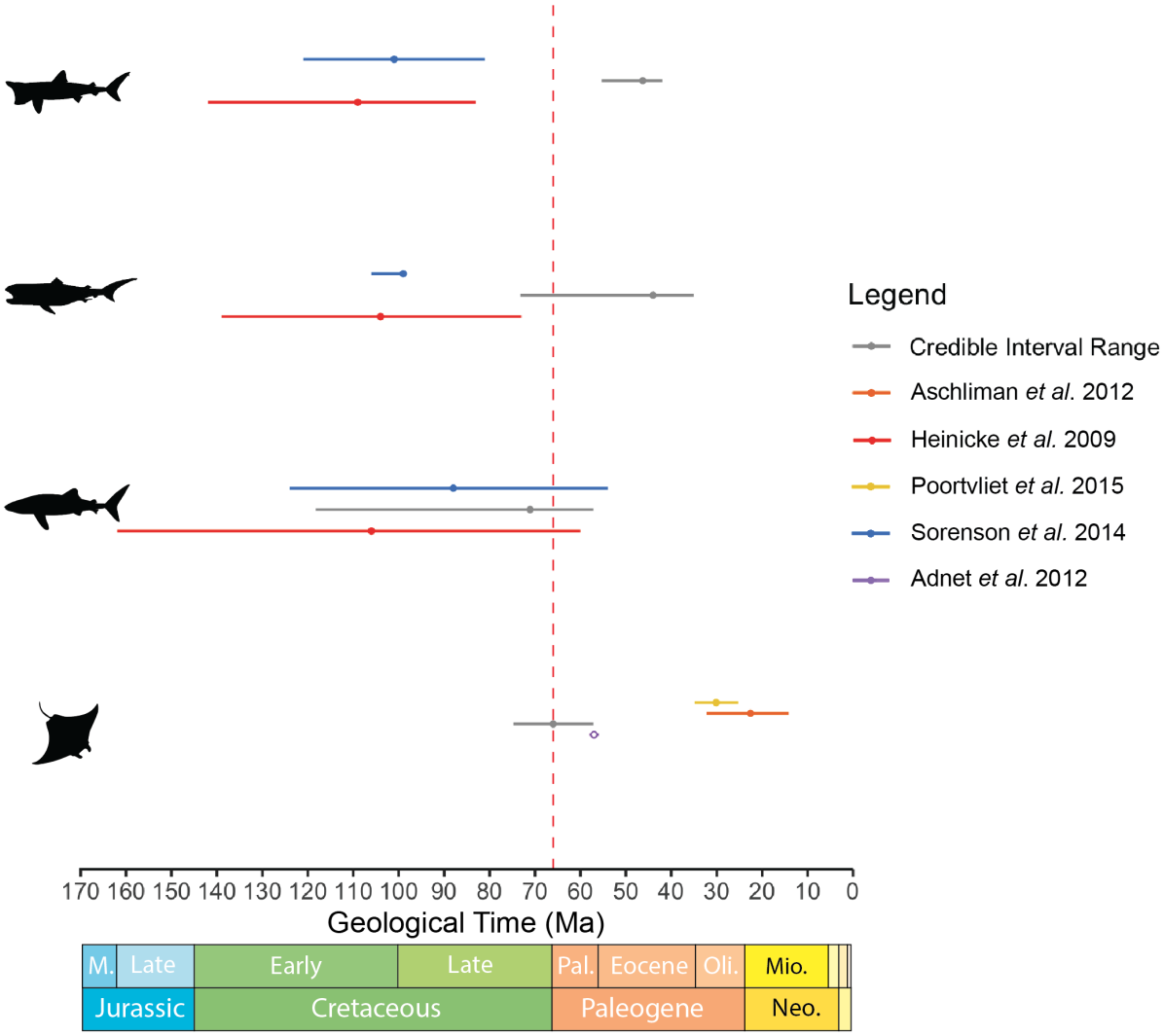

Figure 4.5 – The point estimate and 95% credible intervals of the emergence of the suspension-feeding ecology in modern chondrichthyan radiations compared to molecular clock estimates of total-group divergences. For the molecular clock estimates are represented by closed points (Cetorhinidae; Megachasmidae; Rhincodontidae; Mobulidae), and fossil record estimates are represented by open points (Adnet *et al.* 2012; Mobulidae only). For Mobulidae, the underestimates of mobulid divergence (Aschliman *et al.* 2012; Poortvliet *et al.* 2015) are shown to demonstrate the disparity between estimates of mobulid divergence from molecular clock analyses and estimates derived from the fossil record. The emergence of the suspension-feeding ecology for each lineage, as found in this study, is shown in grey. Taxa listed top to bottom: Cetorhinidae; Megachasmidae; Rhincodontidae; and Mobulidae.

However, the large overlap of these estimates with the emergence of the suspension-feeding ecology makes it unclear when suspension-feeding evolved in relation to the divergence of rhincodontids from other orectolobiforms. This may, in part, be due to the long, but sparse, fossil record of *R. typus* that limits the precision of these estimates (as shown by the wide credible intervals of this study; Fig. 4.5). Looking at the point estimates alone shows a much clearer sequence of events, with the Ginglymostomatidae+Stegosomatidae+Rhincodontidae clade diverging at 106 Ma (Fig. 4.5; Heinicke *et al.* 2009), total-group Rhincodontidae diverging at approximately 88 Ma (Fig. 4.5; Sorenson *et al.* 2014), and the suspension-feeding ecology emerging at approximately 71 Ma (Figs. 4.3–4.5). However, the overlap of credible intervals in this study and the molecular clock studies mean that I can only verify that my estimate fall within a credible range of total-group Rhincodontidae is estimated to have diverged based on molecular studies (Heinicke *et al.* 2009; Sorenson *et al.* 2014).

Placement of putative suspension-feeding taxa

As mentioned earlier, there are a number of putative suspension-feeders identified in the fossil record that have sometimes been placed as early members of lamniforms (Noubhani & Cappetta 1997; Duffin 1998; Cappetta 2006; Shimada 2007; Shimada *et al.* 2015) or mobulids (Case *et al.* 1990; Bronson & Maiseyv 2018). While this study has not included the fossil records of these taxa because of their uncertain placements, it is possible to consider the plausibility of their relationships with lamniforms and mobulids based on current total-group divergence estimates, the respective known fossil record of these putative suspension-feeders, and the morphological evidence to support their placement within these groups.

Lamniformes. It has been hypothesised that crown lamniforms radiated in the Cretaceous (162 Ma; 137–189 Ma 95% HPD; Sorenson *et al.* 2014), but the origin of the group is unclear. There are several taxa that could represent the lamniform stem, but their relationships to crown lamniforms are unresolved due to a poorly understood fossil record (Cappetta 1987, 2012; Maisey 2012): *Serratolamna* (Upper Cretaceous), *Cretodus* (Cretaceous), *Dwardius* (Cretaceous), *Eostriatolamia* (Cretaceous), *Palaeocarcharodon* (Paleocene), *Paranomotodon* (Upper Cretaceous), *Priscusurus* (Lower Cretaceous) and *Trigonotodus* (Eocene). The earliest occurring, and most widely accepted, putative stem lamniform is *Palaeocarcharias stromeri* which was described from the Kimmeridgian of Solnhofen, Germany (de Beaumont 1960; Duffin 1988; Maisey 2012), but recent studies have also placed it as a sister group to both Lamniformes and Carcharhiniformes (Landemaine *et al.* 2018). The most recent study identified that *Palaeocarcharias* shared tooth histology that is unique to lamniforms, thereby placing it as the earliest known lamniform (Jambura *et al.* 2019). If true, this would place the emergence of the lamniform total-group in the Middle Jurassic (at least 163.5 Ma; Jambura *et al.* 2019).

Pseudocetorhinus. Of the putative suspension-feeders discussed in this study, the earliest-emerging is *Pseudocetorhinus pickfordi*,, which is described from the Rhaetian of Devon (Duffin 1998). Despite being initially attributed to cetorhinids, this fossil predates the first fossil record emergence of cetorhinids (Lutian; Cione & Reguero 1998) by approximately 153–167 million years, and the molecular clock emergence of cetorhinids by 66–123 million years (Heinicke *et al.* 2009; Sorenson *et al.* 2014). This would also predate the earliest putative lamniform, *Palaeocarcharias*, by 44–56 million years, and shift the origin of

lamniforms to the Upper Triassic. In addition, the variation in tooth morphology between *Pseudocetorhnius* and other cetorhinids does not support its placement within Cetorhinidae (Andreev & Cuny 2012) and does not resemble the teeth of other chondrichthyan suspension-feeders, making it unlikely to be even an early example of suspension-feeding in chondrichthyans (Cappetta 2012; Shimada et al. 2015). Therefore, both its morphology and its placement in the fossil record make it unlikely to be a member of the lamniform stem (Fig. 4.6), and an unlikely example of other suspension-feeding chondrichthyan lineages.

Pseudomegachamsa. Originally attributed to *Megachasma*, *Pseudomegachasma comanchensis* is known from the mid-late Cenomanian (Shimada 2007; Shimada *et al.* 2015), which supported the hypothesis of a Mesozoic origin of megachasmids (Shimada 2007; Heinicke *et al.* 2009; Shimada & Ward 2016), but pre-dated the first undisputed fossil megachasmid by 70 million years (Shimada *et al.* 2014, 2015). In addition, its tooth morphology was considered strikingly similar to Miocene teeth attributed to megachasmids by Shimada (2007), which suggests that *P. comanchensis* was a suspension-feeder like the other megachasmids. However, later studies placed it in the Odontaspididae because of its much closer morphological similarity to *Johnlongia* – another suspension-feeding odonotaspidid – making its megachasmid-like tooth morphology, as well as the evolution of suspension-feeding, convergent from megachasmids. Similarly, the early Cenomanian putative suspension-feeder *Eorhincodon casei* was also attributed to *Pseudomegachasma* on account of its tooth morphology, which is unlike the tooth records of any other rhincodontids tooth records, but a close resemblance those of *Johnlongia* and *Pseudomegachasma comanchensis* (Shimada *et al.* 2015).

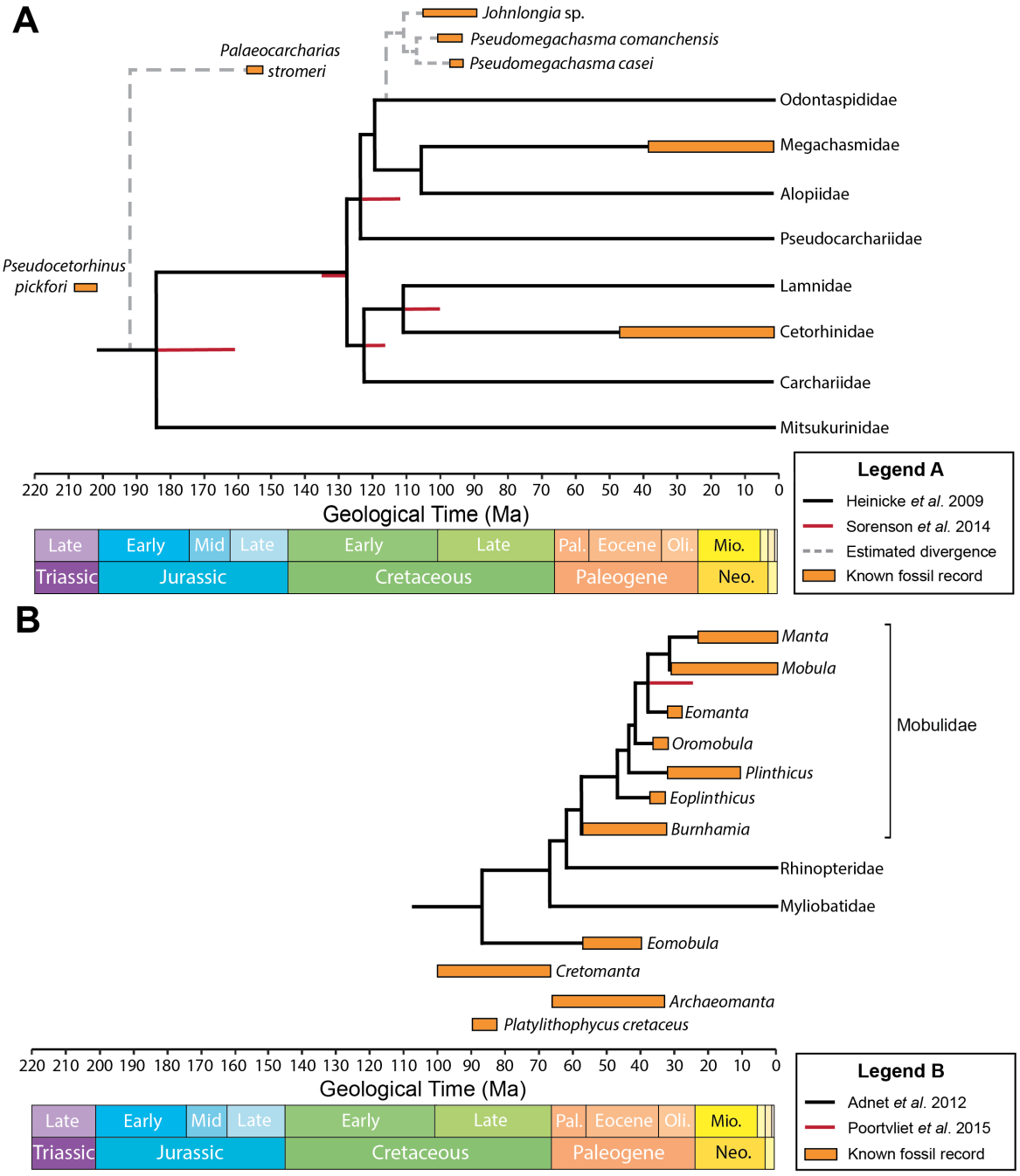

Figure 4.6 – The interrelationships of lamniform and mobulid suspension-feeders, and their divergence dates. A) The phylogeny and divergence estimates of the major families within lamniforms, based on the molecular clock estimates by Heinicke *et al.* (2009, fig. 2). Where phylogeny corroborates, the divergence estimates from Sorenson *et al.* (2014, fig. 1) are shown in red. Grey dashed lines show the divergences of other hypothesised suspension-feeders from the Cretaceous (*Pseudomegachasma* and *Johnlongia*; from Shimada *et al.* 2015, fig. 7), and the putative stem lamniform *Palaeocarcharias*, based on their known fossil record (shown in orange). B) The phylogeny and divergence dates of stem and crown mobulids (Adnet *et al.* 2012, fig. 9), with the molecular clock divergence estimate of crown mobulids shown in red (Poortvliet *et al.* 2015). The known fossil records of stem mobulids and putative suspension-feeding non-mobulids (*Archaeomanta*, *Cretomanta*, *Eomanta* and *Platylithophycus*) are shown in orange.

Given the evidence from morphological studies and the fossil record, it seems unlikely that these taxa are related to extant suspension-feeding lineages, but our poor understanding of early lamniform taxa and relationships limit the inferences that can be made about early lamniform evolution. Even if *Pseudocetorhinus* was an early suspension-feeder, the fossil records of both these taxa (*Pseudocetorhinus* and *Pseudomegachasma*) pre-date the fossil record of extant suspension-feeding families by between 70–167 million years, and *Pseudocetorhinus* even predates the earliest accepted stem lamniform by up to 56 million years, which supports their exclusion from Cetorhinidae and Megachasmidae (Andreev & Cuny 2012; Shimada *et al.* 2015; Shimada & Ward 2016). However, the fossil record of both *Pseudomegachasma* species fall within molecular estimates of the origin of megachasmids (Heinicke *et al.* 2009; Sorenson *et al.* 2014; Fig. 4.6), and the morphological similarity of its teeth to those of megachasmids is not inconsiderable (Shimada 2007; Shimada *et al.* 2015). Therefore, for now, I agree with the current evidence that supports convergent evolution of these putative suspension-feeders from cetorhinids and megachasmids based on their known fossil distribution, but an improvement of the known fossil record of early lamniforms, megachasmids and *Pseudomegachasma* may shed more light on their origin and evolution.

Mobulidae. Although there is some contention around the broader relationships of mobulids within myliobatiforms as sister-group to rhinopterids (Mobulinae) or as a sister-group to all other myliobatiforms (Mobulidae; Adnet *et al.* 2012; fig. 1A), the mobulid stem is well documented in the fossil record (Adnet *et al.* 2012; Cappetta 2012; Enault *et al.* 2013). The most widely accepted earliest mobulid is *Burnhamia*, which has been found in deposits as early as the Thanetian (Baut & Genault 1995). This would then place the origin of the

mobulid total-group in the early Paleocene, but it is not possible to confirm whether they emerged before or after the K-Pg boundary.

Platylithophycus cretaceus. This taxon has been identified and re-identified several times, with the most recent analysis suggesting it may be a mobulid gill raker from the Coniacian–Santonian of the Niobrara Formation (Bronson & Maisey 2018). If it is a mobulid raker, this would make *Platylithophycus* the earliest mobulid fossil by approximately 27–30 million years (Fig. 4.6). The authors also suggested that it may be a close relative to the other Cretaceous suspension-feeding ray, *Cretomanta*, but there is still approximately 11–14 million years between their fossil records. This, along with its currently accepted taxonomic ranking of Elasmobranchii incertae sedis (Bronson & Maisey 2018), makes it poorly supported candidate for a Cretaceous mobulid, and more evidence would be needed (particularly of any tooth remains; see Adnet *et al.* 2012) before it could be assigned to mobulids with any certainty.

Cretomanta. There is also a large gap between the first uncontested mobulid fossils and *Cretomanta* (Case *et al.* 1990; Underwood & Cumbaa 2010), which appears approximately 40 million years before the first mobulids (Fig. 4.6). Therefore, support for the inclusion of *Cretomanta* within mobulids is largely based on its peg-like tooth morphology (Adnet *et al.* 2012), which is considered one of the three major tooth morphologies of mobulids (Adnet *et al.* 2012). In 2013, a study into the histology of mobulid teeth identified that *Cretomanta* teeth have a tooth composition resembling selachimorphs, making its similar morphology convergent to mobulids (Enault *et al.* 2013). This would more strongly

support the hypothesis that *Cretomanta* is actually a suspension-feeding shark (Enault *et al.* 2013) lamniform (Noubhani & Cappetta 1997; Cappetta 2006), not a batoid or mobulid ray (Underwood & Cumbaa 2010), but its placement within sharks or lamniforms is unclear.

Other putative suspension-feeding rays. As with *Cretomanta*, the tooth composition of *Archaeomanta*, namely the presence of a well-developed pulp cavity, placed it outside the mobulid radiation (Underwood *et al.* 2011; Adnet *et al.* 2012; Enault *et al.* 2013). Although, its fossil record overlaps with *Burnhamia* (Adnet *et al.* 2012; Enault *et al.* 2013), making it a plausible candidate that could be part of the mobulid radiation, if only the morphological evidence supported it (Fig. 4.6). Like *Archaeomanta*, the fossil record of *Eomobula* would support its placement as a stem mobulid (Adnet *et al.* 2012; Enault *et al.* 2013), but its tooth morphology does not closely resemble any other mobulid taxa, so it is considered an intermediary taxon between mobulids and other myliobatids (Adnet *et al.* 2012; Enault *et al.* 2013).

Despite their similar morphologies and ecological roles, current evidence does not support the placement of these Cretaceous suspension-feeding chondrichthyans as part of modern suspension-feeding chondrichthyan lineages. Moreover, their fossil records suggest that these Cretaceous taxa represent suspension-feeding lineages that occupied the large bodied suspension-feeder ecology before the modern lineages emerged. Therefore, much like the giant suspension-feeding pachycormiforms, *Archaeomanta* and *Eomobula* (Adnet *et al.* 2012) these taxa are convergent to modern large bodied suspension-feeders, and unrelated.

Ecological drivers behind giant bodied suspension-feeder extinction and emergence

Previous studies hypothesized that suspension-feeding chondrichthyans emerged to fill the niches left vacant following the extinction of pachycormiforms during the K-Pg mass extinction (Friedman *et al.* 2010; Pimiento *et al.* 2019). My results cannot exclude a Cretaceous origin for suspension-feeding megachasmids, mobulids and rhincodontids, or an Eocene extinction for pachycormiforms (Fig. 4.3). However, I can reject a Cretaceous origin for suspension-feeding cetorhinids. This does not necessarily disprove the previous hypothesis as the proposed pattern of extinction and replacement is not excluded by the credible intervals of my results.

A major challenge to understanding the possible ecological drivers of extinction and origination within the large bodied suspension-feeder guild is the diversity of significant major environmental and evolutionary events falling within the credible intervals inferred for most groups, including the end Cretaceous mass extinction and the Paleocene–Eocene Thermal Maximum (PETM). The PETM (approximately 55–56 Ma; Zachos *et al.* 2008) falls within the credible intervals of emergence for suspension-feeding cetorhinids and megachasmids (Figs. 4.3, 4.4). This caused deep sea temperatures to increase by approximately 5°C–6°C, and surface temperatures to increase by up to 8°C. This resulted in widespread extinction of benthic foraminifera (Thomas 1998), a radiation of planktic foraminifera (Lu *et al.* 1998), and a marked rise in marine productivity (Bains *et al.* 2000), that rearranged foodweb structures throughout benthic and pelagic environments, potentially opening niches for taxa to exploit in new environments.

The youngest bound on pachycormiform extinction (47.6 Ma; Table 1; Figs. 4.3, 4.4) also includes this thermal maximum, though it seems unlikely that pachycormiforms would go extinct during a time of increased ocean productivity (55 Ma onwards; Zachos *et al.* 2008; Pimiento *et al.* 2019), because the most severe extinction occurred in benthic environments. It is, however, also possible that pachycormiforms did go extinct at the end of the Cretaceous, and their disappearance from the fossil record at the K-Pg boundary is a true extinction event. Oceanic-anoxic events around the K-Pg boundary (potentially as a result of the flood-basalt eruption of the Deccan Traps or asteroid impact; Rampino & Caldeira 2018) are associated with a presumed collapse in primary productivity contributing to planktonic turn over (Tajika *et al.* 2018; Pimiento *et al.* 2019) that caused, among others, the extinction of Cretaceous ammonites and belemnites. Tajika *et al.* (2018) suggested a close trophic link between pachycormiforms and these ammonites and belemnites due to their coinciding disappearance, but this impossible to verify as they are among many taxa to disappear from the fossil record during the K-Pg mass extinction event. Tajika *et al.* (2018; figs. 3, 4) also points out that the taxa that radiate following the extinction of ammonites and belemnites: juvenile Thecosomata (Gastropoda; Corse *et al.* 2013, Janssen & Goedert 2016) and Euphausiidae (zooplankton) would have been a similar size to juvenile ammonites, and therefore candidate prey items for pachycormiforms if they had survived into the Paleogene.

The definitive survival of smaller suspension-feeders from this time, such as clupeomorphs (Grande 1985), also indicates that prey choice alone is not the single contributing factor to suspension-feeding pachycormiform extinction. Large bodied taxa have been found to be more at risk of extinction during mass extinction events (e.g. McKinney 1997), particularly

those occupying a high trophic level — though this second criteria does not apply to suspension-feeding pachycormiforms, which consume a greater proportion of biomass individually than smaller analogues (Friedman 2009; Pimiento *et al.* 2019). Large bodied taxa are also associated with a longer life cycle and later age of maturity, which would hinder recovery during a mass extinction or times where food sources are scarce (Hutchings *et al.* 2012).

It therefore seems plausible that suspension-feeding pachycormiforms disappeared during the faunal turnover of the K-Pg, in which approximately 50% of genera, including nearly all genera of planktonic foraminifera, disappeared, leading to a substantial collapse in primary productivity (D'Hondt 2005; McCallum 2015; Tajika *et al.* 2018). This led to the restructuring of oceanic foodwebs in a way that disproportionately affected large bodied fishes (Friedman 2009). The loss of these planktonic foraminifera would have directly affected suspension-feeding pachycormiforms as their consumers. This would beg the question of how suspension-feeding chondrichthyans, such as megachasmids, mobulids and rhincodontids for which a Cretaceous origin are cannot be rejected (Figs. 4.3, 4.4) survived if pachycormiforms did not when a major food source disappeared.

However, while the credible intervals of the suspension-feeding chondrichthyans do extend into the Cretaceous, a Paleocene origin cannot be excluded. There are a number of chondrichthyan taxa in the Cretaceous hypothesized to be large bodied suspension-feeders: *Archaeomanta*, *Eomobula*, *Cretomanta*, *Platylithophycus*, and *Pseudomegachasma*. Perhaps significantly, these suspension-feeders are not known in Cenozoic deposits, and appear

unrelated to modern suspension-feeding chondrichthyan radiations, but their presence may indicate higher diversity of giant suspension-feeders before the faunal turnover of the K-Pg boundary. They are also much more poorly known from the fossil record than pachycormiforms, but this may be due to a lack of recognition of these fossils in known deposits, or because they are simply not being actively searched for.

If these taxa were giant bodied suspension-feeders as hypothesized, like the pachycormiforms, their large size and long life cycle could made them vulnerable to an extinction event such as the K-Pg mass extinction. Previous studies have shown that large body size is often selected against during extinction events (Ehrenfeld 1970; McKinney 1997; Friedman 2009) and is a major indicator of increased extinction risk in modern chondrichthyans (Dulvy *et al.* 2014). While I cannot elucidate the pattern of ecological replacement during this study, the presence of these Cretaceous giant suspension-feeders and their apparent replacement with modern lineages after a mass extinction event is compelling. How sudden or gradual this replacement was is unclear, and it is possible that some modern lineages emerged in the Cretaceous (as suggested in this study), but it is as of yet unclear how or why Cretaceous-emerging modern lineages would have survived if other suspension-feeding lineages disappeared.

Conclusions

The results of this study cannot reject an origin of suspension-feeding in emerged as early as the Cretaceous for megachasmids, mobulids and rhincodontids, but suggests an Eocene emergence for cetorhinids. These credible intervals share overlap substantially with those for

the extinction of suspension-feeding pachycormiforms (Figs. 4.3, 4.4). While this does not reject the replacement hypothesis previously suggested by Friedman *et al.* (2010), it also fails to deliver strong support for it. However, the presence of putative suspension-feeding chondrichthyans in the Cretaceous that are not part of the modern radiations suggests that there was a faunal turnover of suspension-feeders at or just before the K-Pg boundary, potentially linked to the planktonic turnover of the K-Pg mass extinction. Further study could focus on the putative Cretaceous suspension-feeders identified in this study, using the methods applied here, to estimate the credible time range for extinction (as found with pachycormiforms here), and build a clearer picture of how these taxa were replaced by the modern suspension-feeders. However, fossil records of these putative suspension-feeders are scant, and so analysis into their emergence and extinction would require recognition of further fossils (the minimum occurrence records for the Strauss and Sadler 1989 method is three). Until then, while these results do not confirm or reject the replacement hypothesis suggested by Friedman *et al.* (2010), patterns of faunal turnover, risk of extinction for giant bodied pachycormiforms, loss of oceanic productivity at the end of the Cretaceous, and an increase in productivity at the PETM make the replacement hypothesis a compelling explanation for the observed patterns in the fossil record and this study.

Chapter 5

Conclusions and future study

In this thesis, I provide new data that improves our understanding of pachycormiforms, one of the earliest diverging groups on the teleost stem, and which are also sometimes considered one of the most mysterious and incomprehensible (Liston 2006, 2010, 2015). My first and second research chapters provide new and reinterpreted morphological data by describing three-dimensionally preserved, articulated fossils of both suspension-feeding and predatory pachycormiforms. These descriptions informed a phylogenetic analysis to estimate pachycormiform interrelationships and divergence times using maximum parsimony and Bayesian analyses, the latter of which included molecular and stratigraphic data. This has allowed me to consider pachycormiforms in the broader context of teleost evolution. As well as estimating the timing of pachycormiform emergence, I used the fossil record of suspension-feeding pachycormiforms to place constraints on their time of extinction, and whether their disappearance coincided with the emergence of modern giant suspension-feeders. My thesis has therefore provided new avenues to explore concerning pachycormiform relationships and their placement on the teleost stem, and also how their extinction might have broader implications for the emergence of modern diversity.

The morphology of *Martillichthys renwickae* and *Pachycormus macropterus* and implications for pachycormiforms

Although both *Martillichthys renwickae* (Chapter 2) and *Pachycormus macropterus* (Chapter 3) have been described previously (Woodward 1897; Rayner 1948; Lehman 1949; Wenz 1967; Patterson 1975; Mainwaring 1978; Liston 2006, 2008*a*; Cawley *et al.* 2018), my observations provided new interpretations and identified previously undescribed structures. This built on previous work by using μCT scanning to view both internal and external structures in their anatomical context and re-examine previous descriptions given their relative topology. In *Martillichthys* (Chapter 2), I identified a putative median vomer, which has never been described in pachycormiforms, and is considered to be a synapomorphy uniting teleosts above *Ichthyokentema* (Patterson 1977*a*; fig. 19; De Pinna 1996). However, a median vomer is also identified in the aspidorhynchid *Vinctifer* (Brito 1992), indicating that a median vomer may be more widely distributed within the teleost total-group, calling into question its reliability as a feature uniting more crownward members of the teleost stem. Although the vomer described in *Martillichthys* would potentially be the earliest reported median vomer within teleost stem phylogeny, paired vomers are described in *Pachycormus* (Chapter 3), and Arratia (1999) points out that a median vomer is also present in *Lepidotes*, *Tetragonolepis*, *Dapedium*, and *Hulettia*, so the feature seems highly homoplastic. I also redescribed aspects of the gill skeleton and hyoid arch, highlighting morphological variation among the giant bodied suspension-feeding pachycormiforms. I compared the newly described gill raker morphologies of *Martillichthys* with the *Asthenocormus* and *Leedsichthys*, which show two patterns of morphology: club-like rakers bearing needle-like teeth (*Asthenocormus* and *Martillichthys*; Lambers 1992), and long, slender rakers bearing fimbriations (*Leedsichthys*;

Liston 2013). Additionally, I highlight the difference in skull geometries between these taxa, *Bonnerichthys* and *Rhinconichthys*, and their sister taxon, *Ohmdenia* (Friedman 2012*a*). This led me — like Liston and Maltese (2016) — to suggest the possibility of a second origin of suspension-feeding in the 'protosphyraenid' clade of pachycormiforms, which I investigated — and rejected — using a stepping stone analysis (Chapter 3).

In *Pachycormus* (Chapter 3), I identified a number of previously undescribed structures, and compared my findings with the most comprehensive — but unpublished — description of *Pachycormus* (i.e. Mainwaring 1978), along with Patterson's (1975) description of the braincase and the external descriptions of other Strawberry Bank specimens (Woodward 1897; Cawley *et al.* 2018). While many of my observations corroborate these previous descriptions, I have reinterpreted aspects of the palate and mandible by confirming the absence of a quadratojugal (contra Mainwaring 1978) and newly describing large fang-like teeth on the anteriormost coronoid toothplates. Most notably, I redescribe aspects of the pectoral girdle, including the scapulocoracoid, and identify six radials (not five, Jessen 1972; or four, Mainwaring 1978). The last of these radials (radial VI) bifurcates distally, resembling the metapterygium found in non-teleost actinopterygians (Coates 1994; Hilton 2011). I also describe a "C"-shaped second radial, "paddle-shaped" third and fourth radials, and an "hourglass shaped" fifth radial in *Pachycormus*, that have previously only been described in *Protosphyraena*, *Bonnerichthys* and *Orthocormus* (Friedman *et al.* 2010), suggesting that this radial morphology is more widely distributed among pachycormiforms than previously thought. Finally, I identify a median structure that lies beneath the basibranchial of the gill basket, which I consider to be a urohyal. This structure had been described before by

Mainwaring (1978: 42–43) but she interpreted it as a median toothplate. If this is a urohyal, it would — like the median vomer of *Martillichthys* — be the earliest (phylogenetically; the pholidophorid urohyal is from temporally older fossils) example of this teleost character on the teleost stem, and support the placement of pachycormiforms within the teleost total-group.

The descriptions provided in this thesis have shown how much is still to be observed and described in even the best known pachycormiforms, through characters either being previously misinterpreted (e.g. the urohyal in *Pachycormus* and the gill rakers in *Martillichthys*) or previously unobserved (e.g. the median vomer in *Martillichthys* and coronoid fangs in *Pachycormus*). My description of *Martillichthys* supports its placement as a pachycormiform, and provides new areas of pachycormiform (particularly in edentulous taxa) morphology to be explored. Such morphology includes the broad, spatulate anterior corpus of the parasphenoid, the median posterior projection of the parietals, and a gap between the frontals, all of which may be more widely distributed among pachycormiforms than currently thought. The presence of skull geometry variation among giant bodied suspension-feeders also indicates variation in feeding mechanisms that could help us understand how these taxa interacted with their environment and their ecological role, particularly when interpreting the remains of less understood taxa such as *Leedsichthys* and *Bonnerichthys*.

Similarly, my description of *Pachycormus* has identified previously unobserved large teeth on the coronoid toothplates that seem to be homologues of the procumbent fangs seen in the

'protosphyraenid' clade, which adds another morphological between the very disparate ecologies of the two major pachycormiform clades: the reduction and loss of these large anterior teeth in the suspension-feeding clade, and the exaggeration of them in the 'protosphyraenid' clade. As with *Martillichthys*, there are also some characters in *Pachycormus* that support the placement of pachycormiforms at the base of the teleost stem. My descriptions have identified a number of teleostean characters (such as the urohyal), along with characters in considered to be present in teleosts, such as the anterodorsal projection of the suboperculum (a holostean character) and a metapterygium-like radial (a non-teleost actinopterygian character; Grande 2010). The discovery of these characters in taxa on the teleost stem demonstrates acquisition and loss of the synapomorphies that unite major actinopterygian clades, and suggest that some of these characters may have originated earlier (e.g. the urohyal) or disappeared later (e.g. the metapterygium and subopercular anterodorsal projection) than previously thought.

Pachycormiform interrelationships and divergence estimates, and their broader placement on the teleost stem

The rest of Chapter 3 builds on the descriptions of *Martillichthys renwickae* and *Pachycormus* provided in Chapters 2 and 3, by incorporating these observations into a pre-existing morphological character matrix (adapted from Friedman 2012*a*). Previous analyses into pachycormiforms and stem teleosts have either focussed purely on pachycormiform interrelationships (Friedman 2012*a*; Wretman *et al.* 2016) or have only included *Pachycormus* in the context of broader analyses of neopterygian relationships (e.g. Gardiner *et al.* 1996; Arratia 1999, 2001, 2004; Hurley *et al.* 2007; Lopéz-Arbarello & Sferco 2018).

The aim of my phylogenetic analyses was to test previous hypotheses of pachycormiform relationships (Friedman 2012*a*; Wretman *et al.* 2016) in the light of new observations and interpretations, while also including molecular and stratigraphic data. My maximum parsimony and Bayesian analyses corroborate previous hypotheses of relationships (Friedman 2012*a*; Wretman *et al.* 2016), but the inclusion of stratigraphic data during the Fossilized Birth-Death model analysis provides an alternative — though less resolved — pattern of relationships. However, while the interrelationships of taxa are changed through the inclusion of stratigraphic data, all my analyses resolve pachycormiforms on the teleost stem, corroborating previous hypotheses of their placement (Patterson 1973, 1977*a*, 1994; Arratia 2004; Friedman *et al.* 2010; Friedman 2012*a*). In addition, my new descriptions of a mix teleostean and non-teleostean characters in pachycormiforms such as the teleostean urohyal and the metapterygium-like radial (as described in chapters 2 and 3), support the placement of pachycormiforms as early diverging teleosts.

This leaves a few areas of further study to improve the disconnect between the interrelationships recovered between analyses including and excluding stratigraphic data. To consider the placement of pachycormiforms more broadly within neopterygians and the teleost stem, this dataset would benefit from being embedded in a matrix that includes more neopterygian (particularly both crown and stem teleost) taxa, with characters that more broadly assess synapomorphies and character states associated with neopterygians. Placing these observations and characters in a larger, more comprehensive dataset (e.g. López-Arbarello & Sferco 2018; Latimer & Giles 2019) would allow for the consideration of characters that focus more specifically on neopterygian and teleost relationships without

risking distorting resolution within the pachycormiform clade. This would also allow for a more comprehensive analysis of pachycormiform taxa based on the descriptions provided here, where characters such as a median vomer, metapterygium and urohyal can be robustly tested for homology among other taxa. Finally, the inclusion of additional taxa to establish node-age minima could help to establish robustly supported divergence dates for major groups within teleosts and holosteans, including the timing of total-group teleost and pachycormiform divergences.

As with Chapter 2, the observations and description provided for *Pachycormus* can now be used to help inform subsequent phylogenetic analyses into pachycormiforms. In particular, *Euthynotus*, as sister taxon to all other pachycormiforms, is a good candidate for further study particularly with respect to establishing anatomical patterns at the very base of the pachycormiform tree. The 'protosphyraenid' clade also warrant further study, perhaps via μCT scanning to resolve the status of *Hypsocormus* and the polytomy of *Orthocormus*, as well as providing an opportunity to compare the 'protosphyraenid' and 'suspension-feeding' pachycormiform clades. Improving the proportion of coded characters in pre-existing datasets, and the observable morphology available for analysis of *Pachycormus* will also be invaluable when it is used as a single representative in broader analyses. Additionally, the presence of putative teleostean characters such as a urohyal could help improve support for the placement of pachycormiforms along the teleost stem either as the single sister-group to all other teleosts (Patterson 1977*a*; fig. 19) or as a clade with aspidorhynchids (Arratia 2017; López-Arbarello & Sferco 2018). It is hoped that new descriptions and phylogenetic analyses will encourage other researchers to re-examine and reinterpret other pachycormiform and

stem teleost specimens using this description for comparison, which could then also be included in future studies into teleost relationships.

Patterns of extinction and emergence of giant bodied suspension-feeders around the K-Pg boundary

The final research chapter of my thesis (Chapter 4) aimed to bring my study of pachycormiforms full circle by investigating the potential timing and implications of their extinction at the end of the Cretaceous. By the Late Cretaceous, only a handful of the family remain: *Bonnerichthys*, *Protosphyraena*, and *Rhinconichthys*, although there is also one Pachycormidae indet. specimen described from the latest Maastrichtian of Antarctica (Cione *et al.* 2018). By the Cretaceous–Paleogene (K-Pg) boundary, only the giant bodied suspension-feeder *Bonnerichthys* and Pachycormidae indet. are reported in the fossil record (Friedman *et al.* 2013; Cione *et al.* 2018). Friedman *et al.* (2010) hypothesized that the extinction of these giant bodied suspension-feeding pachycormiforms paved the way for their ecological replacements — the modern lineages of giant suspension-feeding chondrichthyans — to emerge. I tested this hypothesis by empirically estimating a credible interval during which suspension-feeding pachycormiforms may have existed after they disappeared from the fossil record, and during which modern suspension-feeding chondrichthyans may have emerged before they appear in the fossil record (Strauss & Sadler 1984; Marshall 1997).

Although my results did not give a clear pattern of pachycormiform extinction followed by chondrichthyan emergence (as hypothesized), they did show that these ecologies may have appeared in modern lineages much earlier than the fossil record suggests. Rhincodontids,

mobulids, and megachasmids all had credible interval ranges extending back into the Cretaceous, despite the earliest modern suspension-feeding chondrichthyan fossils occurring in the Thanetian (late Paleocene). Similarly, pachycormiforms may have survived the end Cretaceous mass extinction and lived up to the earliest Lutetian. If these patterns of emergence and extinction are correct, this would raise the question of how the Cretaceous-emerging suspension-feeding chondrichthyans survived if pachycormiforms did not.

However, the Cretaceous yields a number of putative suspension-feeding chondrichthyans that are not known beyond the K-Pg boundary and are not part of the modern radiations, such as *Cretomanta*, *Archeomanta*, *Pseudomegachasma* and *Platylithophycus*. This suggests that there may have been lineages of giant bodied suspension-feeding chondrichthyans within the Cretaceous that are separate from the modern groups. Given that neither pachycormiforms nor these putative suspension-feeders are known beyond the K-Pg boundary, I consider it plausible that giant suspension-feeders were part of the faunal turnover associated with the end of the Cretaceous. This would be consistent with the significant risk mass extinction events pose to large bodied taxa (Friedman 2009), and the collapse of planktonic foraminifera (D'Hondt 2005; Tajika *et al.* 2018) that would have severely depleted food resources during the K-Pg event.

This hypothesis could be tested more robustly with the identification of more specimens of Cretaceous suspension-feeders, and by applying the methods applied in this chapter to the record of the Cretaceous suspension-feeders, it may be possible to build a clearer picture of the faunal turnover at the K-Pg boundary. This would help to elucidate how successful these

groups were throughout the Cretaceous, what the possible drivers were behind their extinction, and when they might have gone extinct. By determining the temporal ranges for these groups, how they related to the suspension-feeding pachycormiforms, and whether they predated the emergence of modern suspension-feeding chondrichthyan lineages, the hypothesis of faunal turnover proposed in this thesis and by Friedman *et al.* (2010) can be explored further.

However, the fossil record of these putative, Cretaceous, suspension-feeding chondrichthyans is even more sparse than the pachycormiform suspension-feeders, and the methods employed in Chapter 4 require a minimum of three occurrence records per focal group (Strauss & Sadler 1989) to calculate the credible intervals for emergence or extinction. Even if three occurrences are recorded for these groups, such a poor fossil record would provide extremely broad confidence intervals (see the results for rhincodontids; Figs. 4.3, 4.4) and would probably tell us very little about patterns of extinction in the Cretaceous. Therefore, this project — while interesting — would need sufficient work to identify these Cretaceous taxa either from poorly sampled deposits or museum collections (that have been misidentified).

Similarly, my study would also benefit from the inclusion of more occurrence records of the modern suspension-feeding chondrichthyans. The groups lacking occurrence data in particular are the rhincodontids and megachasmids, which possess small teeth (up to 3 mm high for rhincodontids and 5 mm high for megachasmids; Yabumoto *et al.* 1997; Cappetta 2012), making their teeth difficult to find. However, more occurrence records for

rhincodontids and megachasmids may help to narrow the large credible intervals seen in my results and potentially rule out the possibility for a Cretaceous emergence.

References

ABEL, R. L., LAURINI, C. R. and RICHTER, M. 2012. A palaeobiologist's guide to 'virtual' micro-CT preparation. *Palaeontologia Electronica*, **15**, 1–17.

ADNET, S., CAPPETTA, H., GUINOT, G. and DI SCIARA, G. N. 2012. Evolutionary history of the devil rays (Chondrichthyes: Myliobatiformes) from fossil and morphological inference. *Zoological Journal of the Linnaean Society*, **166**, 132–159.

AGASSIZ, L. 1832. Untersuchungen über die fossilen Fische der Lias-Formation. *Jahrbuch für Mineralogie, Geognosie, Geologie und Petrefaktenkunde*, **3**, 139–149.

AGASSIZ, L. 1833–1843. *Recherches sur les Poissons Fossils*, Tome II. Petitpierre, Neuchatêl, Switzerland, 1420 pp.

ANDREEV, P. S. and CUNY, G. 2012. New Triassic stem selachimorphs (Chondrichthyes, Elasmobranchii) and their bearing on the evolution of dental enameloid in Neoselachii. *Journal of Vertebrate Paleontology*, **32**, 255–266.

ARAMBOURG, C. 1935*a*. Contribution à l'étude des poisons du Lias supérieur. Annales de Paléontologie, **24**, 1–32.

ARAMBOURG, C. 1935*b*. Observations sur quelques poisons fossiles de l'ordre des Halécostomes et sur l'origins des Clupéidés. *Comptes-Rendus des séances de l'Académie des Sciences, Paris*, **200**, 2110–2112.

ARGYRIOU, T., GILES, S., FRIEDMAN, M., ROMANO, C., KOGAN, I. and SÁNCHEZ-VILLAGRA, M. R. 2018. Internal cranial anatomy of Early Triassic species of †*Saurichthys* (Actinopterygii: †Saurichthyiformes): implications for the phylogenetic

placement of †saurichthyiforms. *BMC Evolutionary Biology*, **18**, 161.

ARRATIA, G. 1997. Basal teleosts and teleostean phylogeny. *Palaeo Ichthyologica*, **7**, 5-168.

ARRATIA, G. 1999. The monophyly of Teleostei and stem group teleosts. 265–334. *In* ARRATIA, G. and SCHULTZE, H. P. (eds.). *Mesozoic Fishes 2— Systematics and Fossil Record*. Verlag Dr Freidrich Pfeil, Münich, Germany, 604 pp.

ARRATIA, G. 2001. The sister-group of Teleostei: consensus and disagreements. *Journal of Vertebrate Paleontology*, **21**, 767–773.

ARRATIA, G. 2004. Mesozoic halecostomes and the early radiation of teleosts. 279–315. *In* ARRATIA, G. and TINTORI, A. (eds.). *Mesozoic Fishes 3 — Systematics, Paleoenvironments and Biodiversity*. Verlag Dr Friedrich Pfeil, Münich, Germany, 649 pp.

ARRATIA, G. 2013. Morphology, taxonomy, and phylogeny of Triassic pholidophorid fishes (Actinopterygii, Teleostei). *Journal of Vertebrate Paleontology*, **33**, 1–138.

ARRATIA, G. 2015. Complexities of early Teleostei and the evolution of particular morphological structures through time. *Copeia*, **103**, 999–1025.

ARRATIA, G. 2017. New Triassic teleosts (Actinopterygii, Teleosteomorpha) from northern Italy and their phylogenetic relationships among the most basal teleosts. *Journal of Vertebrate Paleontology*, **37**, e1312690.

ARRATIA, G. and LAMBERS, P. 1996. The caudal skeleton of pachycormiforms. Parallel evolution? 191–218. *In* ARRATIA, G. and VIOHL, G. (eds). *Mesozoic Fishes 1 — Systematics and Paleoecology*. Verlag Dr Friedrich Pfeil, Münich, Germany, 576 pp.

ARRATIA, G. and SCHULTZE, H. P. 1990. The urohyal: development and homology within osteichthyans. *Journal of Morphology*, **203**, 247–282.

ARRATIA, G. and SCHULTZE, H. P. 2013. Outstanding features of a new Late Jurassic

pachycormiform fish from the Kimmeridgian of Brunn, Germany and comments on current understanding of pachycormiforms. 87–120. *In* ARRATIA, G., SCHULTZE, H. P. and WILSON, M. V. H. (eds.). *Mesozoic Fishes 5 — Global Diversity and Evolution*. Verlag Dr Friedrich Pfeil, Münich, Germany, 560 pp.

ASCHLIMAN, N. C., NISHIDA, M., MIYA, M., INOUE, J. G., ROSANA, K. M. and NAYLOR, G. J. 2012. Body plan convergence in the evolution of skates and rays (Chondrichthyes: Batoidea). *Molecular Phylogenetics and Evolution*, **63**, 28–42.

AX, P. 1984. *Das Phylogenetische System*. Gustav Fischer, Stuttgart, Germany, 349 pp.

AX, P. 1985. Stem species and the stem lineage concept. *Cladistics*, **1**, 279–287.

AX, P. 1987. *The Phylogenetic System: The Systemization of Organisms on the Basis of their Phylogenesis*. Wiley, Chichester, UK, 340 pp.

BACIU, D. S., GRĂDIANU, I., SESERMAN, A. and DUMITRIU, T. C. 2016. Oligocene fish fauna and sedimentological particularities of the Bituminous Marls of the Vrancea Nappe, Eastern Carpathians, Romania. *Analele Stiintifice de Universitatii AI Cuza din Iasi. Sect. 2, Geologie*, **62**, 29–46.

BAINS, S., NORRIS, R. D., CORFIELD, R. M. and FAUL, K. L. 2000. Termination of global warmth at the Palaeocene/Eocene boundary through productivity feedback. *Nature*, **407**, 171–174.

BAMBACH, R. K. 1999. Energetics in the global marine fauna: a connection between terrestrial diversification and change in the marine biosphere. *Geobios*, **32**, 131–44.

BANCROFT, E. N. 1829. On the fish known in Jamaica as the Sea-devil. 444–457. *In* VIGORS, N. A. (ed.). *The Zoological Journal: Volume 4*. W. Phillips Publishing, London, UK, 626 pp.

BARNES, L. G. 2008. Miocene and Pliocene Albireonidae (Cetacea, Odontoceti), rare and unusual fossil dolphins from the eastern North Pacific Ocean. *In* WANG, X. and BARNES, L. G. (eds.). Geology and Vertebrate Paleontology of Western and Southern North America, Contributions in Honor of David P. Whistler. *Natural History Museum of Los Angeles County, Science*, **41**, 99–152.

BARTHEL, K. W., SWINBURNE, N. H. M. and MORRIS, S. C. 1990. *Solnhofen: A Study in Mesozoic Palaeontology.* Cambridge University Press, Cambridge, 236 pp.

BARTHELT, D., FEJFAR, O., PFEIL, F. H. and UNGER, E. 1991. Notizen zu einem Profil der Selachier-Fundstelle Walbertsweiler im Bereich der miozanen Oberen Meeresmolasse Suddeutschlands. *Munchner Geowissenschaftliche Abhandlungen*, **19**, 195–208.

BARTRAM, A. W. H. 1977. The Macrosemiidae, a Mesozoic family of holostean fishes. *Bulletin of the British Museum (Natural History): Geology*, **29**, 137–234.

BAUT, J. P. and GENAULT, B. 1995. Contributiona l'étude des Elasmobranches du Thanetien (Paleocene) du Bassin de Paris. *Belgian Geological Survey Professional Paper*, **278**, 185–259.

BEAUMONT, G. de. 1960. Contribution à l'étude des genres *Orthacodus* Woodw. et *Notidanus* Cuv. (Selachii). *Schweizerischen Paläontologischen Abhandlungen*, **77**, 1–46.

BELLWOOD, D. R. and HOEY, A. 2004. Feeding in Mesozoic fishes: a functional perspective. 639–649. *In* ARRATIA, G. and TINTORI, A. (eds). *Mesozoic Fishes 3 — Systematics, Paleoenvironments and Biodiversity.* Verlag Dr Friedrich Pfeil, Münich, Germany, 649 pp.

BENTON, M. J. 2015. *Vertebrate Palaeontology.* 4th edn. Wiley-Blackwell, Chichester, UK, 506 pp.

BENTON, M. J., WILLS, M. A. and HITCHIN, R. 2000. Quality of the fossil record through time. *Nature*, **403**, 534–537.

BERG, L. S. 1937. A classification of fish-like vertebrates. *Bulletin de l'Académie des Sciences de l'URSS*, **4**, 1277–1280.

BERG, L. S. 1940. Classification of fishes, both Recent and fossil. *Travaux de l'Institut Zoologique de l'Academie des Sciences de l'URSS*, **5**, 87–517.

BERNIER, P., GAILLARD, C., GALL, J. C., BARALE, G., BOURSEAU, J. P., BUFFETAUT, E., and WENZ, S. 1991. Morphogenetic impact of microbial mats on surface structures of Kimmeridgian micritic limestones (Cerin, France). *Sedimentology*, **38**, 127-136.

BERMÚDEZ-ROCHAS, D. D. and POYATO-ARIZA, F. J. 2015. A new semionotiform actinopterygian fish from the Mesozoic of Spain and its phylogenetic implications. *Journal of Systematic Palaeontology*, **13**, 265–285.

BERTIN, L. and ARAMBOURG, C. 1958. Superordre des Téléostéens (Teleostei). 2204–2500. *In* GRASSÉ. P. (ed.). Traité de Zoologie: Anatomie, Systématique, Biologie Tome XIII: Agnathes et Poissons, Fascicules I–III. Masson et Cie, Paris. 2768 pp.

BERTOZZI, T., LEE, M. S. and DONNELLAN, S. C. 2016. Stingray diversification across the end-Cretaceous extinctions. *Memoirs of Museum Victoria*, **74**, 379–390.

BETANCUR-R, R., BROUGHTON, R. E., WILEY, E. O., CARPENTER, K., LÓPEZ, J. A., LI , C., HOLCROFT, N. I., ARCILA, D., SANCIANGCO, M., CURETON, J. C. II, ZHANG, F., BUSER, T., CAMPBELL, M. A., BALLESTEROS, J. A., ROA-VARON, A., WILLIS, S., BORDEN, W. C., ROWLEY, T., RENEAU, P. C., HOUGH, D. J., LU, G., GRANDE, T., ARRATIA, G. and ORTÍ , G. 2013. The tree of life and a new

classification of bony fishes. *PLoS Currents Tree of Life*, published online 18 April 2013. doi:10.1371/currents.tol.53ba26640df0ccaee75bb16 5c8c26288.

BIENKOWSKA-WASILUK, M. and RADWANSKI, A. 2009. A new occurrence of sharks in the Menilite Formation (Lower Oligocene) from the Outer (Flysch) Carpathians of Poland. *Acta Geologica Polonica*, **59**, 235–243.

BLAINVILLE, H. D. de. 1818. *Poissons fossiles; in Nouveau Dictionnaire d'Histoire Naturelle*. Delerville, Paris, 324 pp.

BOESSENECKER, R. W. 2013. A new marine vertebrate assemblage from the Late Neogene Purisima Formation in Central California, Part II: Pinnipeds and cetaceans. *Geodiversitas*, **35**, 815–940.

BOLLIGER, T., KINDLIMANN, R. and WEGMULLER, U. 1995. Die marinen Sedimente (jüngere OMM, St. Galler-Formation) am Südwestrand der Hörnlischüttung (Ostschweiz) und die palökologische Interpretation ihres Fossilinhaltes. *Eclogae Geologicae Helvetiae*, **88**, 885–909.

BOR, T. J. 1990. A new species of mobulid ray (Elasmobranchii, Mobulidae) from the Oligocene of Belgium. *Mededelingen van de Werkgroep voor Tertiaire en Kwartaire Geologie*, **27**, 93–97.

BOURDON, J. 1999. A fossil manta from the Early Pliocene (Zanclean) of North America. *Tertiary Research*, **19**, 79–84

BOWN, P. R. 2005. Calcareous nannoplankton evolution: a tale of two oceans. *Micropaleontology*, **51**, 299–308.

BRIGNON, A. 2017. Le saumon pétrifié de Beaune: histoire de la découverte de l'holotype de *Pachycormus macropterus* (Blainville, 1818). *Geodiversitas*, **39**, 691–704.

BRISSWALTER, G. 2008. Inventaire des Élasmobranches (requins, raies, chimères) des dépôts molassiques du Sud-Luberon (Miocène supérieur). *Courrier Scientifique du Parc naturel Régional du Luberon et de la Réserve de Biosphère Luberon-Lure*, 1–100.

BRITO, P. M. 1992. L'endocrâne et le moulage endocranien de *Vinctifer comptoni* (Actinopterygii, Aspidorhynchiformes) de Cretacé inférieur du Brésil. *Annales de Paléontologie*, **78**, 129–157.

BRITO, P. M. 1997. Révision des Aspidorhynchidae (Pisces, Actinopterygii) du Mésozoïque: ostéologie, relations phylogénétiques, données environnementales et biogéographiques. *Geodiversitas*, **19**, 681–772.

BRONSON, A. W. and MAISEY, J. G. 2018. Resolving the identity of *Platylithophycus*, an enigmatic fossil from the Niobrara Chalk (Upper Cretaceous, Coniacian–Campanian). *Journal of Paleontology*, **92**, 743–750.

BROUGHTON, R. E., BETANCUR-R, R., LI , C., ARRATIA, G. and ORTÍ , G. 2013. Multi-locus phylogenetic analysis reveals the pattern and tempo of bony fish evolution. *PLoS Currents Tree of Life*, **5**, published online 16 April 2013. doi:10.1371/currents.tol.2ca8041495ffafd0c92756e75247483e

BRUSATTE, S. L., O'CONNOR, J. K., and JARVIS, E. D. 2015. The origin and diversification of birds. *Current Biology*, **25**, R888–R898.

BRZOBOHATY, R. and SCHULTZ, O. 1978. Die Fischfauna des Badeniens. 441–465 *In* PAPP, A., CICHA I., SENES, J. and STEININGER, F. (eds.). *Chronostratigraphie und Neostratotypen, Miozän der Zentralen Paratethys, M4 Badenien (Moravien, Wielicien, Kosovien),* Slowakische Akademie der Wissenschaften, Bratislava, 594 pp.

BÜRGIN, T. 2000. *Euthynotus* cf. *incognitus* (Actinopterygii, Pachycormidae) als Mageninhalt eines Fischsauriers aus dem Posidonienschiefer Süddeutschlands (Unterer Juras, Lias epsilon). *Eclogae Geologicae Helvetiae*, **93**, 491–496.

BUSH, A. M. and BAMBACH, R. K. 2011. Paleoecologic megatrends in marine metazoa. *Annual Review of Earth and Planetary Sciences*, **39**, 241–269.

CAPOBIANCO, A. and FRIEDMAN, M. 2019. Vicariance and dispersal in southern hemisphere freshwater fish clades: a palaeontological perspective. *Biological Reviews*, **94**, 662–699.

CAPPETTA, H. 1970, Les sélaciens du Miocene de la region de Montpellier. *Palaeovertebrata, Memoire Extraordinaire*. **1970**, 1–139.

CAPPETTA, H. 1976. Sélaciens nouveaux du London Clay de l'Essex (Yprésien du Bassin de Londres). *Geobios*, **9**, 551–575.

CAPPETTA, H. 1985. Sur un nouvelle espece de *Burnhamia* (Batomorphii, Mobulidae) dans l'Ypresian des Ouled Abdoun, Maroc. *Tertiary Research*, **7**, 27–33.

CAPPETTA, H. 1987. *Handbook of Paleoichthyology. Volume 3B, Chondrichthyes II, Mesozoic and Cenozoic Elasmobranchii*. Gustav Fischer Verlag, Stuttgart, Germany and New York, USA, 193 pp.

CAPPETTA, H. 2006. Elasmobranchii post-Triadici (index specierum et generum). *Fossilium Catalogus, I. Animalia Pars*, **142**, 1–472.

CAPPETTA, H. 2012. *Handbook of Palaeoichthyology, Volume 3E, Chondrichthyes, Mesozoic and Cenozoic Elasmobranchii: Teeth*. Verlag Dr. Friedrich Pfeil, Münich, Germany, 512 pp.

CAPPETTA, H. and STRINGER, G. L. 2002. A new batoid genus (Neoselachii:

Myliobatiformes) from the Yazoo Clay (Upper Eocene) of Louisiana, U.S.A. *Tertiary Research*, **21**, 51–56.

CAPPETTA, H. and TRAVERSE, M. 1988. Une riche faune de Sélaciens dans le bassin à phosphatede Kpogamé-Hahotoé (Éocène moyen du Togo): Note préliminaire et précisions sur la structure et l'âge du gisement. *Geobios*, **21**, 359–365.

CAPPETTA, H., PFEIL, F. and SCHMIDT-KITTLER, N. 2000. New biostratigraphical data on the marine Upper Cretaceous and Palaeogene of Jordan. *Newsletters on Stratigraphy*, **38**, 81–95.

CASE, G. R. 1980. A selachian fauna from the Trent Formation, Lower Miocene (Aquitanian) of Eastern North Carolina, *Palaeontographica Abteilung A*, **171**, 52–79.

CASE, G. R., TOKARYK, T. T. and BAIRD, D. 1990. Selachians from the Niobrara Formation of the Upper Cretaceous (Coniacian) of Carrot River, Saskatchewan, Canada. *Canadian Journal of Earth Sciences*, **27**, 1084–1094.

CASIER, E. 1946 La faune ichthyologique de l'Ypresian de la Belgique. *Mémoires du Musée Royal d'Histoire Naturelle de Belgique*, **104**, 1–267.

CASIER, E. 1966. *Faune ichthyologique du London Clay. Appendice: Otolithes des poisons du London Clay par Frederick Charles Stinton*, British Museum (Natural History), London, 496 pp.

CAVIN, L. and SUTEETHORN, V. 2006. A new semionotiform (Actinopterygii, Neopterygii) from Upper Jurassic-Lower Cretaceous deposits of north-east Thailand, with comments on the relationships of semionotiforms. *Palaeontology*, **49**, 339-353.

CAWLEY, J. J., KRIWET, J., KLUG, S. and BENTON, M. J. 2018. The stem group teleost *Pachycormus* (Pachycormiformes: Pachycormidae) from the Upper Lias (Lower Jurassic)

of Strawberry Bank, UK. *Paläontologische Zeitschrift*, 1–18.

CHATTERJEE, S. 2015. *The Rise of Birds: 225 Million Years of Evolution*. 2nd edn. JHU Press, Baltimore, Maryland, 392 pp.

CHEER, A. Y., OGAMI, Y. and SANDERSON, S. L. 2001. Computational fluid dynamics in the oral cavity of ram suspension-feeding fishes. *Journal of Theoretical Biology*, **210**, 463–474.

CICIMURRI, D. J. and KNIGHT, J. L. 2009. Late Oligocene sharks and rays from the Chandler Bridge Formation, Dorchester County, South Carolina, USA. *Acta Palaeontologica Polonica*, **54**, 627–648.

CIONE, A. L. and REGUERO, M. A. 1998. A middle Eocene basking shark (Lamniformes, Cetorhinidae) from Antarctica. *Antarctic Science*, **10**, 83–88.

CIONE, A. L., SANTILLANA, S., GOUIRIC-CAVALLI, S., HOSPITALECHE, C. A., GELFO, J. N., LÓPEZ, G. M. and REGUERO, M. 2018. Before and after the K/Pg extinction in West Antarctica: New marine fish records from Marambio (Seymour) Island. *Cretaceous Research*, **85**, 250–265.

CLODE, D. 2015. *Prehistoric Marine Life in Australia's Inland Sea*. Museum Victoria, Melbourne, 84 pp.

CLOSE, R. A., FRIEDMAN, M., LLOYD, G. T. and BENSON, R. B. 2015. Evidence for a mid-Jurassic adaptive radiation in mammals. *Current Biology*, **25**, 2137-2142.

COATES, M. 1994. The origin of vertebrate limbs. *Development (Suppl.)*, 169–180.

COATES, M. I. 1999. Endocranial preservation of a Carboniferous actinopterygian from Lancashire, UK, and the interrelationships of primitive actinopterygians. *Philosophical Transactions of the Royal Society of London B: Biological Sciences*, **354**, 435–462.

COHEN, K. M., FINNEY, S. C., GIBBARD, P. L. and FAN, J.-X. 2013. The ICS International Chronostratigraphic Chart. *Episodes*, **36**, 199–204.

COMPAGNO, L. J. V. 1990. Relationships of the megamouth shark, *Megachasma pelagios* (Lamniformes: Megachasmidae), with comments on its feeding habits. 357–379. *In* PRATT Jr., H. L. GRUBER, S. H. and TANIUCHI, T. (eds). *Elasmobranchs as living resources: advances in the biology, ecology, systematics, and the status of the fisheries. NOAA Technical Report NMFS 90*, Seattle, Washington, 518 pp.

COPE, E. D. 1869. Descriptions of some extinct fishes previously unknown. *Proceedings of the Boston Society of Natural History*, **12**, 310–317.

COPE, E. D. 1887. Zittel's Manual of Palaeontology. *American Naturalist*, **17**, 1014–1019.

CORSE, E., RAMPAL, J., CUOC, C., PECH, N., PEREZ, Y. and GILLES, A. 2013. Phylogenetic analysis of Thecosomata Blainville, 1824 (holoplanktonic Opisthobranchia) using morphological and molecular data. *PLOS One*, **8**, e59439.

CROFT, W. N. 1950. A parallel grinding instrument for the investigation of fossils by serial sections. *Journal of Paleontology*, **24**, 693–698.

D'ARGENVILLE, A. J. D. 1742. *Histoire Naturelle Éclaircie dans Deux de ses Parties Principals: L'oryctologie*. De Bure, Paris, 650 pp.

D'HONDT, S. 2005. Consequences of the Cretaceous/Paleogene mass extinction for marine ecosystems. *Annual Review Ecology, Evolution, and Systematics*, **36**, 295–317.

DE BEER, G, R. 1937. *The Development of the Vertebrate Skull*. Oxford University Press, London, UK, 552 pp.

DE PEITRI, V., BERGER, J.-P., PIRKENSEER, C., SCHERLER, L. and MAYR, G. 2010. New skeleton from the early Oligocene of Germany indicates a stem-group position of diomedeoidid birds. *Acta Palaeontologica Polonica*, **55**, 23–34.

DE PINNA, M. 1996. Teleostean monophyly. 147–162. *In* STIASSNY, M. L. J., PARENTI, L. R. and JOHNSON, G. D. (eds.). *Interrelationships of Fishes*. Academic Press, San Diego. 496 pp.

DE SAINT-SEINE, P. 1949. Les poissons des calcaires lithographiques de Cerin (Ain). *Publications du Musée des Confluences*, **2**, 3–79.

DE SAINT-SEINE, P. 1956. L'evolution des actinoptérygiens. *Colloques Internationaux du Centre National de la Recherche Scientifique*, **163**, 27–33.

DE SCHUTTER, P. 2009. The presence of *Megachasma* (Chondrichthyes: Lamniformes) in the Neogene of Belgium, first occurrence in Europe. *Geologica Belgica*, **12**, 179–203.

DELSATE, D. 1999. Haasichthys michelsi, nov. gen., nov. sp., un nouveau Pachycormiforme (Osteichthyes, Actinopterygii) du Toarcien inférieur (Jurassique) luxembourgeois. *Travaux Scientifiques du Musée National d'Histoire Naturelle de Luxembourg*, **32**, 87–140.

DELSATE, D., DUFFIN, C. J. and WEIS, R. 1999. *Les collections paléontologiques du Musée national d'histoire naturelle de Luxembourg: Fossiles du Trias et du Jurassique*. Musée National d'Histoire Naturelle de Luxembourg, Luxembourg. 249 pp.

DEMÉRÉ, T. A. and BERTA, A. 2008. Skull anatomy of the Oligocene toothed mysticete *Aetioceus weltoni* (Mammalia; Cetacea): implications for mysticete evolution and functional anatomy. *Zoological Journal of the Linnaean Society*, **154**, 308–352.

DEMÉRÉ, T. A., BERTA, A. and MCGOWEN, M. R. 2005. The taxonomic and evolutionary history of fossil and modern balaenopteroid mysticetes. *Journal of*

Mammalian Evolution, **12**, 99–143.

DEMÉRÉ, T. A., MCGOWEN, M. R., BERTA, A. and GATESY, J. 2008. Morphological and molecular evidence for a stepwise evolutionary transition from teeth to baleen in mysticete whales. *Systematic Biology*, **57**, 15–37.

DOBSON, C. 2016. The ecological and phylogenetic significance of gill arch and gill raker morphology from micro-computed tomography (μCT) scanning. Unpublished Masters thesis, University College London, London, 31 pp.

DOBSON, C., GILES, S., JOHANSON, Z., LISTON, J. and FRIEDMAN, M. 2019. Cranial osteology of *Martillichthys renwickae* [Neopterygii; Pachycormiformes], and implications for suspension-feeding pachycormids, *Papers in Palaeontology.*

DOLLO, L. 1893. Nouvelle note sur les poissons de la Craie phosphatée. *Bulletin de la Société belge de Géologie, de Paléontologie et d'Hydrologie*, **7**, 180–189.

DOMNING, D.P. 1978. Sirenian evolution in the North Pacific Ocean. *University of California Publications in Geological Sciences*, **18**, 1–176.

DUFFIN, C. J. 1988. The Upper Jurassic selachian *Palaeocarcharias* de Beaumont (1960). *Zoological Journal of the Linnean Society*, **94**, 271–286.

DUFFIN, C. J. 1998. New shark remains from the British Rhaetian (latest Triassic). 1. The earliest basking shark. *Neues Jahrbuch für Geologie und Paläontologie, Monatshefte*, **3**, 157–181.

DUTHEIL, D. B. 1991. A checklist of Neoselachii (Pisces, Chondrichthyes) from the Palaeogene of the Paris Basin, France. *Tertiary Research*, **13**, 27–36.

DULVY, N. K., FOWLER, S. L., MUSICK, J. A., CAVANAGH, R. D., KYNE, P. M., HARRISON, L. R., CARLSON, J. K., DAVIDSON, L. N. K., FORDHAM, S. V.,

FRANCIS, M. P., POLLOCK, C. M., SIMPFENDORFER, C. A., BURGESS, G. H., CARPENTER, K. E., COMPAGNO, L. J. V., EBERT, D. A., GIBSON, C., HEUPEL, M. R., LIVINGSTONE, S. R., SANCIANGO, J. C., STEVENS, J. D., VALENTI, S. and WHITE, W. T. 2014. Extinction risk and conservation of the world's sharks and rays. *eLife*, **3**, e00590.

EHRENFELD, D. W. 1970. *Biological Conservation*. Holt, Rinehart & Winston, New York, 421 pp.

ENAULT, S., CAPPETTA, H. and ADNET, S. 2013. Simplification of the enameloid microstructure of large stingrays (Chondrichthyes: Myliobatiformes): a functional approach. *Zoological Journal of the Linnean Society*, **169**, 144–155.

FAIRCLOTH, B. C., SORENSEN, L., SANTINI, F. and ALFARO, M. E. 2013. A phylogenomic perspective on the radiation of ray-finned fishes based upon targeted sequencing of ultraconserved elements (UCEs). *PLoS One*, **8**, e65923.

FAUJAS DE SAINT-FOND, B. 1803. *Essai de Géologie, ou Mémoires pour servir à l'histoire naturelle du globe, tome 1*. C. F. Patris, Paris, 533 pp.

FELIX, J. 1890. Beiträge zur Kenntniss der Gattung *Protosphyraena* Leidy. *Deutsche Geologische Gesellschaft, Berlin Zeitschrift*, **42**, 278–302.

FERRÓN, H. G., HOLGADO, B., LISTON, J. J., MARTINEZ-PEREZ, C. and BOTELLA, H. 2018. Assessing metabolic constraints on the maximum body size of actinopterygians: locomotion energetics of *Leedsichthys problematicus* (Actinopterygii, Pachycormiformes). *Palaeontology*, **61**, 775–783.

FINNEGAN, S., MCCLAIN, C. M., KOSNIK, M. A. and PAYNE, J. L. 2011. Escargots through time: an energetic comparison of marine gastropod assemblages before and after

the Mesozoic Marine Revolution. *Paleobiology*, **37**, 252–269.

FITCH, J. E. 1970. Fish remains, mostly otoliths and teeth, from the Palos Verdes Sand (late Pleistocene) of California. *Natural History Museum of Los Angeles County, Contributions in Science*, **199**, 1–14.

FOREY, P. L. 2016. Smith Woodward's ideas on fish classification. 115–127. *In* JOHANSON, Z., BARRETT, P. M., RICHTER, M. and SMITH, M. (eds.). *Arthur Smith Woodward: His Life and Influence on Modern Vertebrate Palaeontology*. Geological Society, London, Special Publications, **430**, 362 pp.

FOREY, P. L. and LONGBOTTOM, A. 2010. Bony fishes. 261–269. *In* YOUNG, J. R., GALE, A. S., KNIGHT, R. I. and SMITH, A. B. (eds). *Fossils of the Gault Clay*. Palaeontological Association, Field Guides to Fossils, **12**, 342 pp.

FREDERICKSON, J. A., COHEN, J. E. and BERRY, J. L. 2016. Ontogeny and life history of a large lamniform shark from the Early Cretaceous of North America. *Cretaceous Research*, **59**, 272–277.

FREEDMAN, J. A. and NOAKES, D. L. 2002. Why are there no really big bony fishes? A point-of-view on maximum body size in teleosts and elasmobranchs. *Reviews in Fish Biology and Fisheries*, **12**, 403–416.

FRIEDMAN, M. 2009. Ecomorphological selectivity among marine teleost fishes during the end-Cretaceous extinction. *Proceedings of the National Academy of Sciences*, **106**, 5218–5223.

FRIEDMAN, M. 2012*a*. Parallel evolutionary trajectories underlie the origin of giant suspension-feeding whales and bony fishes. *Proceedings of the Royal Society of London B: Biological Sciences*, **279**, 944–951.

FRIEDMAN, M. 2012*b*. Ray-finned fishes (Osteichthyes, Actinopterygii) from the type Maastrichtian, the Netherlands and Belgium. *Scripta Geologica Special Issue*, **8**, 113–142.

FRIEDMAN, M. 2015. The early evolution of ray-finned fishes. *Palaeontology*, **58**, 213-228.

FRIEDMAN, M. and SALLAN, L. C. 2012. Five hundred million years of extinction and recovery: a Phanerozoic survey of large-scale diversity patterns in fishes. *Palaeontology*, **55**, 707–742.

FRIEDMAN, M., SHIMADA, K., EVERHART, M. J., IRWIN, K. J., GRANDSTAFF, B. S. and STEWART, J. D. 2013*a*. Geographic and stratigraphic distribution of the Late Cretaceous suspension-feeding bony fish *Bonnerichthys gladius* (Teleostei, Pachycormiformes). *Journal of Vertebrate Paleontology*, **33**, 35–47.

FRIEDMAN, M., KECK, B. P., DORNBURG, A., EYTAN, R. I., MARTIN, C. H., HULSEY, C. D., WAINWRIGHT, P. C. and NEAR, T. J. 2013*b*. Molecular and fossil evidence place the origin of cichlid fishes long after Gondwanan rifting. *Proceedings of the Royal Society B: Biological Sciences*, **280**, 20131733.

FRIEDMAN, M., SHIMADA, K., MARTIN, L. D., EVERHART, M. J., LISTON, J., MALTESE, A. and TRIEBOLD, M. 2010. 100-million-year dynasty of giant planktivorous bony fishes in the Mesozoic seas. *Science*, **327**, 990–993.

FRIEDMAN, M., GILES, S. and COATES, M. 2019. Exceptional preservation in a Pennsylvanian ray-finned fish and the limits of neuroanatomical inference from actinopterygian cranial endocasts. *Journal of Morphology*, **280**, S123.

FROHLICHER, H. and WEILER, W. 1952. Die Fischfauna der unterstampischen Molasse des Entlebuchs, Kt. Luzern, und ihre paläogeographische Bedeutung. *Eclogae Geologicae Helvetiae*, **45**, 1–35.

FULGOSI, F. C., CASATI, S., ORLANDINI, A. and PERSICO, D. 2009. A small fossil fish fauna, rich in Chlamydoselachus teeth, from the Late Pliocene of Tuscany (Siena, central Italy). *Cainozoic Research*, **6**, 3–23.

GARDINER, B. G. 1960. A revision of certain actinopterygian and coelacanth fishes, chiefly from the Lower Lias. *Bulletin of the British Museum (Natural History), Geology*, **4**, 239–384.

GARDINER, B. G. 1963. Certain palaeoniscoid fishes and the evolution of the snout in actinopterygians. *Bulletin of the British Museum (Natural History), Geology*, **8**, 255–325.

GARDINER, B. G. 1967. The significance of the preoperculum in actinopterygian evolution. *Zoological Journal of the Linnean Society*, **47**, 197-209.

GARDINER, B. G. 1984. The relationships of the palaeoniscid fishes, a review based on new specimens of *Mimia* and *Moythomasia* from the Upper Devonian of Western Australia. *Bulletin of the British Museum (Natural History), Geology*, **37**, 173–428.

GARDINER, B. G. and SCHAEFFER, B. 1989. Interrelationships of lower actinopterygian fishes. *Zoological Journal of the Linnaean Society*, **97**, 135–187.

GARDINER, B. G., LITTLEWOOD, D. T. J., MAISEY, J. G. 1996. Interrelationships of basal neopterygians. 117–149. *In* STIASSNY, M. L. J., PARENTI, L. R. and JOHNSON, G. D. (eds.). *Interrelationships of Fishes*. Academic Press, San Diego. 496 pp.

GARDINER, B. G., MAISEY, J. G. and LITTLEWOOD, D. T. J. 1996. Interrelationships of basal neopterygians. 117–146. *In* STIASSNY, M. L. J., PARENTI, L. R. and JOHNSON, G. D. (eds.). *Interrelationships of Fishes*, Academic Press, San Diego, California, 496 pp.

GARDINER, B. G., SCHAEFFER, B. and MASSERIE, J. A. 2005. A review of the lower

actinopterygian phylogeny. *Zoological Journal of the Linnaean Society*, **144**, 511–525.

GEISLER, J. H., BOESSENECKER, R. W., BROWN, M. and BEATTY, B. L. 2017. The origin of filter feeding in whales. *Current Biology*, **27**, 2036–2042.

GILES, S. and FRIEDMAN, M. 2014. Virtual reconstruction of endocast anatomy in early ray-finned fishes (Osteichthyes, Actinopterygii). *Journal of Paleontology*, **88**, 636–651.

GILES, S., DARRAS, L., CLÉMENT, G., BLIECK, A. and FRIEDMAN, M. 2015. An exceptionally preserved Late Devonian actinopterygian provides a new model for primitive cranial anatomy in ray-finned fishes. *Proceedings of the Royal Society B: Biological Sciences*, **282**, 20151485.

GILES, S., ROGERS, M. and FRIEDMAN, M. 2016. Bony labyrinth morphology in early neopterygian fishes (Actinopterygii: Neopterygii). *Journal of Morphology*, **279**, 426–440.

GILES, S., XU, G. H., NEAR, T. J. and FRIEDMAN, M. 2017. Early members of 'living fossil' lineage imply later origin of modern ray-finned fishes. *Nature*, **549**, 265–268.

GILL, E. L. 1923. The Permian fishes of the genus *Acentrophorus*. *Proceedings of the Zoological Society*, **93**, 19–40.

GILLE, D., GILLE, A. and FITCHER, J. 2010. Verbreitung und Zusammensetzung der Elasmobranchierfauna im Kasseler Meeressand (Ober-Oligozän, Chattium, Kassel-Formation) Nordhessen, insbesondere im Ahnetal bei Kassel (GK 25, Bl. 4622 Kassel West). *Geologisches Jahrbuch Hessen*, **136**: 5–33.

GOLDBOGEN, J. A., PYENSON, N. D. and SHADWICK, R. E. 2007. Big gulps require high drag for fin whale lunge feeding. *Marine Ecology Progress Series*, **349**, 289–301.

GOLOBOFF, P. A., MATTONI, C. I. and QUINTEROS, A. S. 2006. Continuous characters analyzed as such. *Cladistics*, **22**, 589–601.

GONZÁLEZ-BARBA, G. and THEIS, D. 2000 Asociaciones faunisticas de condrictos en el Cenzoico de la Peninsula de Baja California, Mexico, *Profil*, **18**, 1–4.

GONZÁLEZ-RODRÍGUEZ, K. A., ESPINOZA-ARRUBARRENA, L. and GONZÁLEZ-BARBA, G. 2013. An overview of the Mexican fish fossil record. 9–34. *In* ARRATIA, G., SCHULTZE, H. P. and WILSON, M. V. H. (eds). *Mesozoic Fishes 5 — Global Diversity and Evolution*. Verlag Dr Friedrich Pfeil, Münich, Germany, 560 pp.

GOTTFRIED, M. D. 1995. Miocene basking sharks (Lamniformes: Cetorhinidae) from the Chesapeake Group of Maryland and Virginia. *Journal of Vertebrate Paleontology*, **15**, 443–447.

GOUIRIC-CAVALLI, S. 2013. Sistemática y relaciones biogeográficas de los peces del Titoniano (Jurásico tardío) de la Cuenca Neuquina de Argentina. Unpublished PhD thesis, Universidad Nacional de La Plata, La Plata, 583 pp.

GOUIRIC-CAVALLI, S. 2017. Large and mainly unnoticed: the first Lower Tithonian record of a suspension-feeding pachycormid from southern Gondwana. *Ameghiniana*, **54**, 283–289.

GOUIRIC-CAVALLI, S. and CIONE, A. L. 2015. *Notodectes* is the first endemic pachycormiform genus (Osteichthyes, Actinopterygii, Pachycormiformes) in the Southern Hemisphere. *Journal of Vertebrate Paleontology*, **35**, e933738-1–e933738-11.

GOUIRIC-CAVALLI, S., RASIA, L. L., MÁRQUEZ, G. J., ROSATO, V., SCASSO, R. A. and REGUERO, M. 2019. First pachycormiform (Actinopterygii, Pachycormiformes) remains from the Late Jurassic of the Antarctic Peninsula and remarks on bone alteration by recent bioeroders. *Journal of Vertebrate Paleontology*, **38**, 1–10.

GRADSTEIN, F. M. E., OGG, J. G., SCHMITZ, M. D. and OGG, G. M. 2012. *The Geologic*

Time Scale 2012, Elsevier, Amsterdam, 1140 pp.

GRANDE, L. 1985. Recent and fossil clupeomorph fishes with materials for revision of the subgroups of clupeoids. *Bulletin of the American Museum of Natural History*, **181**, 231–372.

GRANDE, L. 2010. An empirical synthetic pattern study of gars (Lepisosteiformes) and closely related species, based mostly on skeletal anatomy. The resurrection of the Holostei. *American Society of Ichthyologists and Herpetologists Special Publication*, **6**, 1-871.

GRANDE, L. and BEMIS, W. E. 1998. A comprehensive phylogenetic study of amiid fishes (Amiidae) based on comparative skeletal anatomy. An empirical search for interconnected patterns of natural history. *Society of Vertebrate Paleontology, Memoir*, **4**, 1–690.

GRANDSTAFF, B. S., PARRIS, D. C. and JOHNSON, R. O. 2011. *Bonnerichthys gladius* (Osteichthyes) from the Cretaceous of the Atlantic coastal states. *Geological Society of America Abstracts with Programs*, **43**, 87.

GREENWOOD, P. H., ROSEN, D. E., WEITZMAN, S. H. and MYERS, G. S. 1966. Phyletic studies of teleostean fishes, with a provisional classification of living forms. *Bulletin of the American Museum of Natural History*, **131**, 341–455.

GREGORY, W. K. 1923. A Jurassic Fish Fauna from Western Cuba, with an arrangement of the families of Holostean Ganoid Fishes. *Bulletin of the American Museum of Natural History*, **48**, 223–42.

GROSS, W. 1964. Polyphyletische Stämme im System der Wirbeltiere. *Zoologische Anzeiger*, **173**, 1–23.

HABEGGER, M. L., HUBER, D. H., LAJEUNESSE, M. J. and MOTTA, P. J. 2017. Theoretical calculations of bite force in billfishes. *Journal of Zoology*, **303**, 15–26.

HAMPE, O. and BASZIO, S. 2010. Relative warps meet cladistics: A contribution to the phylogenetic relationships of baleen whales based on landmark analyses of mysticete crania. *Bulletin of Geosciences*, **85**, 199–218.

HAUFF, B. 1953*a*. *Ohmdenia multidentata* nov. gen. et nov. sp. Ein neuer großer Fischfund aus den Posidonienschiefern des Lias and von Ohmden/Holzmaden in Württemberg. *Neues Jahrbuch für Geologie und Paläontologie,* **97**, 39–50.

HAUFF, B. 1953*b*. *Das Holzmadenbuch*. Hohenlohe'sche Buchhandlung Ferdinand Rau, Öhringen, Germany, 134 pp.

HAUFF, B. and HAUFF, R. B. 1981. *Das Holzmadenbuch*. REPRO-DRUCK, Fellbach, Germany, 136 pp.

HAY, O. P. 1903. On certain genera and species of North American Cretaceous actinopterous fishes. *Bulletin of the American Museum of Natural History*, **91**, 1–95.

HAYE, T., REINICKE, T., GURS, K. and PIEHL, A. 2008. Die Elasmobranchier des Neochattiums (Oberoligozän) von Johannistal, Ostholstein, und Ergänzungen zu deren Vorkommen in der Ratzeburg-Formation (Neochattium) des südö stlichen. *Nordseebeckens. Palaeontos*, **14**, 55–97.

HEATH, T. A., HUELSENBECK, J. P. and STADLER, T. 2014. The fossilized birth-death process for coherent calibration of divergence-time estimates. *Proceedings of the National Academy of Sciences*, **111**, E2957–E2966.

HEINICKE, M., NAYLOR, G. and HEDGES, S. 2009. Cartilaginous fishes (Chondrichthyes). 320–327. *In* KUMAR, S. and HEDGES, S. (eds). *The Timetree of Life*. New York, Oxford University Press, Oxford, UK, 576 pp.

HENNIG, W. 1966. *Phylogenetic Systematics* [tr. DAVIS, D. D. and ZANGERL, R. D.],

University of Illinois Press, Urbana, Illinois, 263 pp.

HERMAN, J. 1974. Compléments paléoichthyologiques a la faune éocene de la Belgique. 1. *Palaeorhincodon*, genre nouveau de l'Eocene Belge, *Bulletin de la Societe Belge de Geologie*, **83**, 7–13.

HERMAN, J. 1977. Additions to the Eocene fish fauna of Belgium. 3. Revision of the Orectolobiforms. *Tertiary Research*, **1**, 127–138.

HERMAN, J. 1979. Reflexions sur la systematique des Galeoidei et sur les affinités du genre *Cetorhinus* a l'occasion de la découverte d'éléments de la denture d'un exemplaire fossile dans les sables du Kattendijk a Kallo (Pliocene inférieur, Belgique). *Annales de la Société Géologique de Belgique*, **102**, 357–377.

HILTON, E. J. 2011. Bony fish skeleton. 434–448. *In* A. P. Farrell (ed.). *Encyclopedia of fish physiology: From genome to environment*. San Diego, Academic Press, 2272 pp.

HJELM, J. and JOHANSSON, F. 2003. Temporal variation in feeding morphology and size-structured population dynamics in fishes. *Proceedings of the Royal Society of London B: Biological Sciences*, **270**, 1407–1412.

HOVESTADT, D. C. and HOVESTADT-EULER, M. 2011. A partial skeleton of *Cetorhinus parvus* Leriche, 1910 (Chondrichthyes, Cetorhinidae) from the Oligocene of Germany. *Paläontologische Zeitschrift*, **86**, 71–83.

HOVESTADT, D. C., HOVESTADT-EULER, M. and MICKLICH, N. 2010. A review of the chondrichthyan fauna of Grube Unterfeld (Frauenweiler) clay pit. *Kaupia*, **17**, 57–71.

HUDDLESTON, R. W. and TAKEUCHI, G. T. 2006. A new late Miocene species of sciaenid fish based primarily on an *in situ* otolith from California. *Bulletin of the Southern California Academy of Sciences*, **105**, 30–43.

HUDSON, J. D. and MARTILL, D. M. 1994. The Peterborough Member (Callovian, Middle Jurassic) of the Oxford Clay Formation at Peterborough, UK. *Journal of the Geological Society*, **151**, 113–124.

HULL, P. M. 2017. Emergence of modern marine ecosystems. *Current Biology*, **27**, R466–R469.

HURLEY, I. A., MUELLER, R. L., DUNN, K. A., SCHMIDT, E. J., FRIEDMAN, M., HO, R. K., PRINCE, V. E., YANG, Z., THOMAS, M. G. and COATES, M. I. 2007. A new time-scale for ray-finned fish evolution. *Proceedings of the Royal Society B: Biological Sciences*, **274**, 489–498.

HUTCHINGS, J. A., MYERS, R. A., GARCÍA, V. B., LUCIFORA, L. O. and KUPARINEN, A. 2012. Life-history correlates of extinction risk and recovery potential. *Ecological Applications*, **22**, 1061–1067.

INOUE, J. G., MIYA, M., LAM, K., TAY, B. H., DANKS, J. A., BELL, J., WALKER, T. I. and VENKATESH, B. 2010. Evolutionary origin and phylogeny of the modern holocephalans (Chondrichthyes: Chimaeriformes): a mitogenomic perspective. *Molecular Biology and Evolution*, **27**, 2576–2586.

JACKSON, J. A., BAKER, C. S., VANT, M., STEEL, D. J., MEDRANO-GONZALEZ, L. and PALUMBI, S. R. 2009. Big and slow: phylogenetic estimates of molecular evolution in baleen whales (Suborder Mysticeti). *Molecular Biology and Evolution*, **26**, 2427–2440.

JAIN, S. L. and ROBINSON, P. L. 1963. Some new specimens of the fossil fish *Lepidotes* from the English Upper Jurassic. *Proceedings of the Zoological Society of London*, **141**, 119–135.

JAMBURA, P. L., KINDLIMANN, R., LÓPEZ-ROMERO, F., MARRAMÀ, G., PFAFF,

C., STUMPF, S., TÜRTSCHER, J., UNDERWOOD, C. J., WARD, D. J. and KRIWET, J., 2019. Micro-computed tomography imaging reveals the development of a unique tooth mineralization pattern in mackerel sharks (Chondrichthyes; Lamniformes) in deep time. *Scientific Reports*, **9**, 1–13.

JANSSEN, A.W. and GOEDERT, J. L. 2016. Notes on the systematics, morphology and biostratigraphy of fossil holoplanktonic Mollusca, 24. First observation of a genuinely Late Mesozoic thecosomatous pteropod. *Basteria*, **80**, 59–63.

JEFFERIES, R. P. S. 1979. The origin of chordates: a methodological essay. 443–447. In HOUSE, M. R. *The Origin of Major Invertebrate Groups*. Systematics Association Special Volume 12. Academic Press, London, UK, 515 pp.

JESSEN, H. 1972**.** Schultergürtel und Pectoralflosse bei Actinopterygiern. *Fossils and Strata*, **1**, 1–101.

JOHNSON, J. H. and HOWELL, B. F. 1948. A new Cretaceous calcareous alga from Kansas. *Journal of Paleontology*, **22**, 632–633.

JOLLIE, M. 1962. *Chordate morphology*, Rheinhold, New York, USA, 478 pp.

JOLLIE, M. 1984. Development of cranial bones and pectoral girdle bones of *Lepisosteus* with a note on scales. *Copeia*, **1984**, 476–502.

JOLLIE, M. 1962. *Chordate morphology*, Rheinhold, New York, USA, 478 pp.

JONET, S. 1947. Présence d'un Squale du genre *Cetorhinus* dans l'Oligocène de Roumanie. *Bulletin de la Société Belge de Géologie, de Paléontologie et d'Hydrologie*, **56**, 17–19.

JONET, S. 1976. Notes d'Ichthyologie Miocene. VII. La famille des Mobulidae au Portugal. *Boletim da Sociedade Geológica de Portugal*, **20**, 53–64.

JORDAN, D. S. and HANNIBAL, H. 1923. Fossil sharks and rays of the Pacific Slope of North America. *Bulletin of the Southern California Academy of Sciences*, **22**, 27–63.

JUANES, F., BUCKEL, J. A. and SCHARF, F. S. 2002. 12 Feeding Ecology of Piscivorous Fishes. 267–283. *In* HART, P. J. B. and REYNOLDS, J. D. (eds.). *Handbook of fish biology and fisheries: Fish Biology*. Wiley-Blackwell, Hoboken New Jersey, USA. 428 pp.

JUNE, F. C. and CARLSON, F. T. 1971. Food of young Atlantic Menhaden, *Brevoortia tyrannus*, in relation to metamorphosis. *Fisheries Bulletin*, **68**, 493–512.

KANAKOFF, G. 1956. Fish records from the Pleistocene of southern California. *Bulletin of the Southern California Academy of Sciences*, **55**, 47–49.

KARASAWA, H. 1989. Late Cenozoic elasmobranchs from the Hokuriku district, central Japan. *The Science Reports of Kanazawa University*, **34**, 1–57.

KASS, R. E. and RAFTERY, A. E. 1995. Bayes factors. *Journal of the American Statistical Association*, **90**, 773–795.

KEAR, B. P. 2007. First record of pachycormid fish (Actinopterygii: Pachycormiformes) from the Lower Cretaceous of Australia. *Journal of Vertebrate Palaeontology*, **27**, 1033–1038.

KEMP, T. S. 2005. *The Origin and Evolution of Mammals*. Oxford University Press, Oxford UK, 331 pp.

KERMACK, D. M. 1970. True serial-sectioning of fossil material. *Biological Journal of the Linnean Society*, **2**, 47–53.

KIRCHNER, J. W. and WEIL, A. 2000. Delayed biological recovery from extinctions throughout the fossil record. *Nature*, **404**, 177–180.

KLUG, S. 2010. Monophyly, phylogeny and systematic position of the †Synechodontiformes (Chondrichthyes, Neoselachii). *Zoologica Scripta*, **39**, 37–49.

KNOLL, A. H. and FOLLOWS, M. J. 2016. A bottom-up perspective on ecosystem change in Mesozoic oceans. *Proceedings of the Royal Society B: Biological Sciences*, **283**, 20161755.

KORNEISEL, D., GALLOIS, R. W., DUFFIN, C. J. and BENTON, M. J. 2015. Latest Triassic marine sharks and bony fishes from a bone bed preserved in a burrow system, from Devon, UK. *Proceedings of the Geologists' Association*, **126**, 130–142.

KRIWET, J. 2005. A comprehensive study of the skull and dentition of pycnodont fishes. *Zitteliana*, **45**, 135–188.

LANDEMAINE, O., THEIS, D. and WASCHKEWITZ, J. 2018. The Late Jurassic shark *Palaeocarcharias* (Elasmobranchii, Selachimorpha) – functional morphology of teeth, dermal cephalic lobes and phylogenetic position. *Palaeontographica Abteilung A*, 103–165.

LAMBERS, P. H. 1988. *Orthocormus teyleri* nov. spec., the first pachycormid (Pisces, Actinopterygii) from the Kimmeridge [sic] Lithographic Limestone at Cerin (Ain), France; with remarks on the genus *Orthocormus* Weitzel. *Proceedings of the Koninklijke Nederlandse Akademie van Wetenschappen Series B*, **91**, 369–391.

LAMBERS, P. H. 1992. On the ichthyofauna of the Solnhofen Lithographic Limestone (Upper Jurassic, Germany). Unpublished PhD thesis, Rijkuniversiteit Groningen, Groningen, 336 pp.

LAMBERS, P. H. 1999. The actinopterygian fish fauna of the Late Kimmeridgian and Early Tithonian 'Plattenkalke' near Solnhofen (Bavaria, Germany): state of the art. *Geologie en Mijnbouw*, **78**(2), 215–229.

LATIMER, A. E. and GILES, S. 2018. A giant dapediid from the Late Triassic of Switzerland and insights into neopterygian phylogeny. *Royal Society Open Science*, **5**, 180497.

LAUDER, G. V. 1989. Caudal fin locomotion in ray-finned fishes: historical and functional analyses. *American Zoologist*, **29**, 85–102.

LAUDER, G. V. 1995. On the inference of function from structure. 1–18. *In* THOMASON, J. J. (ed.). *Functional morphology in vertebrate palaeontology*, Cambridge University Press, Cambridge, UK, 293 pp.

LAUDER, G. V. and LIEM, K. F. 1983. The evolution and interrelationships of the actinopterygian fishes. *Bulletin of the Museum of Comparative Zoology*, **150**, 95–197.

LÊ, H. L. V., LECOINTRE, G. and PERASSO, R. 1993. A 28S rRNA-based phylogeny of the gnathostomes: first steps in the analysis of conflict and congruence with morphologically based cladograms. *Molecular Phylogenetics and Evolution*, **2**, 31–51.

LEHMAN, J. P. 1949. Étude d'un *Pachycormus* du Lias de Normandie. *Kungliga Svenska Vetenskapsakademiens Handlingar*, **4**, 1–44.

LEHMAN, J. P. 1966. Actinopterygii. 1–243. *In* PIVETEAU, J. (ed.). *Traité de Paléontologie*, Volume 4, part 3. Masson et Cie, Paris, 442 pp.

LEIDY, J. 1857, Remarks on *Saurocephalus* and its allies. *Transactions of the American Philosophical Society*, **11**, 91–95.

LERICHE, M. 1910. Les poissons tertiaris de la Belgique. III. Les poissons oligocenes. *Mémoires du Musée Royal d'Histoire Naturelle de Belgique*, **5**, 229–263.

LERICHE, M. 1927. Les Poissons de la Molasse suisse. *Mémoires de la Société Paléontologique Suisse*, **46**, 1–55.

LERICHE, M. 1948. Note sur les rapports entre la faune ichthyologique de l'Argile à septaria (Septarienton) du bassin de Mayence et celle de l'Argile de Boom (Rupelien moyen), suivie

d'observations nouvelles sur quelques-unes des espèces communes aux deux faunes. *Bulletin de la Société Belge de Géologie, de Paléontologie et d'Hydrologie*, **57**, 176–185.

LINDKVIST, M. 2012. A Phylogenetic Appraisal of *Pachycormus bollensis*: Implications for Pachycormiform Evolution, Unpublished Dissertation, Uppsala University, Uppsala, Sweden, 44 pp.

LISTON, J. 2004. An overview of the pachycormiform *Leedsichthys*. 379–390. *In* ARRATIA, G. and TINTORI, A. (eds.). *Mesozoic Fishes 3 — Systematics, Paleoenvironments and Biodiversity*. Verlag Dr Friedrich Pfeil, Münich, Germany, 649 pp.

LISTON, J. 2006. A fish fit for Ozymandias?: the ecology, growth and osteology of *Leedsichthys* (Pachycormidae, Actinopterygii). Unpublished PhD thesis, University of Glasgow, Glasgow, 464 pp.

LISTON, J. 2007. A fish fit for Oxymandias?: The ecology, growth and osteology of *Leedsichthys* (Pachycormidae, Actinopterygii). PhD thesis, University of Glasgow, Glasgow, UK.

LISTON, J. 2008*a*. A review of the characters of the edentulous pachycormiforms *Leedsichthys*, *Asthenocormus* and *Martillichthys* nov. gen. 181–198. *In* ARRATIA, G., SCHULTZE, H. P. and WILSON, M. V. H. (eds). *Mesozoic Fishes 4 — Homology and Phylogeny*. Verlag Dr Friedrich Pfeil, Münich, Germany, 502 pp.

LISTON, J. 2008*b*. *Leedsichthys* des Vaches Noires au peigne fin (translation by M-C Buchy). *L'Écho des Falaises*, **12**, 41–49.

LISTON, J. 2010. The occurrence of the Middle Jurassic pachycormid fish *Leedsichthys*. *Oryctos*, **9**, 1–36.

LISTON, J. 2013. The plasticity of gill raker characteristics in suspension feeders:

implications for Pachycormiformes. 121–143. *In* ARRATIA, G., SCHULTZE, H. P. and WILSON, M. V. H. (eds.). *Mesozoic Fishes 5 — Global Diversity and Evolution*. Verlag Dr Friedrich Pfeil, Münich, Germany, 560 pp.

LISTON, J. 2016. *Leedsichthys problematicus*: Arthur Smith Woodward's 'most embarrassing enigma'. *Geological Society London: Special Publications*, **430**, 235–259.

LISTON, J. and GENDRY, D. 2015. Le Python de Caen, les algues géantes d'Amblie, et autres specimens perdus de *Leedsichthys* d'Alexandre Bourienne, Jules Morière, Eugène Eudes-Deslongchamps et Alexandre Bigot. *L'Écho des Falaises*, **19**, 17–33.

LISTON, J. and MALTESE, A. 2016. Daggers, swords, scythes and sickles: Pachycormid fins as ecological predictors. *PeerJ Preprints*, **4**, e2550v1.

LISTON, J., NEWBERY, M. G., CHALLANDS, T. J. and ADAMS, C. 2013. Growth, age and size of the Jurassic pachycormid *Leedsichthys problematicus* (Osteichthyes: Actinopterygii). 145–175. *In* ARRATIA, G., SCHULTZE, H. P. and WILSON, M. V. H. (eds). *Mesozoic Fishes 5 — Global Diversity and Evolution*. Verlag Dr Friedrich Pfeil, Münich, Germany, 560 pp.

LONG, D. J. 1993. Late Miocene and early Pliocene fish assemblages from the north coast of Chile. *Tertiary Research*, **17**, 117–126.

LOOMIS, F. B. 1900. Die anatomie und die verwandtschaft der Ganoid- und Knochen-fische aus der Kreide-Formation von Kansas, U.S.A. *Paleontographica*, **46**, 213–283.

LÓPEZ-ARBARELLO, A. 2012. Phylogenetic interrelationships of ginglymodian fishes (Actinopterygii: Neopterygii). *PLoS One*, **7**, e39370.

LÓPEZ-ARBARELLO, A. and SFERCO, E. 2018. Neopterygian phylogeny: the merger assay. *Royal Society Open Science*, **5**, 172337.

LU, G. Y., ADATTE, T., KELLER, G. and ORITZ, N. 1998. Abrupt climatic, oceanographic and ecologic changes near the Paleocene-Eocene transition in the deep Tethys basin: The Alademilla section, southern Spain. *Eclogae Geologicae Helveticae*, **91**, 293–306.

LUO, Z. X. 2007. Transformation and diversification in early mammal evolution. *Nature*, **450**, 1011–1019.

MADDISON, D. R. and MADDISON, W. P. 2005. *MacClade 4: Analysis of phylogeny and character evolution*. Version 4.08a. http://macclade.org

MADDISON, W. P. and MADDISON, D. R. 2018. *Mesquite: a modular system for evolutionary analysis*. Version 3.51. http://www.mesquiteproject.org

MARX, F. G. and FORDYCE, R. E. 2015. Baleen boom and bust: a synthesis of mysticete phylogeny, diversity and disparity. *Royal Society Open Science*, **2**, 140434.

MAINWARING, A. J. 1978. Anatomical and systematic revision of the Pachycormidae, a family of Mesozoic fishes. Unpublished PhD thesis, Westfield College, London, 127 pp.

MAISEY, J. G. 1985. Relationships of the megamouth shark, Megachasma. *Copeia*, **1985**, 228–231.

MAISEY, J. G. 2012. What is an 'elasmobranch'? The impact of palaeontology in understanding elasmobranch phylogeny and evolution. *Journal of Fish Biology*, **80**, 918–951.

MAISEY, J. G., NAYLOR, G. P. and WARD, D. J. 2004. Mesozoic elasmobranchs, neoselachian phylogeny and the rise of modern elasmobranch diversity. 17–57. *In* ARRATIA, G. and TINTORI, A. (eds.). *Mesozoic fishes 3 — Systematics, Paleoenvironments and Biodiversity*. Verlag Dr Friedrich Pfeil, Münich, Germany, 649 pp.

MAREK, R. D., MOON, B. C., WILLIAMS, M. and BENTON, M. J. 2015. The skull and

endocranium of a Lower Jurassic ichthyosaur based on digital reconstructions. *Palaeontology*, **58**, 723–742.

MARSHALL, C. R. 1990. The fossil record and estimating divergence times between lineages: Maximum divergence times and the importance of reliable phylogenies. *Journal of Molecular Evolution*, **30**, 400–408.

MARSHALL, C. R. 1995. Distinguishing between sudden and gradual extinctions in the fossil record: predicting the position of the Cretaceous-Tertiary iridium anomaly using the ammonite fossil record on Seymour Island, Antarctica. *Geology*, **23**, 731–734.

MARSHALL, C. R. 1997. Confidence intervals on stratigraphic ranges with non-random distributions of fossil horizons. *Paleobiology*, **23**, 165–173.

MARSHALL, C. R. and WARD, P. D. 1996. Sudden and gradual molluscan extinctions in the latest Cretaceous of western European Tethys. *Science*, **274**, 1360–1363.

MARTILL, D. M. 1986. The stratigraphic distribution and preservation of fossil vertebrates in the Oxford Clay of England. *Philosophical Transactions of the Royal Society of London B: Biological Sciences*, **311**, 155–165.

MARTILL, D. M. 1988. *Leedsichthys problematicus*, a giant filter-feeding teleost from the Jurassic of England and France. *Neues Jahrbuch fur Geologie und Palaontologie-Monatshefte*, **11**, 670–680.

MARTILL, D. M. 1990. Predation on *Kosmoceras* by semionotid fish in the Middle Jurassic Lower Oxford Clay of England. *Palaeontology*, **33**, 739–742.

MARTILL, D. M. 1991. Fish. 197–225. *In* MARTILL, D. M. and HUDSON, J. D. (eds). *Fossils of the Oxford Clay*. Palaeontological Association Field Guide to Fossils, **4**, The Palaeontological Association, 286 pp.

MARTILL, D. M. 2007. The age of the Cretaceous Santana Formation fossil Konservat Lagerstätte of north-east Brazil: a historical review and an appraisal of the biochronostratigraphic utility of its palaeobiota. *Cretaceous Research*, **28**, 895–920.

MARTIN, A. P. and NAYLOR, G. J. 1997. Independent origins of filter-feeding in megamouth and basking sharks (order Lamniformes) inferred from phylogenetic analysis of cytochrome *b* gene sequences. 39–50. *In* YANO, K., MORRISSEY, J. F., YABUMOTO, Y. and NAKAYA, K. (eds). *Biology of Megamouth Shark*. Tokai University Press, Tokyo, 203 pp.

MARTIN, A. P., PARDINI, A. T., NOBLE, L. R. and JONES, C. S. 2002. Conservation of a dinucleotide simple sequence repeat locus in sharks. *Molecular Phylogenetics and Evolution* **23**, 205–213.

MARTIN, R. E. 1996. Secular increase in nutrient levels through the Phanerozoic: implications for productivity, biomass, and diversity of the marine biosphere. *Palaios*, **11**, 209–219.

MCCALLUM, M. L. 2015. Vertebrate biodiversity losses point to a sixth mass extinction. *Biodiversity and Conservation*, **24**, 2497–2519.

MCCLUNG, C. E. 1908. Ichthyological notes of the Kansas Cretaceous, I. *Kansas University Science Bulletin*, **9**, 235–246.

MCKINNEY, M. L. 1997. Extinction vulnerability and selectivity: combining ecological and paleontological views. *Annual Review of Ecology and Systematics*, **28**, 495–516.

MERLE, D., BAUT, J.-P., GINSBURG, L., SAGNE, C., HERVET, S., CARRIOL, R.-P., VENEC-PEYRE, T., BLANC- VALLERON, M., MOURER-CHAUVIRET, C., ARAMBOL, D. and VIETTE, P. 2002. Découverte d'une faune de vertébrés dans

l'Oligocène inférieur de Vayres-sur-Essonne (bassin de Paris, France): biodiversité et paléoenvironnement. *Comptes Rendus Palevol*, **1**, 111–116.

MICKLICH, N. and PARIN, N. 1996. The fishfauna of Frauenweiler (Middle Oligocene, Rupelian; Germany): first results of a review. *Publicaciones Especpeciales Instituto Español de Oceanografia*, **21**, 129–148.

MILLER, H. W. and WALKER, M. V. 1968. *Echinoteuthis melanae* and *Kansasteuthis lindneri*, new genera and species of teuthids, and a sepiid from the Niobrara Formation of Kansas. *Transactions of the Kansas Academy of Science*, **71**, 176–183.

MITCHELL, E. and TEDFORD, R.H. 1973. The Enaliarctinae, a new group of extinct aquatic Carnivora and a consideration of the origin of the Otariidae. *Bulletin of the American Museum of Natural History*, **151**, 203–284.

MOORE, C. 1853. On the palaeontology of the Middle and Upper Lias. *Proceedings of the Somersetshire Archaeological and Natural History Society*, **3**, 61–76.

MOSS, S. 1977. Feeding mechanisms in sharks. *American Zoologist*, **17**, 355–364.

MOTTA, P. J. 2004. Prey capture behavior and feeding mechanics of elasmobranchs. 165–203. *In* CARRIER, J. C., MUSICK, J. A. and HEITHAUS, M. R. (eds.). *Biology of Sharks and Their Relatives*. 2nd edn. CRC Press, Boca Raton, Florida, 666 pp.

MOTTA, P. J., MASLANKA, M., HUETER, R. E., DAVIS, R. L., DE LA PARRA, R., MULVANY, S. L., HABEGGER, M. L., STROTHER, J. A., MARA, K. R., GARDINER, J. M., TYMINSKI, J. P. and ZEIGLER, L. D. 2010. Feeding anatomy, filter-feeding rate, and diet of whale sharks *Rhincodon typus* during surface ram filter feeding off the Yucatan Peninsula, Mexico. *Zoology*, **113**, 199–212.

MÜLLER, A. 1976. Beiträge zur Kenntnis der Fauna des Rupels der sü dlichen Leipziger Tieflandbucht. TeilI: Die Selachier des Leipziger Rupels. *Abhandlungen und Berichte des Naturkundlichen Museums Mauritianum Altenburg*, **9**, 83–117.

MÜLLER, J. 1844. Über den Bau und die Grenzen der Ganoiden und über das natürliche System der Fische. *Bericht Über die zur Bekanntmachung geeigneten Verhandlungen der Akademis der Wissenschaften, Berlin*, **1844**, 117–216.

MÜLLER, J. 1845. Über den Bau und die Grenzen der Ganoiden und über das natürliche System der Fische. *Archiv für Naturgeschichte*, **11**, 91–141.

NAYLOR, G. J., MARTIN, A. P., MATTISON, E. G. and BROWN, W. M. 1997. Interrelationships of lamniform sharks: testing phylogenetic hypotheses with sequence data. 199–218. *In* KOCHER, T. D. and STEPIEN, C. A. (eds.). *Molecular Systematics of Fishes*, Elsevier, Amsterdam, 314 pp.

NEAR, T. J., EYTAN, R. I., DORNBURG, A., KUHN, K. L., MOORE, J. A., DAVIS, M. P., WAINWRIGHT, P. C., FRIEDMAN, M. and SMITH, W. L. 2012. Resolution of ray-finned fish phylogeny and timing of diversification. *Proceedings of the National Academy of Sciences of the United States of America*, **109**, 13698–13703.

NIELSEN, E. 1942. Studies on Triassic fishes from East Greenland I. *Glaucolepis* and *Boreosomus*. *Palaeozoologica Groenlandica*, **1**, 1–403.

NELSON, G. 1969. Gill Arches and the Phylogeny of Fishes, with Notes on the Classification of Vertebrates. *Bulletin of the American Museum of Natural History*, **141**, 475–552.

NELSON, J. S., GRANDE, T. C. and WILSON, M. V. 2016. *Fishes of the World*. 5th Edition. John Wiley & Sons.

NESSOV, L. A. 1999. [Whale shark *Eorhincodon* gen. nov. (Rhincodontidae)—oldest and

very large rhincodontid from the Cenomanian (Late Cretaceous) of Belgorod and Volgograd provinces]. *Proceedings of the Zoological Institute (Russian Academy of Sciences)*, **227**, 95–103. [Russian with English abstract]

NICHOLSON, H. A. and LYDEKKER, R. 1889. *A Manual of Palaeontology*. Second edition. William Blackwood & Sons, Edinburgh, 1642 pp.

NORMARK, B. B., MCCUNE, A. R. and HARRISON, R. G. 1991. Phylogenetic relationships of neopterygian fishes, inferred from mitochondrial DNA sequences. *Molecular Biology and Evolution*, **8**, 819–834.

NORRIS, R. D. 2000. Pelagic species diversity, biogeography, and evolution. *Paleobiology*, **26**, 236–258.

NOUBHANI, A. and CAPPETTA, H. 1997. Les Orectolobiformes, Carcharhiniformes et Myliobatiformes (Elasmobranchii, Neoselachii) des bassins à phosphate du Maroc (Maastrichtien-Lutétien basal). Systématique, biostratigraphie, évolution et dynamique des faunes. *Palaeo Ichthyologica*, **8**, 1–327.

NURSALL, J. R. 1996. The phylogeny of pycnodonts fishes. 125–152. *In* ARRATIA, G. and VIOHL, G. (eds.). *Mesozoic Fishes 1 — Systematics and Paleoecology*. Verlag Dr Freidrich Pfeil, Münich, Germany, 576 pp.

NYEBLIN, O. 1961. Über die Frage der Abstammung der rezenten primitiven Teleostier. *Paläontologische Zeitschrift*, **35**, 114–117.

NYEBLIN, O. 1964. Versuch einer taxonomischen Revision der jurassischen Fischgattung *Thrissops* Agassiz. *Göteborgs kungl. vetenskaps-och vitterhets Samhälles Handlingar. Series B*, **9**, 1–44.

NYLANDER, J. A., RONQUIST, F., HUELSENBECK, J. P., & NIEVES-ALDREY, J. 2004.

Bayesian phylogenetic analysis of combined data. *Systematic Biology*, **53**, 47–67.

OLSEN, P. E. 1984. The skull and pectoral girdle of the parasemionotid fish *Watsonulus eugnathoides* from the Early Triassic Sakamena Group of Madagascar, with comments on the relationships of the holosteans fishes. *Journal of Vertebrate Paleontology*, **4**, 481–499.

OLSEN, P. E. and MCCUNE, A. R. 1991. Morphology of the Semionotus elegans species group from the Early Jurassic part of the Newark Supergroup of Eastern North America with comments on the family Semionotidae (Neopterygii). *Journal of Vertebrate Paleontology*, **11**, 269–292.

PAIG-TRAN, M. E. W. and SUMMERS, A. P. 2014. Comparison of the structure and composition of the branchial filters in suspension-feeding elasmobranchs. *The Anatomical Record*, **297**, 701–715.

PARKER, G. A. 1992. The evolution of sexual size dimorphism in fish. *Journal of Fish Biology*, **41**, 1–20.

PARRIS, D. C., GRANDSTAFF, B. S. and GALLAGHER, W. B. 2007. Fossil fish from the Pierre Shale Group (Late Cretaceous): clarifying the biostratigraphic record. *Geological Society of America, Special Paper*, **427**, 99–109.

PATTERSON, C. 1967. Are the teleosts a polyphyletic group?. *Colloques Internationaux du Centre National de la Recherche Scientifique*, **163**, 93–109.

PATTERSON, C. 1968. The caudal skeleton in Lower Liassic pholidophorid fishes. *Bulletin of the British Museum of Natural History, Geology*, **16**, 201–239.

PATTERSON, C. 1973. Interrelationships of holosteans. 233–305. *In* GREENWOOD, P. H., MILES, R. S. and PATTERSON, C. (eds.). *Interrelationships of Fishes*, **53**, Academic Press, Cambridge, Massachusetts, 496 pp.

PATTERSON, C. 1975. The braincase of pholidophorid and leptolepid fishes, with a review of the actinopterygian braincase. *Philosophical Transactions of the Royal Society of London B: Biological Sciences*, **269**, 275–579.

PATTERSON, C. 1977*a*. The contribution of paleontology to teleostean phylogeny. 579–643. *In* HECHT, M. K., GOODY, P. C. and HECHT, B. M. (eds). *Major patterns in vertebrate evolution*. Plenum Press, New York, 908 pp.

PATTERSON, C. 1977*b*. Cartilage bones, dermal bones and membrane bones or the exoskeleton versus the endoskeleton. 77–121. *In* WESTOLL, T. S., ANDREWS S. M., MILES, R. S. and WALKER, A. D. (eds). *Problems in Vertebrate Evolution: Essays Presented to Professor T. S. Westoll*. Linnaean Society Symposium Series, **4**, Academic Press, London, UK, 411 pp.

PATTERSON, C. 1982. Morphology and interrelationships of primitive actinopterygian fishes. *American Zoologist*, **22**, 241–259.

PATTERSON, C. 1994. Bony fishes. *Short courses in Paleontology*, **7**, 57–84.

PATTERSON, C. and ROSEN, D. E. 1977. Review of ichthyodectiform and other Mesozoic teleost fishes and the theory and practice of classifying fossils. *Bulletin of the American Museum of Natural History*, **158**, 81–172.

PEREDO, C. M., PYENSON, N. D., MARSHALL, C. D. and UHEN, M. D. 2018. Tooth loss precedes the origin of baleen in whales. *Current Biology*, **28**, 3992–4000.

PFEIL, F. H. 1981. Eine nektonische Fischfauna aus dem unteroligozänen Schönecker Fischschiefer des Galon-Grabens in Oberbayern. *Geologica Bavarica*, **82**, 357–388.

PHARISAT, A. 1998. Marine fish biodiversity in the Oligocene of Froidefontaine (Belfort Territory, France). *Italian Journal of Zoology*, **65**, 189–191.

PIERCE, S. and BENTON, M. J. 2006. *Pelagosaurus typus* Bronn, 1841 (Mesoeucrocodylia: Thalattosuchia) from the Upper Lias (Toarcian; Lower Jurassic) of Somerset, England. *Journal of Vertebrate Paleontology*, **26**, 621–635.

PIMIENTO, C., GONZÁLEZ-BARBA, G., EHRET, D. J., HENDY, A. J., MACFADDEN, B. J. and JARAMILLO, C. 2013. Sharks and rays (Chondrichthyes, Elasmobranchii) from the late Miocene Gatun formation of Panama. *Journal of Paleontology*, **87**, 755–774.

PIMIENTO, C., CANTALAPIEDRA, J. L., SHIMADA, K., FIELD, D. J. and SMAERS, J. B. 2019. Evolutionary pathways toward gigantism in sharks and rays. *Evolution*, **73**, 588–599.

POORTVLIET, M., OLSEN, J. L., CROLL, D. A., BERNARDI, G., NEWTON, K., KOLLIAS, S., O'SULLIVAN, J., FERNANDO, D., STEVENS, G., GALVÁN MAGAÑA, F., SERET, B., WINTNER, S. and HOURAU, G. 2015. A dated molecular phylogeny of manta and devil rays (Mobulidae) based on mitogenome and nuclear sequences. *Molecular Phylogenetics and Evolution*, **83**, 72–85.

POYATO-ARIZA, F. J. 2015. Studies on pycnodont fishes (I): evaluation of their phylogenetic position among actinopterygians. *Rivista Italiana di Paleontologia e Stratigrafia*, **121**, 329–343.

PŘIKRYL, T., KOŠTÁK, M., MAZUCH, M. and MIKULÁŠ, R. 2012. Evidence for fish predation on a coleoid cephalopod from the Lower Jurassic Posidonia Shale of Germany. *Neues Jahrbuch für Geologie und Paläontologie-Abhandlungen*, **263**, 25–33.

PURDY, R. W., SCHNEIDER, V. P., APPLEGATE, S. P., MCLELLAN, J. H., MEYER, R. L. and SLAUGHTER, B. H. 2001. The Neogene sharks, rays, and bony fishes from Lee

Creek Mine, Aurora, North Carolina, III. *Smithsonian Contributions to Paleobiology*, **90**, 71–202.

QUENSTEDT, F. A. 1847. *Ueber Lepidotus im Lias E Württembergs: Mit 2 Tafeln Abbildungen*. L. Frdr. Fues, Germany.

QUENSTEDT, F. A. 1858. *Der Jura*, Laupp'schen, Tübingen, Germany, 842 pp.

QUENSTEDT, F. A. 1852. *Handbuch der Petrefactenkunde. Laupp'sche Buchhandlung*, Tübingen, Germany, 792 pp.

QUENTAL, T. B. and MARSHALL, C. R. 2010. Diversity dynamics: molecular phylogenies need the fossil record. *Trends in Ecology & Evolution*, **25**, 434–441.

RAFINESQUE, C. S. 1810. *Carrateri di alcuni nuovi generi e nuove specie di animali e pianti della sicilia convarie osservazioni sopra i medesimi*. San Filipo, Palermo, 105 pp.

RAMBAUT, A., DRUMMOND, A. J., XIE, D., BAELE, G. and SUCHARD, M. A. 2018. Posterior summarisation in Bayesian phylogenetics using Tracer 1.7. Systematic Biology, syy032. doi:10.1093/sysbio/syy032.

RAMPINO, M. R. and CALDEIRA, K. 2018. Comparison of the ages of large-body impacts, flood-basalt eruptions, ocean-anoxic events and extinctions over the last 260 million years: a statistical study. *International Journal of Earth Sciences*, **107**, 601–606.

RAVI, V. and VENKATESH, B. 2018. The Divergent Genomes of Teleosts. *Annual Review of Animal Biosciences*, **6**, 47–68.

RAYNER, D. H. 1948. The structure of certain Jurassic holostean fishes, with special reference to their neurocrania. *Philosophical Transactions of the Royal Society of London B: Biological Sciences*, **233**, 287–345.

REGAN, C. T. 1923. The skeleton of *Lepidosteus*, with remarks on the origin and evolution

of the lower neopterygian fishes. *Journal of Zoology*, **93**, 445–461.

RENZ, A. J., MEYER, A. and KURAKU, S. 2013. Revealing less derived nature of cartilaginous fish genomes with their evolutionary time scale inferred with nuclear genes. *PLOS One*, **8**, e66400.

RIDGWELL, A. 2005. A Mid Mesozoic Revolution in the regulation of ocean chemistry. *Marine Geology*, **217**, 339–357.

RONQUIST, F., TESLENKO, M., VAN DER MARK, P., AYRES, D. L., DARLING, A., HÖHNA, S., LARGET, B., LIANG, L., SUCHARD, M. A. and HUELSENBACK, J. P. 2012. MrBayes 3.2: efficient Bayesian phylogenetic inference and model choice across a large model space. *Systematic Biology*, **61**, 539–542.

SAHNI, A. and MEHROTRA, D. K. 1981. The elasmobranch fauna of coastal Miocene sediments of peninsular India. *Biological Memoirs Lucknow*, **5**, 83–121.

SALLAN, L. C. 2014. Major issues in the origins of ray-finned fish (Actinopterygii) biodiversity. *Biological Reviews*, **89**, 950–971.

SANDERSON, S. L. and WASSERSUG, R. 1993. Convergent and Alternative Designs for Vertebrate Suspension Feeding. 37–112. *In* HANKEN, J. and HALL, B. K. (eds.). *The Skull: Volume 3*, University of Chicago Press, Chicago, Illinois, 470 pp.

SANZ, J. L., WENZ, S., YEBENES, A., ESTES, R., MARTINEZ-DELCLOS, X., JIMENEZ-FUENTES, E., DIÉGUEZ, C., BUSCALIONI, A. D., BARBADILLO, L. J. and VIA, L. 1988. An Early Cretaceous faunal and floral continental assemblage: Las Hoyas fossil site (Cuenca, Spain). *Geobios*, **21**, 611–635.

SASAKI, T., NIKAIDO, M., HAMILTON, H., GOTO, M., KATO, H., KANDA, N., PASTENE, L. A., CAO, Y., FORDYCE, R. E., HASEGAWA, M. and OKADA, N. 2005.

Mitochondrial phylogenetics and evolution of mysticete whales. *Systematic Biology*, **54**, 77–90.

SAUVAGE, H. E. 1894. Note sur un ganoïde de genre nouveau du Lias de Vassey. *Bulletin de la Société des Sciences Historiques et Naturelles de L'Yonne*, **48**, 3–5.

SCHAEFFER, B. and PATTERSON, C. 1984. Jurassic fishes from the western United States, with comments on Jurassic fish distribution. *American Museum Noviates*, **2796**, 1–86.

SCHMID, H.-P., HARZHAUSER, M., KROH, A., CORIC, S., ROGL, F. and SCHULTZ, O. 2001. Hypoxic events on a middle Miocene carbonate platform of the central paratethys (Austria, Badenian, 14 Ma). *Annalen des Naturhistorischen Museums in Wien*, **102**, 1–50.

SCHULTZ, O. 1977. Elasmobranch and teleost fish remains from the Korytnica Clays (Middle Miocene; Holy Cross Mountains, Poland). *Acta Geologica Polonica*, **27**, 201–209.

SCHULTZ, O. 1978. Neue und fehlinterpretierte Fischformen aus dem Miozän des Wiener Beckens. *Annalen des Naturhistorischen Museums in Wien*, **81**, 203–219.

SCHULTZ, O., BRZOBOHATY, R. and KROUPA, O. 2010. Fish teeth from the Middle Miocene of Kienberg at Mikulov, Czech Republic, Vienna Basin. *Annalen des Naturhistorischen Museums in Wien*, **112**, 489–506.

SCHULTZE, H. P. and WILEY, E. O. 1984. The neopterygian *Amia* as a living fossil. 153-159. *In* ELDREDGE, N. and STANLEY, S. (eds.). *Living Fossils.* Springer-Verlag, New York, 291 pp.

SCHUMACHER, B. A., SHIMADA, K., LISTON, J. and MALTESE, A. 2016. Highly specialized suspension-feeding bony fish *Rhinconichthys* (Actinopterygii: Pachycormiformes) from the mid-Cretaceous of the United States, England, and Japan.

Cretaceous Research, **61**, 71–85.

SHIMADA, K. 2007. Mesozoic origin for megamouth shark (Lamniformes: Megachasmidae). *Journal of Vertebrate Paleontology*, **27**, 512–516.

SHIMADA, K. and WARD, D. J. 2016. The oldest fossil record of the megamouth shark from the late Eocene of Denmark and comments on the enigmatic megachasmid origin. *Acta Palaeontologica Polonica*, **61**, 839–846.

SHIMADA, K., POPOV, E. V., SIVERSSON, M., WELTON, B. J. and LONG, D. J. 2015. A new clade of putative plankton-feeding sharks from the Upper Cretaceous of Russia and the United States. *Journal of Vertebrate Paleontology*, **35**, e981335.

SHIMADA, K., SCHUMACHER, B. A., PARKIN, J. A. and PALERMO, J. M. 2006. Fossil Marine Vertebrates from the Lowermost Greenhorn Limestone (Upper Cretaceous: Middle Cenomanian) in Southeastern Colorado. *Journal of Paleontology Memoir*, **63**, 1–45.

SHIMADA, K., WELTON, B. J. and LONG, D. J. 2014. A new fossil megamouth shark (Lamniformes, Megachasmidae) from the Oligocene-Miocene of the western United States. *Journal of Vertebrate Paleontology*, **34**, 281–290.

SHIRAI, S. 1996. Phylogenetic interrelationships of neoselachians (Chondrichthyes: Euselachii). 9–34. *In* STIASSNY, M. L. J., PARENTI, L. R. and JOHNSON, G. D. (eds.). *Interrelationships of Fishes*. Academic Press, San Diego, 496 pp.

SIGNOR, P. W. and LIPPS, J. H. 1982. Sampling bias, gradual extinction patterns, and catastrophes in the fossil record. *Geological Society of America – Special Paper*, **190**, 291–296.

SMITH, J. C. and SANDERSON, S. L. 2013, Particle retention in suspension-feeding fish after removal of filtration structures, *Zoology*, **116**, 348–355.

SOLLAS, I. B. and SOLLAS, W. J. 1913. A study of the skull of a *Dicynodon* by means of serial sections. *Philosophical Transactions of the Royal Society of London B: Biological Sciences*, **204**, 201–205.

SORENSON, L., SANTINI, F. and ALFARO, M. E. 2014. The effect of habitat on modern shark diversification. *Journal of Evolutionary Biology*, **27**, 1536–1548.

SPANDINI, V. and MANGANELLI, G. 2015. A megachasmid shark tooth (Chondrichthyes, Lamniformes) from the Zanclean (early Pliocene) of San Quirico d'Orcia, central Italy. *Bollettino della Società Paleontologica Italiana*, **54**, 68.

STEWART, J. D. 1988. The stratigraphic distribution of Late Cretaceous *Protosphyraena* in Kansas and Alabama. 80–94. *In* NELSON, M. E. (ed). *Paleontology and Biostratigraphy of Western Kansas*: *Articles in Honor of Myrl V. Walker*. Fort Hays Studies, **3**, Fort Hays State University, Kansas, 127 pp.

STEWART, J. D. 1990. Niobrara formation vertebrate stratigraphy. 19–30. *In* BENNETT, S. C. (ed.), *Niobrara Chalk Excursion Guidebook*. Museum of Natural History and Kansas Geological Survey, Lawrence, Kansas, 81 pp.

STRAUSS, D. and SADLER, P. M. 1989. Classical confidence intervals and Bayesian probability estimates for ends of local taxon ranges. *Mathematical Geology*, **21**, 411–427.

SWOFFORD, D. L. 2003. *PAUP*: Phylogenetic Analysis Using Parsimony (*and Other Methods)*. Version 4.0a63. Sinauer Associates, Sunderland, MA.

TAJIKA, A., NÜTZEL, A. and KLUG, C. 2018. The old and the new plankton: ecological replacement of associations of mollusc plankton and giant filter feeders after the Cretaceous?. *PeerJ*, **6**, e4219.

TAVERNE, L. 1977. On the actinopterygian fishes from the Cenomanian of the Kyi River

(Burma, Pakokku District). *Geologisches Jahrbuch*, **23**, 47–59.

TAVERNE, L. and LISTON, J. 2017. On the presence of the plethodid fish *Dixonanogmius* (Teleostei, Tselfatiiformes) in the marine Upper Cretaceous of Burma (Myanmar), tropical Asia. *Geo-Eco-Trop*, **41**, 77–84.

TAYLOR, L. R., CAMPAGNO, L. J. V and STRUHSAKER, P. J. 1983. Megamouth, a new species, genus and family of lamnoid shark (*Megachasma pelagios*, family Megachasmidae) from the Hawaiian Islands. *Proceedings of the Californian Academy of Science*, **43**, 87–110.

THAYER, C. W. 1983. Sediment-mediated biological disturbance and the evolution of the marine benthos. 479–625. *In* TEVESZ, M. J. S. and MCCALL, P. L. (eds.). *Biotic Interactions in Recent and Fossil Benthic Communities,* Springer, New York, 837 pp.

THEIS, D. and WASCHKEWITZ, J. 2016. Redescription of *Dapedium pholidotum* (Agassiz, 1832) (Actinopterygii, Neopterygii) from the Lower Jurassic Posidonia Shale, with comments on the phylogenetic position of *Dapedium* Leach, 1822. *Journal of Systematic Palaeontology*, **14**, 339–364.

THOMAS, E. 1998. Biogeography of the Late Paleocene Benthic Foraminiferal Extinction. 214–243. *In* AUBRY, M. P., LUCAS, S. G. and BERGGEN, W. A. (eds.). *Late Paleocene Early Eocene Climatic and Biotic Events in the Marine and Terrestrial Records*. Columbia University Press, New York, 513 pp.

TOMITA, T. and OJI, T. 2010. Habitat reconstruction of Oligocene elasmobranchs from Yamaga Formation, Ashiya Group, western Japan. *Paleontological Research*, **14**, 69–80.

UHEN, M. D. 2010. The origin(s) of whales. *Annual Review of Earth and Planetary Sciences*, **38**, 189–219.

UNDERWOOD, C. J. 2006. Diversification of the Neoselachii (Chondrichthyes) during the Jurassic and Cretaceous. *Paleobiology*, **32**, 215–235.

UNDERWOOD, C. J. and CUMBAA, S. L. 2010. Chondrichthyans from a Cenomanian (Late Cretaceous) bonebed, Saskatchewan, Canada. *Palaeontology*, **53**, 903–944.

UNDERWOOD, C. J., KOLMANN, M. A. and WARD, D. J. 2017. Paleogene origin of planktivory in the Batoidea. *Journal of Vertebrate Paleontology*, **37**, e1293068.

UNDERWOOD, C. J., WARD, D. J., KING, C., ANTAR, S. M., ZALMOUT, I.S. and GINGERICH, P. D. 2011. Shark and ray faunas in the Middle and Late Eocene of the Fayum Area, Egypt. *Proceedings of the Geologists' Association of London*, **122**, 47–66.

UNDERWOOD, C. J., JOHANSON, Z., WELTEN, M., METSCHER, B., RASCH, L. J., FRASER, G. J., and SMITH, M. M. 2015. Development and evolution of dentition pattern and tooth order in the skates and rays (Batoidea; Chondrichthyes). *PloS One*, **10**, e0122553.

UYENO, T. and MATSUSHIMA, Y. 1974. Early Pleistocene remains of basking shark, hammerhead shark, and others found in Yokohama, Japan. *Bulletin of the Kanagawa Prefectural Museum, Natural Science*, **7**, 57–66.

VAN DEN BOSCH, M. 1984. Oligocene to recent Cetorhinidae (Vertebrata, basking sharks); problematical finds of teeth, dermal scales and gill-rakers. *Mededelingen van de Werkgroep voor Tertiaire en Kwartaire Geologie*, **21**, 205–232.

VAN DER BRUGGHEN, W. 2005. Over fossiele resten van *Cetorhinus* cf. *maximus* uit het Plioceen van Kallo (België). *Grondboor en Hamer*, **1**, 8–12.

VERMEIJ, G. J. 1977. The Mesozoic marine revolution: evidence from snails, predators and grazers. *Paleobiology*, **3**, 245–258.

VERMEIJ, G. J. 1995. Economics, volcanoes, and Phanerozoic revolutions. *Paleobiology*, **21**, 125–52.

VERMEIJ, G. J. 1999. Inequality and the directionality of history. *American Naturalist*. **153**, 243–53.

VIALLE, N., ADNET, S. and CAPPETTA, H. 2011. A new shark and ray fauna from the Middle Miocene of Mazan, Vaucluse (southern France) and its importance in interpreting the paleoenvironment of marine deposits in the southern Rhodanian Basin. *Swiss Journal of Palaeontology*, **130**, 241 258.

WAGNER, A. 1860. Zur Charakteristik der Gattungen *Sauropsis* und *Pachycormus* nebst ihren Verwandten. *Gelehrte Anzeigen der Königlich Bayerischen Akademie eder Wissenschaften*, **1**, 209–227.

WAGNER, A. 1863. *Monographie der fossilen Fische aus den lithographischen Schiefern Bayerns*. Verlag der Akad, Münich, Germany, 138 pp.

WAINWRIGHT, P. C. and BELLWOOD, D. R. 2002. Ecomorphology of feeding in coral reef fishes. 33–56. *In* SALE, P. F. (ed.). *Coral Reef Fishes: Dynamics and Diversity in a Complex Ecosystem*, Elsevier, Amsterdam, Netherlands, 549 pp.

WAINWRIGHT, P. C. and RICHARD, B. A. 1995. Predicting patterns of prey use from morphology in fishes. *Environmental Biology of Fishes*, **44**, 97–113.

WALSH, S. 2001. The Bahía Inglesa Formation Bonebed: Genesis and Palaeontology of a Neogene Konzentrat Lagerstätte from north-central Chile. Postgraduate Thesis, University of Portsmouth, 440 pp.

WEILER, W. 1922. Beitrage zur Kenntnis der tertiären Fische des Mainzer Beckens I. *Abhandlungen der hessischen Geologischen Landesanstalt zu Darmstadt*, **6**, 69–135.

WEILER, W. 1931. Revision der Fischfauna des Septarientones von Wiesloch bei Heidelberg. Sitzungsberichte der Heidelberger Akademie der Wissenschaften, *Mathematisch-Naturwissenschaftliche Klasse*, **11**, 3–15.

WEITZEL, K. 1930. Drei Riesenfische aus den Solnhofener Schiefern von Langenaltheim. *Abhandlungen der Senckenbergischen Naturforschenden Gesellschaft*, **42**, 85–113.

WELTON, B. J. 2013*a*. *Cetorhinus* cf. *C. maximus* (Gunnerus) (Lamniformes: Cetorhinidae), a basking shark from the late Miocene empire formation, Coos Bay, Oregon. *Bulletin, Southern California Academy of Sciences*, **112**, 74–93.

WELTON, B. J. 2013*b*. *A New Archaic Basking Shark (Lamniformes: Cetorhinidae) from the Late Eocene of Western Oregon, USA, and Description of the Dentition, Gill Rakers and Vertebrae of the Recent Basking Shark* Cetorhinus maximus *(Gunnerus)*, New Mexico Museum of Natural History and Science, Albuquerque, New Mexico, 48 pp.

WELTON, B. J. 2014. A new fossil basking shark (Lamniformes: Cetorhinidae) from the middle Miocene Sharktooth Hill bonebed, Kern County, California. *Contributions in Science*, **522**, 29–44.

WENZ, S. 1967. *Complements a l'étude des poissons actinopterygiens du Jurassique francaise*, Cahiers de Paléontologie. CNRS, Paris, 276 pp.

WESTNEAT, M. W. 2005. Skull biomechanics and suction feeding in fishes. *Fish Physiology*, **23**, 29–75.

WESTOLL, T. S. 1944. The Haplolepidae, a new family of late Carboniferous bony fishes. *Bulletin of the American Museum of Natural History*, **83**, 1–122.

WIJNKER, E., BOR, T. J., WESSELINGH, F. P., MUNSTERMAN, D. K., BRINKHUIS, H., BURGER, A. W., VONHOF, H. B., POST, K., HOEDEMAKERS, K., JANSE, A. C.

and TAVERNE, N. 2008. Neogene stratigraphy of the Langenboom locality (Noord-brabant, the Netherlands). *Netherlands Journal of Geosciences*, **87**, 165–180.

WILEY, E. O. and JOHNSON, G. D. 2010. A teleost classification based on monophyletic groups. 123–182. *In* NELSON, J. S., SCHULTZE, H. P. and WILSON, M. V. H. (eds.). *Origin and Phylogenetic Interrelationships of Teleosts*, Verlag Dr Freidrich Pfeil, Münich, Germany, 480 pp.

WILLIAMS, M., BENTON, M. J. and ROSS, A. 2015. The Strawberry Bank Lagerstätte reveals insights into Early Jurassic life. *Journal of the Geological Society*, **172**, 683–692.

WINKLER, T. C. 1878. *Description d'une espèce nouvelle de* Pachycormus. Héritiers Loosjes, Haarlem, Netherlands, 9 pp.

WOODWARD, A. S. 1889*a*. *Catalogue of Fossil Fishes in the British Museum, Part I.* British Museum (Natural History), London, 474 pp.

WOODWARD, A. S. 1889*b*. On the palaeontology of sturgeons. *Proceedings of the Geologists' Association*, **11**, 24–44.

WOODWARD, A. S. 1890. Notes on some new and little-known British Jurassic fishes. *Report on the 59th Meeting of the British Association for the Advancement of Science*, 585–586.

WOODWARD, A. S. 1891. *Catalogue of Fossil Fishes in the British Museum, Part II.* British Museum (Natural History), London, 567 pp.

WOODWARD, A. S. 1895*a*. *Catalogue of Fossil Fishes in the British Museum, Part III.* British Museum (Natural History), London, 544 pp.

WOODWARD, A. S. 1895*b*. On the Fossil Fishes of the Upper Lias of Whitby, Part I. *Proceedings of the Yorkshire Geological Society*, **13**, 25–42.

WOODWARD, A. S. 1896. On the Fossil Fishes of the Upper Lias of Whitby, Part II. *Proceedings of the Yorkshire Geological Society*, **13**, 155–170.

WOODWARD, A. S. 1897. Notes on the collection of fossil fishes from the Upper Lias of Ilminster in the Bath Museum. *Proceedings of the Bath Natural History and Antiquarian Field Club*, **8**, 233–242.

WOODWARD, A. S. 1901. *Catalogue of Fossil Fishes in the British Museum, Part IV*. British Museum (Natural History), London, 636 pp.

WOODWARD, A. S. 1908*a*. On some remains of *Pachycormus* and *Hypsocormus* from the Jurassic of Normandy. *Memoires de Societe Linneanne de Normandie*, **23**, 29–34.

WOODWARD, A. S. 1908*b*. The Fossil Fishes of the English Chalk. Part IV. Plates XXVII–XXXII. *Monographs of the Palaeontographical Society*, **62**, 129–152.

WOODWARD, A. S. 1909. The Fossil Fishes of the English Chalk. Part V. Plates XXXIII–XXXVIII. *Monographs of the Palaeontographical Society*, **63**, 153–184.

WOODWARD, A. S. 1916. I.—On a New Specimen of the Liassic Pachycormid Fish *Saurostomus esocinus*, Agassiz. *Geological Magazine*, **3**, 49–51.

WOODWARD, A. S. 1942. LXXI.—The Beginning of the Teleostean Fishes. *Journal of Natural History*, **9**, 902–912.

WRETMAN, L., BLOM, H. and KEAR, B. P. 2016. Resolution of the Early Jurassic actinopterygian fish *Pachycormus* and a dispersal hypothesis for Pachycormiformes. *Journal of Vertebrate Paleontology*, **36**, e1206022-1–e1206022-8.

WRIGHT, D. F. 2017*a*. Phenotypic innovation and adaptive constraints in the evolutionary radiation of Palaeozoic crinoids. *Scientific Reports*, **7**, 13745.

WRIGHT, D. F. 2017*b*. Bayesian estimation of fossil phylogenies and the evolution of early

to middle Paleozoic crinoids (Echinodermata). *Journal of Paleontology*, **91**, 799–814.

XIE, W., LEWIS, P. O., FAN, Y., KUO, L. and CHEN, M. H. 2010. Improving marginal likelihood estimation for Bayesian phylogenetic model selection. *Systematic Biology*, **60**, 150–160.

YABUMOTO, Y. and UYENO, T. 1994. Late Mesozoic and Cenozoic fish faunas of Japan. *Island Arc*, 3, 255–269.

YABUMOTO, Y., GOTO, M. and UYENO, T. 1997. Dentition of a female megamouth, *Megachasma pelagios*, collected from Hakata Bay, Japan. 63–75. *In* YANO, K., MORRISSEY, J. F., YABUMOTO, Y. and NAKAYA, K. (eds.). *Biology of Megamouth Shark*. Tokai University Press, Tokyo, 63–75.

ZACHOS, J. C., DICKENS, G. R. and ZEEBE, R. E. 2008. An early Cenozoic perspective on greenhouse warming and carbon-cycle dynamics. *Nature*, **451**, 279.

ZHOU, Z. 2004. The origin and early evolution of birds: discoveries, disputes, and perspectives from fossil evidence. *Naturwissenschaften*, **91**, 455-471.

Appendix A

Supplementary Information associated with Chapter 1 'Introduction'

The known fossil record of pachycormiforms from relevant literature, with specimen numbers, localities and estimates ages given where available

Species	Specimen No.	Locality	Age	Reference
Asthenocormus titanus	JM.SOS 542a+b	Langenaltheim, Eichstätt, Germany	Tithonian	Lambers 1992; Sepkosk 2002
Asthenocormus sp.	IAA-Pv 330	Amenghino Formation, Antarctica	Late Kimmeridgian - Early Tithonian	Gouiric-Cavalli *et al.* 2019
Australopachycormus hurleyi	QM F.52641	Canary Station, Toolebuc Formation	Mid - late Albian	Kear 2007
Australopachycormus hurleyi	SAM P.40514	Warra Station, Toolebuc Formation, Australia	Mid - late Albian	Kear 2007
Australopachycormus hurleyi	NHMUK PV P.73611	Warra Station, Toolebuc Formation, Australia	Mid - late Albian	Liston & Maltese 2016
Bonnerichthys gladius	AMNH FF 1849	?Rooks county, Niobrara Formation, Kansas, UK	Late Coniacian - early Campanian	Friedman *et al.* 2013*a*
Bonnerichthys gladius	KUVP 50179	Barbour county, Alabama, USA	Late Santonian - early Campanian	Friedman *et al.* 2013*a*
Bonnerichthys gladius	NJSM 14668	Marshalltown Formation, Delaware, USA	Early late Campanian	Friedman *et al.* 2013*a*
Bonnerichthys gladius	SMU 76850	Clark county, Arizona, USA	Late Campanian	Friedman *et al.* 2013*a*

Bonnerichthys gladius	MMNS 5257	Clay county, Eutaw, Mississippi	Santonian	Friedman *et al.* 2013*a*
Bonnerichthys gladius	AUMP 1269	Dallas county, Alabama, USA	Late Santonian - early Campanian	Friedman *et al.* 2013*a*
Bonnerichthys gladius	AUMP 2050	Dallas county, Alabama, USA	Late Santonian - early Campanian	Friedman *et al.* 2013*a*
Bonnerichthys gladius	UAM PV2005.006.0124	Dallas county, Alabama, USA	Late Santonian - early Campanian	Friedman *et al.* 2013*a*
Bonnerichthys gladius	UAM PV2006.002.0004	Dallas county, Alabama, USA	Late Santonian - early Campanian	Friedman *et al.* 2013*a*
Bonnerichthys gladius	FMNH P 27365	Dallas county, Alabama, USA	Late Santonian - early Campanian	Friedman *et al.* 2013*a*
Bonnerichthys gladius	AMNH FF 19288	Fall River county, South Dakota, USA	Middle Campanian	Friedman *et al.* 2013*a*
Bonnerichthys gladius	NJSM 22466-70	Fannin county, Texas, UK	Mid-Campanian	Friedman *et al.* 2013*a*
Bonnerichthys gladius	LACM 10125	Fresno county, California, USA	Late early - early late Maastrichtian	Friedman *et al.* 2013*a*
Bonnerichthys gladius	UCMP 137224	Fresno county, California, USA	Late early - early late Maastrichtian	Friedman *et al.* 2013*a*
Bonnerichthys gladius	FHSM VP-212	Gove county, Niobrara Formation, Kansas, USA	Late Coniacian - early Campanian	Friedman *et al.* 2013*a*
Bonnerichthys gladius	FHSM VP-17428	Gove county, Niobrara Formation, Kansas, USA	Late Coniacian - early Campanian	Friedman *et al.* 2013*a*
Bonnerichthys gladius	FHSM VP-17457	Gove county, Niobrara Formation, Kansas, USA	Late Coniacian - early Campanian	Friedman *et al.* 2013*a*
Bonnerichthys gladius	FHSM VP-18986	Gove county, Niobrara Formation, Kansas, USA	Coniacian	Friedman *et al.* 2013*a*
Bonnerichthys gladius	FHSM VP-18987	Gove county, Niobrara Formation, Kansas, USA	Coniacian	Friedman *et al.* 2013*a*
Bonnerichthys gladius	KUVP 49505	Gove county, Niobrara Formation, Kansas, USA	Latest Coniacian	Friedman *et al.* 2013*a*
Bonnerichthys gladius	KUVP 55592	Gove county, Niobrara Formation, Kansas, USA	Santonian - Campanian	Friedman *et al.* 2013*a*
Bonnerichthys gladius	KUVP 65702	Gove county, Niobrara Formation, Kansas, USA	Santonian - Campanian	Friedman *et al.* 2013*a*
Bonnerichthys gladius	KUVP 66692	Gove county, Niobrara Formation, Kansas, USA	Santonian - Campanian	Friedman *et al.* 2013*a*

Bonnerichthys gladius	MCZ 13254	Gove county, Niobrara Formation, Kansas, USA	Late Coniacian - early Campanian	Friedman *et al.* 2013*a*
Bonnerichthys gladius	MCZ 13255	Gove county, Niobrara Formation, Kansas, USA	Late Coniacian - early Campanian	Friedman *et al.* 2013*a*
Bonnerichthys gladius	ROM 37168	Gove county, Niobrara Formation, Kansas, USA	Late Coniacian - early Campanian	Friedman *et al.* 2013*a*
Bonnerichthys gladius	AMNH FF 6316	Gove county, Niobrara Formation, Kansas, USA	Late Coniacian - early Campanian	Friedman *et al.* 2013*a*
Bonnerichthys gladius	KUVP 439	Graham county, Niobrara Formation, Kansas, USA	Santonian - Campanian	Friedman *et al.* 2013*a*
Bonnerichthys gladius	FMNH PF 27363	Hale county, Alabama, USA	Late Santonian - early Campanian	Friedman *et al.* 2013*a*
Bonnerichthys gladius	FMNH P 27364	Hale county, Alabama, USA	Late Santonian - early Campanian	Friedman *et al.* 2013*a*
Bonnerichthys gladius	UNSM 88507	Harlan county reservoir, Nebraska, USA	Middle Campanian	Friedman *et al.* 2013*a*
Bonnerichthys gladius	SDSM 7033	Hyde county, South Dakota, USA	Late Campanian	Friedman *et al.* 2013*a*
Bonnerichthys gladius	UNSM 50999	Knox county, Nebraska, USA	Early Maastrichtian	Friedman *et al.* 2013*a*
Bonnerichthys gladius	KUVP 84867	Lane county, Niobrara Formation, Kansas, USA	Santonian - Campanian	Friedman *et al.* 2013*a*
Bonnerichthys gladius	MMNS 3625	Lee county, Mississippi, USA	Middle - late Campanian	Friedman *et al.* 2013*a*
Bonnerichthys gladius	AMNH FF 2064	Logan county, Niobrara Formation, Kansas, USA	Santonian - Campanian	Friedman *et al.* 2013*a*
Bonnerichthys gladius	FHSM VP-17427	Logan county, Niobrara Formation, Kansas, USA	Late Coniacian - early Campanian	Friedman *et al.* 2013*a*
Bonnerichthys gladius	KUVP 465	Logan county, Niobrara Formation, Kansas, USA	Santonian - Campanian	Friedman *et al.* 2013*a*
Bonnerichthys gladius	KUVP 13995	Logan county, Niobrara Formation, Kansas, USA	Santonian - Campanian	Friedman *et al.* 2013*a*
Bonnerichthys gladius	KUVP 60620	Logan county, Niobrara Formation, Kansas, USA	Late Coniacian - early Campanian	Friedman *et al.* 2013*a*
Bonnerichthys gladius	KUVP 60692	Logan county, Niobrara Formation, Kansas, USA	Santonian - Campanian	Friedman *et al.* 2013*a*
Bonnerichthys gladius	LACM 126520	Logan county, Niobrara Formation, Kansas, USA	Santonian - Campanian	Friedman *et al.* 2013*a*

Bonnerichthys gladius	ROM 00876	Logan county, Niobrara Formation, Kansas, USA	Late Coniacian - early Campanian	Friedman *et al.* 2013*a*
Bonnerichthys gladius	KUVP 338	Logan county, Niobrara Formation, Kansas, USA	Middle Campanian	Friedman *et al.* 2013*a*
Bonnerichthys gladius	RMM 2794	Lowndes county, Alabama, USA	Middle - late Campanian	Friedman *et al.* 2013*a*
Bonnerichthys gladius	NJSM 15140	Marlboro Township, New Jersey, UK	Late Campanian	Friedman *et al.* 2013*a*
Bonnerichthys gladius	MMNS 3613	Monroe/Clay county, Mississippi, USA	Late Santonian - early Campanian	Friedman *et al.* 2013*a*
Bonnerichthys gladius	UCM 55412	Niobrara county, Wyoming, USA	Middle Campanian	Friedman *et al.* 2013*a*
Bonnerichthys gladius	MMNS 392	Noxubee county, Mississippi, USA	Middle - late Campanian	Friedman *et al.* 2013*a*
Bonnerichthys gladius	MMNS 5427	Noxubee county, Mississippi, USA	Middle - late Campanian	Friedman *et al.* 2013*a*
Bonnerichthys gladius	MMNS 5428	Noxubee county, Mississippi, USA	Middle - late Campanian	Friedman *et al.* 2013*a*
Bonnerichthys gladius	AMNH FF 6314	Western Kansas, Niobrara Formation, Kansas, USA	Late Coniacian - early Campanian	Friedman *et al.* 2013*a*
Bonnerichthys gladius	AMNH FF 6315	Western Kansas, Niobrara Formation, Kansas, USA	Late Coniacian - early Campanian	Friedman *et al.* 2013*a*
Euthynotus sp.	SMNH P.1037	Holzmaden, Posidonia Shale, Germany	Toarcian	Arratia & Lambers 1996
Euthynotus incognitus	SMNK 54051	Holzmaden, Posidonia Shale, Germany	Toarcian	Bürgin 2000
Euthynotus incognitus	SMNK 50166	Holzmaden, Posidonia Shale, Germany	Toarcian	Bürgin 2000
Euthynotus incognitus	MNHN P.10537/8	Holzmaden, Posidonia Shale, Germany	Toarcian	Blainville 1818; Wenz 1967
Euthynotus incognitus	AMNH FF 7540	Holzmaden, Posidonia Shale, Germany	Toarcian	Friedman 2012*a*
Euthynotus intermedius	MNHN P.821/ST C 32	Saint-Colombe, Yonne, France	Toarcian	Arambourg 1935; Wenz 1967; Friedman 2012*a*
Euthynotus sp.	T.2563/2564	-	Toarcian	Lambers 1992
Euthynotus sp.	T.7067	-	Toarcian	Lambers 1992
Euthynotus sp.	CM 677	-	Toarcian	Lambers 1992

Euthynotus incognitus	NHMUK P.881a	Ohmden, Posidonia Shale, Germany	Lower Toarcian	Lambers 1992
Euthynotus incognitus	NHMUK P.2044	Ohmden, Posidonia Shale, Germany	Lower Toarcian	Lambers 1992
Euthynotus incognitus	NHMUK P.4366	-	Toarcian	Lambers 1992
Euthynotus sp.	MB 1485	-	Lower Jurassic	Gouiric-Cavalli & Cione 2015
Euthynotus sp.	TU224	Grancourt Shale Base, Luxembourg	Toarcian	Delsate *et al.* 1999
Euthynotus sp.	TU228a/b	Grancourt Shale Base, Luxembourg	Toarcian	Delsate *et al.* 1999
Euthynotus sp.	MICJ00	Grancourt Shale Base, Luxembourg	Toarcian	Delsate *et al.* 1999
Euthynotus sp.	TU173	Grancourt Shale Base, Luxembourg	Toarcian	Delsate *et al.* 1999
Euthynotus sp.	P11	Grancourt Shale Base, Luxembourg	Toarcian	Delsate *et al.* 1999
Euthynotus sp.	P13	Grancourt Shale Base, Luxembourg	Toarcian	Delsate *et al.* 1999
Euthynotus sp.	P08a/b	Grancourt Shale Base, Luxembourg	Toarcian	Delsate *et al.* 1999
Hypsocormus macrodon	CM 5399	Birkhof, Solnhofen, Germany	Tithonian	Lambers 1992; Friedman 2012*a*
Hypsocormus macrodon	MCZ 3096	Birkhof, Solnhofen, Germany	Tithonian	Lambers 1992; Friedman 2012*a*
Hypsocormus macrodon	NHMUK P.6011	Birkhof, Solnhofen, Germany	Tithonian	Lambers 1992; Friedman 2012*a*
Hypsocormus insignis	SMNH P.5698	Birkhof, Solnhofen, Germany	Upper Jurassic	Arratia & Lambers 1996
Hypsocormus tenuirostris	NHMUK P.10579	Dogsthorpe pit, Peterborough, Cambridgeshire, UK	Middle Callovian	Lambers 1992
Hypsocormus insignis	BSPG AS V.4a/b	-	Middle - Late Jurassic	Lambers 1992
Hypsocormus insignis	NHMUK P.954	Solnhofen, Germany	Kimmeridgian	Woodward 1895*a*; Lambers 1992
Hypsocormus insignis	NHMUK P.6942	Solnhofen, Germany	Kimmeridgian	Woodward 1895*a*; Lambers 1992

Hypsocormus insignis	NHMUK P.7181	Solnhofen, Germany	Kimmeridgian	Woodward 1895*a*; Lambers 1992
Hypsocormus insignis	CM 5398	-	Middle - Late Jurassic	Lambers 1992
Hypsocormus insignis	JM.SOS 539a	-	Middle - Late Jurassic	Lambers 1992
Hypsocormus insignis	JM.SOS 3554	-	Middle - Late Jurassic	Lambers 1992
Hypsocormus insignis	JM.SOS 3557	-	Middle - Late Jurassic	Lambers 1992
Hypsocormus macrodon	JM.SOS 3574	-	Middle - Late Jurassic	Lambers 1992
Hypsocormus leedsi	NHMUK P.6913	Huntingdonshire, UK	Oxfordian	Woodward 1895*a*; Lambers 1992
Hypsocormus tenuirostris	NHMUK P.10906	-	Middle - Late Jurassic	Lambers 1992
Hyspcormus sp.	P37	Grancourt Shale Base, Luxembourg	Toarcian	Delsate *et al.* 1999
Leedsichthys problematicus	Private	Alan Dawn Quest Pit, Cambridgeshire, UK	Middle Callovian	Liston 2010
Leedsichthys problematicus	PETMG F121	Buntings Lane, near Farcet, UK	Middle Callovian	Liston 2010
Leedsichthys problematicus	BMNH P.62054	Buntings Lane, near Farcet, UK	Middle Callovian	Liston 2010
Leedsichthys problematicus	GLAHM 132787	Cap de la Hève, Normandy, France	Upper Kimmeridgian	Liston 2010; Liston 2015
Leedsichthys problematicus	BMNH 46355	Christian Malford, Wiltshire, UK	Middle Callovian	Liston 2010
Leedsichthys problematicus	BMNH P.6921	Dogsthorpe pit, Peterborough, Cambridgeshire, UK	Middle Callovian	Liston 2010
Leedsichthys problematicus	BMNH P.6922	Dogsthorpe pit, Peterborough, Cambridgeshire, UK	Middle Callovian	Liston 2010
Leedsichthys problematicus	BMNH P.10000	Dogsthorpe pit, Peterborough, Cambridgeshire, UK	Middle Callovian	Liston 2010
Leedsichthys problematicus	BMNH P.10156	Dogsthorpe pit, Peterborough, Cambridgeshire, UK	Middle Callovian	Liston 2010

Leedsichthys problematicus	BMNH P.66340	Dogsthorpe pit, Peterborough, Cambridgeshire, UK	Middle Callovian	Liston 2010
Leedsichthys problematicus	LEICT G1.2010.2	Dogsthorpe pit, Peterborough, Cambridgeshire, UK	Middle Callovian	Liston 2010
Leedsichthys problematicus	LEIUG 96085	Dogsthorpe pit, Peterborough, Cambridgeshire, UK	Middle Callovian	Liston 2010
Leedsichthys problematicus	I-190173	East of Antofagasta, Chile	Oxfordian	Liston 2010
Leedsichthys problematicus	I8-021173	East of Antofagasta, Chile	Oxfordian	Liston 2010
Leedsichthys problematicus	CAMSM J.46873	Fletton, Peterborough, Cambridgeshire, UK	Middle Callovian	Liston 2010
Leedsichthys problematicus	LEICT G472.1897	Fletton, Peterborough, Cambridgeshire, UK	Middle Callovian	Liston 2010
Leedsichthys problematicus	CAMSM J.27416	Fletton, Huntingdonshire, UK	Middle Callovian	Liston 2010
Leedsichthys problematicus	CAMSM J.27417	Fletton, Huntingdonshire, UK	Middle Callovian	Liston 2010
Leedsichthys problematicus	CAMSM J.27418	Fletton, Huntingdonshire, UK	Middle Callovian	Liston 2010
Leedsichthys problematicus	CAMSM J.27419	Fletton, Huntingdonshire, UK	Middle Callovian	Liston 2010
Leedsichthys problematicus	CAMSM J.27420	Fletton, Huntingdonshire, UK	Middle Callovian	Liston 2010
Leedsichthys problematicus	CAMSM J.27421	Fletton, Huntingdonshire, UK	Middle Callovian	Liston 2010
Leedsichthys problematicus	CAMSM J.27422	Fletton, Huntingdonshire, UK	Middle Callovian	Liston 2010
Leedsichthys problematicus	CAMSM J.27423	Fletton, Huntingdonshire, UK	Middle Callovian	Liston 2010
Leedsichthys problematicus	CAMSM J.46876	Fletton, Huntingdonshire, UK	Middle Callovian	Liston 2010
Leedsichthys problematicus	CAMSM J.66920	Fletton, Huntingdonshire, UK	Middle Callovian	Liston 2010
Leedsichthys problematicus	CAMSM J.66921	Fletton, Huntingdonshire, UK	Middle Callovian	Liston 2010

Leedsichthys problematicus	CAMSM J.66922	Fletton, Huntingdonshire, UK	Middle Callovian	Liston 2010
Leedsichthys problematicus	CAMSM J.66923	Fletton, Huntingdonshire, UK	Middle Callovian	Liston 2010
Leedsichthys problematicus	CAMSM J.66924	Fletton, Huntingdonshire, UK	Middle Callovian	Liston 2010
Leedsichthys problematicus	CAMSM J.66925	Fletton, Huntingdonshire, UK	Middle Callovian	Liston 2010
Leedsichthys problematicus	CAMSM J.66926	Fletton, Huntingdonshire, UK	Middle Callovian	Liston 2010
Leedsichthys problematicus	CAMSM J.66928	Fletton, Huntingdonshire, UK	Middle Callovian	Liston 2010
Leedsichthys problematicus	CAMSM J.66929	Fletton, Huntingdonshire, UK	Middle Callovian	Liston 2010
Leedsichthys problematicus	CAMSM J.66935	Fletton, Huntingdonshire, UK	Middle Callovian	Liston 2010
Leedsichthys problematicus	CAMSM J.66936	Fletton, Huntingdonshire, UK	Middle Callovian	Liston 2010
Leedsichthys problematicus	CAMSM J.66937	Fletton, Huntingdonshire, UK	Middle Callovian	Liston 2010
Leedsichthys problematicus	CAMSM J.66938	Fletton, Huntingdonshire, UK	Middle Callovian	Liston 2010
Leedsichthys problematicus	CAMSM J.66939	Fletton, Huntingdonshire, UK	Middle Callovian	Liston 2010
Leedsichthys problematicus	CAMSM J.66940	Fletton, Huntingdonshire, UK	Middle Callovian	Liston 2010
Leedsichthys problematicus	CAMSM J.66941	Fletton, Huntingdonshire, UK	Middle Callovian	Liston 2010
Leedsichthys problematicus	CAMSM J.67413	Fletton, Huntingdonshire, UK	Middle Callovian	Liston 2010
Leedsichthys problematicus	CAMSM J.67414	Fletton, Huntingdonshire, UK	Middle Callovian	Liston 2010
Leedsichthys problematicus	CAMSM J.67415	Fletton, Huntingdonshire, UK	Middle Callovian	Liston 2010
Leedsichthys problematicus	CAMSM J.67416	Fletton, Huntingdonshire, UK	Middle Callovian	Liston 2010
Leedsichthys problematicus	CAMSM J.67417	Fletton, Huntingdonshire, UK	Middle Callovian	Liston 2010

Leedsichthys problematicus	CAMSM J.67418	Fletton, Huntingdonshire, UK	Middle Callovian	Liston 2010
Leedsichthys problematicus	CAMSM J.67419	Fletton, Huntingdonshire, UK	Middle Callovian	Liston 2010
Leedsichthys problematicus	CAMSM J.67420	Fletton, Huntingdonshire, UK	Middle Callovian	Liston 2010
Leedsichthys problematicus	CAMSM J.67421	Fletton, Huntingdonshire, UK	Middle Callovian	Liston 2010
Leedsichthys problematicus	CAMSM J.67422	Fletton, Huntingdonshire, UK	Middle Callovian	Liston 2010
Leedsichthys problematicus	CAMSM J.67423	Fletton, Huntingdonshire, UK	Middle Callovian	Liston 2010
Leedsichthys problematicus	CAMSM J.67424	Fletton, Huntingdonshire, UK	Middle Callovian	Liston 2010
Leedsichthys problematicus	CAMSM J.67425	Fletton, Huntingdonshire, UK	Middle Callovian	Liston 2010
Leedsichthys problematicus	CAMSM J.67426	Fletton, Huntingdonshire, UK	Middle Callovian	Liston 2010
Leedsichthys problematicus	CAMSM J.67427	Fletton, Huntingdonshire, UK	Middle Callovian	Liston 2010
Leedsichthys problematicus	CAMSM J.67428	Fletton, Huntingdonshire, UK	Middle Callovian	Liston 2010
Leedsichthys problematicus	CAMSM J.67429	Fletton, Huntingdonshire, UK	Middle Callovian	Liston 2010
Leedsichthys problematicus	CAMSM J.67432	Fletton, Huntingdonshire, UK	Middle Callovian	Liston 2010
Leedsichthys problematicus	CAMSM J.67437	Fletton, Huntingdonshire, UK	Middle Callovian	Liston 2010
Leedsichthys problematicus	CAMSM J.67438	Fletton, Huntingdonshire, UK	Middle Callovian	Liston 2010
Leedsichthys problematicus	CAMSM J.67439	Fletton, Huntingdonshire, UK	Middle Callovian	Liston 2010
Leedsichthys problematicus	CAMSM J.67440	Fletton, Huntingdonshire, UK	Middle Callovian	Liston 2010
Leedsichthys problematicus	CAMSM J.67471	Fletton, Huntingdonshire, UK	Middle Callovian	Liston 2010
Leedsichthys problematicus	CAMSM J.67472	Fletton, Huntingdonshire, UK	Middle Callovian	Liston 2010

Leedsichthys problematicus	CAMSM J.67473	Fletton, Huntingdonshire, UK	Middle Callovian	Liston 2010
Leedsichthys problematicus	CAMSM J.67474	Fletton, Huntingdonshire, UK	Middle Callovian	Liston 2010
Leedsichthys problematicus	CAMSM J.67475	Fletton, Huntingdonshire, UK	Middle Callovian	Liston 2010
Leedsichthys problematicus	CAMSM J.67476	Fletton, Huntingdonshire, UK	Middle Callovian	Liston 2010
Leedsichthys problematicus	CAMSM J.67477	Fletton, Huntingdonshire, UK	Middle Callovian	Liston 2010
Leedsichthys problematicus	CAMSM J.67479	Fletton, Huntingdonshire, UK	Middle Callovian	Liston 2010
Leedsichthys problematicus	CAMSM J.67480	Fletton, Huntingdonshire, UK	Middle Callovian	Liston 2010
Leedsichthys problematicus	CAMSM J.67481	Fletton, Huntingdonshire, UK	Middle Callovian	Liston 2010
Leedsichthys problematicus	CAMSM J.67483	Fletton, Huntingdonshire, UK	Middle Callovian	Liston 2010
Leedsichthys problematicus	CAMSM X.50109	Fletton, Huntingdonshire, UK	Middle Callovian	Liston 2010
Leedsichthys problematicus	CAMSM X.50110	Fletton, Huntingdonshire, UK	Middle Callovian	Liston 2010
Leedsichthys problematicus	CAMSM X.50111	Fletton, Huntingdonshire, UK	Middle Callovian	Liston 2010
Leedsichthys problematicus	CAMSM X.50112	Fletton, Huntingdonshire, UK	Middle Callovian	Liston 2010
Leedsichthys problematicus	CAMSM X.50113	Fletton, Huntingdonshire, UK	Middle Callovian	Liston 2010
Leedsichthys problematicus	CAMSM X.50114	Fletton, Huntingdonshire, UK	Middle Callovian	Liston 2010
Leedsichthys problematicus	CAMSM X.50115	Fletton, Huntingdonshire, UK	Middle Callovian	Liston 2010
Leedsichthys problematicus	CAMSM X.50116	Fletton, Huntingdonshire, UK	Middle Callovian	Liston 2010
Leedsichthys problematicus	CAMSM J.27426	Fletton, Northamptonshire, UK	Middle Callovian	Liston 2010
Leedsichthys problematicus	CAMSM J.27427	Fletton, Northamptonshire, UK	Middle Callovian	Liston 2010

Leedsichthys problematicus	CAMSM J.27428	Fletton, Northamptonshire, UK	Middle Callovian	Liston 2010
Leedsichthys problematicus	CAMSM J.27429	Fletton, Northamptonshire, UK	Middle Callovian	Liston 2010
Leedsichthys problematicus	CAMSM J.27430	Fletton, Northamptonshire, UK	Middle Callovian	Liston 2010
Leedsichthys problematicus	CAMSM J.27431	Fletton, Northamptonshire, UK	Middle Callovian	Liston 2010
Leedsichthys problematicus	CAMSM J.27432	Fletton, Northamptonshire, UK	Middle Callovian	Liston 2010
Leedsichthys problematicus	CAMSM J.27433	Fletton, Northamptonshire, UK	Middle Callovian	Liston 2010
Leedsichthys problematicus	CAMSM J.27434	Fletton, Northamptonshire, UK	Middle Callovian	Liston 2010
Leedsichthys problematicus	CAMSM J.27435	Fletton, Northamptonshire, UK	Middle Callovian	Liston 2010
Leedsichthys problematicus	CAMSM J.27436	Fletton, Northamptonshire, UK	Middle Callovian	Liston 2010
Leedsichthys problematicus	CAMSM J.27437	Fletton, Northamptonshire, UK	Middle Callovian	Liston 2010
Leedsichthys problematicus	CAMSM J.27438	Fletton, Northamptonshire, UK	Middle Callovian	Liston 2010
Leedsichthys problematicus	CAMSM J.27439	Fletton, Northamptonshire, UK	Middle Callovian	Liston 2010
Leedsichthys problematicus	CAMSM J.27440	Fletton, Northamptonshire, UK	Middle Callovian	Liston 2010
Leedsichthys problematicus	CAMSM J.27441	Fletton, Northamptonshire, UK	Middle Callovian	Liston 2010
Leedsichthys problematicus	CAMSM J.27442	Fletton, Northamptonshire, UK	Middle Callovian	Liston 2010
Leedsichthys problematicus	CAMSM J.27443	Fletton, Northamptonshire, UK	Middle Callovian	Liston 2010
Leedsichthys problematicus	CAMSM J.27444	Fletton, Northamptonshire, UK	Middle Callovian	Liston 2010
Leedsichthys problematicus	CAMSM J.27445	Fletton, Northamptonshire, UK	Middle Callovian	Liston 2010
Leedsichthys problematicus	CAMSM J.35320	Fletton, Northamptonshire, UK	Middle Callovian	Liston 2010

Leedsichthys problematicus	CAMSM J.46874	Fletton, Northamptonshire, UK	Middle Callovian	Liston 2010
Leedsichthys problematicus	CAMSM J.66930	Fletton, Northamptonshire, UK	Middle Callovian	Liston 2010
Leedsichthys problematicus	CAMSM J.66931	Fletton, Northamptonshire, UK	Middle Callovian	Liston 2010
Leedsichthys problematicus	CAMSM J.66932	Fletton, Northamptonshire, UK	Middle Callovian	Liston 2010
Leedsichthys problematicus	CAMSM J.66933	Fletton, Northamptonshire, UK	Middle Callovian	Liston 2010
Leedsichthys problematicus	CAMSM J.66942	Fletton, Northamptonshire, UK	Middle Callovian	Liston 2010
Leedsichthys problematicus	CAMSM J.66943	Fletton, Northamptonshire, UK	Middle Callovian	Liston 2010
Leedsichthys problematicus	CAMSM J.66944	Fletton, Northamptonshire, UK	Middle Callovian	Liston 2010
Leedsichthys problematicus	CAMSM J.67430	Fletton, Northamptonshire, UK	Middle Callovian	Liston 2010
Leedsichthys problematicus	CAMSM J.67431	Fletton, Northamptonshire, UK	Middle Callovian	Liston 2010
Leedsichthys problematicus	CAMSM J.67433	Fletton, Northamptonshire, UK	Middle Callovian	Liston 2010
Leedsichthys problematicus	CAMSM J.67434	Fletton, Northamptonshire, UK	Middle Callovian	Liston 2010
Leedsichthys problematicus	CAMSM J.67435	Fletton, Northamptonshire, UK	Middle Callovian	Liston 2010
Leedsichthys problematicus	CAMSM J.67436	Fletton, Northamptonshire, UK	Middle Callovian	Liston 2010
Leedsichthys problematicus	CAMSM J.67441	Fletton, Northamptonshire, UK	Middle Callovian	Liston 2010
Leedsichthys problematicus	CAMSM J.67442	Fletton, Northamptonshire, UK	Middle Callovian	Liston 2010
Leedsichthys problematicus	CAMSM J.67443	Fletton, Northamptonshire, UK	Middle Callovian	Liston 2010
Leedsichthys problematicus	CAMSM J.67444	Fletton, Northamptonshire, UK	Middle Callovian	Liston 2010
Leedsichthys problematicus	CAMSM J.67445	Fletton, Northamptonshire, UK	Middle Callovian	Liston 2010

Leedsichthys problematicus	CAMSM J.67446	Fletton, Northamptonshire, UK	Middle Callovian	Liston 2010
Leedsichthys problematicus	CAMSM J.67447	Fletton, Northamptonshire, UK	Middle Callovian	Liston 2010
Leedsichthys problematicus	CAMSM J.67448	Fletton, Northamptonshire, UK	Middle Callovian	Liston 2010
Leedsichthys problematicus	CAMSM J.67449	Fletton, Northamptonshire, UK	Middle Callovian	Liston 2010
Leedsichthys problematicus	CAMSM J.67450	Fletton, Northamptonshire, UK	Middle Callovian	Liston 2010
Leedsichthys problematicus	CAMSM J.67451	Fletton, Northamptonshire, UK	Middle Callovian	Liston 2010
Leedsichthys problematicus	CAMSM J.67452	Fletton, Northamptonshire, UK	Middle Callovian	Liston 2010
Leedsichthys problematicus	CAMSM J.67453	Fletton, Northamptonshire, UK	Middle Callovian	Liston 2010
Leedsichthys problematicus	CAMSM J.67454	Fletton, Northamptonshire, UK	Middle Callovian	Liston 2010
Leedsichthys problematicus	CAMSM J.67455	Fletton, Northamptonshire, UK	Middle Callovian	Liston 2010
Leedsichthys problematicus	CAMSM J.67456	Fletton, Northamptonshire, UK	Middle Callovian	Liston 2010
Leedsichthys problematicus	CAMSM J.67457	Fletton, Northamptonshire, UK	Middle Callovian	Liston 2010
Leedsichthys problematicus	CAMSM J.67458	Fletton, Northamptonshire, UK	Middle Callovian	Liston 2010
Leedsichthys problematicus	CAMSM J.67459	Fletton, Northamptonshire, UK	Middle Callovian	Liston 2010
Leedsichthys problematicus	CAMSM J.67460	Fletton, Northamptonshire, UK	Middle Callovian	Liston 2010
Leedsichthys problematicus	CAMSM J.67461	Fletton, Northamptonshire, UK	Middle Callovian	Liston 2010
Leedsichthys problematicus	CAMSM J.67462	Fletton, Northamptonshire, UK	Middle Callovian	Liston 2010
Leedsichthys problematicus	CAMSM J.67463	Fletton, Northamptonshire, UK	Middle Callovian	Liston 2010
Leedsichthys problematicus	CAMSM J.67464	Fletton, Northamptonshire, UK	Middle Callovian	Liston 2010

Leedsichthys problematicus	CAMSM J.67465	Fletton, Northamptonshire, UK	Middle Callovian	Liston 2010
Leedsichthys problematicus	CAMSM J.67466	Fletton, Northamptonshire, UK	Middle Callovian	Liston 2010
Leedsichthys problematicus	LEICT G1.2010.1	Kempston Quarry, Bedfordshire, UK	Middle Callovian	Liston 2010
Leedsichthys problematicus	PETMG F34	King's Dyke, Cambridgeshire, UK	Middle Callovian	Liston 2010
Leedsichthys problematicus	LEIUG 114604	LBC pit, Calvert, Cambridgeshire, UK	Middle Callovian	Liston 2010
Leedsichthys problematicus	LEIUG 96086	Market Deeping, Cambridgeshire, UK	Middle Callovian	Liston 2010
Leedsichthys problematicus	LEIUG 96087	Orton Pit, Cambridgeshire, UK	Middle Callovian	Liston 2010
Leedsichthys problematicus	LEICT G236.1902 /G520.1993	Peterborough, Cambridgeshire, UK	Middle Callovian	Liston 2010
Leedsichthys problematicus	LEICT G473.1897	Peterborough, Cambridgeshire, UK	Middle Callovian	Liston 2010
Leedsichthys problematicus	LEICT G474.1897	Peterborough, Cambridgeshire, UK	Middle Callovian	Liston 2010
Leedsichthys problematicus	LEICT G475.1897	Peterborough, Cambridgeshire, UK	Middle Callovian	Liston 2010
Leedsichthys problematicus	LEICT G476.1897	Peterborough, Cambridgeshire, UK	Middle Callovian	Liston 2010
Leedsichthys problematicus	LEICT G477.1897	Peterborough, Cambridgeshire, UK	Middle Callovian	Liston 2010
Leedsichthys problematicus	LEICT G478.1897	Peterborough, Cambridgeshire, UK	Middle Callovian	Liston 2010
Leedsichthys problematicus	LEICT G479.1897	Peterborough, Cambridgeshire, UK	Middle Callovian	Liston 2010
Leedsichthys problematicus	LEICT G343.1896	Peterborough, Cambridgeshire, UK	Middle Callovian	Liston 2010
Leedsichthys problematicus	LEICT G344.1896	Peterborough, Cambridgeshire, UK	Middle Callovian	Liston 2010
Leedsichthys problematicus	LEICT G345.1896	Peterborough, Cambridgeshire, UK	Middle Callovian	Liston 2010

Leedsichthys problematicus	LEICT G519.1993	Peterborough, Cambridgeshire, UK	Middle Callovian	Liston 2010
Leedsichthys problematicus	LEICT G1312.1899	Peterborough, Cambridgeshire, UK	Middle Callovian	Liston 2010
Leedsichthys problematicus	LEICT G393.1896	Peterborough, Cambridgeshire, UK	Middle Callovian	Liston 2010
Leedsichthys problematicus	LEICT G3348.1898	Peterborough, Cambridgeshire, UK	Middle Callovian	Liston 2010
Leedsichthys notodectes	SMNK 2573.PAL	Quebrada Corral, Atacama Desert, Chile	Oxfordian	Liston 2010
Leedsichthys problematicus	(unnumbered)	Quebrada del Profeta, Chile	Oxfordian	Liston 2010
Leedsichthys problematicus	PETMG F174	Star Pit, Whittlesey, Cambridgeshire, UK	Middle Callovian	Liston 2010
Leedsichthys problematicus	GLAHM 109519	Stormer Quarry, Wiehengebirge, Germany	Kimmeridgian	Liston 2010
Leedsichthys problematicus	MOZ-Pv 1788	Vaca Muerta, Cerro Lorena, Argentina	Tithonian	Gouiric-Cavalli 2017
Leedsichthys problematicus	Private	Villers-sur-Mer, Normandy, France	Callovian	Liston 2010
Leedsichthys problematicus	BMNH 32581	Villers-sur-Mer, Normandy, France	Callovian	Liston 2010
Leedsichthys problematicus	WMfN PM 17006/8	Wallucke, Wiehengebirge, Germany	Middle-Upper Callovian	Liston 2010
Leedsichthys problematicus	WMfN PM 17006/1	Wallucke, Wiehengebirge, Germany	Middle-Upper Callovian	Liston 2010
Leedsichthys problematicus	WMfN PM 17005/2	Wallucke, Wiehengebirge, Germany	Middle-Upper Callovian	Liston 2010
Leedsichthys problematicus	WMfN PM 17005/23	Wallucke, Wiehengebirge, Germany	Middle-Upper Callovian	Liston 2010
Leedsichthys problematicus	WMfN PM 17005/24	Wallucke, Wiehengebirge, Germany	Middle-Upper Callovian	Liston 2010
Leedsichthys problematicus	PHB W 138/4	Wallucke, Wiehengebirge, Germany	Middle-Upper Callovian	Liston 2010

Leedsichthys problematicus	PMM 19.1-21.1, 23.1	Wallucke, Wiehengebirge, Germany	Middle-Upper Callovian	Liston 2010
Leedsichthys problematicus	GLANHM 109518	Wallucke, Wiehengebirge, Germany	Middle-Upper Callovian	Liston 2010
Leedsichthys problematicus	CAMSM J.27425	Whittlesey, Cambridgeshire, UK	Middle Callovian	Liston 2010
Leedsichthys problematicus	CAMSM J.46877	Whittlesey, Cambridgeshire, UK	Middle Callovian	Liston 2010
Leedsichthys problematicus	CAMSM J.46878	Whittlesey, Cambridgeshire, UK	Middle Callovian	Liston 2010
Leedsichthys problematicus	CAMSM J.46879	Whittlesey, Cambridgeshire, UK	Middle Callovian	Liston 2010
Leedsichthys problematicus	CAMSM J.66124	Whittlesey, Cambridgeshire, UK	Middle Callovian	Liston 2010
Leedsichthys problematicus	CAMSM J.66126	Whittlesey, Cambridgeshire, UK	Middle Callovian	Liston 2010
Leedsichthys problematicus	CAMSM J.66127	Whittlesey, Cambridgeshire, UK	Middle Callovian	Liston 2010
Leedsichthys problematicus	CAMSM J.66128	Whittlesey, Cambridgeshire, UK	Middle Callovian	Liston 2010
Leedsichthys problematicus	CAMSM X.50117	Whittlesey, Cambridgeshire, UK	Middle Callovian	Liston 2010
Leedsichthys problematicus	CAMSM X.50118	Whittlesey, Cambridgeshire, UK	Middle Callovian	Liston 2010
Leedsichthys problematicus	PETMG F.174	Whittlesey, Cambridgeshire, UK	Middle Callovian	Liston 2010
Leedsichthys problematicus	OUMNH J.1803/1	Wolvercote, Oxfordshire, UK	Middle Callovian	Liston 2010
Martillichthys renwickae	PETMG F.161	Dogsthorpe pit, Peterborough, Cambridgeshire, UK	Middle Callovian	Liston 2006; Liston 2008
Martillichthys renwickae	NHMUK PV P.61563	Dogsthorpe pit, Peterborough, Cambridgeshire, UK	Middle Callovian	Liston 2006; Liston 2008; Dobson *et al.* 2019
Ohmdenia multidentata	GPIT 1017/1	Ohmden, Posidonia Shale, Germany	Lower Toarcian	Hauff 1953; Friedman 2012*a*
Orthocormus cornutus	JM.SOS 3751a+b	Birkhof, Solnhofen, Germany	Upper Jurassic	Arratia & Schultze 2013

Orthocormus cornutus	JM.SOS 3460	Birkhof, Solnhofen, Germany	Upper Jurassic	Arratia & Schultze 2013
Orthocormus cornutus	SNMH P.6153	Birkhof, Solnhofen, Germany	Toarcian	Friedman 2012*a*
Orthocormus cornutus	AMNH FF 19639	Birkhof, Solnhofen, Germany	Toarcian	Rayner 1948; Jessen 1972; Lambers 1988; Lambers 1992
Orthocormus roeperi	BSPG 1993 XVIII-VFKO B16	Brunn, Germany	Upper Kimmeridgian	Arratia & Schultze 2013
Orthocormus teyleri	T.14836	Cerin, Ain, France	Kimmeridgian	Lamber 1988; Lambers 1992
Orthocormus cornutus	SM 1863	Langenaltheim, Eichstätt, Germany	Tithonian	Weitzel 1930; Lambers 1992
Orthocormus cornutus	JM.SOS 3336	-	Kimmeridgian	Lambers 1992
Pachycormid indet.	NHMUK PV P.41669	Sherbone, Dorset, UK	Bajocian	Friedman *et al.* 2010
Pachycormid indet.	-	Marambio, Antarctica	Latest Maastrichtian - Danian	Cione *et al.* 2018
Pachycormus sp.	MB 2349	Bad Boll, Posidonia Shale, Germany	Toarcian	Arratia & Lambers 1996
Pachycormus macropterus	MNHN-F-JRE 50	Beaune, Côte-d'Or, Bourgogne, France	Toarcian	Blainville 1818
Pachycormus macropterus	NHMUK PV OR 32433	Curcy, Normandy, France	Toarcian	Rayner 1948; Patterson 1975; Mainwaring 1978; Lambers 1992
Pachycormus sp.	MNHN 10530	Curcy, Normandy, France	Toarcian	Wenz 1967
Pachycormus sp.	MNHN 1872-493	Curcy, Normandy, France	Toarcian	Wenz 1967
Pachycormus curtus	NHMUK P.32434	Curcy, Normandy, France	Toarcian	Wenz 1967; Patterson 1975
Pachycormus sp.	NHMUK P.32425	Curcy, Normandy, France	Toarcian	Patterson 1975

Pachycormus macropterus	?	Curcy, Normandy, France	Toarcian	Lehman 1949
Pachycormus sp.	SMNH P.6152	Holzmaden, Posidonia Shale, Germany	Toarcian	Arratia & Lambers 1996
Pachycormus sp.	SMNH P.6151	Holzmaden, Posidonia Shale, Germany	Toarcian	Arratia & Lambers 1996
Pachycormus macropterus	BRLSI M1297	Strawberry Bank, Ilminster, Somerset, UK	Toarcian	Cawley *et al.* 2018
Pachycormus macropterus	BRLSI M1299	Strawberry Bank, Ilminster, Somerset, UK	Toarcian	Cawley *et al.* 2018
Pachycormus macropterus	BRLSI M1320	Strawberry Bank, Ilminster, Somerset, UK	Toarcian	Cawley *et al.* 2018
Pachycormus macropterus	BRLSI M1332	Strawberry Bank, Ilminster, Somerset, UK	Toarcian	Cawley *et al.* 2018
Pachycormus macropterus	BRLSI M1359	Strawberry Bank, Ilminster, Somerset, UK	Toarcian	Cawley *et al.* 2018
Pachycormus macropterus	BRLSI M1389	Strawberry Bank, Ilminster, Somerset, UK	Toarcian	Cawley *et al.* 2018
Pachycormus macropterus	BRLSI M1395	Strawberry Bank, Ilminster, Somerset, UK	Toarcian	Cawley *et al.* 2018
Pachycormus sp.	BRLSI M1341	Strawberry Bank, Ilminster, Somerset, UK	Toarcian	Cawley *et al.* 2018
Pachycormus sp.	BRLSI M1351	Strawberry Bank, Ilminster, Somerset, UK	Toarcian	Cawley *et al.* 2018
Pachycormus sp.	BRLSI M1366	Strawberry Bank, Ilminster, Somerset, UK	Toarcian	Cawley *et al.* 2018
Pachycormus sp.	BRLSI M1393	Strawberry Bank, Ilminster, Somerset, UK	Toarcian	Cawley *et al.* 2018
Pachycormus sp.	BRLSI M1361a	Strawberry Bank, Ilminster, Somerset, UK	Toarcian	**Chapter 3**
Pachycormus macropterus	BRLSI M1311	Strawberry Bank, Ilminster, Somerset, UK	Toarcian	**Chapter 3**
Pachycormus curtus	SMNK U.49.1911	-	Toarcian	Lambers 1992
Pachycormus curtus	NHMUK P.2405b	-	Toarcian	Lambers 1992
Pachycormus curtus	T.18156	-	Toarcian	Lambers 1992
Pachycormus macropterus	SMNK U.338.1984	-	Toarcian	Lambers 1992

Pachycormus macropterus	NHMUK P.12913	-	Toarcian	Mainwaring 1978; Lambers 1992
Pachycormus macropterus	NHMUK P.51667	-	Toarcian	Lambers 1992
Pachycormus bollensis	T.13230	-	Toarcian	Lambers 1992
Pachycormus sp.	T.2566	-	Toarcian	Lambers 1992
Pachycormus sp.	T.17068	-	Toarcian	Lambers 1992
Pachycormus sp.	NHMUK P.59545	-	Toarcian	Mainwaring 1978
Pachycormus curtus	NHMUK P.10145	-	Toarcian	Mainwaring 1978
Pachycormus sp.	NHMUK P.10146	-	Toarcian	Mainwaring 1978
Pachycormus macropterus	NHMUK PV P.24410	-	Toarcian	Mainwaring 1978
Pachycormus sp.	NHMUK P.32438	-	Toarcian	Mainwaring 1978
Pachycormus macropterus	NHMUK P.32432	-	Toarcian	Mainwaring 1978
Pachycormus curtus	NHMUK P.32430	-	Toarcian	Mainwaring 1978
Pachycormus curtus	GPIT/743 32-4	-	Toarcian	Wretman *et al.* 2016
Pachycormus curtus	SMNK 87771	-	Toarcian	Wretman *et al.* 2016
Pachycormus curtus	SMNK 96618	-	Toarcian	Wretman *et al.* 2016
Pachycormus curtus	SMNK 55300	-	Toarcian	Wretman *et al.* 2016
Pachycormus curtus	SMNK 87762	-	Toarcian	Wretman *et al.* 2016
Pachycormus curtus	PMU 24211	-	Toarcian	Wretman *et al.* 2016
Pachycormus macropterus	NHMUK P.7569	-	Toarcian	Wretman *et al.* 2016
Pachycormus bollensis	GPIT/OS /777	-	Toarcian	Wretman *et al.* 2016
Pachycormus bollensis	GPIT/OS /776	-	Toarcian	Wretman *et al.* 2016
Pachycormus bollensis	PMU 24210	-	Toarcian	Wretman *et al.* 2016

Pachycormus sp.	SMNK 87772	-	Toarcian	Wretman *et al.* 2016
Pachycormus sp.	SMNK 87763	-	Toarcian	Wretman *et al.* 2016
Pachycormus sp.	SMNK 95835	-	Toarcian	Wretman *et al.* 2016
Pachycormus sp.	SMNK 65230	-	Toarcian	Wretman *et al.* 2016
Pachycormus sp.	SMNK 51031	-	Toarcian	Wretman *et al.* 2016
Pachycormus sp.	SMNK 18189	-	Toarcian	Wretman *et al.* 2016
Pachycormus macropterus	GPIT/773	-	Toarcian	Wretman *et al.* 2016
Pachycormus macropterus	GPIT/774	-	Toarcian	Wretman *et al.* 2016
Pachycormus bollensis	PMU P1191	-	Toarcian	Wretman *et al.* 2016
Pachycormus sp.	SMNK 87769	-	Toarcian	Wretman *et al.* 2016
Pachycormus sp.	SMNK 87760	-	Toarcian	Wretman *et al.* 2016
Pachycormus sp.	SMNK 53425	-	Toarcian	Wretman *et al.* 2016
Pachycormus curtus	NHMUK P.2037a	-	Toarcian	Wretman *et al.* 2016
Pachycormus curtus	NHMUK P.32435	-	Toarcian	Wretman *et al.* 2016
Pachycormus curtus	NHMUK P.32439	-	Toarcian	Wretman *et al.* 2016
Pachycormus curtus	NHMUK P.32427	-	Toarcian	Wretman *et al.* 2016
Pachycormus curtus	MB 2348	-	Lower Jurassic	Gouiric-Cavalli & Cione 2015
Pachycormus curtus	MB 18092	-	Lower Jurassic	Gouiric-Cavalli & Cione 2015
Pachycormus macropterus	MB 18093	-	Lower Jurassic	Gouiric-Cavalli & Cione 2015
Pachycormus macropterus	MB 18095	-	Lower Jurassic	Gouiric-Cavalli & Cione 2015
Pachycormus macropterus	MB 12215	-	Lower Jurassic	Gouiric-Cavalli & Cione 2015

Pachycormus macropterus	MB 1477	-	Lower Jurassic	Gouiric-Cavalli & Cione 2015
Pachycormus sp.	MB 4941	-	Lower Jurassic	Gouiric-Cavalli & Cione 2015
Protosphyraena cf. *P. tenuis*	KUVP 119500	Gove county, Niobrara formation, Kansas, USA	Late Coniacian - early Campanian	Arratia & Lambers 1996
Protosphyraena pernicosa	KUVP 49530	Trego county, Niobrara formation, Kansas, USA	Late Coniacian - early Campanian	Arratia & Lambers 1996
Protosphyraena tenuis	KUVP 49419	Trego county, Niobrara formation, Kansas, USA	Late Coniacian - early Campanian	Arratia & Lambers 1996
Protosphyraena cf. *P. pernicosa*	KUVP 67877	Trego county, Niobrara formation, Kansas, USA	Late Coniacian - early Campanian	Arratia & Lambers 1996
Protosphyraena sp.	KUVP 49418	Trego county, Niobrara formation, Kansas, USA	Late Coniacian - early Campanian	Arratia & Lambers 1996
Protosphyraena sp.	KUVP 55500	Trego county, Niobrara formation, Kansas, USA	Late Coniacian - early Campanian	Arratia & Lambers 1996
Protosphyraena sp.	BSPG 1893.X.72	-	Upper Cretaceous	Lambers 1992
Protosphyraena sp.	BSPG 1893.X.53 6a	-	Upper Cretaceous	Lambers 1992
Protosphyraena sp.	NHMUK P.3954	-	Upper Cretaceous	Lambers 1992
Protosphyraena sp.	NHMUK P.5635	-	Upper Cretaceous	Lambers 1992
Protosphyraena sp.	NHMUK P.7256	Cambridge Greensand, Cambridgeshire, UK	Cenomanian	Woodward 1895*a*; Lambers 1992
Protosphyraena sp.	NHMUK P.7258	Cambridge Greensand, Cambridgeshire, UK	Cenomanian	Woodward 1895*a*; Lambers 1992
Protosphyraena sp.	NHMUK P.7573	-	Upper Cretaceous	Lambers 1992
Protosphyraena sp.	NHMUK P.30259	Cambridge Greensand, Cambridgeshire, UK	Cenomanian	Woodward 1895*a*; Lambers 1992
Protosphyraena sp.	NHMUK P.35160a	Cambridge Greensand, Cambridgeshire, UK	Cenomanian	Woodward 1895*a*; Lambers 1992
Protosphyraena sp.	NHMUK P.36438	Merstham, Surrey, UK	Albian	Woodward 1895*a*; Lambers 1992
Protosphyraena ferox	NHMUK P.39438	-	Upper Cretaceous	Lambers 1992

Protosphyraena sp.	NHMUK P.41079	Merstham, Surrey, UK	Albian	Woodward 1895*a*; Lambers 1992
Protosphyraena ferox	NHMUK P.49012	Burham Chalk, Kent, UK	Cenomanian	Woodward 1895*a*; Lambers 1992
Protosphyraena sp.	NHMUK P.10732	-	Upper Cretaceous	Lambers 1992
Protosphyraena sp.	NHMUK P.11155	-	Upper Cretaceous	Lambers 1992
Protosphyraena sp.	KUVP 1019	-	Upper Cretaceous	Lambers 1992
Rhinconichthys taylori	NHMUK PV OR 33219	Burham Chalk, Kent, UK	Cenomanian	Schumacher *et al.* 2016
Rhinconichthys uyenoi	NSM VP21868	Mikasa city, Japan	Cenomanian	Schumacher *et al.* 2016
Rhinconichthys purgatoirensis	DMNH 63794	Otero county, Colorado, USA	Lower middle Turonian	Schumacher *et al.* 2016
Saurostomus esocinus	NHMUK PV P.11126	Holzmaden, Posidonia Shale, Germany	Toarcian	Woodward 1916
Saurostomus esocinus	SMNK 51144	Holzmaden, Posidonia Shale, Germany	Toarcian	Liston & Maltese 2016
Saurostomus esocinus	SMNK 56982	Holzmaden, Posidonia Shale, Germany	Toarcian	Liston & Maltese 2016
Saurostomus esocinus	NHMUK OR3731 L	Holzmaden, Posidonia Shale, Germany	Toarcian	Liston & Maltese 2016
Saurostomus esocinus	SMNK 50736 L+R	Holzmaden, Posidonia Shale, Germany	Toarcian	Liston & Maltese 2016
Saurostomus esocinus	SMNK 53987	Holzmaden, Posidonia Shale, Germany	Toarcian	Lambers 1992
Saurostomus esocinus	SMNK 55309	Holzmaden, Posidonia Shale, Germany	Toarcian	Lambers 1992
Saurostomus esocinus	MNHN 1955-1-18	Holzmaden, Posidonia Shale, Germany	Toarcian	Wenz 1967
Saurostomus esocinus	MNHN 1897-13-6	Saint-Colombe, Yonne, France	Toarcian	Sauvage 1891; Wenz 1967
Saurostomus esocinus	TU463	Grancourt Shale Base, Luxembourg	Toarcian	Delsate *et al.* 1999
Saurostomus esocinus	TU987	Grancourt Shale Base, Luxembourg	Toarcian	Delsate *et al.* 1999

Saurostomus esocinus	TU940	Grancourt Shale Base, Luxembourg	Toarcian	Delsate *et al.* 1999
Saurostomus esocinus	P47	Grancourt Shale Base, Luxembourg	Toarcian	Delsate *et al.* 1999
Saurostomus esocinus	IRSNB JG	Grancourt Shale Base, Luxembourg	Toarcian	Delsate *et al.* 1999
Saurostomus esocinus	SMNK 55859	Grancourt Shale Base, Luxembourg	Toarcian	Delsate *et al.* 1999

Appendix B

Supplementary Information associated with Chapter 2 'Cranial osteology of *Martillichthys renwickae* with comments on the evolution and ecology of edentulous pachycormiforms'

μCT Scanning Parameters

Specimen Name	Specimen Number	Filter	Filter size (mm)	μA	kV	Voxel size (mm)	Projections
Martillichthys renwickae	NHMUK PV P.61563	Copper	1	150	190	0.126	3141
Pachycormus macropterus	NHMUK PV OR 32433	Copper	2	220	205	0.104	3141
Pachycormus macropterus	BRLSI M1297	Copper	2.5	519	225	0.09	3141
Pachycormus macropterus	BRLSI M1361a	Copper	2	176	225	0.048	3141

Appendix C

Supplementary Information associated with Chapter 3 'Cranial osteology of *Pachycormus*, relationships and divergence times among pachycormiforms'

μCT Scanning Parameters

Specimen Name	Specimen Number	Filter	Filter size (mm)	μA	kV	Voxel size (mm)	Projections
Pachycormus macropterus	BRLSI M1361a	Copper	2	176	225	0.048	3141
Pachycormus macropterus	NHMUK PV OR 32433	Copper	2	220	205	0.104	3141
Pachycormus macropterus	BRLSI M1297	Copper	2.5	519	225	0.09	3141
Pachycormus macropterus	BRLSI M1311	Copper	2	357	225	0.06	3141
Pachycormus macropterus	BRLSI M1395	Copper	3	352	225	0.06	3141
Hypsocormus tenuirostris	NHMUK PV P.10579	Copper	1	170	195	0.126	3141
Martillichthys renwickae	NHMUK PV P.61563	Copper	1	150	190	0.126	3141

Specimens analysed for composite taxa

The following taxa were analysed from multiple specimens of different species, or from specimens of uncertain species assignment during the Friedman *et al.* (2010) and Friedman (2012*a*) analyses. For this study, characters were verified using the relevant literature during a literature review to verify correct character coding.

Caturus sp.

Caturus furcatus Agassiz. Two acid-prepared individuals from the Upper Jurassic (Tithonian) Solnhofen Limestone, Germany. AMNH FF 7492; AMNH FF 19074. Specimens described in Rayner (1948), Patterson (1975), Bartram (1977), Lambers (1992) and Grande and Bemis (1998) were also used for codings.

Caturus sp. An acid-prepared skull from the Upper Jurassic (Kimmeridgian) Solnhofen Limestone, Germany. AMNH FF 8763.

Euthynotus sp.

Euthynotus incognitus (Blainville). A complete individual from the Lower Jurassic (Toarcian) Posidonia Shale of Holzmaden, Germany (AMNH FF 7540). Additional codings were made from descriptions in Wenz (1967).

Euthynotus cf. *E. incognitus*. Specimen described in Bürgin (2000).

Euthynotus intermedius (Agassiz). Specimens described in Arambourg (1935*a*).

Euthynotus sp. Caudal specimen from Arratia and Lambers (1996).

Euthynotus incognitus (Blainville). AMNH FF 7540 is from the Lower Jurassic (Toarcian) Posidonia Shale of Holzmaden, Germany, and MNHN 10578 is from an uncertain stratigraphy and locality (Wenz 1967).

Euthynotus intermedius (Agassiz). MNHN STC 32 is from the Lower Jurassic of Sante-Colombe, France. Specimen descriptions in Arambourg (1935*a*) and Wenz (1967) were also used.

Lepidotes sp.

Lepidotes elvensis (Blainville). AMNH FF 7537 (complete individual) from the Lower Jurassic (Toarcian) Posidonia Shale of Holzmaden, Germany. Additional characters are coded from specimens described in Quenstedt (1847).

Lepidotes sp. AMNH FF 11442 (complete individual) from the Middle Jurassic (Bathonian) Sundance Formation, Burnt Hollow, Wyoming, USA.

Lepidotes spp. Additional codings were based on material described in Jain and Robinson (1963) and Patterson (1973, 1975).

Protosphyraena sp.

Protosphyraena sp. Five individuals, all from the Upper Cretaceous (Coniacian – lowermost Campanian) Smoky Hill Member of the Niobrara Formation, Kansas, USA. Scapulocoracoid and incomplete cleithrum, AMNH FF 1901, south fork of Solomon River (labelled *Protosphyraena perniciosa*); complete skull and mandibles, AMNH FF 1966, NE of WaKeeny, Trego County; complete skull and mandibles, AMNH FF 4318 (labeled as *Protosphyraena* perniciosa); cleithrum and scapulocoracoid, KUVP 466, near Banner, Trego

County; caudal fin and incomplete axial column, KUVP 49419; Logan County. Additional codings made from material described in Felix (1890).

Protosphyraena nitida (Cope). Three individuals, all from the Upper Cretaceous (Coniacian-lowermost Campanian) Smoky Hill Member of the Niobrara Formation, Kansas, USA. Complete skull, pectoral and pelvic fins, BMNH P.10341, locality unknown; skull plus fragmentary pectoral fins and girdles, AMNH FF 1634, Gove County; skull plus pectoral girdles and partial fins, cast of LACM 129752, Ellis County (upper Coniacian).

Protosphyraena cf. *P. tenuis* Loomis. Four specimens from the Upper Cretaceous (Coniacian-lowermost Campanian) Smoky Hill Member, Niobrara Formation, Kansas, USA. Incomplete skull, KUVP 420; mandibles, sclerotic ring, partial suspensorium, neurocranium, KUVP 398, Gove County; skull and pectoral fins, KUVP 55489, Trego County; scapulocoracoids and partial suspensorium, KUVP 55499, Logan County.

Protosphyraena perniciosa (Cope). Three individuals from the Upper Cretaceous (Coniacian-lowermost Campanian) Smoky Hill Member, Niobrara Formation, Kansas, USA. Pectoral fins and girdle, AMNH FF 2009, Rooks County; pectoral fin and girdle, KUVP 367, Gove County; fragmented scapulocoracoid, pectoral fin and radials, KUVP 56612, Trego County.

Pteronisculus sp.

Pteronisculus sp. (Nielsen). Codings were made based on the specimens described in Nielsen (1942) under *Glaucolepis* spp. from the Lower Triassic (Induan) of the Stegocelaphian horizon, Kap Stosch, East Greenland.

Character List

The following matrix was adapted from Friedman (2012*a*). Characters denoted with an asterisk (*****) have been modified for the purposes of this chapter. Characters denoted with double asterisk (******) have been removed during the analysis. Sources for similar or identical characters are given in brackets after each character.

1. Ethmoid ossification(s) [Grande 2010]: **(0)** Present; **(1)** Absent.

2. Anterior myodome [Patterson 1977*a*; Gardiner *et al.* 1996; Arratia 1997; Coates 1999; Cavin & Suteethorn 2006; Hurley *et al.* 2007; Friedman *et al.* 2010]: **(0)** Present; **(1)** Absent.

3. Basipterygoid process [Patterson 1973; Gardiner & Schaeffer 1989; Gardiner *et al.* 1996; Hurley *et al.* 2007; Friedman *et al.* 2010]: **(0)** Well-developed dermal process with endoskeletal component; **(1)** Basipterygoid process absent.

4. Posterior myodome [Patterson 1973; Patterson 1977*a*; Gardiner & Schaeffer 1989; Gardiner *et al.* 1996; Coates 1999; Cavin & Suteethorn 2006; Hurley *et al.* 2007; Friedman *et al.* 2010]: **(0)** Present; **(1)** Absent.

5. Endoskeletal floor of posterior myodome [Patterson 1973; Patterson 1977*a*; Gardiner & Schaeffer 1989; Gardiner *et al.* 1996; Coates 1999; Cavin & Suteethorn 2006; Hurley *et al.* 2007; Friedman *et al.* 2010]: **(0)** Complete; **(1)** Fenestrate.

6. Lateral commissure breadth [Hurley *et al.* 2007; Friedman *et al.* 2010]: **(0)** Anteroposteriorly broad; **(1)** Slender.:

7. Spiracular canal [Patterson 1977*a*; Patterson 1982; Gardiner & Schaeffer 1989; Arratia 1997; Hurley *et al.* 2007; Friedman *et al.* 2010]: **(0)** Present; **(1)** Absent.

8. Dermal component of sphenotic bone or sphenotic region of braincase [Grande 2010]: **(0)** Absent; **(1)** Present.

9. Opisthotic [Cavin & Suteethorn 2006; Hurley *et al.* 2007; Friedman *et al.* 2010]: **(0)** Present; **(1)** Absent.

10. Pterotic [Hurley *et al.* 2007; Friedman *et al.* 2010]: **(0)** Present; **(1)** Absent.

11. Pterotic fused with dermopterotic [Gardiner *et al.* 1996; Hurley *et al.* 2007; Friedman *et al.* 2010]: **(0)** Absent; **(1)** Present.

12. Epioccipital [Gardiner *et al.* 1996; Hurley *et al.* 2007; Friedman *et al.* 2010]: **(0)** Epioccipital bordered anteriorly by cranial fissure; **(1)** Epioccipital contacts otic region.

13. Intercalar [Patterson 1973; Gardiner *et al.* 1996; Cavin & Suteethorn 2006; Hurley *et al.* 2007; Friedman *et al.* 2010]: **(0)** Present; **(1)** Absent.

14. Membranous outgrowths of intercalar [Gardiner *et al.* 1996; Hurley *et al.* 2007; Friedman *et al.* 2010]: **(0)** Minor; **(1)** Extensive.

15. Position of membranous outgrowths of intercalar [Gardiner *et al.* 1996; Hurley *et al.* 2007; Friedman *et al.* 2010]: **(0)** Medial to jugular; **(1)** Lateral to jugular.

16. Lateral cranial canal [Coates 1999; Friedman *et al.* 2010]: **(0)** Present; **(1)** Absent.

17. Subtemporal fossa [Gardiner & Schaeffer 1989; Hurley *et al.* 2007; Friedman *et al.* 2010]: **(0)** Absent; **(1)** Present.

18. Posttemporal fossae [Patterson 1973; Patterson 1977*a*; Gardiner & Schaeffer 1989; Gardiner *et al.* 1996; Cavin & Suteethorn 2006; Hurley *et al.* 2007; Friedman *et al.* 2010]: **(0)** Absent; **(1)** Present.

19. Communication between posttemporal fossa and fossa Bridgei [Patterson 1973; Patterson 1977*a*; Gardiner & Schaeffer 1989; Gardiner *et al.* 1996; Cavin & Suteethorn 2006; Hurley *et al.* 2007; Friedman *et al.* 2010]: **(0)** Absent; **(1)** Present.

20. Cranial fissures [Patterson & Rosen 1977*a*; Grande 2010; Hurley *et al.* 2007; Friedman *et al.* 2010]: **(0)** Ventral otic and otico-occipital fissure confluent via vestibular fontanelle; **(1)** Fissures non-persistent (closed), or pattern obscured by incomplete ossification.

21. Foramen for vagus nerve enclosed completely within exoccipital [Gardiner *et al.* 1996; Cavin & Suteethorn 2006; Hurley *et al.* 2007; Friedman *et al.* 2010]: **(0)** Absent; **(1)** Present.

22. Relationship of dorsal aorta to basicranial region (in taxa where this vessel is not enclosed) [Gardiner *et al.* 1996; Arratia 1997; Coates 1999; Hurley *et al.* 2007; Friedman *et al.* 2010]: **(0)** Accommodated in a pronounced aortic groove; **(1)** Accommodated in a shallow depression.

23. Vertebrae fused into adult occipital condyle [Grande 2010]**: **(0)** Absent; **(1)** Present.

24. Vomer(s) [Patterson 1973; Patterson 1977*a*; Friedman *et al.* 2010]: **(0)** Paired; **(1)** Unpaired (median).

25. Parasphenoid corpus in sphenethmoid region [Friedman *et al.* 2010]: **(0)** Narrow; **(1)** Broad.

26. Parasphenoid dentition [Arratia 1997; Friedman *et al.* 2010]: **(0)** Present; **(1)** Absent.

27. Internal carotid foramen through parasphenoid [Patterson 1977*a*; Gardiner *et al.* 1996; Hurley *et al.* 2007; Friedman *et al.* 2010]: **(0)** Absent; **(1)** Present.

28. Efferent pseudobranchial foramen through parasphenoid [Patterson 1977*a*; Gardiner *et al.* 1996; Hurley *et al.* 2007; Friedman *et al.* 2010]: **(0)** Absent; **(1)** Present.

29. Ornament on dermal bones of skull: **(0)** Absent; **(1)** Present.

30. Rostral bone [Gardiner *et al.* 1996; Lambers 1992; Hurley *et al.* 2007; Friedman *et al.* 2010]: **(0)** Cap on snout apex partially or wholly separating the nasals; **(1)** Reduced to a narrow tube with lateral process.

31. Contribution of rostral bone to oral margin: **(0)** Absent; **(1)** Present.

32. Rostrodermethmoid [Mainwaring 1978; Lambers 1992; Liston 2007; Friedman *et al.* 2010]: **(0)** Terminates at anterior tip of mandibular symphysis; **(1)** Forms a produced rostrum, extending anterior to mandibular symphysis.

33. Marginal teeth on rostrodermethmoid [Friedman *et al.* 2010]: **(0)** Present; **(1)**

Absent.

34. Paramedial fangs on rostrodermethmoid [Mainwaring 1978; Lambers 1992; Liston 2007; Friedman *et al.* 2010]: **(0)** Absent; **(1)** Present.

35. Parietals [Arratia 1997; Friedman *et al.* 2010]: **(0)** Paired; **(1)** Single midline ossification.

36. Posterior boss on skull roof [Mainwaring 1978; Lambers 1992; Liston 2007; Friedman *et al.* 2010]: **(0)** Absent; **(1)** Present.

37. Posterior margin of skull roof [Friedman *et al.* 2010]******: **(0)** Straight or concave; **(1)** 'W'-shaped.

38. Free, elongated posterior processes of dermopterotics [Friedman *et al.* 2010]: **(0)** Absent; **(1)** Present.

39. Independent extrascapulars [Mainwaring 1978]: **(0)** Present; **(1)** Absent.

40. Number of extrascapulars on each side of the skull [Grande 2010]: **(0)** Single; **(1)** Multiple.

41. Dermosphenotic [Patterson 1973; Gardiner *et al.* 1996; Hurley *et al.* 2007; Friedman *et al.* 2010]: **(0)** Hinged to skull roof; **(1)** Bound or fused to anterior margin of sphenotic.

42. Dermosphenotic forms dorsal margin of orbit [Mainwaring 1978; Lambers 1992; Liston 2007; Friedman *et al.* 2010]: **(0)** No; **(1)** Yes.

43. Supraorbitals [Hurley *et al.* 2007; Friedman *et al.* 2010]: **(0)** Absent; **(1)** Present.

44. Contact between anterior supraorbitals and bones carrying the infraorbital canal (infraorbitals or antorbital) [Gardiner *et al.* 1996; Hurley *et al.* 2007; Friedman *et al.* 2010]: **(0)** Absent; **(1)** Present.

45. Anterior supraorbitals contact [Gardiner *et al.* 1996; Hurley *et al.* 2007; Friedman *et al.* 2010]: **(0)** Antorbital; **(1)** Infraorbitals only.

46. Suborbitals [Patterson 1973; Cavin & Suteethorn 2006; Friedman *et al.* 2010]: **(0)** Present; **(1)** Absent.

47. Suborbital size [Mainwaring 1978; Lambers 1992; Liston 2007; Friedman *et al.* 2010]: **(0)** Equal in size or smaller than adjacent infraorbital(s); **(1)** Much larger than adjacent infraorbital(s).

48. Suborbital number [Mainwaring 1978; Lambers 1992; Cavin & Suteethorn 2006; Liston 2007; Hurley *et al.* 2007; Friedman *et al.* 2010]: **(0)** Single; **(1)** Two; **(2)** Numerous bones.

49. Broad overlap of preoperculum by the suborbitals: **(0)** Absent; **(1)** Present.

50. Antorbital shape [Hurley *et al.* 2007; Friedman *et al.* 2010]: **(0)** Platelike, with minimal (if any) distinct anterior process; **(1)** Tapering towards slender anterior process; tri-radiate canal with broader, posterior portion.

51. Infraorbitals behind orbit [Lambers 1992; Liston 2007; Friedman *et al.* 2010]: **(0)** Six or fewer; **(1)** More than six.

52. Infraorbitals anterior to circumorbital ring [Olsen & McCune 1991; Cavin & Suteethorn 2006; Hurley *et al.* 2007; Friedman *et al.* 2010]: **(0)** Absent; **(1)** Present.

53. Posteriorly extensive infraorbital [Friedman *et al.* 2010]: **(0)** Present; **(1)** Absent.

54. Preoperculum [Olsen & McCune 1991; Lambers 1992; Hurley *et al.* 2007; Friedman *et al.* 2010]: **(0)** With broad dorsal margin; **(1)** With narrow ascending limb.

55. Dorsal limb of preoperculum: **(0)** Plate like; **(1)** Narrow splint with no posterior lamina.

56. Dentary dentition [Lambers 1992]*****: **(0)** Present; **(1)** Absent.

57. Carinae extending length of teeth [Friedman *et al.* 2010]: **(0)** Absent; **(1)** Present.

58. Supraorbital canal in premaxilla [Grande 2010]: **(0)** Absent; **(1)** Present.

59. Premaxilla forms much of dermal skull roof in snout region [Grande 2010]: **(0)** No; **(1)** Yes.

60. Form of premaxillary dentition [Lambers 1992; Liston 2007; Friedman *et al.* 2010]: **(0)** Similar to maxillary teeth; **(1)** Enlarged relative to maxillary teeth.

61. Mobile premaxilla [Patterson 1973; Patterson 1977*a*; Gardiner & Schaeffer 1989; Gardiner *et al.* 1996; Cavin & Suteethorn 2006; Hurley *et al.* 2007; Friedman *et al.* 2010]: **(0)** Absent; **(1)** Present.

62. Grooved, notched or perforated premaxillary ascending process [Patterson 1973; Gardiner & Schaeffer 1989; Gardiner *et al.* 1996; Cavin & Suteethorn 2006; Hurley

et al. 2007; Friedman *et al.* 2010]: **(0)** Absent; **(1)** Present.

63. Maxilla [Patterson 1973; Gardiner & Schaeffer 1989; Gardiner *et al.* 1996; Hurley *et al.* 2007; Friedman *et al.* 2010]: **(0)** Fixed to cheek; **(1)** Free.

64. Maxilla length [Gardiner *et al.* 1996; Lambers 1992; Cavin & Suteethorn 2006; Hurley *et al.* 2007; Friedman *et al.* 2010]*****: **(0)** One third or less; **(1)** Between one and two thirds; **(2)** Over two thirds.

65. Position of orbit relative to maxilla [Lambers 1992]: **(0)** Centred over maxilla; **(1)** Restricted to posterior half of maxilla; **(2)** Fully posterior to the maxilla.

66. Posterior margin of maxilla [Gardiner *et al.* 1996; Lambers 1992; Cavin & Suteethorn 2006; Hurley *et al.* 2007; Friedman *et al.* 2010]: **(0)** Straight or convex; **(1)** Indented.

67. Thickened ridge on external surface of maxilla [Friedman *et al.* 2010]: **(0)** Absent; **(1)** Present.

68. Supramaxilla [Patterson 1973; Gardiner & Schaeffer 1989; Gardiner *et al.* 1996; Arratia 1997; Cavin & Suteethorn 2006; Hurley *et al.* 2007; Friedman *et al.* 2010]: **(0)** Absent; **(1)** Present.

69. Supramaxilla position [Lambers 1992; Liston 2007; Friedman *et al.* 2010]: **(0)** Dorsal to maxilla; **(1)** Posterodorsal to maxilla.

70. Hyomandibular: **(0)** Strongly waisted, with concave anterior and/or posterior margins; **(1)** Straight anterior and posterior margins.

71. Quadratojugal [Patterson 1973; Patterson 1977*a*; Gardiner *et al.* 1996; Cavin & Suteethorn 2006; Hurley *et al.* 2007; Friedman *et al.* 2010]: **(0)** Present; **(1)** Absent.

72. Jaw joint [Patterson 1973; Olsen & McCune 1991; Gardiner *et al.* 1996; Cavin & Suteethorn 2006; Hurley *et al.* 2007; Friedman *et al.* 2010; Grande 2010]: **(0)** Single; **(1)** Double.

73. Symplectic [Grande 2010]: **(0)** Slender and splint shaped; **(1)** Broad and hatchet shaped.

74. Symplectic position relative to quadrate [Patterson 1973; Olsen & McCune 1991; Gardiner *et al.* 1996; Cavin & Suteethorn 2006; Hurley *et al.* 2007; Friedman *et al.* 2010]: **(0)** Medial to quadrate; **(1)** Posterior to quadrate.

75. Membranous ossification binding symplectic and preoperculum [Gardiner *et al.* 1996]: **(0)** Absent; **(1)** Present.

76. Position of jaw joint [Mainwaring 1978; Lambers 1992; Arratia 1997; Cavin & Suteethorn 2006; Liston 2007; Friedman *et al.* 2010]******: **(0)** Well behind orbit; **(1)** Below or anterior to orbit.

77. Quadrate with elongate posteroventral process [Arratia 1997; Cavin & Suteethorn 2006; Hurley *et al.* 2007; Friedman *et al.* 2010]: **(0)** Absent; **(1)** Present.

78. Contact or close association between quadrate and metapterygoid [Grande 2010]: **(0)** Present; **(1)** Absent.

79. Ectopterygoid participation in the palate [Grande 2010]: **(0)** Makes up less than half

of palate; **(1)** Makes up majority of palate.

80. Entopterygoid/dermopalatine contact [Grande 2010]: **(0)** Present; **(1)** Absent.

81. Dentary tooth row(s) [Mainwaring 1978; Lambers 1992; Liston 2007; Friedman *et al.* 2010]: **(0)** Labial row plus lingual row; **(1)** Single row.

82. Form of anterior dentary dentition [Mainwaring 1978; Lambers 1992; Liston 2007; Friedman *et al.* 2010]: **(0)** Similar to posterior teeth; **(1)** Enlarged, procumbent fangs.

83. Surangular in lower jaw [Patterson 1977*a*; Patterson & Rosen 1977; Patterson 1982; Gardiner & Schaeffer 1989; Hurley *et al.* 2007; Friedman *et al.* 2010]: **(0)** Present; **(1)** Absent.

84. Coronoid process of lower jaw [Grande 2010]: **(0)** Absent; **(1)** Present.

85. Coronoid bones [Grande 2010]: **(0)** Present; **(1)** Absent.

86. Anterior coronoid plate [Mainwaring 1978; Friedman *et al.* 2010]: **(0)** Not inflated; **(1)** Inflated.

87. Prearticular [Patterson 1977*a*; Patterson & Rosen 1977; Friedman *et al.* 2010]: **(0)** Present; **(1)** Absent.

88. Prearticular dentition [Friedman *et al.* 2010]: **(0)** Present; **(1)** Absent.

89. Hypohyal [Patterson 1977*a*; Friedman *et al.* 2010]: **(0)** Single ossification; **(1)** Separate dorsal and ventral ossifications.

90. Exposed dorsal projection of suboperculum between preoperculum and operculum [Friedman *et al.* 2010]: **(0)** Absent; **(1)** Present.

91. Gulars [Lambers 1992; Gardiner *et al.* 1996; Arratia 1997; Coates 1999; Cavin & Suteethorn 2006; Hurley *et al.* 2007; Friedman *et al.* 2010]: **(0)** Present; **(1)** Absent.

92. Number of hypobranchials [Grande 2010]: **(0)** Three; **(1)** Four.

93. Uncinate processes on epibranchials [Patterson 1973; Gardiner & Schaeffer 1989; Gardiner *et al.* 1996; Hurley *et al.* 2007; Friedman *et al.* 2010]: **(0)** Absent; **(1)** Present.

94. Relative position of dorsal and anal fins [Mainwaring 1978; Lambers 1992; Liston 2007; Friedman *et al.* 2010]: **(0)** Overlap between dorsal- and anal-fin bases; **(1)** Dorsal-fin base lies anterior to anal-fin base.

95. Caudal fin segmentation [Lambers 1992; Liston 2007; Friedman *et al.* 2010]: **(0)** Segmented; **(1)** Unsegmented.

96. Ossification of vertebral centra [Lambers 1992; Liston 2007; Friedman *et al.* 2010]: **(0)** Absent; **(1)** Present.

97. Opisthocoelus vertebral centra [Grande 2010]: **(0)** Absent; **(1)** Present.

98. Long epineural intermuscular bones [Grande 2010]: **(0)** Absent; **(1)** Present.

99. Caudal diplospondyly [Gardiner *et al.* 1996]: **(0)** Absent; **(1)** Present.

100. Lateral keels of caudal peduncle (greatly expanded urodermals) [Lambers 1992;

Friedman *et al.* 2010]: **(0)** Absent; **(1)** Present.

101. Uroneurals [Patterson 1973; Patterson 1977*a*; Gardiner *et al.* 1996; Arratia 1997; Cavin & Suteethorn 2006; Hurley *et al.* 2007; Friedman *et al.* 2010; Arratia & Schultze 2013]*****: **(0)** Absent; **(1)** Composed of ural elements; **(2)** Composed of preural elements.

102. Hypural plate [Lambers 1992; Liston 2007; Friedman *et al.* 2010]: **(0)** Absent; **(1)** Present.

103. Geometry of hypural plate [Friedman *et al.* 2010]: **(0)** Length of vertical axis equivalent to or slightly longer than horizontal axis; **(1)** Vertical axis substantially longer than horizontal axis.

104. Main hypural plate notched posterodorsally (incomplete fusion with accessory hypurals) [Friedman *et al.* 2010]: **(0)** Present; **(1)** Absent.

105. Clavicle [Patterson 1973; Gardiner *et al.* 1996; Lambers 1992; Hurley *et al.* 2007]******: **(0)** Present; **(1)** Absent.

106. Medial wing of cleithrum [Grande 2010]: **(0)** Absent; **(1)** Present.

107. Supracleithrum: **(0)** Broad and plate like; **(1)** Splint like.

108. Long axis of supracleithrum: **(0)** Straight; **(1)** With prominent elbow or kink.

109. One or more accessory postcleithra [Arratia 1997; Hurley *et al.* 2007; Friedman *et al.* 2010]: **(0)** Absent; **(1)** Present.

110. Endoskeletal shoulder ossification reduced to mesocoracoid arch [Olsen & McCune 1991; Cavin & Suteethorn 2006; Hurley *et al.* 2007; Friedman *et al.* 2010]: **(0)** No; **(1)** Yes.

111. Pectoral propterygium [Patterson 1977*a*; Patterson 1982; Cavin & Suteethorn 2006; Friedman *et al.* 2010]: **(0)** Free; **(1)** Fused to first pectoral-fin ray.

112. Pectoral-fin radial morphology [Friedman *et al.* 2010]: **(0)** Cylindrical; **(1)** Broad distal area and narrow proximal stalk (paddle-shaped).

113. Scythe-like pectoral fins [Mainwaring 1978; Lambers 1992; Liston 2007; Friedman *et al.* 2010]: **(0)** Absent; **(1)** Present.

114. Complete fusion of fin rays along length of leading edge of pectoral fin [Friedman *et al.* 2010]: **(0)** Absent; **(1)** Present.

115. Bifurcations in pectoral-fin rays [Friedman *et al.* 2010]: **(0)** Present; **(1)** Absent.

116. Bifurcations of pectoral lepidotrichia occurring independently of joints [Lambers 1992; Liston 2007; Friedman *et al.* 2010]: **(0)** Absent; **(1)** Present.

117. Pelvic fins [Mainwaring 1978; Lambers 1992; Liston 2007; Friedman *et al.* 2010]: **(0)** Present; **(1)** Absent.

118. Pelvic fin position [Friedman *et al.* 2010]: **(0)** At or posterior to midpoint between anal and pectoral fins; **(1)** Anterior to midpoint between anal and pectoral fins.

119. Scales: **(0)** Present; **(1)** Absent.

120. Ridge scales [Gardiner *et al.* 1996; Cavin & Suteethorn 2006; Hurley *et al.* 2007; Friedman *et al.* 2010]: **(0)** Absent; **(1)** Present.

121. Scale morphology [Patterson 1973; Patterson 1977*a*; Patterson & Rosen 1977; Friedman *et al.* 2010]: **(0)** Rhombic; **(1)** Round.

In addition, the following novel characters were added:

122. Median projection of parietal posterior margin: **(0)** Absent; **(1)** Present.

This was added following the removal of character 37 (posterior margin of the skull roof), to record the median posterior projection of the parietals identified in Martillichthys renwickae *(Chapter 2). When coupled with character 38 (free-elongated posterior processes of the dermopterotics), the variation of the skull roof posterior margin shapes (straight, concave, and 'W' shaped) measured by character 37 can be measured. Splitting character 37 across two characters (chs. 38 and 122), allows the structures forming the posterior margin of the skull roof (the dermopterotics and the parietals) to be measured separately and in isolation of each other.*

123. Gap between frontals: **(0)** Absent; **(1)** Present.

This character was added following the identification of a frontal gap in Martillichthys *(Chapter 2),* Bonnerichthys *(Friedman* et al. *2010),* Rhinconichthys uyenoi*, and* Rhinconichthys purgatoirensis *(Schumacher* et al. *2016; fig. 8). It was added on the hypothesis that it may be a synapomorphy uniting the edentulous*

pachycormiform, though this is not supported in the results of Chapter 3, but the state of this character in Leedsichthys *and* Asthenocormus *is not known.*

124. Gill rakers [Liston 2013; Dobson 2016]: **(0)** Absent; **(1)** Present.

This character, along with characters 125 and 126, has been formulated based on the wide variation in gill raker morphology seen within teleosts (and most starkly within pachycormiforms). Liston (2013) suggested that gill raker morphology is too plastic both within and between individuals to hold any phylogenetic signal, but analysis of raker morphology in a Masters project (Dobson 2016) identified that longer, ornamented rakers are associated with suspension-feeding pachycormiforms (as seen in suspension-feeding chondrichthyans; Paig-Tran & Summers 2014).

125. Size of gill rakers (if present) [Dobson 2016]: **(0)** Stalk height roughly equal or smaller than base width; **(1)** Stalk height is at least double base width.

As elongated gill rakers are associated with the suspension-feeding ecology, this character quantifies and tests for the distribution of elongate rakers among neopterygians, and whether it is a character that unites the suspension-feeders to the exclusion of other neopterygians.

126. Raker ornamentation [Lambers 1992; Dobson 2016]: **(0)** Absent; **(1)** Present.

Lambers (1992) first included this character to measure whether the presence of "raker teeth" are associated with the suspension-feeding ecology. However, a Masters project (Dobson 2016) found that raker ornamentation is also found on short gill rakers (e.g. in Hypsocormus*) but it is unclear what their role is or how this impacts*

pachycormiform relationships as they have never been recorded in a phylogenetic analysis.

127. Elongate sphenoid region: **(0)** Makes up less than half of skull length; **(1)** Makes up over half of skull length.

This character, along with character 128, are formulated to test the variation in skull geometries seen in the edentulous pachycormiforms (Chapter 2), and whether measuring this character results in an alternative pattern of relationships. While a gradual increase in sphenoid length is seen in the 'protosphyraenid' clade: from the short sphenoid region of Hypsocormus*, the pointed noses of* Protosphyraena *and* Australopachycormus *(Kear 2007), the giant bodied suspension-feeders show more pronounced variation between taxa.* Bonnerichthys *and* Rhinconichthys *both have short sphenoid regions like* Pachycormus *and* Saurostomus*, despite diverging between* Ohmdenia *and the Jurassic pachycormiforms (*Asthenocormus*,* Leedsichthys *and* Martillichthys*), which all have elongated sphenoid regions. Because this variation has never been included in a phylogenetic analysis of pachycormiforms, its impact on relationships within suspension-feeding pachycormiforms were unclear.*

128. Short hyomandibula relative to jaw length: **(0)** Height is less the one third jaw length; **(1)** Height is over one third jaw length.

Like character 127, this is based on the observations made in Chapter 2, where the short sphenoid region of Bonnerichthys *and* Rhinconichthys *also results in a taller hyomandibula relative to jaw length. This could have implications for suspension-feeding pachycormiform relationships, which is tested in Chapter 3.*

129. Opercular process of the hyomandibula: **(0)** Absent; **(1)** Present.

It was noted in Chapter 2 that an opercular process of the hyomandibula is absent in Asthenocormus *(Lambers 1992),* Rhinconichthys *(Schumacher* et al. *2016) and in* Ohmdenia *(if the hyomandibula has been correctly identified; Friedman 2012a), but it is present in* Martillichthys *and* Bonnerichthys*. Its distribution among pachycormiforms and other neopterygians has not been tested.*

130. Occipital stalk length: **(0)** Terminates at posterior margin of skull roof; **(1)** Extends beyond skull roof.

Chapter 2 noted that the length of the occipital stalk varies in pachycormiforms, but the distribution of this character within pachycormiforms is untested.

131. Maxillary dentition: **(0)** Absent; **(1)** Present.

By splitting character 56 (originally "marginal dentition"; Friedman 2012a) into three characters (ch. 56; dentary dentition; ch. 88; prearticular dentition; and ch. 131; maxillary dentition) the variation in dentition among taxa, and how gradual loss of dentition (such as the absence of maxillary dentition in Ohmdenia*; Friedman 2012a) marks the evolutionary steps towards edentulous taxa, such as the suspension-feeding pachycormiforms.*

132. Shoulder girdle element: **(0)** Caps/Anterior to the cleithrum; **(1)** Dorsal to the cleithrum.

This is designed to test the homology of the paired element that sits antero-lateral to the cleithra in Pachycormus *(Chapter 3), which is interpreted as embedded squamation. The terms here are carefully chosen to avoid any assumptions of*

homology that would come with using the terms "serrated organ" or "clavicle" (as outlined in Grande & Bemis 1998; Arratia 2015). To avoid repeating the states measured in character 105 (clavicle; present/absent), character 105 was excluded from analyses.

133. Midline ossification lying ventral to basibranchial: **(0)** Absent; **(1)** Present.

This character tests the homology of the unpaired element that sits ventral to the basibranchial in Pachycormus *(Chapter 3). Originally, Mainwaring (1978) identified this as a ventral toothplate, but . The terms here are carefully chosen to avoid any assumptions of homology that would come with using the terms "serrated organ" or "clavicle" (see Arratia & Schultze 2010). To avoid repeating the states measured in character 105 (clavicle; present/absent), character 105 was excluded from analyses.*

Character Matrix

	1	2	3	4	5	6	7	8	9	10	11	12	13	14	15	16	17	18	19	20	21	22
Pteronisculus spp.	0	0	0	0	0	0	0	0	?	?	0	0	-	-	-	0	0	0	-	0	?	?
Amia calva	0	0	1	0	1	0	0	1	1	1	-	1	0	1	0	1	0	1	0	1	0	1
Caturus spp.	0	0	1	0	1	1	?	1	1	1	-	1	0	1	0	0	1	1	0	1	0	1
Macrepistius arenatus	0	0	1	0	1	1	?	1	0	0	1	1	0	1	0	?	1	1	0	1	0	?
Watsonulus eugnathoides	0	0	0	0	1	1	0	1	-	-	?	0	-	?	?	0	?	1	?	0	-	1
Lepidotes spp.	1	?	0	0	1	1	?	?	1	1	-	1	1	-	-	0	1	1	?	1	1	0
Semionotus elegans	1	?	0	0	1	?	?	1	1	1	-	1	1	-	-	?	?	?	0	?	1	1
Lepisosteus platostomus	1	1	0	1	-	0	0	1	1	1	-	1	1	-	-	0	0	0	-	1	1	1
Dentilepisosteus laevis	1	1	0	1	-	1	?	1	1	1	-	1	1	-	-	?	?	?	?	1	1	0
Macrosemius rostratus	0	?	0	0	1	?	?	0	1	0	0	1	?	?	?	0	?	?	?	1	1	1
Asthenocormus titanus	?	?	?	?	?	?	?	?	?	?	?	?	?	?	?	?	?	?	?	?	?	?
Leedsichthys problematicus	?	?	?	?	?	?	?	?	?	?	?	?	?	?	?	?	?	?	?	?	?	1
Martillichthys renwickae	0	?	1	?	?	?	?	0	?	?	?	?	?	?	?	?	?	?	?	?	?	1
Rhinconichthys taylori	0	?	1	0	1	1	?	?	?	?	?	?	?	?	?	?	?	1	?	?	?	1
Bonnerichthys gladius	0	?	1	?	?	1	?	0	0	0	0	?	0	0	-	?	?	1	?	?	?	0
Ohmdenia multidentata	?	?	?	?	?	?	?	?	?	?	?	?	?	?	?	?	?	?	?	?	?	?
Saurostomus esocinus	?	?	1	?	?	?	?	?	?	?	?	?	?	?	?	?	?	?	?	?	?	?
Pachycormus sp.	0	?	1	0	?	?	0	0	0	0	0	?	0	?	?	?	1	1	1	0	0	0
Australopachycormus hurleyi	0	?	?	?	?	?	?	?	0	0	?	?	0	?	?	?	?	?	?	?	?	?
Protosphyraena spp.	0	?	1	?	?	1	?	0	0	0	0	-	0	0	-	?	1	1	?	?	0	0
Orthocormus cornutus	0	?	?	?	?	1	?	?	0	?	?	?	0	?	?	?	?	?	?	?	0	?
Orthocormus roeperi	0	?	?	?	?	?	?	?	?	?	?	?	?	?	?	?	?	?	?	?	?	?
Orthocormus teyleri	0	?	?	?	?	?	?	?	?	?	?	?	?	?	?	?	?	?	?	?	?	?
Hypsocormus tenuirostris	0	?	1	?	?	?	?	?	?	?	?	?	?	?	?	?	?	?	?	?	?	0
Hypsocormus macrodon	?	?	?	?	?	?	?	?	?	?	?	?	?	?	?	?	?	?	?	?	?	?
Hypsocormus insignis	?	?	?	?	?	?	?	?	?	?	?	?	?	?	?	?	?	?	?	?	?	?
Euthynotus spp.	?	?	?	?	?	?	?	0	?	?	?	?	?	?	?	?	?	?	?	?	?	?
Aspidorhynchus acutirostris	0	?	1	0	?	?	?	0	0	?	?	1	0	?	?	?	?	?	?	?	0	1
Vinctifer comptoni	0	?	1	0	?	?	?	0	0	?	?	1	0	?	?	?	?	?	?	?	0	1
Belonostomus tenuirostris	0	?	?	0	?	?	?	0	0	?	?	1	0	?	?	?	?	1	?	?	0	1
Elops hawaiensis	0	0	1	0	1	1	1	0	1	0	1	1	0	1	1	1	1	1	1	1	1	1
Hiodon alosoides	0	0	1	0	1	1	1	0	1	0	1	1	0	1	1	1	1	1	1	1	1	0
Dorsetichthys bechei	0	0	0	0	1	1	0	0	0	0	1	0	-	?	?	0	1	1	0	0	0	2

	23	24	25	26	27	28	29	30	31	32	33	34	35	36	37	38	39	40	41	42	43	44
Pteronisculus spp.	?	0	0	0	0	0	1	0	0	-	-	-	0	0	0	0	0	1	0	0	0	-
Amia calva	1	0	0	0	0	0	1	0	0	-	-	-	0	0	0	0	0	0	1	0	0	-
Caturus spp.	?	0	0	0	0	0	0	1	0	-	-	-	0	0	0	1	0	0	1	0	1	1
Macrepistius arenatus	?	?	0	1	0	0	1	?	0	-	-	-	0	0	0	0	0	0	1	0	1	1
Watsonulus eugnathoides	?	0	0	0	0	0	1	1	0	-	-	-	0	0	0	0	0	0	1	0	1	1
Lepidotes spp.	1	0	0	1	0	0	1	1	0	-	-	-	0	0	0	0	0	0	0	0	1	1
Semionotus elegans	?	0	0	0	0	0	0	1	0	-	-	-	0	0	0	0	0	0	0	0	1	1
Lepisosteus platostomus	1	0	0	0	0	0	1	1	0	-	-	-	0	0	0	0	0	1	0	0	1	1
Dentilepisosteus laevis	?	0	0	0	0	0	1	?	?	-	-	-	0	0	0	?	0	1	1	0	1	1
Macrosemius rostratus	?	0	0	1	0	1	1	1	0	-	-	-	0	0	0	0	0	0	0	0	0	-
Asthenocormus titanus	?	?	?	?	?	?	0	0	1	0	-	-	0	0	1	0	1	-	?	?	0	-
Leedsichthys problematicus	?	?	1	1	?	?	0	?	?	?	-	-	?	?	?	?	?	?	?	?	?	?
Martillichthys renwickae	?	?	1	1	?	?	0	0	1	0	0	0	0	0	1	1	1	-	0	1	0	-
Rhinconichthys taylori	?	0	1	?	?	?	0	?	?	?	-	-	0	0	1	1	1	-	?	?	?	?
Bonnerichthys gladius	?	0	1	1	1	0	0	0	1	0	-	-	?	?	?	1	1	-	0	1	0	-
Ohmdenia multidentata	?	?	?	?	?	?	1	?	?	?	?	?	?	?	?	?	?	?	?	?	?	?
Saurostomus esocinus	?	?	1	?	?	?	1	0	1	0	0	0	?	1	?	1	1	-	?	?	?	?
Pachycormus sp.	?	0	0	0	1	0	1	0	1	0	0	0	0	1	0	0	1	-	0	1	0	-
Australopachycormus hurleyi	?	?	?	?	?	?	1	0	1	1	1	1	1	0	0	?	?	?	?	?	?	?
Protosphyraena spp.	?	0	0	0	1	0	1	0	1	1	1	1	1	1	0	1	?	?	0	1	0	-
Orthocormus cornutus	?	?	?	?	?	?	1	0	1	1	1	1	0	1	?	?	1	-	0	?	0	-
Orthocormus roeperi	?	?	?	?	?	?	1	0	1	1	1	1	?	1	?	?	1	-	0	0	0	-
Orthocormus teyleri	?	0	?	?	?	?	1	0	1	1	1	1	?	1	?	?	1	-	?	?	0	-
Hypsocormus tenuirostris	?	0	0	0	1	0	1	0	1	1	0	1	?	1	0	0	?	?	?	?	?	?
Hypsocormus macrodon	?	?	?	?	?	?	1	0	1	0	0	1	?	1	?	?	?	?	?	?	0	-
Hypsocormus insignis	?	?	?	?	?	?	1	0	1	0	0	1	?	1	?	0	?	?	?	?	0	-
Euthynotus spp.	?	?	0	?	?	?	1	0	1	0	0	0	?	1	0	?	0	0	0	1	0	-
Aspidorhynchus acutirostris	?	1	0	0	1	1	1	0	0	-	-	-	2	0	0	0	0	0	0	0	1	1
Vinctifer comptoni	?	1	0	1	1	1	1	0	0	-	-	-	2	0	0	0	0	0	0	0	1	1
Belonostomus tenuirostris	?	?	?	1	1	1	1	0	0	-	-	-	2	0	0	0	0	0	0	0	1	1
Elops hawaiensis	0	?	?	?	1	0	0	0	0	-	-	-	0	0	0	0	0	0	0	0	1	1
Hiodon alosoides	0	1	0	0	1	1	0	0	0	-	-	-	0	0	0	0	0	0	0	0	0	-
Dorsetichthys bechei	?	1	0	0	1	1	1	0	0	-	-	-	0	-	0	0	0	0	0	0	1	0

	45	46	47	48	49	50	51	52	53	54	55	56	57	58	59	60	61	62	63	64	65	66
Pteronisculus spp.	-	0	0	1	0	0	0	0	0	0	0	0	0	0	0	0	0	0	0	1	-	0
Amia calva	-	1	-	-	-	1	0	0	0	1	0	0	0	0	0	0	0	1	1	1	0	1
Caturus spp.	0	0	1	1	1	1	0	0	1	1	0	0	0	0	0	0	0	1	1	1	0	1
Macrepistius arenatus	0	0	1	2	1	?	0	0	1	1	0	0	0	?	0	0	0	?	1	1	1	1
Watsonulus eugnathoides	0	0	0	2	0	1	0	0	1	0	0	0	0	0	0	0	0	1	1	1	0	1
Lepidotes spp.	1	0	1	2	1	1	0	1	1	1	0	0	0	0	0	0	0	1	1	0	2	0
Semionotus elegans	1	0	1	0	1	1	0	1	1	1	0	0	0	0	0	0	0	1	1	1	2	0
Lepisosteus platostomus	1	0	0	2	1	1	0	1	1	1	0	0	0	1	1	0	0	1	0	0	2	0
Dentilepisosteus laevis	1	0	0	2	?	?	0	1	0	1	0	0	0	1	1	0	0	?	1	0	2	0
Macrosemius rostratus	-	1	-	-	-	1	0	1	1	1	1	0	0	0	0	0	0	1	1	0	-	0
Asthenocormus titanus	-	?	?	?	?	?	?	?	?	?	?	1	-	?	0	-	?	?	1	0	2	0
Leedsichthys problematicus	?	?	?	?	?	?	?	?	?	1	1	1	-	?	?	-	?	?	1	?	?	?
Martillichthys renwickae	-	0	?	?	?	0	?	?	?	?	?	1	-	0	0	-	?	?	1	0	2	0
Rhinconichthys taylori	?	?	?	?	?	?	?	?	?	?	?	1	-	?	?	-	?	?	1	1	0	0
Bonnerichthys gladius	-	?	?	?	?	0	?	?	?	?	?	1	-	?	0	-	0	-	1	1	0	0
Ohmdenia multidentata	?	?	?	?	?	?	?	?	?	1	1	0	?	0	?	?	?	?	1	?	1	0
Saurostomus esocinus	?	?	?	?	?	?	?	?	?	1	1	0	0	?	0	0	?	?	1	1	1	0
Pachycormus sp.	-	0	1	1	0	0	1	0	1	1	1	0	0	0	0	0	0	0	1	1	0	0
Australopachycormus hurleyi	?	?	?	?	?	?	?	?	?	?	?	0	1	?	0	1	0	0	?	?	?	0
Protosphyraena spp.	-	0	1	?	?	0	?	0	?	?	?	0	1	?	0	1	0	0	1	?	0	0
Orthocormus cornutus	-	0	1	1	?	0	?	?	?	?	?	0	0	?	0	1	0	0	1	0	0	0
Orthocormus roeperi	-	0	?	?	?	?	1	?	?	?	?	0	0	?	0	1	0	0	1	0	0	0
Orthocormus teyleri	-	0	1	?	?	0	?	?	?	1	0	0	0	?	0	1	0	0	1	0	0	0
Hypsocormus tenuirostris	?	0	1	1	?	?	1	?	1	1	0	0	0	?	0	1	0	0	1	?	0	0
Hypsocormus macrodon	?	0	1	1	?	?	1	?	1	?	?	0	0	?	?	0	0	0	1	?	0	0
Hypsocormus insignis	-	0	1	1	?	?	1	?	1	1	0	0	0	?	0	0	0	?	1	?	0	0
Euthynotus spp.	-	0	1	1	0	0	?	0	1	1	0	0	0	?	0	0	?	-	1	?	0	0
Aspidorhynchus acutirostris	1	0	1	1	0	?	0	1	1	1	1	0	?	0	1	1	0	0	0	0	1	0
Vinctifer comptoni	1	0	1	1	0	?	0	1	1	1	1	0	?	0	1	-	0	0	0	0	1	0
Belonostomus tenuirostris	1	0	1	2	0	?	0	1	1	1	1	0	?	0	1	1	0	0	0	1	1	0
Elops hawaiensis	0	1	-	-	-	0	0	0	0	1	0	0	0	0	0	0	1	0	1	1	0	0
Hiodon alosoides	-	1	-	-	-	-	0	0	0	1	0	0	0	0	0	0	1	0	1	1	0	0
Dorsetichthys bechei	-	0	1	0	0	0	0	0	0	1	0	0	0	0	0	0	1	0	1	1	0	0

	67	68	69	70	71	72	73	74	75	76	77	78	79	80	81	82	83	84	85	86	87	88
Pteronisculus **spp.**	0	0	-	0	0	0	?	-	?	0	0	0	0	0	0	0	0	0	0	0	0	0
Amia calva	0	1	0	0	1	1	1	1	1	0	0	0	0	0	1	0	0	1	0	0	0	0
Caturus **spp.**	0	1	0	0	1	1	1	1	1	0	0	?	0	0	1	0	0	1	0	0	0	0
Macrepistius arenatus	0	1	0	?	?	1	?	?	1	1	?	?	?	?	?	0	?	1	?	?	0	0
Watsonulus eugnathoides	0	1	0	0	1	1	1	1	0	0	0	0	0	0	1	0	0	1	0	0	0	0
Lepidotes **spp.**	0	1	0	0	0	0	?	1	0	-	0	0	0	?	1	0	?	1	0	0	0	0
Semionotus elegans	0	1	0	0	0	0	0	1	0	-	0	0	0	?	1	0	0	1	0	0	0	0
Lepisosteus platostomus	0	0	-	0	0	0	0	1	0	-	0	1	1	1	0	0	0	1	0	0	0	0
Dentilepisosteus laevis	0	1	0	0	0	0	?	?	?	1	0	1	1	1	1	0	0	1	0	?	0	?
Macrosemius rostratus	0	0	-	1	0	0	0	?	0	-	0	0	0	0	1	0	0	1	0	0	0	0
Asthenocormus titanus	?	0	-	0	?	?	?	?	0	1	?	?	?	?	-	-	?	0	?	?	?	?
Leedsichthys problematicus	?	?	?	0	?	0	?	?	?	?	?	?	?	?	-	-	?	?	?	?	?	?
Martillichthys renwickae	1	0	-	0	1	0	1	0	0	1	0	0	0	?	-	-	0	?	0	1	0	-
Rhinconichthys taylori	1	0	-	1	?	0	?	?	?	0	?	0	0	?	-	-	?	0	?	?	0	?
Bonnerichthys gladius	1	0	-	1	1	0	?	?	?	0	0	?	?	?	-	-	?	?	?	?	0	1
Ohmdenia multidentata	?	?	?	1	?	0	?	?	?	0	0	?	?	?	0	0	0	0	?	?	?	?
Saurostomus esocinus	0	1	1	0	?	0	?	0	?	0	0	0	?	?	0	0	0	0	?	?	?	?
Pachycormus **sp.**	0	1	1	0	1	0	1	0	0	0	0	0	0	0	1	0	0	0	0	0	0	0
Australopachycormus hurleyi	?	?	?	?	?	?	?	?	?	?	?	?	?	?	1	1	?	?	0	1	?	?
Protosphyraena **spp.**	?	0	-	0	1	0	?	0	?	0	0	?	0	?	0	1	0	0	0	1	0	0
Orthocormus cornutus	0	1	1	?	?	0	?	?	?	0	?	?	?	?	0	1	?	?	?	?	?	?
Orthocormus roeperi	0	1	1	?	?	0	?	?	?	0	?	?	?	?	1	1	?	?	?	?	?	?
Orthocormus teyleri	0	?	?	?	?	0	?	?	?	0	?	?	?	?	0	1	?	?	?	?	?	?
Hypsocormus tenuirostris	0	1	1	0	?	?	?	?	?	0	?	?	0	0	0	1	0	0	0	1	0	0
Hypsocormus macrodon	0	1	1	?	?	?	?	?	?	0	?	?	?	?	?	1	0	0	?	?	?	?
Hypsocormus insignis	?	1	1	0	?	?	?	?	?	0	?	?	?	?	0	0	?	0	?	?	?	?
Euthynotus **spp.**	0	1	1	0	1	?	?	0	?	0	?	?	?	?	1	0	?	0	?	?	?	?
Aspidorhynchus acutirostris	0	1	1	0	1	0	0	0	?	0	?	0	0	?	1	0	1	1	?	?	1	-
Vinctifer comptoni	0	0	-	0	1	1	0	1	?	1	?	0	0	?	1	0	1	1	?	?	1	-
Belonostomus tenuirostris	0	0	-	?	1	0	0	?	?	1	?	0	0	?	1	0	1	?	?	?	1	-
Elops hawaiensis	0	1	0	0	1	0	0	0	0	1	1	0	0	0	?	0	1	1	1	-	1	-
Hiodon alosoides	0	0	-	0	1	0	0	0	0	1	1	0	0	0	1	0	1	1	1	-	1	-
Dorsetichthys bechei	0	1	0	0	1	0	0	0	0	1	1	0	0	?	1	0	0	1	1	?	0	?

	89	90	91	92	93	94	95	96	97	98	99	100	101	102	103	104	105	106	107	108	109	110
Pteronisculus **spp.**	0	0	0	1	0	0	0	0	-	0	?	0	0	0	-	-	0	0	0	0	0	0
Amia calva	0	1	0	1	1	0	0	1	0	0	1	0	0	0	-	-	0	0	0	0	0	0
Caturus **spp.**	0	1	0	1	1	0	0	0	0	0	1	0	0	0	-	-	0	0	0	0	1	0
Macrepistius arenatus	?	1	0	?	?	0	0	1	0	0	1	0	0	0	-	-	?	?	?	?	1	?
Watsonulus eugnathoides	0	1	0	?	?	0	0	0	-	0	?	0	0	0	-	-	0	0	0	0	1	0
Lepidotes **spp.**	?	1	1	?	1	0	0	1	0	0	?	0	0	0	-	-	0	1	0	0	1	?
Semionotus elegans	0	1	1	?	1	0	0	0	-	0	?	0	0	0	-	-	0	1	0	0	1	1
Lepisosteus platostomus	0	1	1	1	0	0	0	1	1	0	0	0	0	0	-	-	0	1	0	0	1	1
Dentilepisosteus laevis	0	1	1	?	?	0	0	1	1	0	0	0	0	0	-	-	0	1	0	0	1	?
Macrosemius rostratus	0	1	1	?	1	0	0	1	0	0	?	0	0	0	-	-	0	1	0	0	1	?
Asthenocormus titanus	?	0	0	?	?	?	1	0	-	0	?	?	?	1	1	1	?	?	?	?	?	?
Leedsichthys problematicus	0	?	0	?	?	?	1	0	-	?	?	?	?	?	?	?	?	?	?	?	?	?
Martillichthys renwickae	0	0	0	?	?	?	1	0	-	?	-	?	?	?	?	?	?	?	?	?	?	?
Rhinconichthys taylori	0	?	0	?	?	?	?	0	-	?	?	?	?	?	?	?	?	?	?	?	?	?
Bonnerichthys gladius	?	0	0	?	?	?	?	0	-	?	?	?	?	1	1	1	1	0	?	?	?	0
Ohmdenia multidentata	?	?	?	?	?	?	0	0	-	0	?	?	?	?	?	?	1	0	1	1	?	?
Saurostomus esocinus	?	0	0	?	?	0	0	0	-	0	?	?	2	1	1	0	1	0	1	1	?	?
Pachycormus **sp.**	0	1	0	1	1	1	0	0	-	?	-	1	2	1	0	0	1	0	1	1	1	0
Australopachycormus hurleyi	?	?	?	?	?	?	1	0	?	?	?	?	?	?	?	?	?	?	?	?	?	?
Protosphyraena **spp.**	0	?	0	?	?	?	0	0	-	?	?	?	2	1	0	-1	1	0	?	?	?	0
Orthocormus cornutus	?	?	?	?	?	1	0	0	-	0	-	?	?	?	?	?	?	?	?	?	?	?
Orthocormus roeperi	?	?	?	?	?	1	0	0	-	?	-	?	2	1	0	?	?	?	?	?	?	?
Orthocormus teyleri	?	?	?	?	?	1	0	0	-	?	-	?	2	1	?	?	?	?	?	?	1	?
Hypsocormus tenuirostris	0	?	?	?	?	?	0	0	-	0	?	?	?	1	0	1	1	0	?	?	?	?
Hypsocormus macrodon	?	?	?	?	?	0	0	0	-	0	?	?	?	?	?	?	?	?	?	?	?	?
Hypsocormus insignis	?	0	0	?	?	0	0	0	-	0	?	1	?	1	0	0	?	0	0	0	?	?
Euthynotus **spp.**	?	0	?	?	?	0	0	1	0	0	?	0	2	1	0	0	1	0	0	0	1	?
Aspidorhynchus acutirostris	0	1	1	?	?	0	1	0	-	0	-	?	(1 2)	0	-	-	1	?	0	?	0	?
Vinctifer comptoni	0	1	1	?	?	0	0	1	?	0	?	?	1	0	-	-	1	1	0	?	0	0
Belonostomus tenuirostris	0	1	1	?	?	0	0	1	?	0	?	?	(1 2)	0	-	-	1	?	0	?	0	?
Elops hawaiensis	1	0	0	0	1	1	0	1	0	1	0	0	1	0	-	-	1	0	1	0	1	0
Hiodon alosoides	1	0	1	0	1	0	0	1	0	1	0	0	1	0	-	-	1	0	0	0	0	0
Dorsetichthys bechei	0	0	0	?	?	1	0	0	0	1	1	0	1	0	-	-	1	0	0	0	0	?

	111	112	113	114	115	116	117	118	119	120	121	122	123	124	125	126	127	128	129	130	131	132	133
Pteronisculus **spp.**	0	0	0	0	0	0	0	0	0	0	0	0	0	?	?	?	0	?	?	?	1	0	1
Amia calva	0	0	0	0	0	0	0	0	0	0	1	0	0	1	0	1	0	?	?	?	1	0	2
Caturus **spp.**	0	0	0	0	0	0	0	0	0	0	0	0	0	1	0	0	0	1	1	0	1	?	2
Macrepistius arenatus	?	0	?	?	?	?	?	?	0	0	0	0	0	?	?	?	0	?	?	0	1	?	?
Watsonulus eugnathoides	?	?	0	0	?	0	0	0	0	0	0	0	0	?	?	?	0	1	1	0	1	?	1
Lepidotes **spp.**	0	0	0	0	0	0	0	0	0	1	0	0	0	?	?	?	0	?	1	?	1	?	?
Semionotus elegans	?	?	0	0	0	0	0	0	0	1	0	0	0	1	?	?	0	1	1	?	1	?	2
Lepisosteus platostomus	0	?	0	0	0	0	0	0	0	0	0	0	0	1	0	1	1	0	1	0	0	0	2
Dentilepisosteus laevis	?	?	0	0	0	0	0	0	0	0	0	0	0	1	0	1	1	1	1	0	1	0	0
Macrosemius rostratus	0	0	0	0	0	0	0	0	0	0	0	0	0	1	0	1	0	1	1	?	1	0	?
Asthenocormus titanus	?	?	1	0	0	1	1	-	1	0	-	1	?	1	1	1	1	0	0	?	0	?	?
Leedsichthys problematicus	?	1	1	0	0	1	?	?	1	?	-	?	?	1	1	1	1	?	?	?	0	?	?
Martillichthys renwickae	?	?	1	0	0	1	0	?	1	0	-	1	1	1	1	1	1	0	1	1	0	?	?
Rhinconichthys taylori	?	?	?	?	?	?	?	?	?	?	?	1	1	1	1	?	0	1	0	1	0	?	?
Bonnerichthys gladius	?	1	1	1	0	1	?	?	1	?	-	?	1	?	?	?	0	1	1	0	0	?	?
Ohmdenia multidentata	?	1	1	1	0	1	1	-	1	0	-	?	?	?	?	?	?	0	?	?	1	?	?
Saurostomus esocinus	?	1	1	0	0	1	1	-	0	0	0	?	?	?	?	?	0	?	?	?	1	?	?
Pachycormus **sp.**	1	1	1	0	0	1	1	-	0	0	0	0	0	1	0	0	0	1	1	0	1	1	1
Australopachycormus hurleyi	?	?	1	?	1	-	?	?	?	?	?	0	0	?	?	?	0	?	?	0	1	?	?
Protosphyraena **spp.**	0	1	1	1	1	-	0	1	1	0	-	?	?	?	?	?	?	?	?	?	1	?	?
Orthocormus cornutus	0	?	1	0	0	1	0	1	0	?	0	0	0	?	?	?	1	?	?	?	1	?	?
Orthocormus roeperi	0	?	1	0	?	?	0	1	0	0	0	0	0	?	?	?	1	?	?	?	1	?	?
Orthocormus teyleri	0	?	1	0	0	1	0	1	0	?	0	0	0	?	?	?	1	?	?	?	1	?	?
Hypsocormus tenuirostris	0	?	1	0	?	?	?	?	0	0	0	?	?	1	0	1	?	?	?	?	1	?	?
Hypsocormus macrodon	?	?	1	0	0	1	0	0	0	0	0	?	?	?	?	?	?	?	?	?	1	?	?
Hypsocormus insignis	?	1	1	0	0	1	0	1	0	0	0	?	?	?	?	?	?	?	?	?	1	?	?
Euthynotus **spp.**	?	?	1	0	0	1	0	1	0	0	0	?	?	?	?	?	?	?	?	?	1	?	?
Aspidorhynchus acutirostris	0	?	0	0	1	-	0	0	0	1	0	0	0	?	?	?	1	?	?	0	1	?	0
Vinctifer comptoni	0	0	0	0	1	-	0	0	0	1	0	0	0	?	?	?	1	?	1	0	0	?	0
Belonostomus tenuirostris	0	?	0	0	1	-	0	0	0	1	0	0	0	?	?	?	1	?	?	0	1	?	0
Elops hawaiensis	1	?	0	0	?	0	0	0	0	0	1	?	?	?	?	?	?	?	?	?	1	1	0
Hiodon alosoides	1	0	0	0	0	0	0	0	0	0	1	0	0	1	1	0	0	1	1	0	1	1	0
Dorsetichthys bechei	1	?	0	0	0	0	0	0	0	0	0	?	?	1	1	0	0	?	?	?	1	?	?

Character Optimizations

Character optimizations are included below. Because it is too small to be read here, this has also been included in the digital supplementary information.

Figure A1 – ACTRAN and DELTRAN character optimizations from the maximum parsimony analysis. This is an output file from MacClade, and a key is included.

PAUP analyses script*

```
log file=pachycormids.log;
execute Pachycormidmatrix.nex;
outgroup Pteronisculus_spp;
set root=outgroup;
Exclude 76 23 105 37;
set maxtrees=35000 increase=NO;
hsearch addseq=random hold=5 nreps=500;
condense collapse;
savetrees /file=pachycormids.tre;
contree /strict=yes adams=yes majrule=yes;
file=consensus_pachycormids.tre;
```

MrBayes analyses code blocks

The code given here is the parameter block written at the end of each nexus file. The character matrix is given above, and the 12 nuclear genes used (where molecular data are included) are from Broughton *et al.* (2013). Full nexus files for MrBayes are provided in the digital supplementary information.

Morphology-only Bayesian analyses

```
begin mrbayes;
exclude 23 76 37 105;
outgroup Pteronisculus_spp;
lset coding=variable rates=gamma;
mcmcp filename=AllMorph;
mcmcp nchains=4 savebrlens=yes;
mcmcp nruns=2 diagnfreq=1000 diagnstat=maxstddev;
mcmcp ngen=5000000 printfreq=100 samplefreq=100;
mcmc;
sump filename=AllMorph;
sumt filename=AllMorph;
end;
```

Bayesian analysis including morphological and nuclear data

```
begin mrbayes;
      charset p1 = 1-990\3; [molecular]
      charset p2 = 2-990\3 9740-10674\3; [molecular]
      charset p3 = 3-990\3 1824-2448\3 3426-4206\3 4209-4887\3
9054-9738\3 9741-10674\3; [molecular]
      charset p4 = 991-1821\3 5593-7080\3 7081-7914\3 9052-9738\3;
[molecular]
```

```
     charset p5 = 992-1821\3 1823-2448\3 2450-3423\3 3425-4206\3
4889-5592\3 5594-7080\3 7082-7914\3 7916-9051\3; [molecular]
     charset p6 = 993-1821\3 2451-3423\3 4890-5592\3 7083-7914\3
7917-9051\3; [molecular]
     charset p7 = 1822-2448\3 2449-3423\3 3424-4206\3 4207-4887\3
4888-5592\3 7915-9051\3 9739-10805\3; [molecular]
     charset p8 = 4208-4887\3 9053-9738\3; [molecular]
     charset p9 = 5595-7080\3; [molecular]
     charset p10 = 10675-10805; [morphological]

     partition bypartition=10:p1,p2,p3,p4,p5,p6,p7,p8,p9,p10;
     set partition=bypartition;
    lset applyto=(1,2,6,9) nst=6 rates=invgamma; prset
revmatpr=dirichlet(1,1,1,1,1,1) statefreqpr=fixed(equal)
shapepr=uniform(0.1,50) pinvarpr=uniform(0,1);[SYM+G+I]
    lset applyto=(3,4,5,7) nst=6 rates=invgamma; prset
revmatpr=dirichlet(1,1,1,1,1,1) statefreqpr=dirichlet(1)
shapepr=uniform(0.1,50) pinvarpr=uniform(0,1);[GTR+G+I]
     lset applyto=(8) nst=6 rates=gamma; prset
revmatpr=dirichlet(1,1,1,1,1,1) statefreqpr=dirichlet(1)
shapepr=uniform(0.1,50); [GTR+G]
     lset applyto=(10) rates=gamma coding=variable;
     unlink shape=(all) revmat=(1,2,3,4,5,6,7,8,9)
pinvar=(1,2,3,4,5,6,7,9,10) statefreq=(all);

outgroup Pteronisculus_spp;
exclude 10697 10750 10711 10779;
     prset applyto = (all)  ratepr = variable;
     prset applyto=(all) brlenspr=unconstrained:exp(100);
     mcmc ngen=5000000 append=no;
sump burninfrac=0.5;
sumt burninfrac=0.5;
end;
```

Fossilized Birth-Death analysis (including morphological, molecular and stratigraphic data)

```
begin mrbayes;
      charset p1 = 1-990\3; [molecular]
      charset p2 = 2-990\3 9740-10674\3; [molecular]
      charset p3 = 3-990\3 1824-2448\3 3426-4206\3 4209-4887\3
9054-9738\3 9741-10674\3; [molecular]
      charset p4 = 991-1821\3 5593-7080\3 7081-7914\3 9052-9738\3;
[molecular]
      charset p5 = 992-1821\3 1823-2448\3 2450-3423\3 3425-4206\3
4889-5592\3 5594-7080\3 7082-7914\3 7916-9051\3; [molecular]
      charset p6 = 993-1821\3 2451-3423\3 4890-5592\3 7083-7914\3
7917-9051\3; [molecular]
      charset p7 = 1822-2448\3 2449-3423\3 3424-4206\3 4207-4887\3
4888-5592\3 7915-9051\3 9739-10674\3; [molecular]
      charset p8 = 4208-4887\3 9053-9738\3; [molecular]
      charset p9 = 5595-7080\3; [molecular]
      charset p10 = 10675-10807; [morphological]

      partition bypartition=10:p1,p2,p3,p4,p5,p6,p7,p8,p9,p10;
      set partition=bypartition;
    lset applyto=(1,2,6,9) nst=6 rates=invgamma; prset
revmatpr=dirichlet(1,1,1,1,1,1) statefreqpr=fixed(equal)
shapepr=uniform(0.1,50) pinvarpr=uniform(0,1);[SYM+G+I]
    lset applyto=(3,4,5,7) nst=6 rates=invgamma; prset
revmatpr=dirichlet(1,1,1,1,1,1) statefreqpr=dirichlet(1)
shapepr=uniform(0.1,50) pinvarpr=uniform(0,1);[GTR+G+I]
      lset applyto=(8) nst=6 rates=gamma; prset
revmatpr=dirichlet(1,1,1,1,1,1) statefreqpr=dirichlet(1)
shapepr=uniform(0.1,50); [GTR+G]
      lset applyto=(10) rates=gamma coding=variable;
      unlink shape=(all) revmat=(1,2,3,4,5,6,7,8,9)
pinvar=(1,2,3,4,5,6,7,9,10) statefreq=(all);

outgroup Pteronisculus_spp;
exclude 10697 10750 10711 10779;
```

```
calibrate
      Pteronisculus_spp=uniform(251.2, 251.9)
      Amia_calva=fixed(0)
      Caturus_spp=uniform(150.9, 152.1)
      Macrepistius_arenatus=uniform(100.5, 113)
      Watsonulus_eugnathoides=uniform(251.2, 251.9)
      Lepidotes_spp=uniform(180.4, 181.7)
      Semionotus_elegans=uniform(200.8, 201.1)
      Lepisosteus_osseus [Lepisosteus_platostomus]=fixed(0)
      Dentilepisosteus_laevis=uniform(100.5, 113)
      Macrosemius_rostratus=uniform(150.9, 152.1)
      Asthenocormus_titanius=uniform(150.9, 152.1)
      Leedsichthys_problematicus=uniform(164, 164.7)
      Martillichthys_NEW=uniform(164, 164.7)
      Rhinconichthys_taylori=uniform(98.5, 100.3)
      Bonnerichthys_gladius=uniform(85.6, 86.7)
      Ohmdenia_multidentata=uniform(180.4, 181.7)
      Saurostomus_esocinus=uniform(180.4, 181.7)
      Pachycormus_NEW=uniform(180.4, 181.7)
      Australopachycormus_hurleyi=uniform(100.5, 113)
      Protosphyraena_spp=uniform(87.9, 89.8)
      Orthocormus_cornutus=uniform(150.9, 152.1)
      Orthocormus_roeperi=uniform(152.1, 153.5)
      Orthocormus_teyleri=uniform(152.1, 153.5)
      Hypsocormus_tenuirostris=uniform(164, 164.7)
      Hypsocormus_macrodon=uniform(150.9, 152.1)
      Hypsocormus_insignis=uniform(150.9, 152.1)
      Euthynotus_spp=uniform(180.4, 181.7)
      Aspidorhynchus_acutirostris=uniform(150.9, 152.1)
      Vinctifer_comptoni=uniform(100.5, 113)
      Belonostomus_tenuirostris=uniform(152.1, 153.5)
      Elops_saurus [Elops_hawaiensis]=fixed(0)
      Hiodon_alosoides=fixed(0)
      Dorsetichthys_bechei=uniform(200.8, 201.1)
      ;
```

```
      prset ratepr = variable;
      prset brlenspr=clock:fossilization;
      prset speciationpr=exp(20);
      prset extinctionpr=beta(1,1);
      prset fossilizationpr=beta(1,1);
      prset sampleprob=0.00013 samplestrat=diversity 4: 182.7 0,
166.1 0, 145 0, 113 0; [Toarcian-Bathonian, Callovian-Tithonian,
Berriasian-Aptian, Albian-present]
      prset clockvarpr=tk02 tk02varpr=exp(10);
      prset clockratepr=gamma(1,2);
      prset nodeagepr=calibrated;
      mcmc ngen=100000000 append=no;
sump burninfrac=0.5;
sumt burninfrac=0.5;
end;
```

Stepping stone analysis – Currently accepted relationships

```
begin mrbayes;
outgroup Euthynotus_spp;
exclude 23 76 37 105;
calibrate
      Asthenocormus_titanius=uniform(64.75, 65.95)
      Leedsichthys_problematicus=uniform(77.85, 78.55)
      Martillichthys_NEW=uniform(77.85, 78.55)
      Rhinconichthys_taylori=uniform(12.35, 14.15)
      Bonnerichthys_gladius=fixed(0)
      Ohmdenia_multidentata=uniform(94.25, 95.55)
      Saurostomus_esocinus=uniform(94.25, 95.55)
      Pachycormus_NEW=uniform(94.25, 95.55)
      Australopachycormus_hurleyi=uniform(14.35, 26.85)
      Protosphyraena_spp=fixed(0)
      Orthocormus_cornutus=uniform(64.75, 65.95)
      Orthocormus_roeperi=uniform(65.95, 67.35)
      Orthocormus_teyleri=uniform(65.95, 67.35)
      Hypsocormus_tenuirostris=uniform(77.85, 78.55)
```

```
      Hypsocormus_macrodon=uniform(64.75, 65.95)
      Hypsocormus_insignis=uniform(64.75, 65.95)
      Euthynotus_spp=uniform(94.25, 95.55);

      constraint edent= Bonnerichthys_gladius
Leedsichthys_problematicus Asthenocormus_titanius
Martillichthys_NEW Rhinconichthys_taylori;
      prset topologypr=constraints(edent);
      prset ratepr = variable;
      prset brlenspr=clock:fossilization;
      prset speciationpr=exp(20);
      prset extinctionpr=beta(1,1);
      prset fossilizationpr=beta(1,1);
      prset sampleprob=0.117; [2/17]
      prset clockvarpr=tk02 tk02varpr=exp(10);
      prset clockratepr=gamma(1,2);
      prset nodeagepr=calibrated;
      ss ngen=150000000 burninss=-1 append=no;
end;
```

Stepping stone analysis – Alternative relationships hypothesis

```
begin mrbayes;
outgroup Euthynotus_spp;
exclude 23 76 37 105;
calibrate
      Asthenocormus_titanius=uniform(64.75, 65.95)
      Leedsichthys_problematicus=uniform(77.85, 78.55)
      Martillichthys_NEW=uniform(77.85, 78.55)
      Rhinconichthys_taylori=uniform(12.35, 14.15)
      Bonnerichthys_gladius=fixed(0)
      Ohmdenia_multidentata=uniform(94.25, 95.55)
      Saurostomus_esocinus=uniform(94.25, 95.55)
      Pachycormus_NEW=uniform(94.25, 95.55)
      Australopachycormus_hurleyi=uniform(14.35, 26.85)
      Protosphyraena_spp=fixed(0)
```

```
      Orthocormus_cornutus=uniform(64.75, 65.95)
      Orthocormus_roeperi=uniform(65.95, 67.35)
      Orthocormus_teyleri=uniform(65.95, 67.35)
      Hypsocormus_tenuirostris=uniform(77.85, 78.55)
      Hypsocormus_macrodon=uniform(64.75, 65.95)
      Hypsocormus_insignis=uniform(64.75, 65.95)
      Euthynotus_spp=uniform(94.25, 95.55);

      constraint newclade= Bonnerichthys_gladius
Australopachycormus_hurleyi Protosphyraena_spp;
      prset topologypr=constraints(newclade);
      prset ratepr = variable;
      prset brlenspr=clock:fossilization;
      prset speciationpr=exp(20);
      prset extinctionpr=beta(1,1);
      prset fossilizationpr=beta(1,1);
      prset sampleprob=0.117; [2/17]
      prset clockvarpr=tk02 tk02varpr=exp(10);
      prset clockratepr=gamma(1,2);
      prset nodeagepr=calibrated;
      ss ngen=150000000 burninss=-1 append=no;
end;
```

Appendix D

Occurrence records

Suspension-feeding pachycormiform occurrence records

Below is the compiled list of suspension-feeding pachycormiform occurrences from a literature review. A full list of the actinopterygian yielding horizons (collected from the Paleobiology Database) can be found in RData.xlsx in the digital supplementary information.

Reference	Genus	Specimen No.	Horizon	Age
Gouiric-Cavalli *et al.* 2019	*Asthenocormus*	IAA-Pv 330	Tierra de San Martin, Amenghino Formation	Latest Kimmeridgian - Early Tithonian
Lambers 1992	*Asthenocormus*	JM.SOS 542a+b	Langenaltheim	Tithonian
Friedman *et al.* 2013*a*	*Bonnerichthys*	NJSM 14668	Chesapeake and Delaware Canal, DE	Early Late Campanian
Friedman *et al.* 2013*a*	*Bonnerichthys*	NJSM 15140	Marlboro Township, NJ	Late Campanian
Friedman *et al.* 2013*a*	*Bonnerichthys*	AMNH FF 1849	Rooks County, KA	Santonian-Campanian
Friedman *et al.* 2013*a*	*Bonnerichthys*	AMNH FF 2064	Logan county, KA	Santonian-Campanian
Friedman *et al.* 2013*a*	*Bonnerichthys*	AMNH FF 6314	Western Kansas	Santonian-Campanian
Friedman *et al.* 2013*a*	*Bonnerichthys*	AMNH FF 6315	Western Kansas	Santonian-Campanian
Friedman *et al.* 2013*a*	*Bonnerichthys*	AMNH FF 6316	Western Kansas	Santonian-Campanian
Friedman *et al.* 2013*a*	*Bonnerichthys*	FHSM VP-212	Gove county, KA	Santonian-Campanian
Friedman *et al.* 2013*a*	*Bonnerichthys*	FHSM VP-17427	Logan county, KA	Santonian-Campanian
Friedman *et al.* 2013*a*	*Bonnerichthys*	FHSM VP-17428	Gove county, KA	Santonian-Campanian
Friedman *et al.* 2013*a*	*Bonnerichthys*	FHSM VP-17457	Gove county, KA	Santonian-Campanian

Friedman *et al.* 2013*a*	*Bonnerichthys*	FHSM VP-18986	Gove county, KA	Coniacian
Friedman *et al.* 2013*a*	*Bonnerichthys*	FHSM VP-18987	Gove county, KA	Coniacian
Friedman *et al.* 2013*a*	*Bonnerichthys*	KUVP 439	Graham county, KA	Santonian-Campanian
Friedman *et al.* 2013*a*	*Bonnerichthys*	KUVP 465	Logan county, KA	Santonian-Campanian
Friedman *et al.* 2013*a*	*Bonnerichthys*	KUVP 13995	Logan county, KA	Santonian-Campanian
Friedman *et al.* 2013*a*	*Bonnerichthys*	KUVP 49505	Gove county, KA	Latest Coniacian
Friedman *et al.* 2013*a*	*Bonnerichthys*	KUVP 55592	Gove county, KA	Santonian-Campanian
Friedman *et al.* 2013*a*	*Bonnerichthys*	KUVP 60620	Logan county, KA	Santonian-Campanian
Friedman *et al.* 2013*a*	*Bonnerichthys*	KUVP 60692	Logan county, KA	Santonian-Campanian
Friedman *et al.* 2013*a*	*Bonnerichthys*	KUVP 65702	Gove county, KA	Santonian-Campanian
Friedman *et al.* 2013*a*	*Bonnerichthys*	KUVP 66692	Gove county, KA	Santonian-Campanian
Friedman *et al.* 2013*a*	*Bonnerichthys*	KUVP 84867	Lane County, KA	Santonian-Campanian
Friedman *et al.* 2013*a*	*Bonnerichthys*	LACM 126520	Logan county, KA	Santonian-Campanian
Friedman *et al.* 2013*a*	*Bonnerichthys*	MCZ 13254	Gove county, KA	Santonian-Campanian
Friedman *et al.* 2013*a*	*Bonnerichthys*	MCZ 13255	Gove county, KA	Santonian-Campanian
Friedman *et al.* 2013*a*	*Bonnerichthys*	ROM 00876	Logan county, KA	Santonian-Campanian
Friedman *et al.* 2013*a*	*Bonnerichthys*	ROM 37168	Gove county, KA	Santonian-Campanian
Friedman *et al.* 2013*a*	*Bonnerichthys*	AMNH FF 19288	Fall River County, SD	Middle Campanian
Friedman *et al.* 2013*a*	*Bonnerichthys*	UCM 55412	Niobrara county, WY	Middle Campanian
Friedman *et al.* 2013*a*	*Bonnerichthys*	KUVP 338	Logan county, KA	Middle Campanian
Friedman *et al.* 2013*a*	*Bonnerichthys*	UNSM 88507	Harlan County reservoir, NE	Middle Campanian

Friedman *et al.* 2013*a*	*Bonnerichthys*	SDSM 7033	Hyde county, SD	Late Campanian
Friedman *et al.* 2013*a*	*Bonnerichthys*	UNSM 50999	Knox county, NE	Early Maastrichtian
Friedman *et al.* 2013*a*	*Bonnerichthys*	MMNS 5257	Clay county, MS	Upper Cretaceous
Friedman *et al.* 2013*a*	*Bonnerichthys*	AUMP 1269	Dallas county, AL	Santonian-Campanian
Friedman *et al.* 2013*a*	*Bonnerichthys*	AUMP 2050	Dallas county, AL	Santonian-Campanian
Friedman *et al.* 2013*a*	*Bonnerichthys*	UAM PV2005.006.0124	Dallas county, AL	Santonian-Campanian
Friedman *et al.* 2013*a*	*Bonnerichthys*	UAM PV2006.0002.0004	Dallas county, AL	Santonian-Campanian
Friedman *et al.* 2013*a*	*Bonnerichthys*	FMNH PF 27363	Hale county, AL	Santonian-Campanian
Friedman *et al.* 2013*a*	*Bonnerichthys*	FMNH P 27364	Hale county, AL	Santonian-Campanian
Friedman *et al.* 2013*a*	*Bonnerichthys*	FMNH P 27365	Dallas county, AL	Santonian-Campanian
Friedman *et al.* 2013*a*	*Bonnerichthys*	KUVP 50179	Barbour county, AL	Santonian-Campanian
Friedman *et al.* 2013*a*	*Bonnerichthys*	MMNS 3613	Monroe/Clay county, MS	Santonian-Campanian
Friedman *et al.* 2013*a*	*Bonnerichthys*	MMNS 392	Noxubee county, MS	Middle to late Campanian
Friedman *et al.* 2013*a*	*Bonnerichthys*	MMNS 3625	Lee county, MS	Middle to late Campanian
Friedman *et al.* 2013*a*	*Bonnerichthys*	MMNS 5427	Noxubee county, MS	Middle to late Campanian
Friedman *et al.* 2013*a*	*Bonnerichthys*	MMNS 5428	Noxubee county, MS	Middle to late Campanian
Friedman *et al.* 2013*a*	*Bonnerichthys*	RMM 2794	Lowndes county, AL	Middle to late Campanian
Friedman *et al.* 2013*a*	*Bonnerichthys*	NJSM 22466-70	Fannin County, TX	Mid-Campanian
Friedman *et al.* 2013*a*	*Bonnerichthys*	SMU 76850	Clark county, AR	Late Campanian
Friedman *et al.* 2013*a*	*Bonnerichthys*	LACM (CIT locality 355) 10125	Fresno county, CA	Middle Maastrichtian
Friedman *et al.* 2013*a*	*Bonnerichthys*	UCMP 137224	Fresno county, CA	Middle Maastrichtian

Liston 2010; 2015	*Leedsichthys*	GLAHM 132787	Cap de la Heve	Upper Kimmeridgian
Liston 2010	*Leedsichthys*	Private	Villers-sur-Mer	Callovian
Liston 2010	*Leedsichthys*	BMNH 32581	Villers-sur-Mer	Callovian
Liston 2010	*Leedsichthys*	WMfN PM 17006/8	Wallucke	Middle-Upper Callovian
Liston 2010	*Leedsichthys*	WMfN PM 17006/1	Wallucke	Middle-Upper Callovian
Liston 2010	*Leedsichthys*	WMfN PM 17005/2	Wallucke	Middle-Upper Callovian
Liston 2010	*Leedsichthys*	WMfN PM 17005/23	Wallucke	Middle-Upper Callovian
Liston 2010	*Leedsichthys*	WMfN PM 17005/24	Wallucke	Middle-Upper Callovian
Liston 2010	*Leedsichthys*	PHBW 138/4	Wallucke	Middle-Upper Callovian
Liston 2010	*Leedsichthys*	PMM 19.1-21.1, 23.1	Wallucke	Middle-Upper Callovian
Liston 2010	*Leedsichthys*	GLANHM 109518	Wallucke	Middle-Upper Callovian
Liston 2010	*Leedsichthys*	BMNH P.6921	Dogsthorpe pit, UK	Middle Callovian
Liston 2010	*Leedsichthys*	BMNH P.6922	Dogsthorpe pit, UK	Middle Callovian
Liston 2010	*Leedsichthys*	BMNH P.10000	Dogsthorpe pit, UK	Middle Callovian
Liston 2010	*Leedsichthys*	BMNH P.10156	Dogsthorpe pit, UK	Middle Callovian
Liston 2010	*Leedsichthys*	BMNH P.66340	Dogsthorpe pit, UK	Middle Callovian
Liston 2010	*Leedsichthys*	BMNH 46355	Christian Malford	Middle Callovian
Liston 2010	*Leedsichthys*	PETMG F.174	Whittlesey	Middle Callovian
Liston 2010	*Leedsichthys*	CAMSM J.46873	Fletton	Middle Callovian
Liston 2010	*Leedsichthys*	SMNK 2573.PAL	Quebrada Corral	Oxfordian
Liston 2010	*Leedsichthys*	I-190173	East of Antofagasta	Oxfordian
Liston 2010	*Leedsichthys*	I8-021173	East of Antofagasta	Oxfordian
Liston 2010	*Leedsichthys*	(unnumbered)	Quebrada del Profeta	Oxfordian
Liston 2010	*Leedsichthys*	CAMSM J.27416	Fletton, Huntingdonshire	Middle Callovian
Liston 2010	*Leedsichthys*	CAMSM J.27417	Fletton, Huntingdonshire	Middle Callovian
Liston 2010	*Leedsichthys*	CAMSM J.27418	Fletton, Huntingdonshire	Middle Callovian

Liston 2010	*Leedsichthys*	CAMSM J.27419	Fletton, Huntingdonshire	Middle Callovian
Liston 2010	*Leedsichthys*	CAMSM J.27420	Fletton, Huntingdonshire	Middle Callovian
Liston 2010	*Leedsichthys*	CAMSM J.27421	Fletton, Huntingdonshire	Middle Callovian
Liston 2010	*Leedsichthys*	CAMSM J.27422	Fletton, Huntingdonshire	Middle Callovian
Liston 2010	*Leedsichthys*	CAMSM J.27423	Fletton, Huntingdonshire	Middle Callovian
Liston 2010	*Leedsichthys*	CAMSM J.27425	Whittlesea	Middle Callovian
Liston 2010	*Leedsichthys*	CAMSM J.27426	Fletton, Northamptonshire	Middle Callovian
Liston 2010	*Leedsichthys*	CAMSM J.27427	Fletton, Northamptonshire	Middle Callovian
Liston 2010	*Leedsichthys*	CAMSM J.27428	Fletton, Northamptonshire	Middle Callovian
Liston 2010	*Leedsichthys*	CAMSM J.27429	Fletton, Northamptonshire	Middle Callovian
Liston 2010	*Leedsichthys*	CAMSM J.27430	Fletton, Northamptonshire	Middle Callovian
Liston 2010	*Leedsichthys*	CAMSM J.27431	Fletton, Northamptonshire	Middle Callovian
Liston 2010	*Leedsichthys*	CAMSM J.27432	Fletton, Northamptonshire	Middle Callovian
Liston 2010	*Leedsichthys*	CAMSM J.27433	Fletton, Northamptonshire	Middle Callovian
Liston 2010	*Leedsichthys*	CAMSM J.27434	Fletton, Northamptonshire	Middle Callovian
Liston 2010	*Leedsichthys*	CAMSM J.27435	Fletton, Northamptonshire	Middle Callovian
Liston 2010	*Leedsichthys*	CAMSM J.27436	Fletton, Northamptonshire	Middle Callovian
Liston 2010	*Leedsichthys*	CAMSM J.27437	Fletton, Northamptonshire	Middle Callovian
Liston 2010	*Leedsichthys*	CAMSM J.27438	Fletton, Northamptonshire	Middle Callovian
Liston 2010	*Leedsichthys*	CAMSM J.27439	Fletton, Northamptonshire	Middle Callovian
Liston 2010	*Leedsichthys*	CAMSM J.27440	Fletton, Northamptonshire	Middle Callovian
Liston 2010	*Leedsichthys*	CAMSM J.27441	Fletton, Northamptonshire	Middle Callovian

Liston 2010	*Leedsichthys*	CAMSM J.27442	Fletton, Northamptonshire	Middle Callovian
Liston 2010	*Leedsichthys*	CAMSM J.27443	Fletton, Northamptonshire	Middle Callovian
Liston 2010	*Leedsichthys*	CAMSM J.27444	Fletton, Northamptonshire	Middle Callovian
Liston 2010	*Leedsichthys*	CAMSM J.27445	Fletton, Northamptonshire	Middle Callovian
Liston 2010	*Leedsichthys*	CAMSM J.35320	Fletton, Northamptonshire	Middle Callovian
Liston 2010	*Leedsichthys*	CAMSM J.46873	Fletton, Northamptonshire	Middle Callovian
Liston 2010	*Leedsichthys*	CAMSM J.46874	Fletton, Northamptonshire	Middle Callovian
Liston 2010	*Leedsichthys*	CAMSM J.46876	Fletton, Huntingdonshire	Middle Callovian
Liston 2010	*Leedsichthys*	CAMSM J.46877	Whittlesea	Middle Callovian
Liston 2010	*Leedsichthys*	CAMSM J.46878	Whittlesea	Middle Callovian
Liston 2010	*Leedsichthys*	CAMSM J.46879	Whittlesea	Middle Callovian
Liston 2010	*Leedsichthys*	CAMSM J.66124	Whittlesea	Middle Callovian
Liston 2010	*Leedsichthys*	CAMSM J.66126	Whittlesea	Middle Callovian
Liston 2010	*Leedsichthys*	CAMSM J.66127	Whittlesea	Middle Callovian
Liston 2010	*Leedsichthys*	CAMSM J.66128	Whittlesea	Middle Callovian
Liston 2010	*Leedsichthys*	CAMSM J.66920	Fletton, Huntingdonshire	Middle Callovian
Liston 2010	*Leedsichthys*	CAMSM J.66921	Fletton, Huntingdonshire	Middle Callovian
Liston 2010	*Leedsichthys*	CAMSM J.66922	Fletton, Huntingdonshire	Middle Callovian
Liston 2010	*Leedsichthys*	CAMSM J.66923	Fletton, Huntingdonshire	Middle Callovian
Liston 2010	*Leedsichthys*	CAMSM J.66924	Fletton, Huntingdonshire	Middle Callovian
Liston 2010	*Leedsichthys*	CAMSM J.66925	Fletton, Huntingdonshire	Middle Callovian
Liston 2010	*Leedsichthys*	CAMSM J.66926	Fletton, Huntingdonshire	Middle Callovian
Liston 2010	*Leedsichthys*	CAMSM J.66928	Fletton, Huntingdonshire	Middle Callovian
Liston 2010	*Leedsichthys*	CAMSM J.66929	Fletton, Huntingdonshire	Middle Callovian

Liston 2010	*Leedsichthys*	CAMSM J.66930	Fletton, Northamptonshire	Middle Callovian
Liston 2010	*Leedsichthys*	CAMSM J.66931	Fletton, Northamptonshire	Middle Callovian
Liston 2010	*Leedsichthys*	CAMSM J.66932	Fletton, Northamptonshire	Middle Callovian
Liston 2010	*Leedsichthys*	CAMSM J.66933	Fletton, Northamptonshire	Middle Callovian
Liston 2010	*Leedsichthys*	CAMSM J.66935	Fletton, Huntingdonshire	Middle Callovian
Liston 2010	*Leedsichthys*	CAMSM J.66936	Fletton, Huntingdonshire	Middle Callovian
Liston 2010	*Leedsichthys*	CAMSM J.66937	Fletton, Huntingdonshire	Middle Callovian
Liston 2010	*Leedsichthys*	CAMSM J.66938	Fletton, Huntingdonshire	Middle Callovian
Liston 2010	*Leedsichthys*	CAMSM J.66939	Fletton, Huntingdonshire	Middle Callovian
Liston 2010	*Leedsichthys*	CAMSM J.66940	Fletton, Huntingdonshire	Middle Callovian
Liston 2010	*Leedsichthys*	CAMSM J.66941	Fletton, Huntingdonshire	Middle Callovian
Liston 2010	*Leedsichthys*	CAMSM J.66942	Fletton, Northamptonshire	Middle Callovian
Liston 2010	*Leedsichthys*	CAMSM J.66943	Fletton, Northamptonshire	Middle Callovian
Liston 2010	*Leedsichthys*	CAMSM J.66944	Fletton, Northamptonshire	Middle Callovian
Liston 2010	*Leedsichthys*	CAMSM J.67413	Fletton, Huntingdonshire	Middle Callovian
Liston 2010	*Leedsichthys*	CAMSM J.67414	Fletton, Huntingdonshire	Middle Callovian
Liston 2010	*Leedsichthys*	CAMSM J.67415	Fletton, Huntingdonshire	Middle Callovian
Liston 2010	*Leedsichthys*	CAMSM J.67416	Fletton, Huntingdonshire	Middle Callovian
Liston 2010	*Leedsichthys*	CAMSM J.67417	Fletton, Huntingdonshire	Middle Callovian
Liston 2010	*Leedsichthys*	CAMSM J.67418	Fletton, Huntingdonshire	Middle Callovian
Liston 2010	*Leedsichthys*	CAMSM J.67419	Fletton, Huntingdonshire	Middle Callovian

Liston 2010	*Leedsichthys*	CAMSM J.67420	Fletton, Huntingdonshire	Middle Callovian
Liston 2010	*Leedsichthys*	CAMSM J.67421	Fletton, Huntingdonshire	Middle Callovian
Liston 2010	*Leedsichthys*	CAMSM J.67422	Fletton, Huntingdonshire	Middle Callovian
Liston 2010	*Leedsichthys*	CAMSM J.67423	Fletton, Huntingdonshire	Middle Callovian
Liston 2010	*Leedsichthys*	CAMSM J.67424	Fletton, Huntingdonshire	Middle Callovian
Liston 2010	*Leedsichthys*	CAMSM J.67425	Fletton, Huntingdonshire	Middle Callovian
Liston 2010	*Leedsichthys*	CAMSM J.67426	Fletton, Huntingdonshire	Middle Callovian
Liston 2010	*Leedsichthys*	CAMSM J.67427	Fletton, Huntingdonshire	Middle Callovian
Liston 2010	*Leedsichthys*	CAMSM J.67428	Fletton, Huntingdonshire	Middle Callovian
Liston 2010	*Leedsichthys*	CAMSM J.67429	Fletton, Huntingdonshire	Middle Callovian
Liston 2010	*Leedsichthys*	CAMSM J.67430	Fletton, Northamptonshire	Middle Callovian
Liston 2010	*Leedsichthys*	CAMSM J.67431	Fletton, Northamptonshire	Middle Callovian
Liston 2010	*Leedsichthys*	CAMSM J.67432	Fletton, Huntingdonshire	Middle Callovian
Liston 2010	*Leedsichthys*	CAMSM J.67433	Fletton, Northamptonshire	Middle Callovian
Liston 2010	*Leedsichthys*	CAMSM J.67434	Fletton, Northamptonshire	Middle Callovian
Liston 2010	*Leedsichthys*	CAMSM J.67435	Fletton, Northamptonshire	Middle Callovian
Liston 2010	*Leedsichthys*	CAMSM J.67436	Fletton, Northamptonshire	Middle Callovian
Liston 2010	*Leedsichthys*	CAMSM J.67437	Fletton, Huntingdonshire	Middle Callovian
Liston 2010	*Leedsichthys*	CAMSM J.67438	Fletton, Huntingdonshire	Middle Callovian
Liston 2010	*Leedsichthys*	CAMSM J.67439	Fletton, Huntingdonshire	Middle Callovian
Liston 2010	*Leedsichthys*	CAMSM J.67440	Fletton, Huntingdonshire	Middle Callovian

Liston 2010	*Leedsichthys*	CAMSM J.67441	Fletton, Northamptonshire	Middle Callovian
Liston 2010	*Leedsichthys*	CAMSM J.67442	Fletton, Northamptonshire	Middle Callovian
Liston 2010	*Leedsichthys*	CAMSM J.67443	Fletton, Northamptonshire	Middle Callovian
Liston 2010	*Leedsichthys*	CAMSM J.67444	Fletton, Northamptonshire	Middle Callovian
Liston 2010	*Leedsichthys*	CAMSM J.67445	Fletton, Northamptonshire	Middle Callovian
Liston 2010	*Leedsichthys*	CAMSM J.67446	Fletton, Northamptonshire	Middle Callovian
Liston 2010	*Leedsichthys*	CAMSM J.67447	Fletton, Northamptonshire	Middle Callovian
Liston 2010	*Leedsichthys*	CAMSM J.67448	Fletton, Northamptonshire	Middle Callovian
Liston 2010	*Leedsichthys*	CAMSM J.67449	Fletton, Northamptonshire	Middle Callovian
Liston 2010	*Leedsichthys*	CAMSM J.67450	Fletton, Northamptonshire	Middle Callovian
Liston 2010	*Leedsichthys*	CAMSM J.67451	Fletton, Northamptonshire	Middle Callovian
Liston 2010	*Leedsichthys*	CAMSM J.67452	Fletton, Northamptonshire	Middle Callovian
Liston 2010	*Leedsichthys*	CAMSM J.67453	Fletton, Northamptonshire	Middle Callovian
Liston 2010	*Leedsichthys*	CAMSM J.67454	Fletton, Northamptonshire	Middle Callovian
Liston 2010	*Leedsichthys*	CAMSM J.67455	Fletton, Northamptonshire	Middle Callovian
Liston 2010	*Leedsichthys*	CAMSM J.67456	Fletton, Northamptonshire	Middle Callovian
Liston 2010	*Leedsichthys*	CAMSM J.67457	Fletton, Northamptonshire	Middle Callovian
Liston 2010	*Leedsichthys*	CAMSM J.67458	Fletton, Northamptonshire	Middle Callovian
Liston 2010	*Leedsichthys*	CAMSM J.67459	Fletton, Northamptonshire	Middle Callovian
Liston 2010	*Leedsichthys*	CAMSM J.67460	Fletton, Northamptonshire	Middle Callovian
Liston 2010	*Leedsichthys*	CAMSM J.67461	Fletton, Northamptonshire	Middle Callovian

Liston 2010	*Leedsichthys*	CAMSM J.67462	Fletton, Northamptonshire	Middle Callovian
Liston 2010	*Leedsichthys*	CAMSM J.67463	Fletton, Northamptonshire	Middle Callovian
Liston 2010	*Leedsichthys*	CAMSM J.67464	Fletton, Northamptonshire	Middle Callovian
Liston 2010	*Leedsichthys*	CAMSM J.67465	Fletton, Northamptonshire	Middle Callovian
Liston 2010	*Leedsichthys*	CAMSM J.67466	Fletton, Northamptonshire	Middle Callovian
Liston 2010	*Leedsichthys*	CAMSM J.67471	Fletton, Huntingdonshire	Middle Callovian
Liston 2010	*Leedsichthys*	CAMSM J.67472	Fletton, Huntingdonshire	Middle Callovian
Liston 2010	*Leedsichthys*	CAMSM J.67473	Fletton, Huntingdonshire	Middle Callovian
Liston 2010	*Leedsichthys*	CAMSM J.67474	Fletton, Huntingdonshire	Middle Callovian
Liston 2010	*Leedsichthys*	CAMSM J.67475	Fletton, Huntingdonshire	Middle Callovian
Liston 2010	*Leedsichthys*	CAMSM J.67476	Fletton, Huntingdonshire	Middle Callovian
Liston 2010	*Leedsichthys*	CAMSM J.67477	Fletton, Huntingdonshire	Middle Callovian
Liston 2010	*Leedsichthys*	CAMSM J.67479	Fletton, Huntingdonshire	Middle Callovian
Liston 2010	*Leedsichthys*	CAMSM J.67480	Fletton, Huntingdonshire	Middle Callovian
Liston 2010	*Leedsichthys*	CAMSM J.67481	Fletton, Huntingdonshire	Middle Callovian
Liston 2010	*Leedsichthys*	CAMSM J.67483	Fletton, Huntingdonshire	Middle Callovian
Liston 2010	*Leedsichthys*	CAMSM X.50109	Fletton, Huntingdonshire	Middle Callovian
Liston 2010	*Leedsichthys*	CAMSM X.50110	Fletton, Huntingdonshire	Middle Callovian
Liston 2010	*Leedsichthys*	CAMSM X.50111	Fletton, Huntingdonshire	Middle Callovian
Liston 2010	*Leedsichthys*	CAMSM X.50112	Fletton, Huntingdonshire	Middle Callovian
Liston 2010	*Leedsichthys*	CAMSM X.50113	Fletton, Huntingdonshire	Middle Callovian

Liston 2010	*Leedsichthys*	CAMSM X.50114	Fletton, Huntingdonshire	Middle Callovian
Liston 2010	*Leedsichthys*	CAMSM X.50115	Fletton, Huntingdonshire	Middle Callovian
Liston 2010	*Leedsichthys*	CAMSM X.50116	Fletton, Huntingdonshire	Middle Callovian
Liston 2010	*Leedsichthys*	CAMSM X.50117	Whittlesea	Middle Callovian
Liston 2010	*Leedsichthys*	CAMSM X.50118	Whittlesea	Middle Callovian
Liston 2010	*Leedsichthys*	LEICT G520.1993	Oxford Clay, Peterborough	Middle Callovian
Liston 2010	*Leedsichthys*	LEICT G472.1897	Fletton	Middle Callovian
Liston 2010	*Leedsichthys*	LEICT G473.1897	Oxford Clay, Peterborough	Middle Callovian
Liston 2010	*Leedsichthys*	LEICT G474.1897	Oxford Clay, Peterborough	Middle Callovian
Liston 2010	*Leedsichthys*	LEICT G475.1897	Oxford Clay, Peterborough	Middle Callovian
Liston 2010	*Leedsichthys*	LEICT G476.1897	Oxford Clay, Peterborough	Middle Callovian
Liston 2010	*Leedsichthys*	LEICT G477.1897	Oxford Clay, Peterborough	Middle Callovian
Liston 2010	*Leedsichthys*	LEICT G478.1897	Oxford Clay, Peterborough	Middle Callovian
Liston 2010	*Leedsichthys*	LEICT G479.1897	Oxford Clay, Peterborough	Middle Callovian
Liston 2010	*Leedsichthys*	LEICT G343.1896	Oxford Clay, Peterborough	Middle Callovian
Liston 2010	*Leedsichthys*	LEICT G344.1896	Oxford Clay, Peterborough	Middle Callovian
Liston 2010	*Leedsichthys*	LEICT G345.1896	Oxford Clay, Peterborough	Middle Callovian
Liston 2010	*Leedsichthys*	LEICT G519.1993	Oxford Clay, Peterborough	Middle Callovian
Liston 2010	*Leedsichthys*	LEICT G1312.1899	Oxford Clay, Peterborough	Middle Callovian
Liston 2010	*Leedsichthys*	LEICT G393.1896	Oxford Clay, Peterborough	Middle Callovian
Liston 2010	*Leedsichthys*	LEICT G1.2010.1	Kempston Quarry	Middle Callovian
Liston 2010	*Leedsichthys*	LEICT G1.2010.2	Dogsthorpe Pit	Middle Callovian
Liston 2010	*Leedsichthys*	LEIUG 96085	Dogsthorpe Pit	Middle Callovian
Liston 2010	*Leedsichthys*	LEIUG 96086	Market Deeping	Middle Callovian

Liston 2010	*Leedsichthys*	LEIUG 96087	Orton Pit	Middle Callovian
Liston 2010	*Leedsichthys*	LEIUG 114604	LBC pit, Calvert	Middle Callovian
Liston 2010	*Leedsichthys*	OUMNH J.1803/1	Wolvercote, Oxford	Middle Callovian
Liston 2010	*Leedsichthys*	PETMG F34	King's Dyke	Middle Callovian
Liston 2010	*Leedsichthys*	PETMG F121	Buntings Lane, near Farcet	Middle Callovian
Liston 2010	*Leedsichthys*	PETMG F174	Star Pit, Whittlesey	Middle Callovian
Liston 2010	*Leedsichthys*	GLAHM 109519	Stormer Quarry, Wallucke	Kimmeridgian
Liston 2010	*Leedsichthys*	BMNH 32581	Oxford Clay	Middle Callovian
Liston 2010	*Leedsichthys*	BMNH P.62054	Buntings Lane, near Farcet	Middle Callovian
Liston 2010	*Leedsichthys*	Private	Alan Dawn Quest Pit, Stewartby	Middle Callovian
Gouiric-Cavalli 2017	*Leedsichthys*	MOZ-Pv 1788	Vaca Muerta, Cerro Lorena	Lower Tithonian
Liston 2006, 2008*a*	*Martillichthys*	PETMG F.161	Dogsthorpe pit, UK	Middle Callovian
Liston 2006, 2008*a*; Dobson *et al.* 2019	*Martillichthys*	NHMUK PV P.61563	Dogsthorpe pit, UK	Middle Callovian
Cione *et al.* 2018	*Pachycormidae indet.*	(unnumbered)	Marambio	Latest Maastrichtian
Friedman *et al.* 2010	*Pachycormidae indet.*	NHMUK PV P.41669	Sherborne	Bajocian
Schumacher *et al.* 2016	*Rhinconichthys*	DMNH 63794	Otero county, CO	Lower middle Turonian
Friedman *et al.* 2010	*Rhinconichthys*	NSM VP21868	Mikasa city, Japan	Cenomanian
Friedman *et al.* 2010	*Rhinconichthys*	NHMUK PV OR 33219	Burham, UK	Cenomanian

Suspension-feeding chondrichthyan occurrence records

Below is the compiled list of suspension-feeding chondrichthyan occurrences from a literature review. A full list of the chondrichthyan yielding horizons (collected from the Paleobiology Database) can be found in RData.xlsx in the digital supplementary information.

Reference	**Group**	**Genus**	**Horizon**	**Age**
Applegate 1978	Cetorhinidae	*Cetorhinus*	Gloria	Zanclean
Mitchell & Tedford 1973	Cetorhinidae	*Cetorhinus*	Pyramid Hill	Chattian - Aquitanian
Baciu *et al.* 2016	Cetorhinidae	*Cetorhinus*	Piatra Neamt, Colza	Rupelian
Barnes 2008	Cetorhinidae	*Cetorhinus*	Almejas	Messinian
Barthelt *et al.* 1991	Cetorhinidae	*Cetorhinus*	Walbertsweiler	Burdigalian
Bienkowska-Wasiluk & Radwanski 2009	Cetorhinidae	*Cetorhinus*	Menilite	Oligocene
Boessenecker 2012	Cetorhinidae	*Cetorhinus*	Purisima	Zanclean - Gelasian
Bollinger *et al.* 1995	Cetorhinidae	*Cetorhinus*	St Gallen	Burdigalian
Brisswalter 2009	Cetorhinidae	*Cetorhinus*	Cabrieres d'Aigues	Langhian - Serravallian
Van Der Brugghen 2005	Cetorhinidae	*Cetorhinus*	Kattendijk	Zanclean
Brzobohaty & Schultz 1978	Cetorhinidae	*Cetorhinus*	Steinebrunn	Serravallian
Cicimurri & Knight 2009	Cetorhinidae	*Cetorhinus*	Chandler Bridge	Rupelian-Chattian
Cione & Reguero 1998	Cetorhinidae	*Cetorhinus*	La Meseta	Lutetian
De Pietri *et al.* 2010	Cetorhinidae	*Cetorhinus*	Rheinweiler	Rupelian
Domning 1978	Cetorhinidae	*Cetorhinus*	Ysidro	Aquitanian
Duheil 1991	Cetorhinidae	*Cetorhinus*	Faluns de Jeurre et de Morigny, Paris Basin	Rupelian

Duheil 1991	Cetorhinidae	*Cetorhinus*	Faluns de Vauroux, Paris Basin	Rupelian
Fitch 1970	Cetorhinidae	*Cetorhinus*	Palos Verdes Sand	Late Pleistocene
Fitch 1970	Cetorhinidae	*Cetorhinus*	Palos Verdes Sand	Late Pleistocene
Frohlicher & Wilhelm 1952	Cetorhinidae	*Cetorhinus*	Entlebuchs, Molasse Basin	Rupelian
Fulgosi *et al.* 2009	Cetorhinidae	*Cetorhinus*	Castelnuovo Berardenga	Zanclean - Piacenzian
Gille *et al.* 2010	Cetorhinidae	*Cetorhinus*	Kassel	Chattian
Gonzalez-Barba & Theis 2000	Cetorhinidae	*Cetorhinus*	Almejas	Tortonian - Messinian
Gonzalez-Barba & Theis 2000	Cetorhinidae	*Cetorhinus*	Purisima	Zanclean - Piacenzian
Gonzalez-Barba & Theis 2000	Cetorhinidae	*Cetorhinus*	Rosarito Beach	Langhian - Serravallian
Gottfried 1995	Cetorhinidae	*Cetorhinus*	Calvert	Langhian
Haye *et al.* 2008	Cetorhinidae	*Cetorhinus*	Johannistal	Chattian
Haye *et al.* 2008	Cetorhinidae	*Cetorhinus*	Ratzeburg	Chattian
Herman 1979	Cetorhinidae	*Cetorhinus*	Kattendijk	Zanclean
Herman *et al.* 1974	Cetorhinidae	*Cetorhinus*	Kattendijk	Zanclean
Hovestadt & Hovestadt-Euler 2011	Cetorhinidae	*Cetorhinus*	Fraunweiler	Rupelian
Hovestadt *et al.* 2010	Cetorhinidae	*Cetorhinus*	Fraunweiler	Rupelian
Huddleston & Takeuchi 2006	Cetorhinidae	*Cetorhinus*	Puente	Tortonian
Jonet 1947	Cetorhinidae	*Cetorhinus*	Teleajen Nappes	Rupelian
Jordan & Hannibal 1923	Cetorhinidae	*Cetorhinus*	Barker's Ranch	Burdigalian - Langhian
Jordan & Hannibal 1923	Cetorhinidae	*Cetorhinus*	Bena	Burdigalian - Langhian
Jordan & Hannibal 1923	Cetorhinidae	*Cetorhinus*	Monterey	Miocene
Jordan & Hannibal 1923	Cetorhinidae	*Cetorhinus*	Temblor	Langhian - Serravallian
Kanakoff 1956	Cetorhinidae	*Cetorhinus*	Palos Verdes Sand	Late Pleistocene

Kanakoff 1956	Cetorhinidae	*Cetorhinus*	Palos Verdes Sand	Late Pleistocene
Karasawa 1989	Cetorhinidae	*Cetorhinus*	Maenami	Langhian - Serravallian
Leriche 1910	Cetorhinidae	*Cetorhinus*	Boom	Rupelian
Leriche 1927	Cetorhinidae	*Cetorhinus*	Conglomerates of Porrentury	Rupelian
Leriche 1948	Cetorhinidae	*Cetorhinus*	Boom	Rupelian
Long 1993	Cetorhinidae	*Cetorhinus*	Coquimbo	Serravallian
Merle *et al.* 2002	Cetorhinidae	*Cetorhinus*	Vayres-sur-Essonne	Rupelian
Micklich & Parin 1996	Cetorhinidae	*Cetorhinus*	Fraunweiler	Rupelian
Muller 1976	Cetorhinidae	*Cetorhinus*	Rupel Beds	Rupelian
Pfeil 1981	Cetorhinidae	*Cetorhinus*	Schoneck Formation	Rupelian
Pharisat 1998	Cetorhinidae	*Cetorhinus*	Froidefontaine	Rupelian
Purdy *et al.* 2001	Cetorhinidae	*Cetorhinus*	Pungo River	Langhian - Serravallian
Schmid *et al.* 2001	Cetorhinidae	*Cetorhinus*	St Margarethen, Eisenstadt-Soporon Basin	Serravallian
Schultz 1978	Cetorhinidae	*Cetorhinus*	Steinebrunn	Serravallian
Schultz *et al.* 2010	Cetorhinidae	*Cetorhinus*	Hrusky	Langhian - Serravallian
Tomita & Oji 2010	Cetorhinidae	*Cetorhinus*	Ashiya Group	Rupelian - Chattian
Uyeno & Masushima 1974	Cetorhinidae	*Cetorhinus*	Nakazato	Pleistocene
van den Bosch 1984	Cetorhinidae	*Cetorhinus*	Breda	Tortonian - Zanclean
van den Bosch 1984	Cetorhinidae	*Cetorhinus*	Stemerdink Beds	Langhian - Serravallian
van den Bosch 1984	Cetorhinidae	*Cetorhinus*	Sylt Stufe, Morsum Cliff	Messinian - Zanclean
Vialle *et al.* 2011	Cetorhinidae	*Cetorhinus*	Mazan, Vaucluse	Rupelian
Walsh 2001	Cetorhinidae	*Cetorhinus*	Bahia Inglesa	Messinian - Piacenzian
Weiler 1922	Cetorhinidae	*Cetorhinus*	Alzey	Rupelian
Weiler 1931	Cetorhinidae	*Cetorhinus*	Weisloch, Upper Rhine	Rupelian
Welton 2013*a*	Cetorhinidae	*Cetorhinus*	Empire	Tortonian
Welton 2013*b*	Cetorhinidae	*Cetorhinus*	Alzey	Rupelian

Welton 2013*b*	Cetorhinidae	*Keasius*	Keasey	Bartonian - Priabonian
Welton 2014	Cetorhinidae	*Cetorhinus*	Temblor	Langhian - Serravallian
Wijnker *et al.* 2008	Cetorhinidae	*Cetorhinus*	Oosterhaut	Zanclean - Piacenzian
Yabumoto & Uyeno 1994	Cetorhinidae	*Cetorhinus*	Matsuyama Group	Miocene
Yabumoto & Uyeno 1994	Cetorhinidae	*Cetorhinus*	Mizunami Group	Middle Miocene
Yabumoto & Uyeno 1994	Cetorhinidae	*Cetorhinus*	Suso	Middle Miocene
Yabumoto & Uyeno 1994	Cetorhinidae	*Cetorhinus*	Ashiya Group	Rupelian - Chattian
De Schutter 2009	Megachasmidae	*Megachasma*	Kattendijk	Zanclean
De Schutter 2009	Megachasmidae	*Megachasma*	Nye	Aquitanian
De Schutter 2009	Megachasmidae	*Megachasma*	Pyramid Hill	Chattian - Aquitanian
De Schutter 2009	Megachasmidae	*Megachasma*	Yaquina	Chattian
Gonzalez-Barba & Theis 2000	Megachasmidae	*Megachasma*	Rosarito Beach	Langhian - Serravallian
Purdy *et al.* 2001	Megachasmidae	*Megachasma*	Pungo River	Langhian - Serravallian
Shimada & Ward 2016	Megachasmidae	*Megachasma*	Sovind Marl	Priabonian (NP19-20)
Shimada *et al.* 2014	Megachasmidae	*Megachasma*	Nye	Aquitanian
Shimada *et al.* 2014	Megachasmidae	*Megachasma*	Pyramid Hill	Aquitanian
Shimada *et al.* 2014	Megachasmidae	*Megachasma*	Skooner Gulch	Serravallian - Tortonian
Shimada *et al.* 2014	Megachasmidae	*Megachasma*	Yaquina	Chattian
Spadini & Manganelli 2015	Megachasmidae	*Megachasma*	San Quirico d'Orcia	Zanclean
Taylor *et al.* 1983	Megachasmidae	*Megachasma*	Nye	Chattian - Aquitanian
Taylor *et al.* 1983	Megachasmidae	*Megachasma*	Topanga	Burdigalian - Langhian
Adnet & Cappetta 2008	Mobulidae	*Burnhamia*	Glennes Sands	Late Ypresian (NP12)
Adnet *et al.* 2010	Mobulidae	*Burnhamia*	Samlat	Bartonian–Priabonian
Adnet *et al.* 2010	Mobulidae	*Mobula*	Samlat	Bartonian–Priabonian
Adnet *et al.* 2012	Mobulidae	*Eoplinthicus*	Samlat	Bartonian–Priabonian
Adnet *et al.* 2012	Mobulidae	*Oromobula*	Samlat	Bartonian–Priabonian
Baut & Genault 1995	Mobulidae	*Burnhamia*	Rollot, Paris Basin	Thanetian
Bor 1990	Mobulidae	*Plinthicus*	Boom	Rupelian

Bourdon 1999	Mobulidae	*Manta*	Yorktown	Zanclean
Brisswalter 2009	Mobulidae	*Mobula*	Cabrieres d'Aigues	Langhian - Serravallian
Cappetta & Stringer 2002	Mobulidae	*Eoplinthicus*	Yazoo	Priabonian
Cappetta & Traverse 1988	Mobulidae	*Burnhamia*	Kpogame-Hahotoe	Middle Eocene
Cappetta & Traverse 1988	Mobulidae	*Mobula*	Kpogame-Hahotoe	Middle Eocene
Cappetta 1970	Mobulidae	*Manta*	Herault, Loupian	Langhian
Cappetta 1970	Mobulidae	*Mobula*	Herault, Loupian	Langhian
Cappetta 1976	Mobulidae	*Burnhamia*	London Clay	Ypresian
Cappetta 1985	Mobulidae	*Burnhamia*	Ouled Abdoun	Ypresian
Cappetta *et al.* 2000	Mobulidae	*Burnhamia*	Umm Rijam Chert	Lutetian
Case 1980	Mobulidae	*Manta*	Trent	Aquitanian
Casier 1946	Mobulidae	*Burnhamia*	London Clay	Ypresian
Casier 1966	Mobulidae	*Burnhamia*	London Clay	Ypresian
Casier 1966	Mobulidae	*Burnhamia*	London Clay	Ypresian
Casier 1966	Mobulidae	*Burnhamia*	London Clay	Ypresian
Cicimurri & Knight 2009	Mobulidae	*Mobula*	Chandler Bridge	Chattian
Cope 1869	Mobulidae	*Plinthicus*	Kirkwood	Langhian
Gonzalez-Barba & Theis 2000	Mobulidae	*Burnhamia*	Rosarito Beach	Langhian - Serravallian
Gonzalez-Barba & Theis 2000	Mobulidae	*Mobula*	Almejas	Tortonian - Messinian
Gonzalez-Barba & Theis 2000	Mobulidae	*Mobula*	Rosarito Beach	Langhian - Serravallian
Jonet 1976	Mobulidae	*Manta*	Costa da Caparica	Serravallian (Helvetian)
Jonet 1976	Mobulidae	*Mobula*	Costa da Caparica	Serravallian (Helvetian)
Noubhani & Cappetta 1997	Mobulidae	*Burnhamia*	Ouled Abdoun	Thanetian - Ypresian
Pfeil 1981	Mobulidae	*Manta*	Schoneck Formation	Rupelian

Pfeil 1981	Mobulidae	*Mobula*	Schoneck Formation	Rupelian
Pimiento *et al.* 2013	Mobulidae	*Mobula*	Gatun	Tortonian
Pimiento *et al.* 2013	Mobulidae	*Mobula*	Gatun	Tortonian
Pimiento *et al.* 2013	Mobulidae	*Mobula*	Gatun	Tortonian
Purdy *et al.* 2001	Mobulidae	*Manta*	Yorktown	Zanclean
Purdy *et al.* 2001	Mobulidae	*Mobula*	Pungo River	Langhian - Serravallian
Purdy *et al.* 2001	Mobulidae	*Plinthicus*	Pungo River	Langhian - Serravallian
Sahni & Mehrotra 1981	Mobulidae	*Mobula*	Baripada	Aquitanian - Burdigalian
Schultz 1977	Mobulidae	*Mobula*	Korytnica Clays	Langhian - Serravallian
Underwood *et al.* 2011	Mobulidae	*Burnhamia*	Birket Qarun	Priabonian
Underwood *et al.* 2011	Mobulidae	*Burnhamia*	Gehannam	Late Bartonian - Priabonian
Underwood *et al.* 2011	Mobulidae	*Burnhamia*	Qasr El-Sagha	Priabonian
Underwood *et al.* 2011	Mobulidae	*Eoplinthicus*	Birket Qarun	Priabonian
Underwood *et al.* 2011	Mobulidae	*Eoplinthicus*	Gehannam	Late Bartonian - Priabonian
Underwood *et al.* 2017	Mobulidae	*Burnhamia*	London Clay	Ypresian
Woodward 1889*a*	Mobulidae	*Burnhamia*	London Clay	Ypresian
Cappetta & Traverse 1988	Rhincodontidae	*Palaeorhincodon*	Kpogame-Hahotoe	Middle Eocene
Cappetta 1970	Rhincodontidae	*Rhincodon*	Herault, Loupian	Langhian
Cicimurri & Knight 2009	Rhincodontidae	*Palaeorhincodon*	Chandler Bridge	Chattian
Cicimurri & Knight 2009	Rhincodontidae	*Rhincodon*	Chandler Bridge	Chattian
Gonzalez-Barba & Theis 2000	Rhincodontidae	*Rhincodon*	San Gregorio	Chattian
Herman 1974	Rhincodontidae	*Palaeorhincodon*	Brussels	Lutetian
Herman 1974	Rhincodontidae	*Palaeorhincodon*	Lede Sands	Lutetian
Herman 1977	Rhincodontidae	*Palaeorhincodon*	Brussels	Lower Lutetian
Herman 1977	Rhincodontidae	*Palaeorhincodon*	Ieper	Ypresian
Herman 1977	Rhincodontidae	*Palaeorhincodon*	Lede Sands	Upper Lutetian
Herman 1977	Rhincodontidae	*Palaeorhincodon*	Vlierzele	Bartonian (Auversian)

Herman 1977	Rhincodontidae	*Palaeorhincodon*	Wemmel Sands	Lutetian - Bartonian
Noubhani & Cappetta 1997	Rhincodontidae	*Palaeorhincodon*	Ouled Abdoun	Thanetian
Purdy *et al.* 2001	Rhincodontidae	*Rhincodon*	Pungo River	Langhian - Serravallian

R scripts

Pachycormiform extinction (adapted from script in Capobianco & Friedman 2018)

```
library(dplyr)
library(xlsx)

# Load fossil horizon data and eliminate duplicates (if present)

data <- read.xlsx("RData.xlsx", sheetIndex = 8) #loads horizons
yielding actinopt fossils
form.idx <- which(duplicated(data$formation))
if (length(form.idx) > 0) {
  data <- data[-c(form.idx),]
}

# Extract relevant information

max <- 202-data[, c("min_ma")] # convert earliest appearance to
latest appearance
min <- 202-data[, c("max_ma")] # convert latest appearance to
earliest appearance
ave <- rep(NA, length(max))
for (i in 1:length(max)){
  ave[i] <- (max[i]+min[i])/2
}
formation_name <- data[, c("formation")]
continents <- data[, c("continent")] # set to one continent name
formation.list <- data.frame(formation_name, continents, max,
min, ave, data[,c("early_interval")], data[,c("late_interval")])

table(formation.list$continents)

# Load fossil occurrences for the clade of interest
lepido <- read.xlsx("RData.xlsx", sheetIndex = 6) # sheet number
changes depending on the focal group (See RData.xlsx)

```

```
#Check that every formation where fossils of the focal clade have
been found are in the formation list
lepido$Formation.locality <- gsub(" Formation", "",
lepido$Formation.locality)

check <- lepido$Formation.locality %in%
formation.list$formation_name
which(check == FALSE)

form.idx <- match(lepido$Formation.locality,
formation.list$formation_name)
lepido$max <- formation.list$max[form.idx]
lepido$min <- formation.list$min[form.idx]
lepido$ave <- formation.list$ave[form.idx]

#Cumulative density function used in subsequent BayesianPosterior
function
cdf <- function (posterior.p, x, quantile) {
  area <- 0
  j <- 1
  while (area <= quantile*(sum (posterior.p))){

    area <- area + posterior.p[j]
    j <- j+1

  }

  x [j]
}

#For horizon-based calculations, FAD is measured in numbers of
horizons

Bayesian.posterior <- function(FAD, LAD, n, old.bound,
young.bound, n.bins) {

```

```
  #first, rescale variables on to the scale [0,1]

  interval <- old.bound-young.bound

  z <- (FAD-young.bound)/interval

  y <- (LAD-young.bound)/interval


  #u.n, Strauss and Sadler (1989: formula 25)

  u.n <- (z-y)^(-n-2)-(1-y)^(-n+2)+1-z^(-n+2)

  u.n1 <- (z-y)^(-(n-1)-2)-(1-y)^(-(n-1)+2)+1-z^(-(n-1)+2)

  #create a vector of theta.2 values on the scaled interval

  theta.2 <- seq (z, 1, length = n.bins)

  h.x <- array (dim = n.bins)

  for (i in 1:n.bins) {

    h.x [i] <- (n-2)*((theta.2[i]-y)^(-n+1)-theta.2[i]^(-
n+1))/u.n

  }

  #plot (theta.2, h.x, xlab = 'relative time', ylab = 'posterior
probability')

  output <- array (dim = 5)

  names (output) <- c("point estimate", "CI 2.5", "CI 50", "CI
90", "CI 97.5")

```

```
106   #Formula 27 in Straus & Sadler (1989)
107   output [1] <- ((n-2)*u.n1)/((n-3)*u.n)+(y*((z-y)^(-n+2)-(1-
108 y)^(-n+2)))/u.n
109
110   output [2] <- cdf (h.x, theta.2, 0.025)
111
112   output [3] <- cdf (h.x, theta.2, 0.5)
113
114   output [4] <- cdf (h.x, theta.2, 0.90)
115
116   output [5] <- cdf (h.x, theta.2, 0.975)
117
118   output <- output * interval
119
120   output
121
122 }
123
124 #Accounting for formation age uncertainty
125
126 binSpan <- 1
127
128 # Function that converts relative age derived from the
129 Bayesian.posterior function in absolute age
130
131 date.converter <- function (horizon.distribution, n){
132
133   age.matrix <- array (dim = c(4, ceiling(202/binSpan)))
134
135   rownames (age.matrix) <- c ("top bin", "bottom bin",
136 "horizons", "cumulative horizons")
137
138   age.matrix [1, ] <- c(seq(0, 202-binSpan, binSpan))
139   age.matrix [2, ] <- c(seq(binSpan, 202, binSpan))
140   age.matrix [3, ] <- horizon.distribution
141   age.matrix [4, ] <- cumsum (horizon.distribution)
```

```
142
143   total <- 0
144
145   i <- 1
146
147   while (total < n) {
148
149
150     total <- age.matrix [4, i]
151
152     i <- i+1
153
154   }
155
156   age.estimate <- ((n-age.matrix [4, (i-2)])/age.matrix[3,(i-
157 1)])*(age.matrix[2, (i-1)]-age.matrix[1, (i-1)]) + age.matrix[1,
158 (i-1)]
159
160   age.estimate
161
162 }
163
164 # Replicates to account for uncertainty in horizon age
165
166 Nreplicates = 1000
167 table <- array(dim=c(Nreplicates, 5))
168 for (u in 1:Nreplicates){
169
170   cat(u, "\n")
171
172   randhorizon <- rep(NA, length(formation.list$min))
173   for (i in 1:length(formation.list$min)){
174     randhorizon[i] <- runif(1, formation.list$min[i],
175 formation.list$max[i])
176   }
```

```
  form.idx <- match(lepido$Formation.locality,
formation.list$formation_name)
  randoccurrence <- randhorizon[form.idx]


  horizons <- cut(randhorizon, breaks=seq(0, 202, by=binSpan))
  horizontable <- as.data.frame(table(horizons))
  colnames(horizontable) <- c("time.bins", "horizons")
  occurrences <-  cut(randoccurrence, breaks=seq(0, 202,
by=binSpan))
  horizontable$occurrences <- table(occurrences)

  horizon.distribution <- horizontable [, "horizons"]

  FAD <- sum (horizontable
[c(1:tail(which(horizontable$occurrences>0),1)), "horizons"])

  n <- sum (horizontable
[c(1:tail(which(horizontable$occurrences>0),1)), "occurrences"])

  maximum <- sum (horizontable [, "horizons"])

  result <- Bayesian.posterior (FAD, 0.0000001, n, maximum, 0,
100000)

  #colnames (summary.table) <- c("point estimate", "upper CI",
"lower CI")

  table [u, 1] <- date.converter(horizon.distribution,
result["point estimate"])
  table [u, 2] <- date.converter(horizon.distribution, result["CI
97.5"])
  table [u, 3] <- date.converter(horizon.distribution, result
["CI 2.5"])
  table [u, 4] <- date.converter(horizon.distribution, result
["CI 50"])
```

```
  table [u, 5] <- date.converter(horizon.distribution, result
["CI 90"])
}

finalresult.Median1 <- 202-(apply(table, 2, median)) #minus from
202 to return flipped values to actual
finalresult.Upper1 <- 202-(apply(table, 2, quantile,
probs=c(0.025)))
finalresult.Lower1 <- 202-(apply(table, 2, quantile,
probs=c(0.975)))

save.image(file='PachycormidsExt.RData') #rename as appropriate
```

Emergence estimates for suspension-feeding chondrichthyans

```
library(dplyr)
library(xlsx)

# Load fossil horizon data and eliminate duplicates (if present)

data <- read.xlsx("RData.xlsx", sheetIndex = 7) #loads horizons
yielding chondrichthyan fossils
form.idx <- which(duplicated(data$formation))
if (length(form.idx) > 0) {
  data <- data[-c(form.idx),]
}

# Extract relevant information

max <- data[, c("max_ma")]
min <- data[, c("min_ma")]
ave <- rep(NA, length(max))
for (i in 1:length(max)){
  ave[i] <- (max[i]+min[i])/2
```

```
}
formation_name <- data[, c("formation")]
continents <- data[, c("continent")] # set to one continent name
formation.list <- data.frame(formation_name, continents, max,
min, ave, data[,c("early_interval")], data[,c("late_interval")])

table(formation.list$continents)

# Load fossil occurrences for the clade of interest
lepido <- read.xlsx("RData.xlsx", sheetIndex = 4) # this would
calculate mobulid emergence, but sheet number (choose between
sheets 2-5 for chondrichthyans) changes depending on the focal
group (See RData.xlsx)

#Check that every formation where fossils of the focal group have
been found are in the formation list
lepido$Formation.locality <- gsub(" Formation", "",
lepido$Formation.locality)

check <- lepido$Formation.locality %in%
formation.list$formation_name
which(check == FALSE)

form.idx <- match(lepido$Formation.locality,
formation.list$formation_name)
lepido$max <- formation.list$max[form.idx]
lepido$min <- formation.list$min[form.idx]
lepido$ave <- formation.list$ave[form.idx]

#Cumulative density function used in subsequent BayesianPosterior
function
cdf <- function (posterior.p, x, quantile) {
  area <- 0
  j <- 1
  while (area <= quantile*(sum (posterior.p))){

```

```
    area <- area + posterior.p[j]
    j <- j+1

  }

  x [j]
}

#For horizon-based calculations, FAD is measured in numbers of
horizons

Bayesian.posterior <- function(FAD, LAD, n, old.bound,
young.bound, n.bins) {

  #first, rescale variables on to the scale [0,1]

  interval <- old.bound-young.bound

  z <- (FAD-young.bound)/interval

  y <- (LAD-young.bound)/interval


  #u.n, Strauss and Sadler (1989: formula 25)

  u.n <- (z-y)^(-n-2)-(1-y)^(-n+2)+1-z^(-n+2)

  u.n1 <- (z-y)^(-(n-1)-2)-(1-y)^(-(n-1)+2)+1-z^(-(n-1)+2)

  #create a vector of theta.2 values on the scaled interval

  theta.2 <- seq (z, 1, length = n.bins)

  h.x <- array (dim = n.bins)

  for (i in 1:n.bins) {
```

```
92
93      h.x [i] <- (n-2)*((theta.2[i]-y)^(-n+1)-theta.2[i]^(-
94  n+1))/u.n
95
96    }
97
98    #plot (theta.2, h.x, xlab = 'relative time', ylab = 'posterior
99  probability')
100
101   output <- array (dim = 5)
102
103   names (output) <- c("point estimate", "CI 2.5", "CI 50", "CI
104 90", "CI 97.5")
105
106   #Formula 27 in Straus & Sadler (1989)
107   output [1] <- ((n-2)*u.n1)/((n-3)*u.n)+(y*((z-y)^(-n+2)-(1-
108 y)^(-n+2)))/u.n
109
110   output [2] <- cdf (h.x, theta.2, 0.025)
111
112   output [3] <- cdf (h.x, theta.2, 0.5)
113
114   output [4] <- cdf (h.x, theta.2, 0.90)
115
116   output [5] <- cdf (h.x, theta.2, 0.975)
117
118   output <- output * interval
119
120   output
121
122 }
123
124 #Accounting for formation age uncertainty
125
126 binSpan <- 1
127
```

```
# Function that converts relative age derived from the
Bayesian.posterior function in absolute age

date.converter <- function (horizon.distribution, n){

  age.matrix <- array (dim = c(4, ceiling(202/binSpan)))

  rownames (age.matrix) <- c ("top bin", "bottom bin",
"horizons", "cumulative horizons")

  age.matrix [1, ] <- c(seq(0, 202-binSpan, binSpan))
  age.matrix [2, ] <- c(seq(binSpan, 202, binSpan))
  age.matrix [3, ] <- horizon.distribution
  age.matrix [4, ] <- cumsum (horizon.distribution)

  total <- 0

  i <- 1

  while (total < n) {


    total <- age.matrix [4, i]

    i <- i+1

  }

  age.estimate <- ((n-age.matrix [4, (i-2)])/age.matrix[3,(i-
1)])*(age.matrix[2, (i-1)]-age.matrix[1, (i-1)]) + age.matrix[1,
(i-1)]

  age.estimate

}

```

```
# Replicates to account for uncertainty in horizon age

Nreplicates = 1000
table <- array(dim=c(Nreplicates, 5))
for (u in 1:Nreplicates){

  cat(u, "\n")

  randhorizon <- rep(NA, length(formation.list$min))
  for (i in 1:length(formation.list$min)){
    randhorizon[i] <- runif(1, formation.list$min[i],
formation.list$max[i])
  }
  form.idx <- match(lepido$Formation.locality,
formation.list$formation_name)
  randoccurrence <- randhorizon[form.idx]


  horizons <- cut(randhorizon, breaks=seq(0, 202, by=binSpan))
  horizontable <- as.data.frame(table(horizons))
  colnames(horizontable) <- c("time.bins", "horizons")
  occurrences <-  cut(randoccurrence, breaks=seq(0, 202,
by=binSpan))
  horizontable$occurrences <- table(occurrences)

  horizon.distribution <- horizontable [, "horizons"]

  FAD <- sum (horizontable
[c(1:tail(which(horizontable$occurrences>0),1)), "horizons"])

  n <- sum (horizontable
[c(1:tail(which(horizontable$occurrences>0),1)), "occurrences"])

  maximum <- sum (horizontable [, "horizons"])

```

```
199   result <- Bayesian.posterior (FAD, 0.0000001, n, maximum, 0,
200 100000)
201
202   #colnames (summary.table) <- c("point estimate", "upper CI",
203 "lower CI")
204
205   table [u, 1] <- date.converter(horizon.distribution,
206 result["point estimate"])
207   table [u, 2] <- date.converter(horizon.distribution, result["CI
208 97.5"])
209   table [u, 3] <- date.converter(horizon.distribution, result
210 ["CI 2.5"])
211   table [u, 4] <- date.converter(horizon.distribution, result
212 ["CI 50"])
213   table [u, 5] <- date.converter(horizon.distribution, result
214 ["CI 90"])
215 }
216
217 finalresult.Median1 <- (apply(table, 2, median))
218 finalresult.Upper1 <- (apply(table, 2, quantile, probs=c(0.025)))
219 finalresult.Lower1 <- (apply(table, 2, quantile, probs=c(0.975)))
220
221 save.image(file='Mobulidae.RData') #rename as appropriate
```